

Spring 1996

Implementation of ALF results to designing flexible pavements in Louisiana

Ludfi Djakfar
Louisiana Tech University

Follow this and additional works at: <https://digitalcommons.latech.edu/dissertations>



Part of the [Civil Engineering Commons](#)

Recommended Citation

Djakfar, Ludfi, "" (1996). *Dissertation*. 168.
<https://digitalcommons.latech.edu/dissertations/168>

This Dissertation is brought to you for free and open access by the Graduate School at Louisiana Tech Digital Commons. It has been accepted for inclusion in Doctoral Dissertations by an authorized administrator of Louisiana Tech Digital Commons. For more information, please contact digitalcommons@latech.edu.

INFORMATION TO USERS

This manuscript has been reproduced from the microfilm master. UMI films the text directly from the original or copy submitted. Thus, some thesis and dissertation copies are in typewriter face, while others may be from any type of computer printer.

The quality of this reproduction is dependent upon the quality of the copy submitted. Broken or indistinct print, colored or poor quality illustrations and photographs, print bleedthrough, substandard margins, and improper alignment can adversely affect reproduction.

In the unlikely event that the author did not send UMI a complete manuscript and there are missing pages, these will be noted. Also, if unauthorized copyright material had to be removed, a note will indicate the deletion.

Oversize materials (e.g., maps, drawings, charts) are reproduced by sectioning the original, beginning at the upper left-hand corner and continuing from left to right in equal sections with small overlaps. Each original is also photographed in one exposure and is included in reduced form at the back of the book.

Photographs included in the original manuscript have been reproduced xerographically in this copy. Higher quality 6" x 9" black and white photographic prints are available for any photographs or illustrations appearing in this copy for an additional charge. Contact UMI directly to order.

UMI

A Bell & Howell Information Company
300 North Zeeb Road, Ann Arbor MI 48106-1346 USA
313/761-4700 800/521-0600

**IMPLEMENTATION OF ALF RESULTS TO
DESIGNING FLEXIBLE PAVEMENTS
IN LOUISIANA**

By

LUDFI DJAKFAR, MS

A Dissertation Presented in Partial fulfillment
of the Requirements for the Degree
Doctor of Engineering

**COLLEGE OF ENGINEERING AND SCIENCE
LOUISIANA TECH UNIVERSITY**

April 1999

UMI Number: 9926822

UMI Microform 9926822
Copyright 1999, by UMI Company. All rights reserved.

**This microform edition is protected against unauthorized
copying under Title 17, United States Code.**

UMI
300 North Zeeb Road
Ann Arbor, MI 48103

LOUISIANA TECH UNIVERSITY
THE GRADUATE SCHOOL

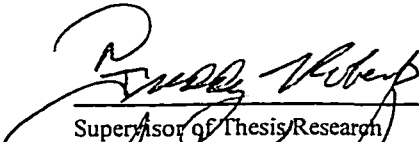
4/8/1999

Date

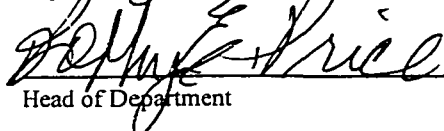
We hereby recommend that the thesis prepared under our supervision by
Ludfi Djakfar

entitled Implementation of ALF Results to Designing Flexible Pavements in Louisiana

be accepted in partial fulfillment of the requirements for the Degree of
Doctor of Engineering



Supervisor of Thesis/Research (FLR)

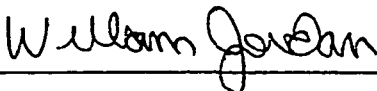


Head of Department (BEP)

Civil Engineering

Department


Recommendation concurred in:



(WMJ)




(RN)

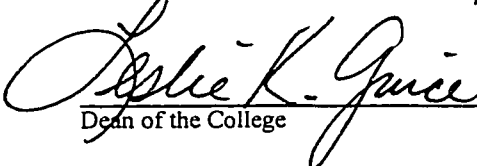


(NDP) Advisory Committee

Approved:

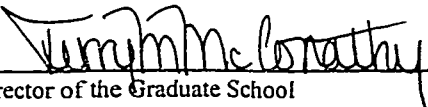


Director of Graduate Studies



Dean of the College

Approved:



Director of the Graduate School

ABSTRACT

The Louisiana Transportation Research Center (LTRC) recently conducted a research effort using the Accelerated Loading Facility (ALF). The objective of the research was to evaluate a limited number of alternative base materials and construction techniques envisioned to provide a significant reduction in the occurrence of shrinkage and reflected block cracking in the cement-stabilized bases. Nine test sections were constructed for this research, using the same wearing course material but having different thicknesses of crushed stone and soil cement bases and subbases. The soil cement base is the most commonly used base material in Louisiana, whereas crushed stone is a preferred base material in North Louisiana.

The objective of this study includes evaluating the ALF test results to determine the performance for each set of materials used in the test sections, and assessing the performance of those materials when constructed at other conditions and environment throughout Louisiana. To accomplish the objective, activities including literature review, data analysis, and performance modeling were performed.

From the analysis it was found that the combination of crushed stone base over a soil cement subbase, known as an inverted pavement, provided better performance than the soil cement bases while resisting rutting and retarding the

occurrence of reflection cracking. This finding confirmed the results from other researches conducted previously.

Based on the analysis it is recommended that an inverted pavement section should definitely be considered for use in Louisiana. The pavement with crushed stone bases should also be considered even in those areas where the subgrade is relatively soft. In addition, soil cement bases of 4 percent cement and mixed in-place should be constructed and their performance observed and compared to the more standard 10 percent plant mixed soil cement bases.

When the ALF materials were used in the pavement structure in the regions having different soil conditions and traffic levels, pavement with soil cement bases outperformed those with crushed stone bases.

Therefore, it is recommended that crushed stone materials similar to those used in the ALF test sections be used only in the areas with ADT not more than 25,000 or the number of ESALs not more than 23,700,00 ESALs for 20 years design period. On the other hand, soil cement bases can structurally be used in any areas with ADT not more than 75,000 or the number of ESALs not more than 44,500,000 for the 20-year design period. However, one should be cautious when using this material in areas where rainfall or water table is high since water may weaken the structure and cause a substantial reduction of pavement life.

It is also concluded that none of the material combination used in the ALF test section can predictably perform satisfactorily in the areas with ADT more

than 75,000. In such a situation, therefore, a rigid pavement should be a better candidate to handle the traffic.

Inverted sections such as those used in lane 009 of ALF test section can be considered as the best of all material combinations even though its performance is somewhat lower than those with soil cement bases. The results from the Louisiana ALF experiment showed that the inverted section has better performance due to its ability to substantially reduce the reflection cracking initiated in the soil cement material underneath.

TABLE OF CONTENTS

| | |
|---|-------|
| ABSTRACT | iii |
| LIST OF FIGURES | x |
| LIST OF TABLES | xv |
| ACKNOWLEDGMENTS..... | xviii |
| CHAPTER 1 | 1 |
| INTRODUCTION..... | 1 |
| Background | 1 |
| Objectives of Study..... | 5 |
| Methodology..... | 5 |
| Literature Review | 5 |
| Data Collection | 5 |
| ALF Data Analysis..... | 6 |
| Performance Modeling | 6 |
| Analysis Tool..... | 6 |
| Modeling Performance Prediction by VESYS 3A-M | 6 |
| Results Implementation | 7 |
| CHAPTER 2 | 8 |
| LITERATURE REVIEW | 8 |
| The ALF Machine | 8 |
| Overview of VESYS 3A-M | 12 |
| Road Roughness as the Performance Indicator | 18 |
| Overview of Available Performance Models | 22 |
| The Use of Falling Weight Deflectometer to Obtain Layer Moduli..... | 30 |
| Correction of AC Modulus Predicted from Backcalculation Method | 33 |

| | |
|--|-----|
| AC Moduli Prediction throughout the Year | 36 |
| Overview of Materials Used in the ALF Sections..... | 39 |
| CHAPTER 3 | 42 |
| DESCRIPTION OF ALF TEST SECTIONS AND PRESENTATION OF THE DATA COLLECTED | 42 |
| Pavement Test Sections..... | 42 |
| Times of Loading | 44 |
| Location of the Test Section | 46 |
| Data Collection Method | 46 |
| Evaluation of Layer Moduli from Backcalculation Method | 48 |
| Surface Moduli Evaluation | 50 |
| Evaluation of Base Moduli | 52 |
| Evaluation of Subbase Moduli..... | 54 |
| Evaluation of Subgrade Moduli | 55 |
| Rutting Calculation..... | 56 |
| Roughness Calculation..... | 58 |
| CHAPTER 4 | 60 |
| PERFORMANCE PREDICTION OF ALF TEST SECTIONS | 60 |
| Introduction | 60 |
| Slope Variance | 60 |
| Present Serviceability Index | 62 |
| Input Data Preparation..... | 63 |
| Analysis of Results and Discussions | 67 |
| Rutting | 67 |
| Cracking..... | 68 |
| Present Serviceability Index | 69 |
| Conclusion | 71 |
| CHAPTER 5 | 100 |
| RELATIVE PERFORMANCE COMPARISON USING OBSERVED DATA | 100 |
| Rut Depth Data | 100 |
| Roughness Data..... | 102 |

| | |
|---|-----|
| Cracking Development..... | 105 |
| CHAPTER 6 | 110 |
| IMPLEMENTATION OF ALF RESULTS..... | 110 |
| Methodology..... | 110 |
| Pavement Design Practices in Louisiana | 111 |
| Surface Materials | 111 |
| Structural Coefficients..... | 111 |
| Serviceability Index | 112 |
| Reliability Level..... | 112 |
| Overall Standard Deviation | 114 |
| Roadbed Condition | 114 |
| Resilient Moduli | 115 |
| Grouping Parishes with Similar Soil Condition | 117 |
| Traffic Analysis..... | 118 |
| Conversion of ADT to ESALs | 119 |
| Growth Rate..... | 120 |
| Directional Distribution..... | 120 |
| Lane Distribution..... | 120 |
| Calculation of the Total Number of ESALs | 121 |
| Analysis Method..... | 125 |
| Performance Criteria | 127 |
| Results and Discussions | 128 |
| Rutting Evaluation..... | 128 |
| Serviceability Evaluation..... | 131 |
| Why is It Different from the ALF Rresults?..... | 133 |
| CHAPTER 7 | 172 |
| CONCLUSIONS AND RECOMMENDATIONS | 172 |
| APPENDIX 1. RESILIENT MODULUS DATA..... | 177 |
| APPENDIX 2. RUTTING DATA | 186 |
| APPENDIX 3. ROUGHNESS DATA..... | 196 |
| APPENDIX 4. PSI DATA | 206 |

| | |
|---|-----|
| APPENDIX 5. THICKNESS DESIGN DATA | 211 |
| REFERENCES | 221 |
| VITAE | 228 |

LIST OF FIGURES

| | |
|--|----|
| Figure 2. 1 The Louisiana ALF machine..... | 9 |
| Figure 2. 2 Modular structure of VESYS [14] | 13 |
| Figure 2. 3 The IRI roughness scale..... | 21 |
| Figure 2. 4 Chart to predict pavement temperature [41] | 35 |
| Figure 2. 5 Estimation of temperature [41] | 39 |
| Figure 3. 1 Cross section of pavement test lanes..... | 43 |
| Figure 3. 2 Predicted HMA modulus for each lane..... | 51 |
| Figure 3. 3 Predicted moduli for stone material base layer..... | 53 |
| Figure 3. 4 Predicted moduli for soil cement base layer | 54 |
| Figure 3. 5 Comparison of select soil subbase moduli | 55 |
| Figure 3. 6 Comparison of subgrade moduli..... | 56 |
| Figure 3. 7 A sample calculation of rut depth from a transverse profile | 57 |
| Figure 3. 8 Moving average filter | 59 |
| Figure 4. 1 Comparison of rutting development between VESYS 3A-M and observed data for lane 002..... | 73 |
| Figure 4. 2 Comparison of rutting development between VESYS 3A-M and observed data for lane 003..... | 74 |
| Figure 4. 3 Comparison of rutting development between VESYS 3A-M and observed data for lane 004..... | 75 |
| Figure 4. 4 Comparison of rutting development between VESYS 3A-M and observed data for lane 005..... | 76 |
| Figure 4. 5 Comparison of rutting development between VESYS 3A-M and observed data for lane 006..... | 77 |
| Figure 4. 6 Comparison of rutting development between VESYS 3A-M and observed data for lane 007 | 78 |
| Figure 4. 7 Comparison of rutting development between VESYS 3A-M and observed data for lane 008..... | 79 |
| Figure 4. 8 Comparison of rutting development between VESYS 3A-M and observed data for lane 009..... | 80 |
| Figure 4. 9 Comparison of rutting development between VESYS 3A-M and observed data for lane 010..... | 81 |
| Figure 4. 10 Comparison of crack development between VESYS 3A-M prediction and observed data for lane 002 | 82 |
| Figure 4. 11 Comparison of crack development between VESYS 3A-M prediction and observed data for lane 003 | 83 |

| | |
|---|-----|
| Figure 4. 12 Comparison of crack development between VESYS 3A-M prediction and observed data for lane 004 | 84 |
| Figure 4. 13 Comparison of crack development between VESYS 3A-M prediction and observed data for lane 005 | 85 |
| Figure 4. 14 Comparison of crack development between VESYS 3A-M prediction and observed data for lane 006 | 86 |
| Figure 4. 15 Comparison of crack development between VESYS 3A-M prediction and observed data for lane 007 | 87 |
| Figure 4. 16 Comparison of crack development between VESYS 3A-M prediction and observed data for lane 008 | 88 |
| Figure 4. 17 Comparison of crack development between VESYS 3A-M prediction and observed data for lane 009 | 89 |
| Figure 4. 18 Comparison of crack development between VESYS 3A-M prediction and observed data for lane 010 | 90 |
| Figure 4. 19 Comparison of PSI development between VESYS 3A-M prediction and observed data for lane 002 | 91 |
| Figure 4. 20 Comparison of PSI development between VESYS 3A-M prediction and observed data for lane 003 | 92 |
| Figure 4. 21 Comparison of PSI development between VESYS 3A-M prediction and observed data for lane 004 | 93 |
| Figure 4. 22 Comparison of PSI development between VESYS 3A-M prediction and observed data for lane 005 | 94 |
| Figure 4. 23 Comparison of PSI development between VESYS 3A-M prediction and observed data for lane 006 | 95 |
| Figure 4. 24 Comparison of PSI development between VESYS 3A-M prediction and observed data for lane 007 | 96 |
| Figure 4. 25 Comparison of PSI development between VESYS 3A-M prediction and observed data for lane 008 | 97 |
| Figure 4. 26 Comparison of PSI development between VESYS 3A-M prediction and observed data for lane 009 | 98 |
| Figure 4. 27 Comparison of PSI development between VESYS 3A-M prediction and observed data for lane 010 | 99 |
| Figure 5. 1 Average rutting development for lanes 002 through 010..... | 101 |
| Figure 5. 2 Performance comparison at a rut depth of 19-mm. (0.75 in.)..... | 103 |
| Figure 5. 3 Summary of roughness development for lanes 002 through 010. | 104 |
| Figure 5. 4 Performance comparison based on rutting and roughness | 106 |
| Figure 5. 5 Crack development for lanes 002 through 010..... | 108 |
| Figure 6. 1 Resilient modulus for typical Louisiana soil types [67] | 116 |
| Figure 6. 2 Soil resilient modulus – R-values correlation [67]..... | 117 |
| Figure 6. 3 Predicted rutting comparison at the end of a 20-year performance period for pavements designed for an average ADT of 4,000 and subgrade modulus of 8,000 psi..... | 136 |

| | |
|--|-----|
| Figure 6. 4 Predicted rutting comparison at the end of a 20-year performance period for pavements designed for an average ADT of 8,000 and subgrade modulus of 8,000 psi..... | 137 |
| Figure 6. 5 Predicted rutting comparison at the end of a 20-year performance period for pavements designed for an average ADT of 15,000 and subgrade modulus of 8,000 psi..... | 138 |
| Figure 6. 6 Predicted rutting comparison at the end of a 20-year performance period for pavements designed for an average ADT of 25,000 and subgrade modulus of 8,000 psi..... | 139 |
| Figure 6. 7 Predicted rutting comparison at the end of a 20-year performance period for pavements designed for an average ADT of 40,000 and subgrade modulus of 8,000 psi..... | 140 |
| Figure 6. 8 Predicted rutting comparison at the end of a 20-year performance period for pavements designed for an average ADT of 75,000 and subgrade modulus of 8,000 psi..... | 141 |
| Figure 6. 9 Predicted rutting comparison at the end of a 20-year performance period for pavements designed for an average ADT of 4,000 and subgrade modulus of 9,150 psi..... | 142 |
| Figure 6. 10 Predicted rutting comparison at the end of a 20-year performance period for pavements designed for an average ADT of 8,000 and subgrade modulus of 9,150 psi..... | 143 |
| Figure 6. 11 Predicted rutting comparison at the end of a 20-year performance period for pavements designed for an average ADT of 15,000 and subgrade modulus of 9,150 psi..... | 144 |
| Figure 6. 12 Predicted rutting comparison at the end of a 20-year performance period for pavements designed for an average ADT of 25,000 and subgrade modulus of 9,150 psi..... | 145 |
| Figure 6. 13 Predicted rutting comparison at the end of a 20-year performance period for pavements designed for an average ADT of 40,000 and subgrade modulus of 9,150 psi..... | 146 |
| Figure 6. 14 Predicted rutting comparison at the end of a 20-year performance period for pavements designed for an average ADT of 75,000 and subgrade modulus of 9,150 psi..... | 147 |
| Figure 6. 15 Predicted rutting comparison at the end of a 20-year performance period for pavements designed for an average ADT of 4,000 and subgrade modulus of 10,600 psi..... | 148 |
| Figure 6. 16 Predicted rutting comparison at the end of a 20-year performance period for pavements designed for an average ADT of 8,000 and subgrade modulus of 10,600 psi..... | 149 |
| Figure 6. 17 Predicted rutting comparison at the end of a 20-year performance period for pavements designed for an average ADT of 15,000 and subgrade modulus of 10,600 psi..... | 150 |

| | |
|--|-----|
| Figure 6. 18 Predicted rutting comparison at the end of a 20-year performance period for pavements designed for an average ADT of 25,000 and subgrade modulus of 10,600 psi..... | 151 |
| Figure 6. 19 Predicted rutting comparison at the end of a 20-year performance period for pavements designed for an average ADT of 40,000 and subgrade modulus of 10,600 psi..... | 152 |
| Figure 6. 20 Predicted rutting comparison at the end of a 20-year performance period for pavements designed for an average ADT of 75,000 and subgrade modulus of 10,600 psi..... | 153 |
| Figure 6. 21 Predicted PSI comparison at the end of a 20-year performance period for pavements designed for an average ADT of 4,000 and subgrade modulus of 8,000 psi..... | 154 |
| Figure 6. 22 Predicted PSI comparison at the end of a 20-year performance period for pavements designed for an average ADT of 8,000 and subgrade modulus of 8,000 psi..... | 155 |
| Figure 6. 23 Predicted PSI comparison at the end of a 20-year performance period for pavements designed for an average ADT of 15,000 and subgrade modulus of 8,000 psi..... | 156 |
| Figure 6. 24 Predicted PSI comparison at the end of a 20-year performance period for pavements designed for an average ADT of 25,000 and subgrade modulus of 8,000 psi..... | 157 |
| Figure 6. 25 Predicted PSI comparison at the end of a 20-year performance period for pavements designed for an average ADT of 40,000 and subgrade modulus of 8,000 psi..... | 158 |
| Figure 6. 26 Predicted PSI comparison at the end of a 20-year performance period for pavements designed for an average ADT of 75,000 and subgrade modulus of 8,000 psi..... | 159 |
| Figure 6. 27 Predicted PSI comparison at the end of a 20-year performance period for pavements designed for an average ADT of 4,000 and subgrade modulus of 9,150 psi..... | 160 |
| Figure 6. 28 Predicted PSI comparison at the end of a 20-year performance period for pavements designed for an average ADT of 8,000 and subgrade modulus of 9,150 psi..... | 161 |
| Figure 6. 29 Predicted PSI comparison at the end of a 20-year performance period for pavements designed for an average ADT of 15,000 and subgrade modulus of 9,150 psi..... | 162 |
| Figure 6. 30 Predicted PSI comparison at the end of a 20-year performance period for pavements designed for an average ADT of 25,000 and subgrade modulus of 9,150 psi..... | 163 |
| Figure 6. 31 Predicted PSI comparison at the end of a 20-year performance period for pavements designed for an average ADT of 40,000 and subgrade modulus of 9,150 psi..... | 164 |

| | |
|--|-----|
| Figure 6. 32 Predicted PSI comparison at the end of a 20-year performance period for pavements designed for an average ADT of 75,000 and subgrade modulus of 9,150 psi..... | 165 |
| Figure 6. 33 Predicted PSI comparison at the end of a 20-year performance period for pavements designed for an average ADT of 4,000 and subgrade modulus of 10,600 psi..... | 166 |
| Figure 6. 34 Predicted PSI comparison at the end of a 20-year performance period for pavements designed for an average ADT of 8,000 and subgrade modulus of 10,600 psi..... | 167 |
| Figure 6. 35 Predicted PSI comparison at the end of a 20-year performance period for pavements designed for an average ADT of 15,000 and subgrade modulus of 10,600 psi..... | 168 |
| Figure 6. 36 Predicted PSI comparison at the end of a 20-year performance period for pavements designed for an average ADT of 25,000 and subgrade modulus of 10,600 psi..... | 169 |
| Figure 6. 37 Predicted PSI comparison at the end of a 20-year performance period for pavements designed for an average ADT of 40,000 and subgrade modulus of 10,600 psi..... | 170 |
| Figure 6. 38 Predicted PSI comparison at the end of a 20-year performance period for pavements designed for an average ADT of 75,000 and subgrade modulus of 10,600 psi..... | 171 |

LIST OF TABLES

| | |
|---|-----|
| Table 2. 1 Features of the Louisiana ALF device..... | 10 |
| Table 2. 2 VESYS 3A-M version features | 15 |
| Table 2. 3 Classification of flexible prediction models based on various condition measures [5]..... | 24 |
| Table 2. 4 Classification of flexible prediction models based on distresses-related [5] | 24 |
| Table 3. 1 Properties of materials used at ALF test sections | 45 |
| Table 3. 2 Loading schemes applied to the ALF test lanes | 46 |
| Table 3. 3 Offset of the FWD geophones [61] | 49 |
| Table 3. 4 Axle load equivalency factor for lanes 002 through 010..... | 50 |
| Table 3. 5 Summary of HMA modulus of ALF test section..... | 51 |
| Table 4. 1 Permanent deformation Alpha and Gnu for lanes 002 through 010 | 66 |
| Table 4. 2 Poisson's ratio for selected materials [64]..... | 66 |
| Table 4. 3 Fatigue coefficients k_1 and k_2 at 25°C (77°F) | 67 |
| Table 4. 4 Tensile strain at the bottom of asphalt layer from VESYS 3A-M analysis | 70 |
| Table 5. 1 Regression model for rut depth versus ESALs | 102 |
| Table 5. 2 Approximate relation between IRI and SI for each lane | 104 |
| Table 6. 1 Pavement type with respect to traffic volume..... | 111 |
| Table 6. 2 Surface lift thickness specification..... | 112 |
| Table 6. 3 Layer coefficients for some materials commonly used in Louisiana | 113 |
| Table 6. 4 Serviceability index suggested for each functional class | 114 |
| Table 6. 5 Reliability level for each location and functional class | 114 |
| Table 6. 6 Range of moduli used in the analysis | 118 |
| Table 6. 7 Traffic level used in the study..... | 119 |
| Table 6. 8 Lane distribution factor guidelines from AASHTO [41] | 121 |
| Table 6. 9 A sample of spreadsheet used to calculate 18-kips ESALs | 122 |
| Table 6. 10 Classification counts (%) of vehicles | 123 |
| Table 6. 11 FHWA functional class description | 124 |
| Table 6. 12 1996 Louisiana equivalency factors for each classification vehicle for $PSI_i = 2.5$ | 124 |
| Table 6. 13 1996 Louisiana equivalency factors for each classification vehicle for $PSI_i = 2.0$ | 125 |

| | |
|--|-----|
| Table 6. 14 Design combinations of subgrade and traffic level included in this study | 126 |
| Table 6. 15 Summary of traffic level used in the analysis | 126 |
| Table 6. 16 Summary of subgrade level used in the study..... | 127 |
| Table 7. 1 Recommended use of ALF test materials based on traffic and subgrade modulus | 176 |
| Table A1. 1 Predicted layer moduli for lane 002..... | 178 |
| Table A1. 2 Predicted layer moduli for lane 003..... | 179 |
| Table A1. 3 Predicted layer moduli for lane 004..... | 179 |
| Table A1. 4 Predicted layer moduli for lane 005..... | 180 |
| Table A1. 5 Predicted layer moduli for lane 006..... | 181 |
| Table A1. 6 Predicted layer moduli for lane 007..... | 182 |
| Table A1. 7 Predicted layer moduli for lane 008..... | 183 |
| Table A1. 8 Predicted layer moduli for lane 009..... | 184 |
| Table A1. 9 Predicted layer moduli for lane 010..... | 185 |
| Table A2. 1 Rut depth for Lane 002 | 187 |
| Table A2. 2 Rut depth for lane 003 | 188 |
| Table A2. 3 Rut depth for lane 004 | 189 |
| Table A2. 4 Rut depth for lane 005 | 190 |
| Table A2. 5 Rut depth for lane 003 | 191 |
| Table A2. 6 Rut depth for lane 007 | 192 |
| Table A2. 7 Rut depth for lane 008 | 193 |
| Table A2. 8 Rut depth for lane 009 | 194 |
| Table A2. 9 Rut depth for lane 010 | 195 |
| Table A3. 1 IRI and RN values for lane 002..... | 197 |
| Table A3. 2 IRI and RN values for lane 003..... | 198 |
| Table A3. 3 IRI and RN values for lane 004..... | 199 |
| Table A3. 4 IRI and RN values for lane 005..... | 200 |
| Table A3. 5 IRI and RN values for lane 006..... | 201 |
| Table A3. 6 IRI and RN values for lane 007..... | 202 |
| Table A3. 7 IRI and RN values for lane 008..... | 203 |
| Table A3. 8 IRI and RN values for lane 009..... | 204 |
| Table A3. 9 IRI and RN values for lane 010..... | 205 |
| Table A4. 1 PSI for lane 002..... | 207 |
| Table A4. 2 PSI for lane 003..... | 207 |
| Table A4. 3 PSI for lane 004..... | 208 |
| Table A4. 4 PSI for lane 005..... | 208 |
| Table A4. 5 PSI for lane 006..... | 208 |
| Table A4. 6 PSI for lane 007..... | 209 |
| Table A4. 7 PSI for lane 008..... | 209 |
| Table A4. 8 PSI for lane 009..... | 210 |
| Table A4. 9 PSI for lane 010..... | 210 |

| | |
|---|-----|
| Table A5. 1 Thickness design using lane 002 materials | 212 |
| Table A5. 2 Thickness design using lane 003 materials | 213 |
| Table A5. 3 Thickness design using lane 004 materials | 214 |
| Table A5. 4 Thickness design using lane 005 materials | 215 |
| Table A5. 5 Thickness design using lane 006 materials | 216 |
| Table A5. 6 Thickness design using lane 007 materials | 217 |
| Table A5. 7 Thickness design using lane 008 materials | 218 |
| Table A5. 8 Thickness design using lane 009 materials | 219 |
| Table A5. 9 Thickness design using lane 010 materials | 220 |

ACKNOWLEDGMENTS

Many people have contributed to the completion of this dissertation. First of all, I would like to express my gratefulness to Dr. Freddy L. Roberts, who with patience and tirelessness has provided guidance and support toward the completion of this report. Special thanks go to other members of my graduate committee Dr. Raja Nassar, Dr. Norman D. Pumphrey, Jr., and Dr. William M. Jordan for their valuable suggestions during the process of completion of this dissertation.

I also wish to thank the Louisiana Transportation Research Center for providing data and financial support for this study. Gratitude is also extended to Mr. Masood Rasoulia, ALF Project Director; and Dr. J.B. Metcalf of Louisiana State University for providing surface-crack and profile data.

Finally, special thanks are due to my dear wife Dyah for her patience and encouragement.

CHAPTER 1

INTRODUCTION

Background

During the last two decades, two significant changes have occurred in the highway system: the magnitude and number of loads have increased and the rate of development of distress has increased as well. Due to the economic forces affecting truck transportation, highway loads have increased dramatically in intensity and in a number of applications. Freeme, *et al.*, [1] indicated that the increase in traffic loading in South Africa exceeded design expectation during the period between 1977 to 1981, and the average single axle load (ESAL) per vehicle increased from 0.3 to 0.5. In the meantime, the predominant distress that occurs in flexible pavements has shifted from fatigue cracking, the dominant distress in the 1970s, to rutting. Based on available data from the Long Term Pavement Performance (LTPP) database, Al-Omary and Darter [2] found that rutting was the predominant distress that occurred in most flexible pavement test sections.

Every year the United States spends more than \$30 billion to maintain and upgrade its highway systems [3]. To secure information on the effect of loads on road conditions, lawmakers and highway agencies have initiated two

programs: long-term pavement performance monitoring programs and accelerated pavement testing programs.

One method of evaluating short-term pavement performance is using full-scale accelerated pavement testing (APT). APT is defined as “the controlled application of a prototype wheel loading, at or above the appropriate legal load limit to a prototype or actual layered, structural pavement system to determine pavement response and performance under a controlled, accelerated accumulation of damage in a compressed time period” [4]. Over 30 such facilities exist in North America alone, with over 21 overseas. These field and laboratory facilities were built to provide data to help better understand the relationships between load and distress and to predict pavement performance with a high degree of accuracy in a short period of time [4].

The Louisiana Department of Transportation and Development (La DOTD) is conducting pavement testing using an accelerated loading facility (ALF), the mechanical loading machine developed in Australia also being used at the Turner-Fairbank Laboratory in Virginia. Along with number of wheel load applications, typical performance data collected during tests of pavements with ALF include:

- Rutting/permanent deformation
- Fatigue cracks
- Roughness
- Pavement temperatures, and

- Nondestructive testing (NDT) data from the falling weight deflectometer (FWD).

Metcalf [4] reported that various analysis techniques have been used for the interpretation of results from full-scale accelerated pavement tests. Most of them related to practical assessment of the behavior and performance of the tested pavement, predicting rut depth development and tire pressure investigations. Metcalf also reported that only nine of these facilities linked the experimental programs to long-term pavement performance monitoring.

The following list contains the phenomena that can be potentially explained using ALF data:

- Permanent deformation and fatigue cracking development
- Changes in load intensity as roughness increases
- Decreases in pavement layer moduli with increases in distress as the number of load applications increases, and
- Development of pavement performance prediction models as a function of load applications. These models can be used in pavement management systems.

As can be seen from the list above, ALF can provide data for broad variety of pavement behavior studies. However, performance data from ALF pavements have several limitations, including:

- Accelerated loading. This type of loading does not permit pavement healing to occur as it does in normal service. As a result, long-term

behavior of a pavement cannot be fully represented from accelerated test results without the application of a shift factor or through validation studies.

- Environmental effect. Due to the short pavement life, the full effect of environment on the material behavior under traffic load will likely not be reflected properly.

In addition, until recently few studies have been conducted to verify and relate the performance data collected from the ALF with that from existing pavements.

Other concerns, particularly for analysis using data from the Louisiana ALF, are as follows:

- After testing pavement configurations, what steps should be taken to correlate the test results with field pavement performance?
- If the materials used in the test section performed satisfactorily, will the same performance occur if used in pavement construction in different environments and soil conditions in Louisiana?
- If there are differences in the performance, what factors influence these differences?

It is the intent of this study to evaluate the applicability of ALF results to other environments and conditions in Louisiana.

Objectives of Study

The objectives of the study are as follows:

1. Evaluate and analyze the ALF test results to assess the performance of each set of materials used in the test sections, and
2. Evaluate the performance of those materials when constructed at other conditions and environments throughout Louisiana.

Methodology

To accomplish the above objectives, the following activities were performed:

Literature Review

The purpose of the literature review was to search for previous works related to the study, including searching for models that have been developed from previous studies. The works by Rao, *et al.* [5] and Rauhut, *et al.* [6], for pavement performance modeling was used as the starting point because of the comprehensiveness of these studies. The details on this activity are discussed in Chapter 2.

Data Collection

LTRC personnel have collected ALF field data from December 1995 to April 1998. The data include longitudinal and transverse profiles, cracking, FWD data, load intensity, and pavement temperatures. These data were secured for distribution in a CD- ROM format. Some of them were also transferred

electronically to Bogard Hall BH-234 of Louisiana Tech University using a modem and PC ANYWHERE software installed on both computers.

Other data from selected sites typical of the Louisiana roads were obtained from the La DOTD including traffic data from the planning office and material parameters from the pavement and geotechnical office.

ALF Data Analysis

The data collected from the ALF sites were analyzed to assess and compare the performance among the lanes of the ALF test sections based on rutting, roughness, and surface cracks. The detailed discussion on this task is presented in Chapter 3.

Performance Modeling

Analysis Tool. There are two analysis tools to be used for this task: LaFLEX, a computer program developed in this study based on AASHTO 1993, and VESYS 3A-M, a pavement analysis computer program developed by FHWA.

Modeling Performance Prediction by VESYS 3A-M. Data secured from the laboratory and the ALF site were used as inputs for VESYS 3A-M to estimate the performance of ALF sections in terms of rutting, fatigue cracking, and roughness/serviceability. The estimated performance was then compared with those observed from the ALF test sections. If a good agreement was obtained between VESYS prediction and the observed data, no further adjustment was needed. However, when no such good agreement was achieved, an adjustment to the

VESYS model was necessary. The detailed discussion on this task is presented in Chapter 4.

Results Implementation

Results from the previous task were used to evaluate the performance of ALF materials when constructed in different traffic levels, and soil conditions. The evaluation was performed in terms of rutting, cracks, and roughness development. The details of this task are presented in Chapter 6.

CHAPTER 2

LITERATURE REVIEW

The ALF Machine

ALF is a full-scale transportable pavement test device that simulates the effect of traffic loading on full-scale pavements by applying controlled wheel loading in a repetitive manner [Z]. The machine was first designed and manufactured for AUSTROADS by the Road Transport Authority (RTA) in New South Wales, Australia. In 1984, the FHWA purchased the U.S. manufacturing rights from the RTA, and the first ALF machine in the U.S. was assembled and located at the Turner-Fairbanks Highway Research Center (TFHRC). The second one was purchased by the LTRC and delivered to the Pavement Research Facility outside Port Allen, Louisiana, in April 1994. A schematic diagram and partial list of features for the Louisiana ALF machine are shown in Figure 2.1 and Table 2.1, respectively.

The ALF machine is constructed from a 30.5 m (100 ft) long structural steel frame with a moving wheel assembly at the front and the rear. This machine travels on rails at speed of 0 to 17.7 km/h (11 mph) on a 11.6 m (38 ft) long test section. The movement is generated by an electric geared motor attached to the wheel, having the capability to maneuver uni-directionally. At the

ends of the frame, the rails curve upward to permit gravity to accelerate, decelerate, and change the direction of the wheel assembly [8]. Loads are applied to the pavement only in one direction, representing the real traffic load, and can be distributed laterally to simulate traffic wander, which produces the wheel path observed on highways. To move from one test site to another, the ALF is erected by cranes whereas for longer moves two loaders are usually used [9].



Figure 2. 1 The Louisiana ALF machine

The ALF can apply approximately 380 load cycles per hour using either a single- or dual-tire wheel assembly that models one-half of a single axle. The loads applied to the pavement can be varied from 40 kN (9,000 lb) to 100 kN (22,500 lb) by adding or subtracting ballast weights [8].

Table 2. 1 Features of the Louisiana ALF device

| Description | Features and Specifications |
|------------------------|---|
| Wheel test loads: | Duals: 34.696 kN (7,800 lb) – 111.2 kN (25,000 lb) Singles: 36.5 kN (8,200 lb) – 53.38 kN (12,000 lb) |
| Rut depth: | 0 – 102 mm (4 in) |
| Speed: | 0 – 17.7 km/h (11 mph) |
| Load application rate: | 360 – 720 per hour |
| Axle loads per day: | 100,000 – 300,000 |
| Power requirements: | Operating: 480 AC, 3 PH, 60 Hz, 10 Amp avg., 30 Amp peak, no hydraulics |
| Instrumentation: | Load cells – four independent, strain gauges with amplifiers; Rut profiles – linear potentiometer with data acquisition software |
| Operating conditions: | Environment: -17.8°C (0°F) to 40°C (105°F) wet or dry |
| Size: | Length – 28.9 m (94.8 ft), width – 4.51 m (14.8 ft), height – 6.4 m (21 ft) |

The ALF can provide many benefits to highway agencies. Principal among these benefits is the ability to observe the behavior and the damage patterns that develop under traffic loads in a short period of time, thereby avoiding the need for full scale pavement tests like the AASHO Road Test. Bonaquist et al. [10] used the ALF to evaluate the effects of tire pressure on flexible pavement response and performance. Sebaaly et al. [11] used data from previous ALF research to evaluate relationships between surface cracking and the structural capacity of both thin and thick pavements.

Another benefit derived from ALF research is the ability to compare performance of new with currently used materials. Before being extensively

used, the performance of a new material can be evaluated and its cost relative to other materials can be assessed. Kadar [12] used the ALF test results to assess the relative performance of a variety of asphalt surface types for pavement rehabilitation. Johnson-Clark et al. [9] employed the ALF to investigate the effectiveness of a geotextile reinforced seal between the subgrade and gravel layers to rehabilitate low volume roads. Metcalf [4] described the application of the accelerated loading into the following categories:

- Pavement performance: empirical comparison and serviceability
- Pavement response: stress/strain modeling, deflection modeling, deformation modeling, deformation modeling, and fatigue modeling
- Material response: backcalculation of modulus
- Material and layer equivalency
- Load equivalency: wheel and axle load configurations

Other benefits attributed to the ALF include (13):

- The generation of higher quality and more reliable data than could be obtained from other forms of full-scale testing,
- The establishment of links between the results from the trials and the laboratory characterization of the materials
- The increased awareness and adoption of rational pavement design methods rather than empirical methods

- Improved-cooperation between researchers and practitioners who are active in the pavement area, and
- Ease of installing instruments in a test section versus in real pavements.

Overview of VESYS 3A-M

The computational sequence in VESYS 3A-M consists of three main steps: primary response analysis, damage modeling, and performance predictions, as shown in Figure 2.2. First, the program calculates the primary response of the layered elastic or viscoelastic pavement section to a vertical surface stress over a finite circular area for a given set of input data. The output of this step (stress, strain, and deflection), combined with additional input data relating to number of load repetitions and empirical damage criteria, is then used to predict distress using the damage models. Finally, the output from the damage model analysis is used to calculate the performance in terms of serviceability index and expected life.

VESYS 3A-M is one of the VESYS computer program series that has been released by the FHWA since 1972. Unlike other series that operate on mainframe computers, VESYS 3A-M is designed to run on a microcomputer. Since there are many differences in configuration and memory between mainframe and microcomputer, modifications have been made to VESYS 3A-M to permit the program to run on a microcomputer system. For example, the probabilistic matrix formulation has been revised to accommodate this

compatibility, as well as the use of finite mathematics to keep exponential values within the operating range for certain types of computers [14].

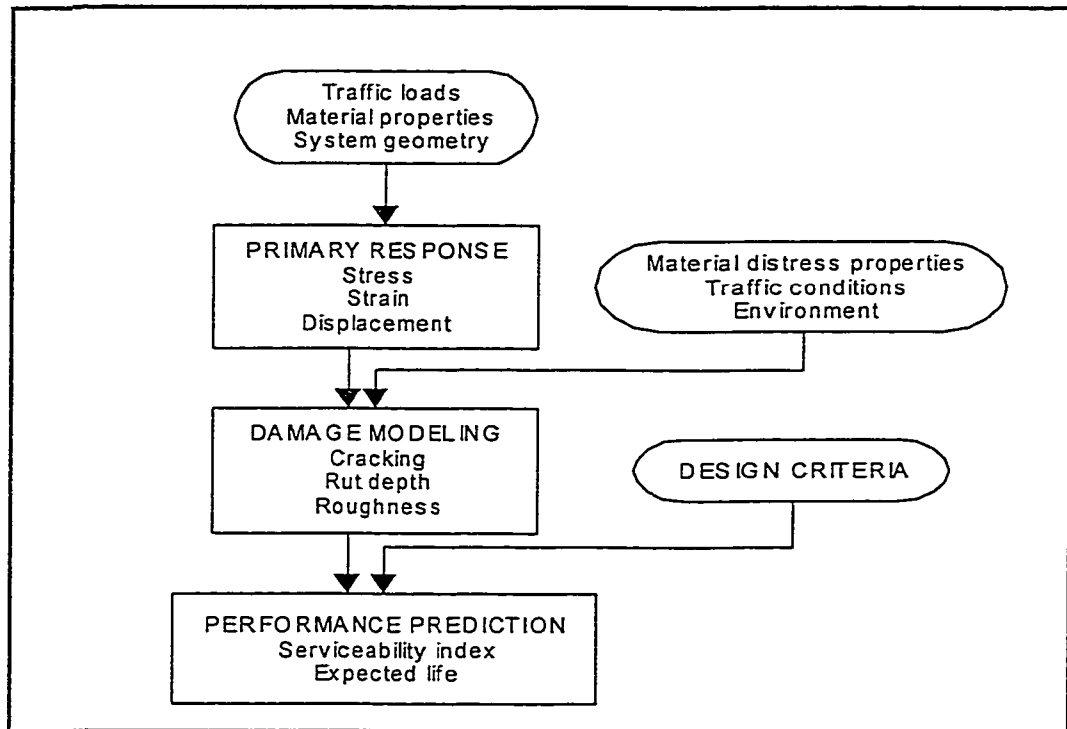


Figure 2. 2 Modular structure of VESYS [14]

However, these modifications do not make VESYS 3A-M less powerful. Table 2.2 shows the VESYS attributes of all versions. It can be seen that VESYS 3A-M has features that are quite powerful and still offers many advantages for use in design and analysis purposes.

In the primary response analysis, the pavement cross-section is analyzed using equations based on the theory of elasticity and a layered elastic medium subjected to vertical stationary surface loads to determine the stresses, strains and deflections taken as an approximation of those due to moving traffic loads. The basic assumptions included in the analysis are as follows:

- The bottom layer is infinite while the upper layers are finite in thickness
- All layers are infinite in the horizontal direction, and
- The material properties are time-dependent [14].

The input data for the primary response analysis include:

- Material properties
- System geometry, and
- The design stationary load

The input material properties for each layer include creep compliance, coefficients of variation, Poisson's ratio, and modulus. To take into account the environmental effects on the pavement, VESYS 3A-M accommodates up to 25 seasonal periods a year. Thus, the effects of seasonal moisture and temperature variations are reflected through the coefficients of variation of materials and layer moduli for each layer for each season.

The system geometry includes thickness of each layer and number of points in the radial and vertical positions where the primary responses are to be evaluated. For example, the primary response and location of interest for fatigue cracking is the horizontal strain at the bottom of asphalt layer directly under the load. Therefore, these locations of interest must be identified by coordinates with the center of the load being 0,0.

Table 2. 2 VESYS 3A-M version features

| FEATURES | VESYS Versions | | | | | | | | | | |
|--------------------------|----------------|---|---|----|----|----|----|----|------|---|---|
| | 2M | A | G | 3I | 3A | 4A | 3B | 4B | 3A-M | D | 5 |
| Closed-form viscoelastic | X | X | | X | | | | | | | |
| 3 layers | X | X | | X | | | | | | | |
| N layers | | | X | X | X | X | | X | X | X | X |
| Viscoelastic (Quasi) | | | X | X | | X | | X | | | |
| General response | X | X | X | X | | X | | X | | | |
| Probability | X | X | X | X | X | X | X | X | X | X | X |
| Minor (crack) | X | X | X | X | X | X | X | X | X | X | X |
| System rutting | X | X | X | X | X | X | X | X | X | | X |
| Multiple seasons & radii | X | | X | X | X | X | X | X | X | X | X |
| Low temperature cracking | | X | | X | X | X | X | X | X | X | X |
| Elastic (only) | | | | | X | X | X | X | X | X | X |
| Elastic w/creep | | | | | | X | | X | | X | X |
| Variable season length | | | | | | X | X | | | X | |
| Stress dependent | | | | | | | X | X | | | |
| Tandem axle factor | | | | | | | X | X | | | |
| Tandem axles | | | | | | | X | X | | | |
| Tridem axles | | | | | | | | | | X | X |
| Dynamic load | | | | | | | | | | X | |
| Layer rutting | | | | | | | | | | X | X |
| Microcomputer | | | | | | | | | X | | |

The stationary load is the intensity of load to be applied to the pavement as specified in the design, expressed as the load in pounds and the radius of the contact area per wheel. For example, if an 80 kN (18-kip) single axle load with a 0.689 MPa (100 psi) tire pressure is used in the analysis, the input must be 40

kN (9,000 lb) for the single tire load intensity and 136 mm (5.35 in) for the radius of contact area.

Pavement damage is estimated using two models: (1) fatigue cracking, and (2) rutting. These two damage models are employed in VESYS since they are the most commonly encountered traffic induced types of damage in flexible pavements. Each model requires additional input data including traffic conditions, material properties related to the distress, and environment. The traffic condition data include the number of repeated loads in axles per day for each analysis period for which damage calculations are desired. The fatigue model requires, for the hot mix asphalt layers, k_1 , k_2 and the coefficients of variation, where k_1 is the coefficient and k_2 is the exponent in Miner's Law. The Miner's law can be expressed as:

$$D = \sum_{i=1}^m \frac{n_i}{N_i} \leq 1 \quad (2.1)$$

where:

n_i = the number of load applications at the state (i)

N_i = the number of cycles to failure for that particular state (i)

$$= k_1 (1/\sigma)^{k_2}$$

m = total number of cycles

The rut depth model requires permanent deformation properties Alpha and Gnu for each layer of the pavement. Alpha and Gnu are obtained from plots of data from the repeated load creep test. The slope variance model, based on the rut depth variation predictions from the rutting model, is used to estimate

the present serviceability index (PSI). Additional input data required are the terminal serviceability level, level of reliability, standard deviation of initial PSI value, and the system performance properties.

Using typical input data for Louisiana materials and conditions, a preliminary run of VESYS 3A-M was performed, and an analysis of the results revealed the following:

1. VESYS 3A-M requires that the design life have at least two seasons. If the user desires to use the same data for the whole year, the number of seasons must still be at least two by assuming the same data for each season. If not, the program does not always function properly, and error messages may appear.
2. VESYS 3A-M requires a microcomputer equipped with a math-coprocessor. The math-coprocessor serves two functions: prevents floating point errors and reduces the computational time for a run.
3. Preliminary runs have shown that VESYS 3A-M is sensitive to the number of seasons, the design life, and the radius of the loaded area. For certain combinations of design life or number of seasons, VESYS 3A-M prints out error messages. Therefore, if VESYS 3A-M prints error messages, one of the three factors mentioned above must be modified.
4. Unlike the mainframe version, the VESYS 3A-M version does not require creep compliance for the pavement materials. Creep compliance data are used only to calculate VARCOEF1, VARCOEF2 and VARCOEF3.

Road Roughness as the Performance Indicator

Two main criteria commonly used to assess road performance are distresses and roughness that occur on that road. These two criteria were also commonly used in the pavement management system. Furthermore, roughness has become the primary operating characteristics of a road [15]. Carey and Irick [16] showed that surface roughness was the primary variable needed to explain the driver's opinion of the quality and serviceability provided by pavement surface. Road roughness not only affects the direct cost of the road but also the indirect cost in terms of user cost. A study by the Transport and Road Research Laboratory (TRRL) and the World Bank from 1971 to 1972 showed that road roughness affected vehicle operating costs [17].

Hudson [15] defined the road roughness as the surface characteristics of a pavement that affect vehicle operating costs and the riding quality of that pavement as perceived by the highway user. Paterson [18] defined roughness as the variation in elevation of a road surface that typically has a complex profile comprising a spectrum of different wavelengths and amplitudes. Sayers [19] defined roughness as the variation in surface elevation that induces vibrations in traversing vehicles.

As of present, the roughness measuring equipment can be grouped into two generic [19]:

- Profilometric Methods. The longitudinal elevation profile of the road is measured and then analyzed to obtain one or more roughness

indices. It includes quasistatic methods and high-speed profilometer systems. Examples of this type include Face Dipstick and ALF profilometer.

- Response type road roughness measuring systems (RTRRMSs). A vehicle is instrumented with a road meter device, producing a roughness reading as the results of the vehicle motions that occur while traversing the road. RTRRMS systems are less accurate compared with the profilometric systems due to their dependence to the vehicle responses which vary by time. Examples of the RTRRMS systems type include Mays meter car, Bump integrator trailer, and Bureau of Public Road roughmeter.

Differences arising between roughness measures are due to the way the measuring instrument responds to the road profile and to the way the data are processed [18]. For example, data secured from the profilometric system represent either some measure of displacement amplitude relative to a moving average amplitude, or they represent the response of a standard vehicle response to roughness. In the RTRRMSs systems, the differences arise primarily through characteristics of each system.

Therefore, in 1982 the IRRE and the World Bank initiated a research effort to study the relationship among those measurements, and they established a standard that is time-stable [19]. The research was held in Brasilia, Brazil, in 1982 by research teams from the United States, the United Kingdom, France, Belgium, and Brazil. Forty-nine road test sites were measured using a variety of

test equipment and measurement conditions. The sites included a full roughness range of asphalt pavement, surface treatment, gravel, and earth roads. The data acquired were analyzed to determine the suitability of equipment and to relate and correlate the roughness statistic among the equipment.

Since then, most agencies have adopted this standard. The Federal Highway Administration (FHWA) has required state highway agencies that roughness data from the Long Term Pavement Performance Monitoring (LTPP) should be in the form of IRI [20]. Figure 2.3 shows the interpretation of common values of IRI. As can be seen from the figure, the common values for asphalt pavements range from 1.5 m/km to 6.0 m/km.

The results of the World Bank research are known as the International Roughness Index (IRI), a standard roughness index which is practical and measurable by most of the equipment used. The equipment used to measure IRI can be divided into four classes [21]:

1. Class 4. A roughness measure is not reproducible or stable with time, and can be measured only compared to IRI by subjective estimation. This class covers panel ratings and measures made with uncalibrated RTRRMSs
2. Class 3. A measure obtained from RTRRMS is calibrated to the IRI scale by correlation with reference measures from a Class 1 or 2 system. An example of this class includes the Mays Ride Meter.
3. Class 2. A profile-based method reproducible and stable with time is used, and also calibrated independently of other roughness measuring

instruments. Examples of this class include the 690 DNC Profilometer, APL Longitudinal Profile Analyzer, and Automatic Road Analyzer (ARAN).

4. Class 1. A profile-based method similar to Class 2 is used. A profile-based measurement qualifies as a Class 1 measure if it is so accurate that further improvements in accuracy would not be apparent. Examples of this class include longitudinal rod and level, Face Dipstick and ALF Profilometer.

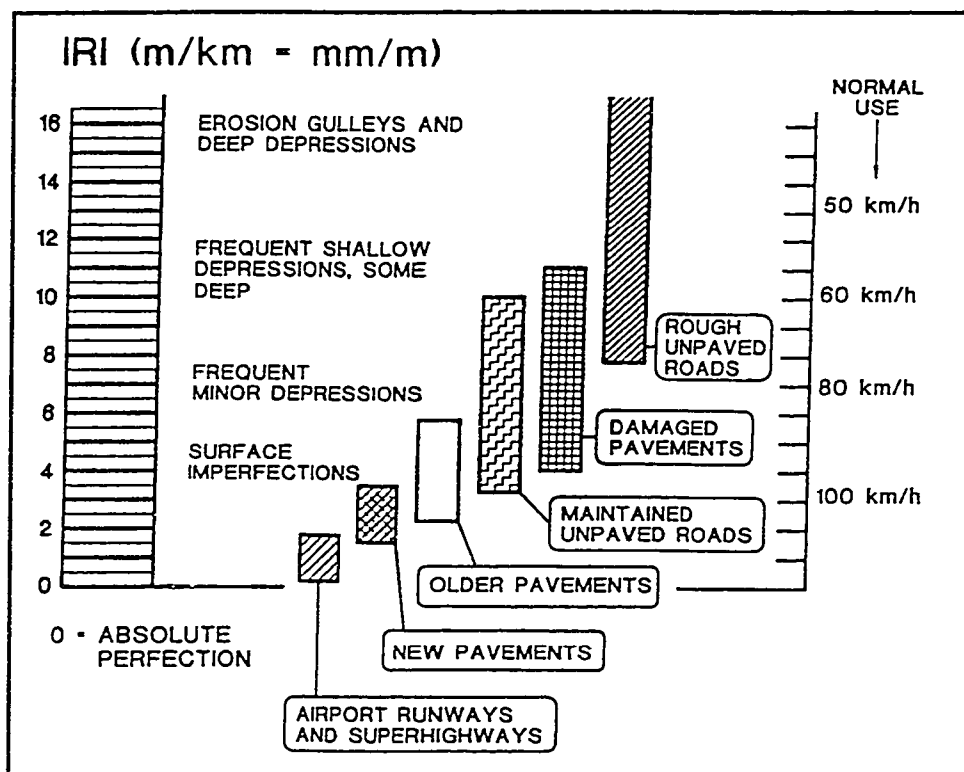


Figure 2.3 The IRI roughness scale

The in-depth discussion on the IRI and how to analyze the profile are discussed elsewhere [22]. For the purpose of this study, a program called

PROFILEANALYZER was developed to analyze data from the ALF site. Details on the calculation are presented in Chapter 3.

Overview of Available Performance Models

Available models for predicting flexible pavement performance, in general, can be put into four categories: roughness, structural, and composite as shown in tables 2.3 and 2.4 [5].

The first approach in evaluating pavement performance based on roughness progression was proposed after the AASHO road test, and is expressed in terms of PSI as:

$$g = \frac{p_o - p_t}{p_o - p_f} = \left(\frac{N_t}{\rho} \right)^\beta \quad (2.2)$$

Where:

- g = dimensionless damage parameter defining the functional loss of serviceability incurred before time t,
- p_o = serviceability index (PSI) at time t = 0,
- p_t = serviceability index at time t,
- p_f = terminal serviceability criterion, at which rehabilitation or reconstruction is indicated,
- N_t = cumulative number of equivalent 80 kN (18-kip) standard axle loads to time t, and

Table 2. 1 Classification of flexible prediction models based on various condition measures [5]

| Roughness | | | Structural | | | Composite | | | |
|------------|---------|--|--|---|-----------------------|--|--|---------|----------------|
| IRI | RCI | Others | Fatigue | Deflection | SAI | PSI | PCR | PQI | PCI |
| World Bank | Alberta | TRRL, Arizona, Australia, PEN DOT | Asphalt Institute, Shell, TRRL, Mobile Manual, Denmark, Belgium, Cost Allocation, NCHRP 1-10B, ARE, VESYS | AASHO, Arizona DOT, Asphalt Institute | Alberta, Minnesota | VESYS, HPMS, Idaho, Minnesota, Fernando Equation | Washington, Mississippi, PARS, Arkansas | Alberta | CERL, Paver |

Table 2. 2 Classification of flexible prediction models based on distresses-related [5]

| Distress - Related | | | | |
|--------------------|--|---|------------|------------|
| Alligator Cracking | Rutting | Permanent Strain | Potholing | Raveling |
| World bank | World Bank, Ohio State, Cost Allocation, SPDM, Monismith, et al., NCHRP 1-10B, VESYS, WATMODE | Monismith, Ogawa-Freeme, Barksdale, Michigan State, TTI | World Bank | World Bank |

ρ, β = functions of axle type, axle load and pavement strength parameters, including the structural number and a soil support parameter.

Hodges, et al [17] proposed a model which explicitly related roughness to pavement strength. The model is expressed as follows:

$$R_t = R_o + s(S) N_t \quad (2. 3)$$

Where:

R_o, R_t = roughness at time = 0 and t, respectively

$s(S)$ = function of modified structural number, and

N_t = cumulative number of equivalent 80 kN (18-kip) standard axle loads at time t

Way and Eisenberg [23] proposed a model based on the relation between change in roughness per unit of time and pavement age. The model takes the following expression:

$$\Delta R_t = a R_t \Delta t - b \quad (2. 4)$$

Where:

ΔR_t = change in roughness,

a, b = parameters obtained from regression analysis and a function of environment (rainfall, elevation, freeze-thaw cycles, temperature, etc.),

R_t = roughness at time t, and

Δt = change of time (age)

Zaniewski, et al [24] conducted a study to evaluate pavement performance data obtained from roughness survey data using Mays meter from 1972 to 1981, and to relate performance to pavement design. They proposed the following model:

$$R_t = C_0 + C_1 t \quad (2.5)$$

Where:

R_t = roughness in a homogenous section, in/mi.,

t = year since the treatment, and

C_0, C_1 = regression coefficients.

Potter [25] developed a model from roughness data similar to that of Zaniewski, et al [24] that takes the form:

$$R_t = C_0 + at^b \quad (2.6)$$

Where:

R_t = roughness at time t ,

t = pavement age, in years

C_0, a, b = regression coefficients

Uzan and Lytton [26, 27] related increase in roughness to the variance of rut depth, cracking area, patching and mean rut depth. Their model takes the following form:

$$P_t = 4.436 - 1.686 \log_{10}[1 + 350 \text{var}(RD)] - 0.881RD^{2.5} - 0.031(C + P)^{0.5} \quad (2.7)$$

Where:

P_t = serviceability index at time t ,

$\text{var}(\text{RD})$ = variance of rut depth, in^2 .,

RD = mean rut depth, $\text{in}.$,

C = cracking area, $\text{ft}^2/1000 \text{ ft}^2$, and

P = patching area, $\text{ft}^2/1000 \text{ ft}^2$.

Unlike previous models that included surface distress, Watanada, et al. [28] and Patterson [29] developed a model that included only age, structural number and traffic:

$$RI_t = [RI_o + 725(1 + SNC)^{-4.99} NE_{4t}]e^{0.0153t} \quad (2.8)$$

Where:

RI_t, RI_o = international roughness index at times t and $t = 0$ respectively, in m/km ,

SNC = modified structural number,

NE_{4t} = cumulative equivalent standard axle loadings to time t , million $80 \text{ kN ESAL}/\text{lane}$, and

t = age of pavement since overlay or construction.

Garzia-Diaz and Riggins of Texas Transportation Institute (TTI) [30] formulated prediction models using a sigmoidal (S-shaped) functions as follows:

$$g = \exp^{-(\rho/N_t)^p} \quad (2.9)$$

Where:

g = normalized damage function,

= number of 80 kN ESALs or the age to reach $g=1$, where $PSI = PSI_f$,

N_t = number of 80 kN ESALs or the age to a prescribed level of g (PSI) at time t ,

ρ, β = site-specific constant developed from performance validation studies.

George, *et al* [31] developed a model based on roughness and distress rating. The model includes age, traffic volume, thickness of surfacing, structural thickness of pavements and surface deflection and takes the form:

$$PCR_t = 90 - a[\exp(\text{Age})^b - 1] \left(\frac{ESAL}{SNC^c} \right) \quad (2.10)$$

Where:

PCR_t = present condition rating (PCR) at time t , which ranges from 0 to 100

Age = time since construction in years,

ESAL = annual rate of 80-kN ESALs for the design lane,

SNC = modified structural number, and

a, b, c = regression constant.

Al-Omary and Darter [2] developed a model based on the deterioration types using data from the LTPP database. They correlated IRI to PSR (0 to 5 scale) and pavement distress. The forms of the model are as follows:

$$PSR = 5e^{-0.0026IRI} \quad (\text{IRI in cm/km}) \quad (2.11)$$

$$PSR = 5e^{-0.0041IRI} \quad (\text{IRI in in./mile}) \quad (2.12)$$

The roughness correlation to rut depth model is as follows:

$$IRI = 57.56RD - 334.28 \quad (2.13)$$

Where:

IRI = international roughness index, in cm/km

RD = mean rut depth, in mm

When all the distresses were included, the model became:

$$PSR = 4.95 - 0.685D - 0.334P - 0.051C - 0.211RD \quad (2.14)$$

Where:

D = high severity depressions (number per 50 m),

P = high severity potholes (number per 50 m),

C = high severity cracks (number per 50 m), and

RD = average rut depth (mm).

Patterson [18] developed a relationship between PSI and IRI as follows:

$$SI = 5e^{-0.18IRI} \quad (2.15)$$

Where:

IRI is in m/km.

Patterson suggested the following comparable values between SI and IRI:

$$\begin{aligned} 4.2 SI &\cong 1.0 (m/km) IRI \\ 2.5 SI &\cong 3.8 (m/km) IRI \\ 2.0 SI &\cong 5.0 (m/km) IRI \\ 1.5 SI &\cong 6.6 (m/km) IRI \end{aligned} \quad (2.16)$$

Cumbaa [32] developed the following relationship for Louisiana conditions:

$$SI = 5.01e^{-[\ln(IRI, ClassIII)/4.977]^{4.738}} \quad (2.17)$$

Where:

IRI =roughness index from Class III devices (such as Mays Rid Meter).

When using other devices, the IRI should be converted to an equivalent Class III values:

For Class I (Face Dipstick):

$$ClassIII = 0.46(IRI, ClassI) - 4.26 \quad (2.18)$$

For Class II (ARAN, APL Longitudinal Profile Analyzer):

$$ClassIII = 0.40(IRI, ClassII) - 2.89 \quad (2.19)$$

Effect of the Initial Condition on Pavement Life. Smith, et al [33] reported that the initial condition of a pavement has a significant effect on the life of a pavement. A 25 percent increase in the initial smoothness increases the pavement life up to 9 percent. A 50 percent increase in smoothness increases 15 percent in pavement life.

The Use of Falling Weight Deflectometer to Obtain Layer Moduli

In lieu of available data from a laboratory, moduli of flexible pavements can be predicted directly from the field using deflection data secured from the Falling Weight Deflectometer (FWD) measurement. The FWD is "an impulse loading device that is used to simulate moving load in both magnitude and

duration. The FWD is typically equipped with a circular loading plate and several deflection sensors positioned at discrete locations from the center of the loading plate" [34].

The basic premise of the method is that the field values of layer moduli have been identified when the surface deflection basin computed using assumed moduli match the measured deflection basin [35]. In most of the backcalculation computer programs the initial values of the layer moduli are assumed and the deflection of the surface caused by the applied load is calculated and compared to the measured deflection. If the deflections match within prescribed limits, the assumed moduli become the layer moduli. If not, the process is repeated until the computed and measured deflections match. The theory of linear elasticity is used in most calculation routines where a circular loaded area and uniform stress distribution under the loaded area are assumed [34].

It should be kept in mind that the layer moduli obtained from non-destructive testing devices (NDT) using backcalculation methods are not unique solutions but are simply sets of moduli that yield the observed deflection [35]. However, many studies, such as that reported by Parker [36] have shown that the results from field NDT generally agreed with layer moduli obtained from laboratory testing.

It is important that the field deflection measurements be as accurate as possible since even small errors can cause differences in modulus values [37]. Another important feature of this methodology is that the assumptions used in the backcalculation must be representative of what happens in the field during

data collection. For example, a study by Touma, et al ([34](#)) showed that "if full contact [of the load plate] is assumed, when in reality it did not occur, significant errors in the backcalculated moduli values of the pavements analyzed may result."

All input parameters, e.g., Poisson's ratio, effective layer thickness, depth to bedrock, load configuration, and maximum number of iterations, have an effect on the values of layer moduli. The depth to bedrock parameter is a significant contributor to the size of errors and may be difficult to assess because it can vary with each deflection site ([35](#)). Uddin, *et al.*, also stated, "Ignorance of rigid bottom considerations may lead to substantial errors in the predicted moduli of a pavement-subgrade system. The subgrade modulus may be significantly overpredicted if a semi-infinite subgrade is falsely assumed, when actual bedrock exists at a shallow depth" ([38](#)).

Chou and Lytton ([35](#)) stated that the moduli of thin layers or sandwiched layers are usually difficult to obtain, because surface deflections are insensitive to changes in the moduli of these layers. Therefore, for pavements having thin layers, a more accurate measurement of the thickness is required to ensure that the backcalculated result is accurate. In addition, surface layer moduli are very sensitive to the layer thickness, followed by base and subbase layer moduli.

Hossain and Scofield ([39](#)) reported that the average backcalculated asphalt moduli compared favorably with the average laboratory-determined moduli when the condition of the pavement is good. Pavement condition is the primary determinant for good agreement between calculated and laboratory-

determined moduli. They concluded that backcalculated asphalt moduli seems to more accurately represent the in-situ moduli of the asphalt concrete. Their conclusion was based on the better agreement found on the moduli obtained from backcalculation method and laboratory-determined for new pavements and distress-free pavement in between wheel path locations on old pavements.

A study by Roberts et al. [40] indicated that moduli predicted from a 9,000 lb. load deflection basin produced better moduli estimates than those calculated at other loads. The study also suggested the use of the 9,000-lb. load unless "the stress sensitivity of the pavement material is of interest."

Several computer programs for backcalculation analyses have been developed, such as BISDEF, BOUSDEF, CHEVDEF, COMDEF, ELMOD, ELSDEF, EVERCALC, MODULUS, and many more. Each program was developed for a particular application and has its own advantages and disadvantages. For the soil, environment, and pavement conditions in Louisiana, MODULUS and WESDEF provided the best match between estimated and laboratory measured moduli [34].

Correction of AC Modulus Predicted from Backcalculation Method

Asphalt modulus obtained from a backcalculation method should be corrected to a standard temperature of 25°C (70°F), as suggested by the 1986 AASHTO guidelines [41]. The relation can be expressed as:

$$E_{std} = \lambda E_{tp} \quad (2.20)$$

Where:

E_{std} = asphalt modulus at a standard temperature of 70°F

λ = asphalt modulus adjustment factor

E_{tp} = asphalt modulus from backcalculation method

Several methods have been proposed to determine λ . AASHTO 1986 provides a chart that can be used to calculate λ , as shown in Figure 2.4.

Baltzer and Jansen [42] proposed the following model for adjustment factor:

$$\lambda = 10^{m(T-20)} \quad (2.21)$$

Where:

T = temperature at time of data collection, in °C

m = a constant with proposed value of 0.018.

Johnson and Baus [43] proposed the following equation:

$$\lambda = 10^{-0.0002175(70^{1.886} - T^{1.886})} \quad (2.22)$$

Where:

T = temperature at the time of FWD data collection

Ullidtz [44] suggested a model developed from the AASHTO Road Test deflection data as follows:

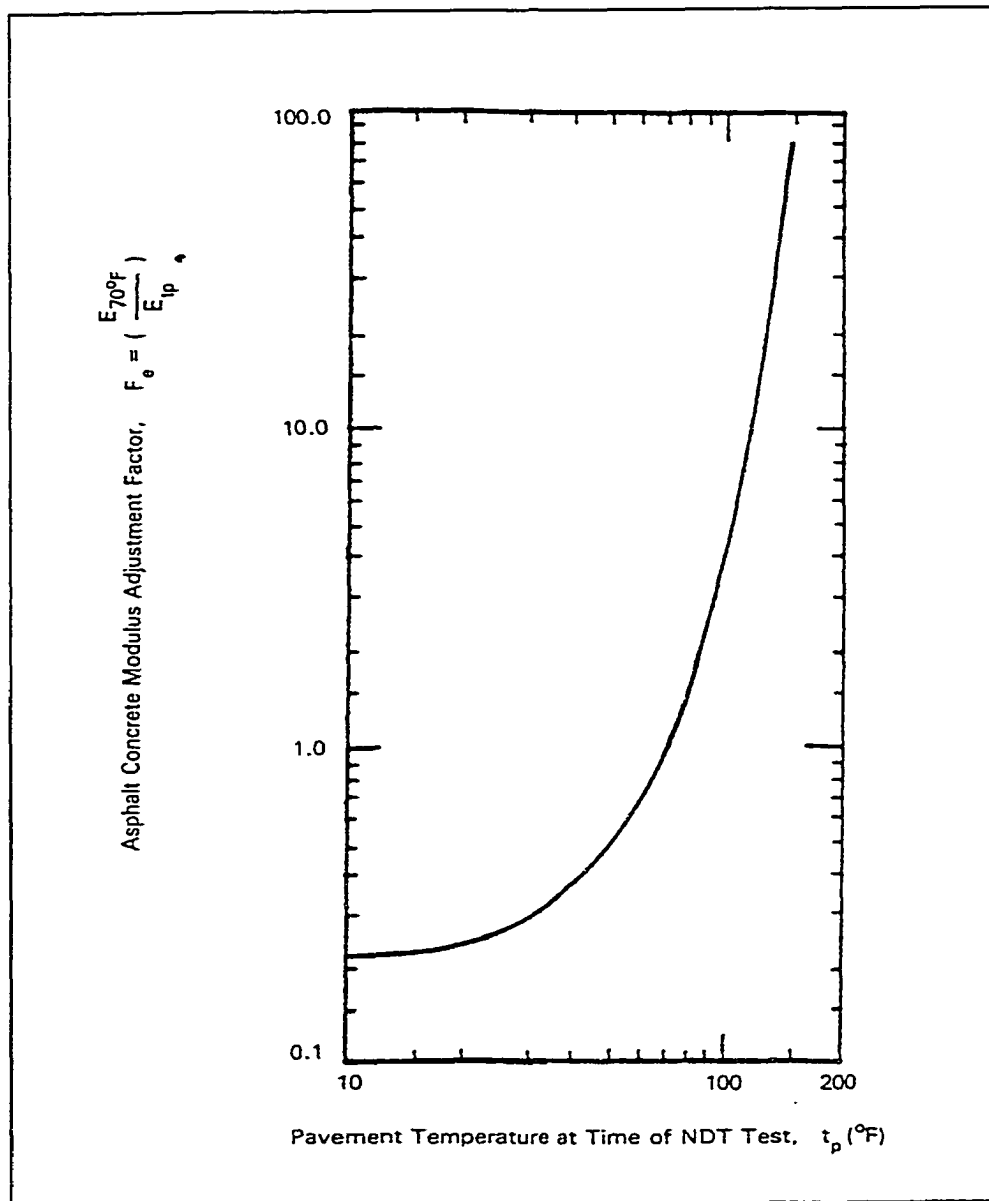


Figure 2. 4 Chart to predict pavement temperature [41]

$$\lambda = \frac{1}{3.177 - 1.673 \log T} \quad (2.23)$$

Where:

T = temperature at time of data collection, in °C, and must be >1°C

AC Moduli Prediction throughout the Year

The modulus of hot mix asphalt changes with temperature. At higher temperatures the modulus decreases, but at lower temperature it increases. It is essential, therefore, to take into account the moduli variation that occurs with temperature changes during ALF testing to properly analyze the performance of a pavement section. For example, the computer program VESYS allows up to 24 seasonal modulus variations within a year.

Commonly, the asphalt modulus is measured in the laboratory at 4.54°C (40°F), 25°C (77°F), and 40°C (104°F). These temperatures represent typical winter, fall/spring, and the summer conditions, respectively, but are not necessarily typical field conditions during ALF testing.

Ali and Parker [45] and Ali and Lopez [46] used a time series analysis to develop a methodology for predicting seasonal pavement temperature and the pavement layer moduli appropriate for those temperatures. The method is based on the assumption that pavement temperature can be predicted from ambient temperature. Since ambient temperature follows some pattern throughout the year, HMA modulus would also follow a similar pattern. If the pattern is sinusoidal, HMA modulus can be expressed as [45]:

$$E_{HMA} = A + B[\text{Sin}((2\pi f T + C)\frac{180}{\pi})] \quad (2.24)$$

Where:

E_{HMA} = HMA elastic modulus,

A = average annual HMA modulus for the whole year,

- B = amplitude of the variation in HMA modulus during the year (if modulus is constant then B equals 0),
- T = time of observation (e.g. month of the year 1 to 12),
- f = frequency (number of time increments per cycle, =1/12 if months are used and there is 1 cycle per year), and
- C = phase angle that controls the starting point on the curve and the peak month or months.

To determine the pavement temperature, Solaimanian and Kennedy [47] proposed a calculation method for estimating the maximum pavement surface temperature profile based on the maximum air temperature and hourly solar radiation. The equation takes the following form:

$$422\alpha\tau_{\alpha}^{1/\cos z} \cos z + 0.7\sigma T_a^4 - h_c(T_s - T_a) - 90k - \epsilon\sigma T_s^4 = 0 \quad (2.25)$$

Where:

- α = solar absorbtivity (default: 0.9),
- τ_{α} = sunshine factor (0.81 for perfectly sunny conditions),
- z = zenith angle (approximately $z = \text{latitude} - 20$ for May through August),
- σ = Stefan-Boltzman constant [0.1714 E-8 Btu/(hr.ft².R⁴)],
- T_a = maximum air temperature (Rankine),
- h_c = surface coefficient of heat transfer [default = 3.5 Btu/(hr.ft².F)],
- T_s = maximum pavement surface temperature (Rankine),

k = thermal conductivity [default: 0.8 Btu/(hr.ft².F)/ft], and

ϵ = surface emissivity [default:0.9].

The above equation must be solved iteratively. If the HMA depth is less than 8 in., the following alternative equation can be used to predict the pavement temperature at any depth [48]:

$$T_d = T_s(1 - 0.063d + 0.007d^2 - 0.0004d^3) \quad (2.26)$$

Where:

T_d = maximum pavement temperature (°F) at any depth,

T_s = maximum pavement temperature (°F) at the surface, and

d = depth (in.).

Ullidtz and Larsen [49] proposed the following equation to predict the pavement temperature of the asphalt based on the air temperature:

$$T_{asp} = 1.2T_{air} + 3.2$$

$$T_{air} = \frac{T_1 + T_2}{2} + \left(\frac{T_1 - T_2}{2} \right) \cos\left(\frac{U - U_0}{26} \right) \pi \quad (2.27)$$

Where:

T_{asp} = asphalt temperature, in °C

T_{air} = mean weekly air temperature, in °C

T_1 = maximum temperature during the year, in °C

T_2 = minimum temperature during the year, in °C

U = week number (counted from New Year)

U_0 = number of weeks from the beginning of the year to the week of maximum temperature

AASHTO 1986 [41] proposed a simple method using a chart to predict the asphalt temperature as shown in Figure 2.5. The method requires two inputs:

1. Pavement surface temperature during the NDT test, and
2. Mean air temperature data at the site for 5 previous days before the NDT test.

Once the two inputs were prepared, the asphalt temperature can be predicted from the chart.

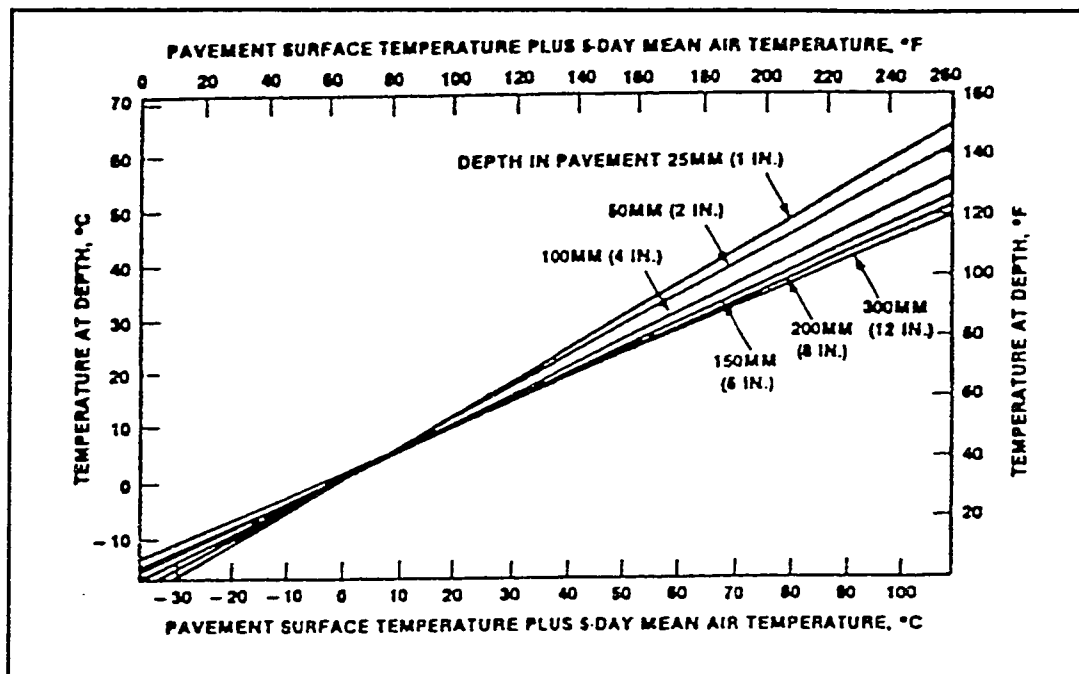


Figure 2. 5 Estimation of temperature [41]

Overview of Materials Used in the ALF Sections

Cement-stabilized bases were usually utilized in the area where aggregate sources for base layers do not meet the required strength or in the area

subjected to heavy loads. The use of cement-stabilized bases had been in practice since 1935 [50]. Tayabji [50] reported that high-quality cement-stabilized bases perform well under very heavy traffic. Huntington, et al., [51] reported that cement-stabilized bases have performed well for years in Wyoming and have provided a cost-effective service life. Other successful use of cement-stabilized bases have also been reported elsewhere [52, 53, 54, 55].

An inverted pavement section consists of an unstabilized crushed stone base sandwiched between a lower cement-stabilized layer and the upper asphalt concrete surfacing [56]. The purpose of putting a crushed stone between the surface and the soil cement base is to reduce the crack propagation induced by soil cement bases to the surface. The performance of the inverted pavement has been studied since the early 1960s as reported by Johnson [57] and McGhee [58].

Overall, inverted pavements had a history of good performance. McGhee [58] reported that the inverted pavement exhibited the lowest overall cost compared with others in his study. A study by Tutumluer and Barksdale [56] showed that inverted pavements had better performance compared with conventional and full-depth hot mix asphalt. In addition, the study also reported that the inverted sections had lower vertical stresses in the subgrade and lower resilient surface deflections. Van Vuuren [59] reported that inverted pavement section performed better than that of cement-treated base section.

Barksdale, et al. [60] reported that the effects of geosynthetic reinforcement on stress, strain, and deflection are relatively small for pavements

designed to carry more than about 200,000 equivalent 18-kip (80 kN) single axle loads (ESALs). Thus, geosynthetic reinforcement of an aggregate base will have relatively little effect on overall pavement stiffness. The greatest beneficial effect of reinforcement appears to be due to small changes in radial stress and strain together with slight reductions of vertical stress in the aggregate base and on the top of the subgrade. Barksdale, et al. [60] study also showed that when geosynthetic was used in a thin pavement ($SN \leq 2.5$ or 3) on a weak subgrade ($CBR \leq 3$), it can significantly reduce the permanent deformations in the subgrade or the aggregate base.

CHAPTER 3

DESCRIPTION OF ALF TEST SECTIONS AND PRESENTATION OF THE DATA COLLECTED

This chapter describes the research conducted at the ALF facility in Port Allen. It is divided into two major sections: a description of the test sections and a presentation of the data collected from the field. The first section describes the structure and the materials used in the nine sections while the second section includes a presentation of the data including calculation of rutting, surface cracks, and roughness.

Pavement Test Sections

The LTRC constructed nine sets of pavement sections divided into three phases: phase 1, 2 and 3. Phase 1 consisted of lanes 002, 003 and 004; phase 2 consisted of lanes 005, 006, and 007; and phase 3 consisted of lanes 008, 009 and 010. The materials in each lane are shown in Figure 3.1. All lanes received the same 89-mm. (3.5 in.) of La DOTD Type 8 wearing course mix.

The noticeable differences among the lanes were the types of materials used and the thickness of the bases. Lanes 002 through 004 used conventional crushed stone bases.

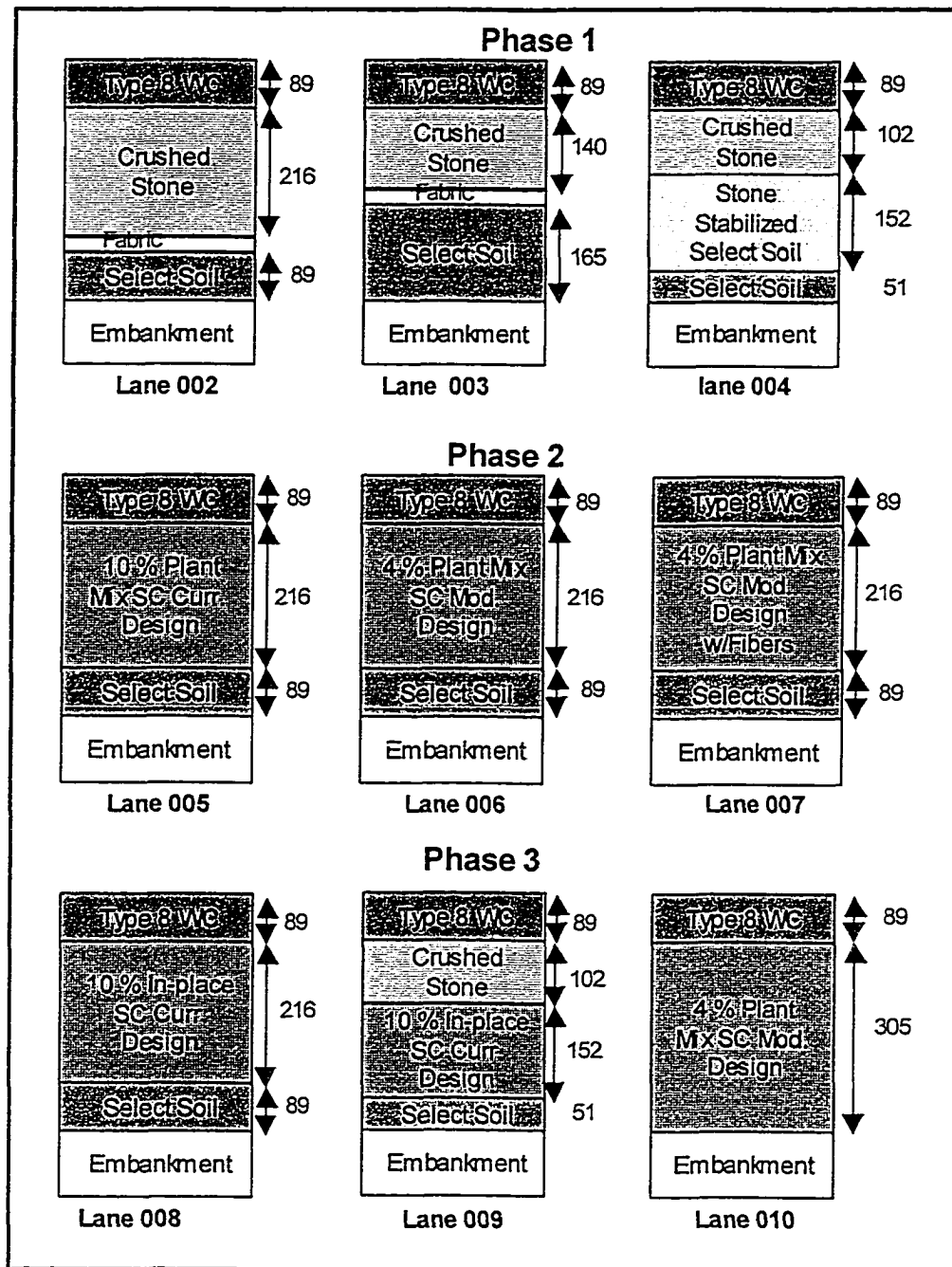


Figure 3. 1 Cross section of pavement test lanes

Fabrics were placed below the base in lanes 002 and 003 to prevent intrusion of the select embankment into the base course. Lanes 005, 006, 007,

008, and 010 included soil cement bases, which include variation in the mixing process and the cement percentages. Lane 009 was an inverted pavement, where a crushed stone base was placed between the surface and a soil cement subbase. The properties of each of the pavement materials are presented in Table 3.1.

Notice in Figure 3.1 that the select A-4 soil had a variable thickness required to make the total thickness of the base and select soil equal 305-mm (12 in). Such an arrangement allowed the elevation of the surface of the test bed to be constant when the wearing course was placed.

Under the base was a 1524-mm (5-ft) of uniform embankment A-4 select soil with a PI between 0 to 10, which was placed over the natural soils at the Port Allen site. The natural soil is a highly variable, highly organic, fat clay with high water content. This clay material was dredge spoil spread over the site from canal construction just across the road. The water table is highly variable and at times there is positive water pressure when the Mississippi River level is high.

Times of Loading

The loads were applied to lanes 002, 003, and 004 between February 2, 1996 through September 27, 1996. At the beginning of the test, the average daily air temperature was about 13°C (55°F), and it rose steadily to about 28°C (82 °F) in mid-July 1996. This average daily air temperature remained steady until the end of August and went down to about 25 °C (77 °F) at the end of the test in September 1996.

Table 3. 1 Properties of materials used at ALF test sections

| Material | Density (kg/m ³) | Moisture Content (%) | CBR | UCS (MPa) | Moduli* (MPa) |
|------------------|---------------------------------|----------------------------|-----|-------------------|------------------|
| Type 8 WC | 2,212 | - | - | - | 2,000 – 3,900 |
| Crushed stone | 2,203 | - | - | - | 135 – 150 |
| Stabilized stone | 1,933 | - | - | - | 135 – 150 |
| Select soil | 1,715 | 12 | - | - | 35 – 75 |
| Embankment | 1,700 | 16 | 10 | - | 25 – 35 |
| Soil Cement: | | | | - | 1,020 – 1, 070 |
| 10% In-place | 1,720 | 14.4 | - | 2.01 (7 days) | |
| | | | - | 2.66 (28 days) | |
| 4% Plant-mixed | 1,720 | 14.1 | - | 0.98 (7 days) | |
| | | | - | 1.35 (28 days) | |

*Predicted from backcalculation

When lanes 008, 009, and 010 were loaded between November 19, 1996, and May 24, 1997, the surface temperature ranged between 10 °C (50 °F) to 40 °C (105 °F). At the beginning of the test, the surface temperature was about 18 °C (65 °F), and went down steadily to about 10 °C (50 °F) in the middle of January 1997. After that the surface temperature rose to reach about 35 °C (95 °F) in the middle of April 1997, remained steady to the end of the month and rose again up to about 40 °C (105 °F) at the end of the loading period.

The ALF loading for lanes 005, 006, and 007 was applied between November 19, 1997 and February 6, 1998. During the loading, the surface temperature ranged between 10 °C (50 °F) to 16 °C (60 °F). At the beginning of the loading period, the surface temperature was about 16 °C (60 °F); then it went

down steadily to about 10 °C (50 °F) at the end of December 1997. The temperature remained steady at 13 °C (55 °F) until the end of the loading period.

Location of the Test Section

The pavement research facility lies just south of Port Allen, Louisiana, across the Mississippi River from Baton Rouge. The facility is located about 1 mile south of I-10 on LA 1 South just past the Intracoastal Waterway on North Line Road, west about two miles. The research facility has a 6-acre tract.

Data Collection Method

Field measurements included the periodic collection of cracking, transverse and longitudinal profile, deflection data, and temperatures. The ALF loading was stopped periodically for maintenance, and surface measurements were made at those times. To simulate highway traffic, the ALF loads were applied only in one direction and were normally distributed about an 813-mm. (32-in.) wheelpath. The ALF was also moved alternately between test lanes at approximately 25,000 passes to offset relative environmental effects occurring during the loading period. The magnitude of the ALF loading varied with number of applications. At the beginning of the test, a 10,000 lb load was applied and after several thousand passes the magnitude was increased as shown in Table 3.2.

Table 3. 2 Loading schemes applied to the ALF test lanes

| Lane | ALF Load , kN (lbf) | Pass Interval | Cumulative ESALs |
|------|------------------------|-------------------|--------------------------|
| 002 | 44.5 (10,000) | 0 – 217,000 | 0 – 322,000 |
| | 64.0 (14,400) | 217,000 – 297,000 | 322,000 – 853,000 |
| 003 | 44.5 (10,000) | 0 – 50,000 | 0 – 74,000 |
| 004 | 44.5 (10,000) | 0 – 258,000 | 0 – 382,000 |
| 005 | 44.5 (10,000) | 0 – 150,000 | 0 – 222,000 |
| 006 | 44.5 (10,000) | 0 – 150,000 | 0 – 222,000 |
| 007 | 44.5 (10,000) | 0 – 175,000 | 0 – 259,000 |
| 008 | 44.5 (10,000) | 0 – 125,000 | 0 – 111,000 |
| | 54.7 (12,300) | 75,000 – 125,000 | 111,000 – 312,000 |
| 009 | 44.5 (10,000) | 0 – 100,000 | 0 – 148,000 |
| | 54.7 (12,300) | 100,000 – 360,000 | 148,000 – 1,193,000 |
| | 64.9 (14,600) | 360,000 – 460,000 | 1,193,000 – 1,864,000 |
| 010 | 44.5 (10,000) | 0 – 75,000 | 0 – 111,000 |
| | 54.7 (12,300) | 75,000 – 250,000 | 111,000 – 815,000 |

Deflection testing was conducted on a periodic basis using the falling weight deflectometer (FWD). The FWD data were used to backcalculate the moduli of each layer of the test sections. The profile data used to calculate rutting and roughness were secured using the ALF profilograph, which consists of a linear variable differential transformer (LVDT) mounted on a metal carriage [61]. It moves transversely across the pavement on a metal frame. The metal frame can be positioned along the pavement section between two rails mounted on the pavement surface, outside the trafficked area.

The ALF profilograph measured both longitudinal and transverse profile. For the longitudinal profile, three profile measurements were secured for each lane, consisting of one measurement at the centerline of the wheelpath and two other measurements at 305-mm (1-ft.) to the left and to the right of the centerline, respectively. For the transverse profile, eight profile measurement stations were located at 1219-mm (48-in.) intervals. The profile readings were taken every 25.4-mm (1-in). Generally, the profile data were collected approximately every 25,000 passes of ALF machine when it was moved to load another test section or stopped for maintenance.

Failure of a test section occurred when either the average rut depth reached 19-mm. (0.75-in.) or the serviceability index reached 2.3.

Evaluation of Layer Moduli from Backcalculation Method

The resilient modulus for each pavement layer was predicted from the falling weight deflectometer (FWD) and Dynaflect data. The primary purpose of the FWD measurement is to predict the deflection of a pavement when subjected to a load. Using the backcalculation methodology, this deflection measurement can be used to predict the resilient moduli of each layer of the pavement. The deflection measurement was created by applying an impulse force generated from a two mass assembly in which the falling weight is dropped onto a second weight/buffer combination [61]. The loading plate sits in the pavement surface

and has a diameter of 300 mm (12 in). the plate is segmented into four quadrants that can move independently.

The measurements were performed on the centerline of the loading path of each pavement test section at 11 stations spaced at intervals of 1.52 m (5 ft) along the centerline. The geophone configuration can be seen in Table 3.3. At each station, 20 deflection bowls were recorded. However, only the last two bowls corresponding to the 9,000-lb load level were used in the backcalculation analysis. In addition to the deflection measurements, temperatures of the air and the pavement surface were also collected using an electronic thermometer and an infrared digital thermometer.

Table 3. 3 Offset of the FWD geophones [61]

| Geophone Number | | 0 | 1 | 2 | 3 | 4 | 5 | 6 |
|-----------------|------|---|-----|-----|-----|-----|-----|------|
| Offset | (in) | 0 | 8 | 12 | 18 | 24 | 36 | 48 |
| | (mm) | 0 | 200 | 300 | 450 | 600 | 900 | 1200 |

The resilient modulus for each layer was predicted using MODULUS 5.0, a backcalculation computer program developed by the Texas Transportation Institute. MODULUS 5.0 was selected as the analysis tool based on the recommendation from previous study by Roberts, et al [40]. According to Roberts, et al, MODULUS provided the most reasonable resilient for Louisiana condition. These resilient moduli were then used to predict the performance of the test sections using VESYS 3A-M.

Tables A1.1 through A1.9 in Appendix 1 show the modulus for each layer for lanes 002 through 010. The ESALs were obtained by multiplying the number of passes, which represent the number of ALF passes obtained from the field, with an axle load coefficient from Appendix D of 1993 AASHTO guide for the design of pavement structures. To determine the axle load coefficient, the structural number (SN) of each section was calculated using the Louisiana "a" values. The load equivalency factors for lanes 002 through 010 were also calculated and the results are presented in Table 3.4.

Table 3. 4 Axle load equivalency factor for lanes 002 through 010

| Load, kN (lb.) | Lane 002 | Lane 003 | Lane 004 | Lane 005 | Lane 006 | Lane 007 | Lane 008 | Lane 009 | Lane 010 |
|-------------------|-------------|-------------|-------------|-------------|-------------|-------------|-------------|-------------|-------------|
| 44.48 (10,000) | 1.48 | 1.49 | 1.48 | 1.48 | 1.48 | 1.48 | 1.48 | 1.48 | 1.48 |
| 54.71 (12,300) | - | - | - | - | - | - | 4.01 | 4.02 | 4.02 |
| 64.94 (14,600) | 6.70 | - | - | - | - | - | - | 6.70 | - |

Surface Moduli Evaluation

All the lanes of the ALF test sections used the same material for the surface layer, a Louisiana Type 8A wearing course. Since the same material was used, the predicted moduli for all layers should be in close agreement. Figure 3.2 shows the corrected and uncorrected moduli for lanes 2 through 10.

As can be seen from Figure 3.2, there is a variability of the HMA modulus when corrected to 20°C (68°F), ranging from the maximum of 3,841 MPa (557

ksi) for lane 009 to the minimum of 1,884 MPa (273 ksi) for lane 006 with average of 2586 MPa (375 ksi). Table 3.5 also shows that the coefficient of variation for the surface layer modulus becomes smaller when the value is corrected to the standard temperature.

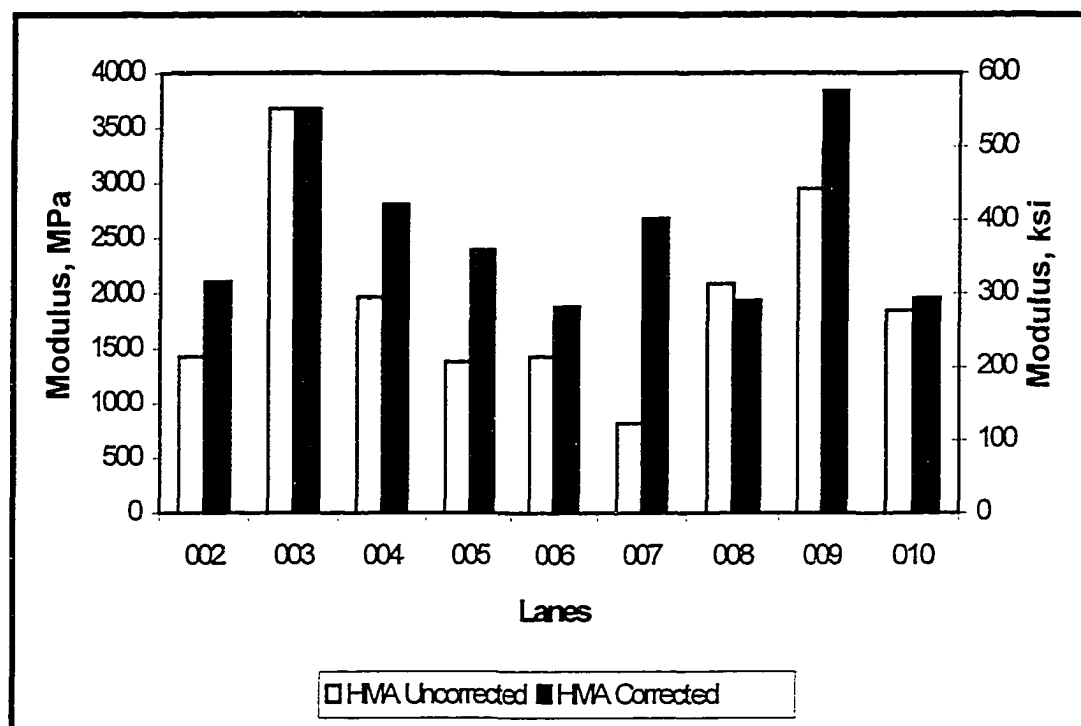


Figure 3. 2 Predicted HMA modulus for each lane

Table 3. 5 Summary of HMA modulus of ALF test section

| | Uncorrected | Corrected to 20°C (68°F) |
|-------------------------------|-------------|--------------------------|
| Average, ksi (MPa) | 283 (1953) | 375 (2586) |
| Standard Deviation, ksi (MPa) | 127 (877) | 108 (742) |
| Coeff. of Variation (%) | 45 | 29 |

Note from Figure 3.2 that lane 003 has the second highest predicted moduli after lane 009 even though the performance evaluation showed it to have the worst performance. Unlike the other lanes where the predicted moduli were based on the average of several FWD measurements, the predicted moduli for lane 003 was based only on single FWD measurements collected at the beginning of loading. Additionally, since the FWD test for lane 003 was performed before loading began, the structure might have not experienced any distresses, which according to the literature affect the modulus value.

Evaluation of Base Moduli

As described previously, two types of base materials were used in the ALF sections: stone and soil cement materials. The predicted base moduli obtained from the backcalculation method are shown in Figures 3.3 and 3.4 for stone and soil cement materials, respectively.

Lanes 002, 003, 004 and 009, constructed using the stone material, have relatively similar moduli values ranging from the minimum of 138.8 MPa (20.1 ksi) to the maximum of 157.7 MPa (22.9 ksi). Lane 007, which included 4 percent plant-mixed soil cement with fiber, has a higher modulus than that of lane 006, which included 4 percent plant-mixed soil cement without fibers. It indicates that the use of fiber in the soil cement may increase the modulus. Lane 010, constructed using the same 4 percent plant-mixed soil cement as that of lane 006, has a higher modulus than that of lane 007. This higher modulus may

be associated with the structure of lane 010, which used similar materials in both the base and subbase.

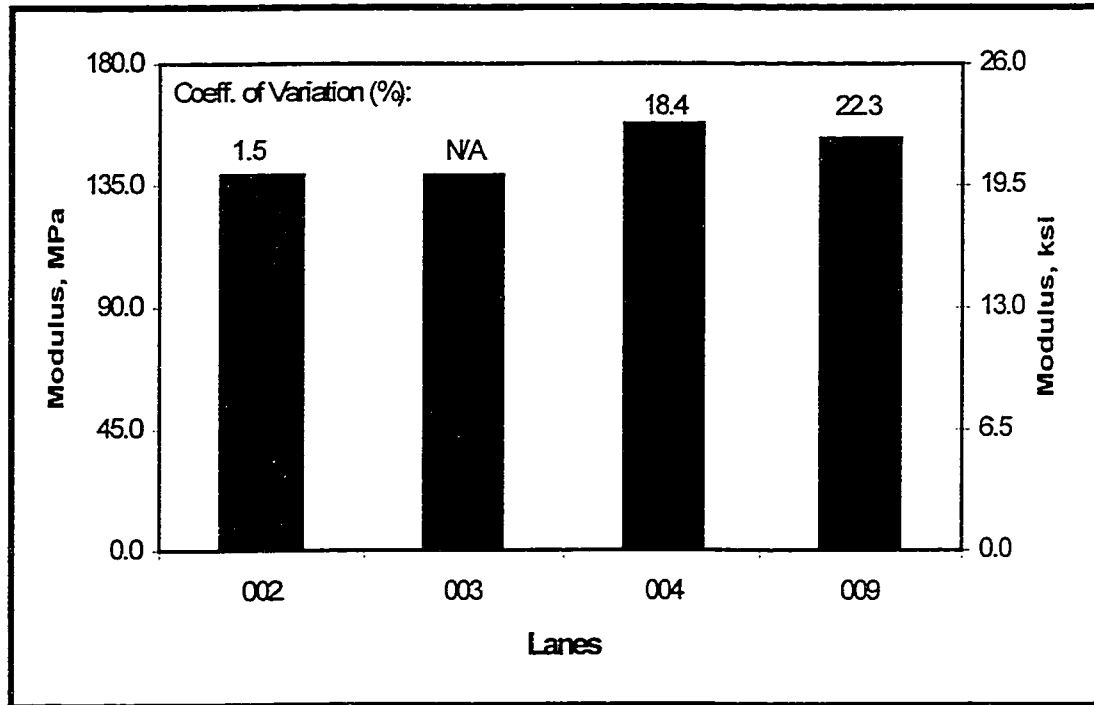


Figure 3. 3 Predicted moduli for stone material base layer

It seems that there is no clear evidence of differences between the plant mixed soil cement materials and the mixed in-place material, as can be seen by comparing lane 005 with lane 008. Lane 005 has a modulus of 1038.8 MPa (150.7 ksi), whereas lane 008 has a modulus of 1054.9 MPa (153.0 ksi). However, higher percentages of cement increased the modulus as shown by comparing lane 005 with lane 006. Lane 005, which included 10 percent cement, has a higher modulus than lane 006, which included 4 percent cement.

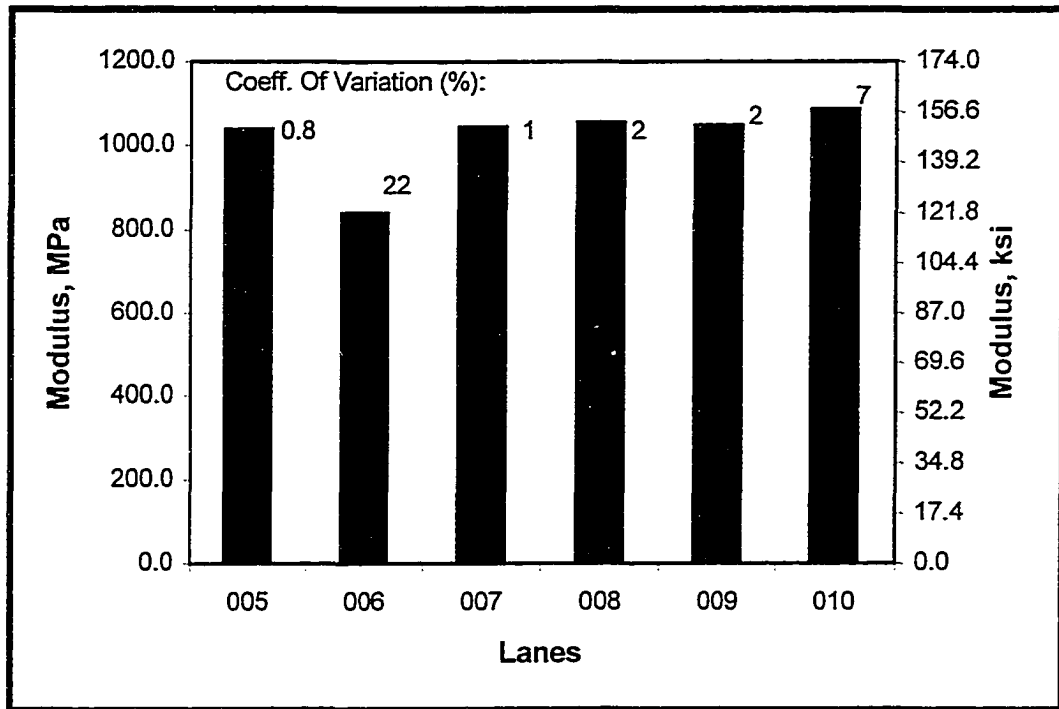


Figure 3. 4 Predicted moduli for soil cement base layer

Evaluation of Subbase Moduli

The predicted subbase modulus for each lane is shown in Figure 3.5. Lanes 002 through 008 included the same material as a subbase, the select soil material. Since all lanes received the same material type, they should in theory have about the same modulus value. However, Figure 3.5 shows that there is considerable variation in the moduli ranging from the minimum of 35.6 MPa (5.2 ksi) for lane 002 to the maximum of 77.6 MPa (11.3 ksi) for lane 008, with an average of 51.7 MPa (7.5 ksi) and coefficient of variation of 33 percent.

This variability may be ascribed to either the variability of the material itself or to the nature of the backcalculation method, or both. These values, however, are still in the range commonly reported for this type of material.

Therefore, a range of 35 MPa (5 ksi) to 75 MPa (11 ksi) can be considered as appropriate for use in mechanistic studies.

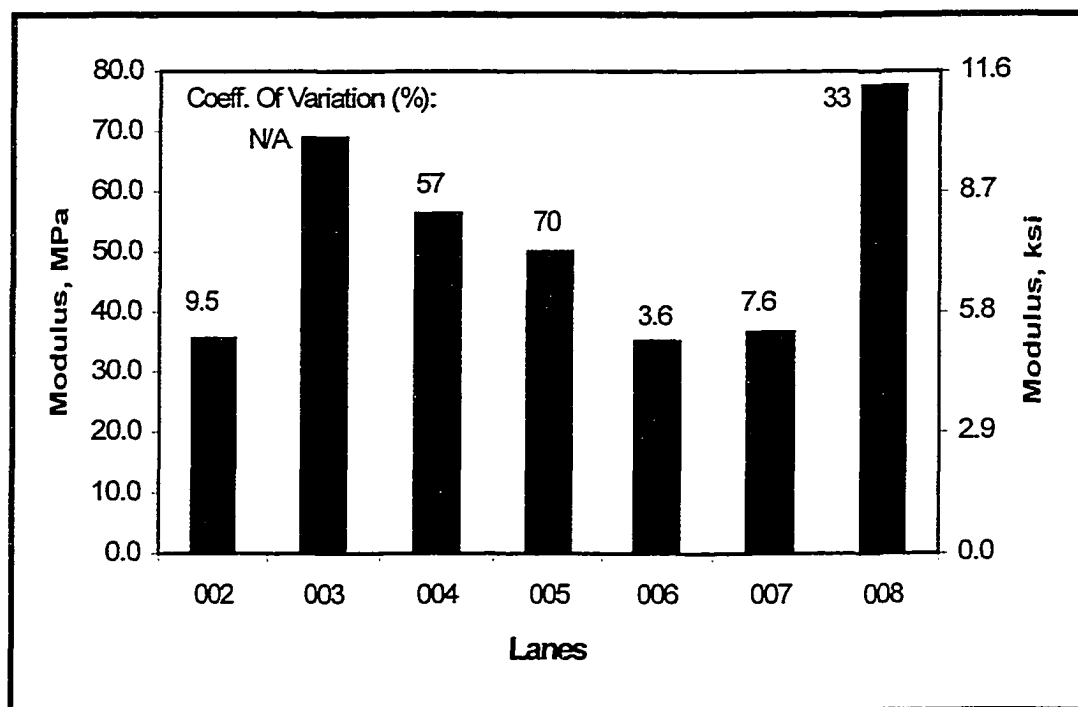


Figure 3. 5 Comparison of select soil subbase moduli

Evaluation of Subgrade Moduli

The average subgrade modulus for each test lane is presented in Figure 3.6. As can be seen from the figure, the average modulus of the subgrade for all lanes is relatively uniform except for lane 009, ranging from a minimum of 19.5 MPa (2.8 ksi) to a maximum of 48 MPa (7.0 ksi) for lane 009 with average of 31 MPa (4 ksi). This result is not surprising because the FWD testing was conducted at different times of the year. The large variability may be associated with the temperature and moisture content ranges during the testing and data collection.

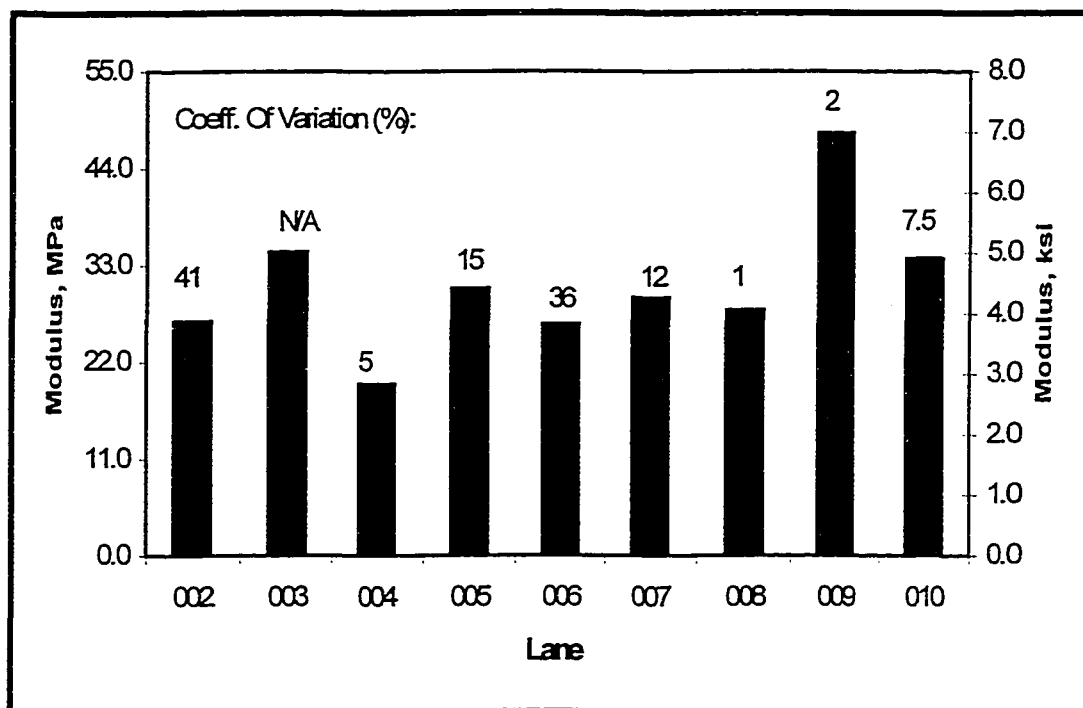


Figure 3. 6 Comparison of subgrade moduli

Rutting Calculation

The maximum rut depth for each station was calculated by plotting the transverse profile data and measuring the maximum difference between the top and bottom elevation of the profile, as shown in Figure 3.7. Note that the vertical scale of Figure 3.7 was exaggerated to show the clear form of the transverse profile. The top elevation was obtained using a 1219-mm (48-in) straightedge beam as suggested by Johnson-Clarke, *et al.* [9].

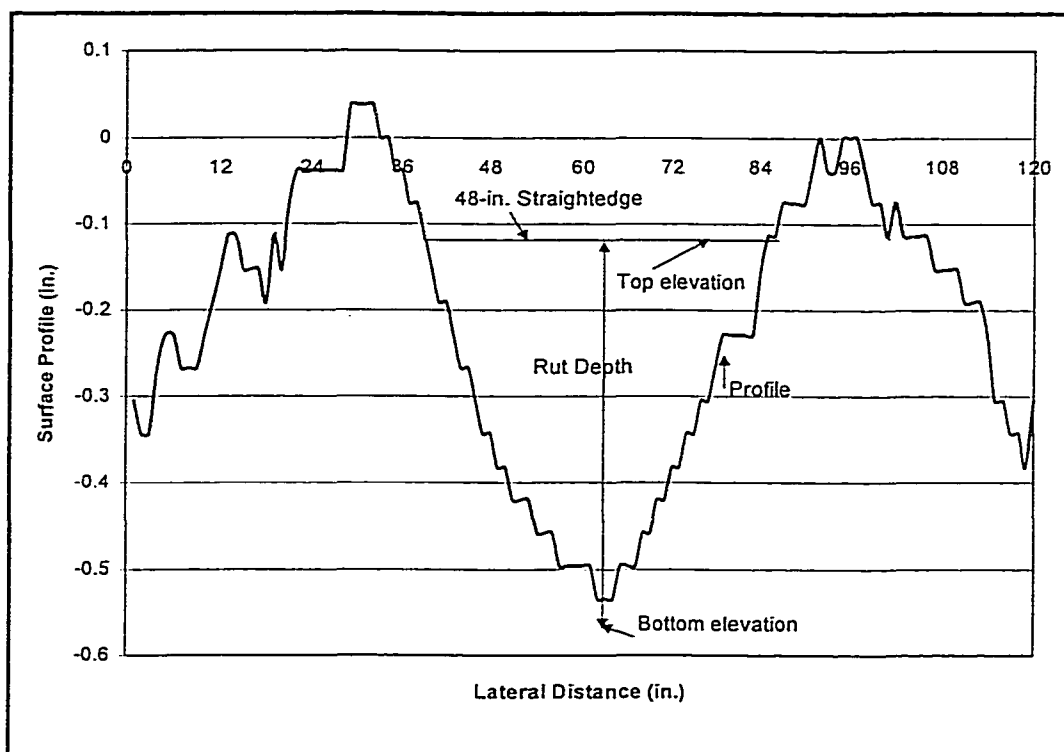


Figure 3. 7 A sample calculation of rut depth from a transverse profile

In each wheel path the largest difference between the top and bottom elevation shown in Figure 3.7 is the rut depth. If the bottom elevation is not smooth, an average value of the bottom elevation was calculated from the profile.

To automate the plotting and calculation process, an MS Excel 97 macro (written in Visual Basic language) was prepared. The macro first converted the transverse profile data in a plain text file format, put the data in MS Excel 97 worksheet, and then created the plot from the data. A 1219-mm. (48-in.) straightedge line was also created so that it can be moved along the chart to determine the top elevation, which should connect the nearest 1219-mm. (48-in.) distance between left and right profile, as shown in Figure 3.7. Each

transverse profile file contains data for stations 2 through 8. Tables A2.1 through A2.9 in Appendix 2 show the rut depth for lanes 002 through 010.

Roughness Calculation

The roughness of the test section, expressed in the international roughness index (IRI), was determined from the longitudinal profile as generated by the ALF profilograph. IRI measurement, expressed in m/km, has a normal range from 0 for perfectly smooth to 20 for unpassable roads [18]. IRI is an index that can be used to express the roughness condition of a pavement that impacts vehicle response. It is calculated for a single longitudinal profile with the sample interval no larger than 1 ft. (300 mm) for accurate calculation. This profile is assumed to have a constant slope between sampled elevation points. The profile is then smoothed with a moving average of 250-mm (1 ft) base length, see Figure 3.8, and further filtered by quarter-car simulation [22]. The simulated suspension motion of the quarter car is linearly accumulated and divided by the length of the profile to yield IRI. Thus, IRI has units of slope such as inch/mile or m/km. The idea of expressing roughness measurements in such units is unlike roughness measurement in metal, which is usually conducted over a short distance, in that roughness measurement for a highway can be in increments as long as 10 miles. Thus, the use of units in in/mile is appropriate for the application.

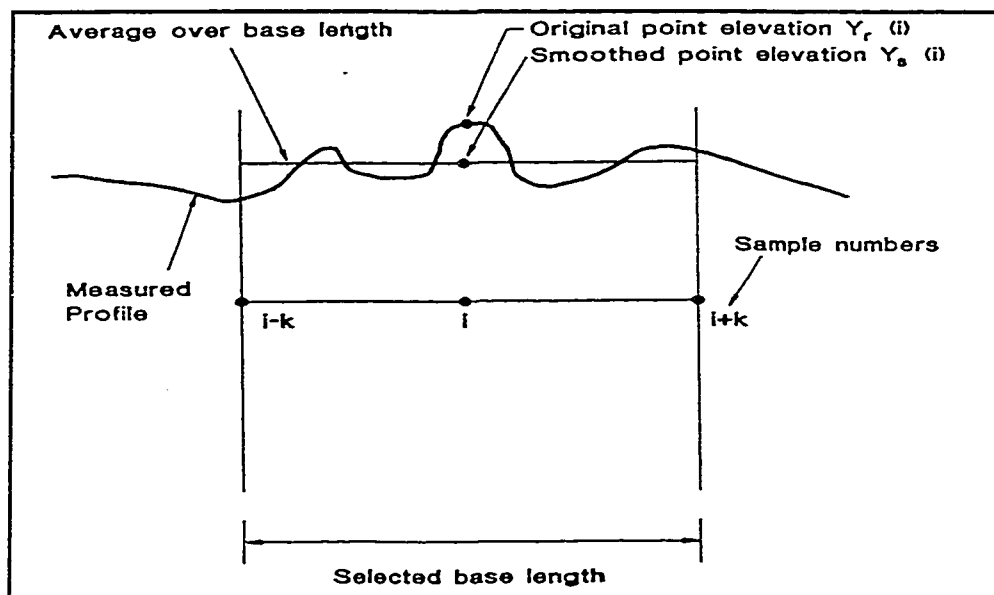


Figure 3. 8 Moving average filter

An MS Excel 97 macro, IRI PROFILER, written to automate the analysis, was based on an algorithm proposed by Sayer [22] using the World Bank definition and computation method for IRI. The output from the analysis is predicted roughness of the profile in IRI units and presented in Tables A3.1 through A3.9 in Appendix 3.

CHAPTER 4

PERFORMANCE PREDICTION OF ALF

TEST SECTIONS

Introduction

To determine the performance of the ALF section materials when constructed in other conditions and environment, a performance prediction study was conducted. There have been a number of similar research studies as reported in Chapter 2. VESYS 3A-M was selected to make the performance predictions in this study because of its capabilities and the familiarity of the researcher with the program.

As discussed in Chapter 2, VESYS 3A-M predicts the pavement performance in terms of rutting, fatigue cracking and serviceability development. To verify the validity of the VESYS model, it is necessary to calculate the rutting, cracking and PSI from field loadings and compare the calculated values with the measured data. Rutting and cracking were discussed in Chapter 3. The calculation of PSI from measured profile data is discussed in the next section.

Slope Variance

One of the components required to calculate PSI is the slope variance of the road profile. Slope variance (SV) is a statistical term that indicates the

variation of slope of a pavement from the mean slope value [63]. It is computed from the longitudinal profile using the following equation:

$$SV = \frac{\sum Y^2 - \frac{1}{n}(\sum Y)^2}{n-1} \quad (4.1)$$

Where:

SV = slope variance, in 10^{-6} rad.

Y = slope between two points 305-mm. (12-in.) apart

n = number of sets of readings

The slope between two elevations (Y) at any point is calculated as follows:

$$Y_i = \frac{h_{i+1} - h_i}{d} \quad (4.2)$$

Where:

Y_i = slope between two points

h_{i+1} = elevation of the profile one reading ahead of i

h_i = elevation at point i

d = distance between the two points = 305-mm. (12-in.)

Since the longitudinal profile measured at the ALF site was in 25.4-mm (1 in.) intervals, an adjustment needs to be made in order to be consistent with the AASHO definition on slope variance as expressed in the equation 4-1. Therefore, pairs of data every 305-mm. (12-in.) were used in the calculation procedure. However, to take into account all the data, as many as 12 slope variance calculations were made using different sets of data at appropriate intervals (1,

13, 25,...), (2, 14, 26,...), (3, 15, 27,...) and so on. The average of this calculation was the slope variance of the longitudinal profile.

To automate the calculation, an MS Excel 97 macro called SLOPEVAR was written. The macro works by first converting the longitudinal profile into MS Excel format, the user is asked to specify the range of the data for each profile and then the slope variance is calculated.

Present Serviceability Index

The present serviceability index (PSI) was developed at the AASHO Road Test as a way of characterizing the riding quality of the road [63]. At the road test, a panel of 15 engineers drove over selected pavements and rated the pavements using a scale of 0 to 5. Zero represents a road that was impassable, while 5 represents a road in perfect condition. Since the ratings may vary among raters because of human nature, the rating numbers assigned to a pavement by panel members were averaged and designated as the Present Serviceability Rating (PSR). The PSR was then correlated to objective measurements made by profile measuring devices through a regression analysis procedure. The resulting present serviceability index (PSI), which is the predicted value of PSR, for flexible pavements is expressed as follows [63]:

$$PSI = 5.03 - 1.91 \log(1 + SV) - 0.01\sqrt{C + P} - 1.38(RD)^2 \quad (4.3)$$

Where:

PSI = present serviceability index ranging between 0 to 5.0

SV = slope variance calculated from the road profile using eq. 4-1

- C = major cracking, in $\text{ft}^2/1,000 \text{ ft}^2$
- P = bituminous patching, in $\text{ft}^2/1,000 \text{ ft}^2$
- RD = Average rut depth of both wheelpaths, in inches measured at the center of a 4-ft. span in the most deeply rutted part of the wheelpath.

Since no patching was performed in the ALF test sections, only rutting, cracking and slope variance were included in the PSI calculation using ALF data. Using the above equation, the PSI for lanes 002 through 010 are shown in Tables A4.1 through A4.9 in Appendix 4.

Input Data Preparation

Following is the list of the primary input data required to run VESYS 3A-M:

1. Seasonal data in terms of temperatures for the whole analysis period. The break periods in the ALF loading were assumed to be the seasonal periods. For example, there are 10 seasonal periods used in analyzing lane 002. For other lanes, see Appendices A1 or A2.
2. Thickness of each layer. The thickness of each layer of each lane is given in Figure 3.1.
3. Materials properties, including resilient moduli, permanent deformation coefficients Alpha and Gnu for each layer, Poisson's ratios, and fatigue coefficients k_1 and k_2 for the surface layer. Resilient moduli are presented in Appendix 1. Permanent deformation coefficients Alpha and Gnu are presented in Table 4.1. Alpha and Gnu were compiled from the previous

works by Hadley [64] for typical Louisiana materials and from Anderson, et al., [65] for granular materials. Notice that data from Anderson, et al., [65] were correlated to the materials used at lanes 002 through 004 of the ALF test sections using the density and moisture content. For example, since the crushed stone material of lane 002 has an average density of 2214 kg/m³ (138.2 lb/ft³), which corresponds to Anderson's pavement no.5, the selected values for Alpha and Gnu were 0.801 and 0.0693, respectively. Poisson's ratios for selected materials are presented in Table 4.2. Fatigue coefficients k_1 and k_2 at 25°C (77°F) are presented in Table 4.3, as calculated from laboratory fatigue tests performed by the LTRC. Values of k_1 and k_2 for all seasonal periods are calculated using equation 4.4 as follows [66]:

$$\begin{aligned} k_1(T) &= k_1(T_R) e^{(0.001336 \cdot X)} \\ k_2(k_1) &= 1.75 - 0.252 \log(k_1) \end{aligned} \quad (4.4)$$

Where:

$k_1(T)$ = fatigue coefficient k_1 at temperature T , °F

$k_1(T_R)$ = fatigue coefficient k_1 at reference temperature T_R , (77°F), see Table 4.3

$k_2(k_1)$ = fatigue coefficient k_2 for the corresponding k_1

X = $T^2 - T_R^2$

4. Traffic in terms of the magnitude and the number of equivalent single axle loads applications per day. Other inputs required to run the VESYS program are traffic data, which include the load magnitude and the number of load applications. The load magnitude is input as the tire pressure and the radius

of the loaded area. In this study the tire pressure is set to 0.689 MPa (100 psi) and the radius of the loaded area is 136 mm (5.35 in). The number of load application is represented by the number of axle load application per day, defined in VESYS as LAMBDA. It is calculated by dividing the number of ESALs at every break of the ALF loading by the number of days the ALF machine operated for that period.

5. Analysis period to be included in the damage analysis. The analysis period is defined in VESYS 3A-M by TRANDOM and NTRANDOM. TRANDOM represents an array of times at which a printout of the values computed in the damage model is desired [14]. In this study, TRANDOM is defined as the number of days of the ALF testing for each lane. NTRANDOM represents the number of points in the TRANDOM and LAMBDA arrays. In this study, it is defined at every regular break of the ALF loading where the field data collection was performed so that the comparison with observed data could be made at the same number of ESALs.
6. Service life in terms of the initial serviceability (PSI_i) and terminal serviceability (PSI_t). The predicted service life is the time required to reduce the initial PSI_i to the final PSI_t . A PSI_i of 3.6 and PSI_t of 2.3 were used as input data. The reason for setting PSI_i at 3.6 and not 4.2, as commonly used for newly constructed, road is that the average PSI from observed data on the ALF construction was about 3.6; the PSI_t was set at 2.5 as recommended by the LTRC.

Table 4. 1 Permanent deformation Alpha and Gnu for lanes 002 through 010

| Lanes | | WC/ Type 8 | Crushed Stone | Soil Cement | Select Soil | Embank ment |
|-------|-------|---------------|------------------|----------------|----------------|----------------|
| 002 | Alpha | 0.4706 | 0.801 | - | 0.689 | 0.735 |
| | Gnu | 0.0247 | 0.0693 | | 0.0505 | 0.048 |
| 003 | Alpha | 0.4706 | 0.808 | - | 0.689 | 0.735 |
| | Gnu | 0.0247 | 0.0688 | | 0.0505 | 0.048 |
| 004 | Alpha | 0.4706 | 0.808 | - | 0.689 | 0.735 |
| | Gnu | 0.0247 | 0.0688 | | 0.0505 | 0.048 |
| 005 | Alpha | 0.4706 | - | 1.00 | 0.881 | 0.735 |
| | Gnu | 0.0247 | | 0.00 | 0.0751 | 0.048 |
| 006 | Alpha | 0.4706 | - | 1.00 | 0.700 | 0.735 |
| | Gnu | 0.0247 | | 0.00 | 0.0518 | 0.048 |
| 007 | Alpha | 0.4706 | - | 1.00 | 0.689 | 0.735 |
| | Gnu | 0.0247 | | 0.00 | 0.0505 | 0.048 |
| 008 | Alpha | 0.4706 | - | 1.00 | 0.635 | 0.735 |
| | Gnu | 0.0247 | | 0.00 | 0.0399 | 0.048 |
| 009 | Alpha | 0.4706 | - | 1.00 | 0.689 | 0.735 |
| | Gnu | 0.0247 | | 0.00 | 0.0505 | 0.048 |
| 010 | Alpha | 0.4706 | - | 1.00 | 0.689 | 0.735 |
| | Gnu | 0.0247 | | 0.00 | 0.0505 | 0.048 |

Table 4. 2 Poisson's ratio for selected materials [64]

| Materials | Poisson's Ratio |
|-----------------------|-----------------|
| Type 8 Wearing Course | 0.35 |
| Crushed Stone | 0.40 |
| Soil Cement | 0.35 |
| Select Soil | 0.40 |
| Subgrade/Embankment | 0.40 |

Table 4. 3 Fatigue Coefficients k_1 and k_2 at 25°C (77°F)

| Sample | # of Cycles to Failure, N_f | Initial Strains, ϵ_i | k_1 | k_2 |
|--------|-------------------------------|-------------------------------|-----------------------|--------|
| 1 | 3251 | 2.227×10^{-3} | 3.93×10^{-4} | 2.6082 |
| 2 | 57451 | 5×10^{-4} | 9.78×10^{-7} | 3.2644 |
| 3 | 8051 | 6.83×10^{-4} | 3.05×10^{-5} | 2.8881 |

Analysis of Results and Discussions

Rutting

Figures 4.1 through 4.9 show the comparison of rutting development for the VESYS 3A-M prediction and the observed data. Only observed data from stations 3 through 6 were used in the comparison to minimize the bias caused by the touchdown effects at Stations 1 and 2 and the lift-off effects at stations 7 and 8 when the ALF load was lifted from the pavement. In addition, instead of averaging the data of stations 3 through 6, an envelope of values was used for the comparison due to the large variability in the field data.

As can be seen from Figures 4.1 through 4.9, in general, good agreement existed between VESYS 3A-M predictions with those observed data even though VESYS tends to underestimate the rutting development for any material configurations used in the lanes. Except for lane 006, the VESYS predictions were near the bottom of the envelope of observed rutting. This phenomenon was expected due to the nature of the problem. VESYS 3A-M model was developed to predict the behavior of normal in-service pavements and not those experiencing accelerated loading. In accelerated loading, a 20-

year lifetime of loads are applied in a period of a few months. As a result, there is no chance for the hot mix asphalt pavement to heal; all the loads may be applied at elevated temperatures, and oxidative hardening of asphalt has no time to develop. The effect of all of these factors reduces the rate of rutting development. Consequently, rutting occurs faster in an accelerated test situation than in a pavement serving traffic in the field.

Based on the figures, it can be concluded that when VESYS 3A-M is to be used to predict the behavior of in-service real pavements, no further adjustment or modification is needed for the model. When more accurate results are needed for accelerated load testing, the agency should perform additional laboratory testing to more accurately determine the material input parameters including resilient moduli, and Alpha and Gnu for each material to be used in the design.

Cracking

Figures 4.10 through 4.18 show the comparison between VESYS 3A-M predictions of cracking with observed cracking data. Two distinctive characteristics were observed from the figures: VESYS 3A-M overestimated the cracking development for test sections with crushed stone bases and underestimated the cracking development for the soil cement bases. In addition, VESYS 3A-M did not predict that any fatigue cracks would occur in the lanes with soil cement bases. The observed data, however, showed the opposite result: lanes with soil cement bases developed more cracks than those with crushed stone bases.

There are two plausible reasons to explain this contradiction:

1. The cracks observed on the lanes with soil cement bases are not fatigue cracks. Rather, they are reflection cracks that develop as the soil cement bases shrink during curing. The VESYS model, however, is designed to model cracks of the fatigue type which are initiated by strain at the bottom of the asphalt layer.
2. Fatigue cracks modeled by VESYS model did not develop in the lanes with soil cement bases because of the much higher resilient moduli of the soil cement base. Consequently, the strain at the bottom of asphalt layer is very small, making crack development very slow. To verify this assertion, a set of sample data using a lower value of moduli for soil cement base was run and fatigue cracks did develop after a reasonable number of load applications. Table 4.4 shows the strain at the bottom of the asphalt layer for lanes 002 through 010. It can be seen that in average the tensile strain at the bottom of asphalt layer for lanes with soil cement bases were only about one tenth of the strains occurring with granular bases.

Present Serviceability Index

Figures 4.19 through 4.27 present the comparison of the present serviceability index (PSI) development between VESYS 3A-M development with those estimated from observed data. Despite the poor estimate of cracking by VESYS 3A-M, the PSI development showed good agreement between predicted PSI and that calculated from field data.

Table 4. 4 Tensile strain at the bottom of asphalt layer from VESYS 3A-M analysis

| Lanes | Tensile Strain, ϵ |
|-------|----------------------------|
| 002 | 0.556×10^{-5} |
| 003 | 0.466×10^{-5} |
| 004 | 0.611×10^{-5} |
| 005 | 0.647×10^{-6} |
| 006 | 0.640×10^{-6} |
| 007 | 0.570×10^{-6} |
| 008 | 0.667×10^{-6} |
| 009 | 0.448×10^{-5} |
| 010 | 0.838×10^{-6} |

This is expected since the VESYS model for PSI is influenced mainly by slope variance and minimally by rutting and cracking. In addition, the slope variance model is calculated from the profile used to predict rutting. VESYS 3A-M relates the mean slope variance to the mean and variance of rut depth using the following equation [14]:

$$E[SV] = \frac{2B}{C^2} \sigma_n^2 (Var[RT] + (E[RT])^2) \quad (1)$$

$$Var[SV] = \left(\frac{4B}{C^2} \sigma_n^2 E[RT]\right)^2 Var[RT]$$

Where:

$E[SV]$ = the mean slope variance

$Var[SV]$ = variance of the slope variance

B, C = pavement roughness properties due to material variability

σ_n = variance of the random variable obtained from the primary response in VESYS 3A-M 3A-M model

$\text{Var}[RT]$ = variance of rut depth prediction

$E[RT]$ = mean value of rut depth prediction

Since there was good agreement between VESYS and field rutting, one can expect good agreement for PSI as well. Note also from the figures that the initial field PSI for all lanes are approximately 3.60, indicating that the test sections stated out in good to fair condition. The common value for the initial PSI is 4.2. This slightly low initial PSI compared with the normal field initial PSI values might contribute to the rate of damage development of the test sections.

Conclusion

Based on the above discussions, it can be concluded that VESYS reasonably predicted the rutting and PSI development over the performance period. The poor agreement in fatigue cracks development between VESYS predictions and observed data is mainly due to the shortcomings of the program to adequately model fatigue behavior of HMA over soil cement bases. In addition, the cracks observed in the field were not fatigue cracks. Rather, they are surface cracks that occurred due to the shrinkage in soil cement bases that reflected to the surface. Therefore, when more accurate prediction is desired, a new performance model needs to be developed for HMA over cement stabilized bases.

It is worth mentioning here that the comparison analysis using VESYS 3A-M made in this chapter is not to be used to predict the performance of in-service

pavements because the data used were from the accelerated ALF experiments and have some limitations for simulating in-service pavement performance.

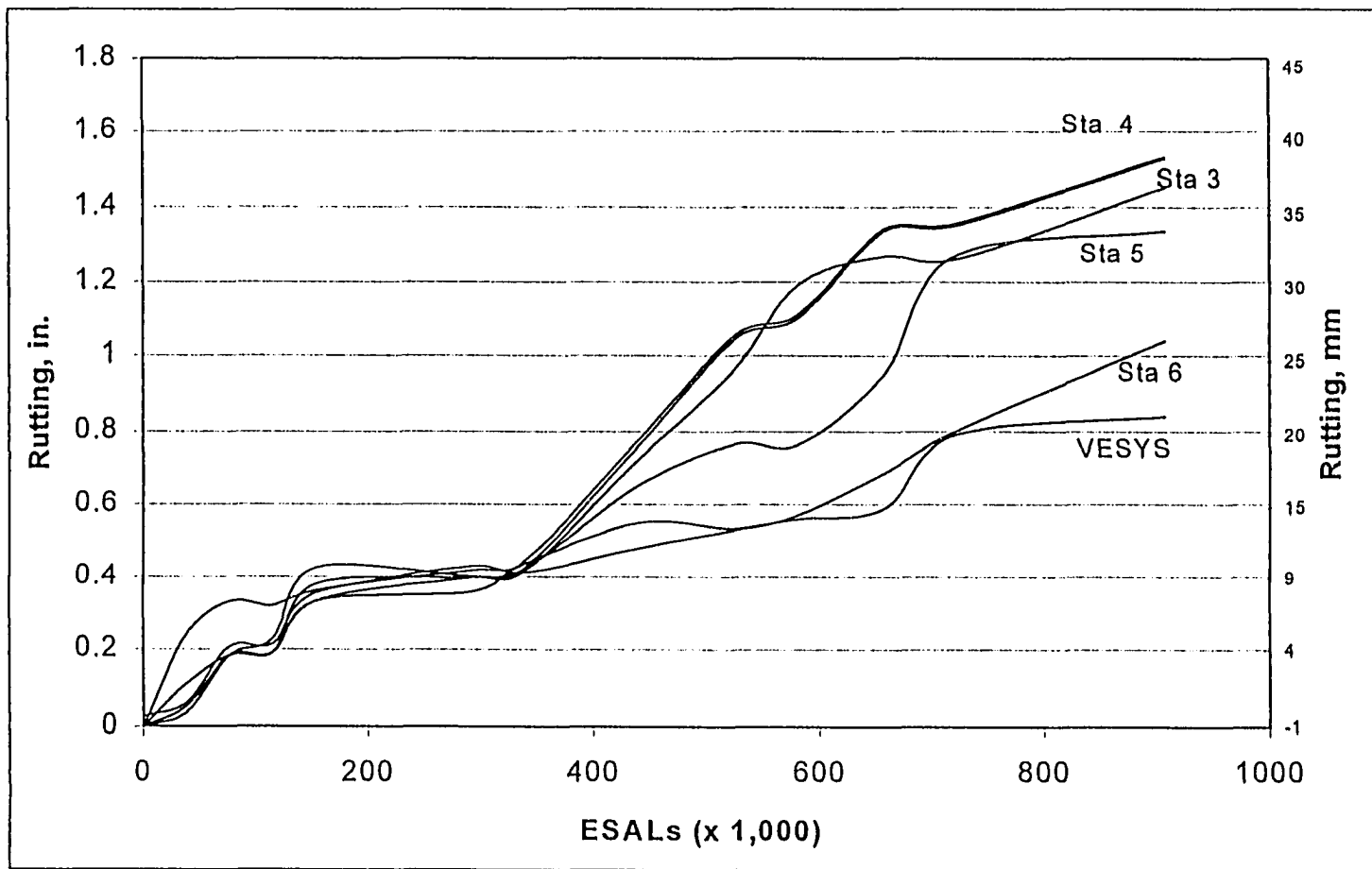


Figure 4. 1 Comparison of rutting development between VESYS 3A-M and observed data for lane 002

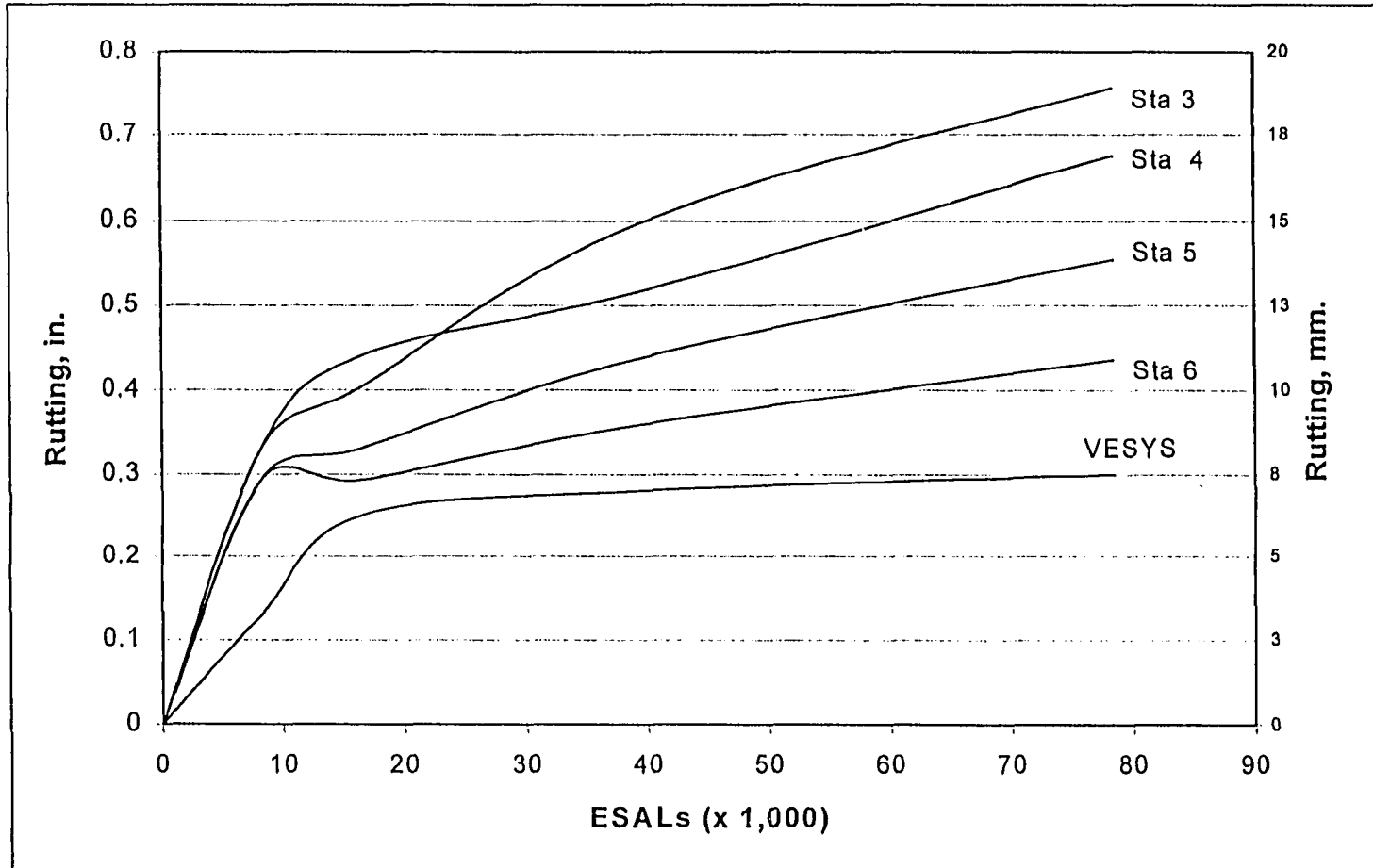


Figure 4. 2 Comparison of rutting development between VESYS 3A-M and observed data for lane 003

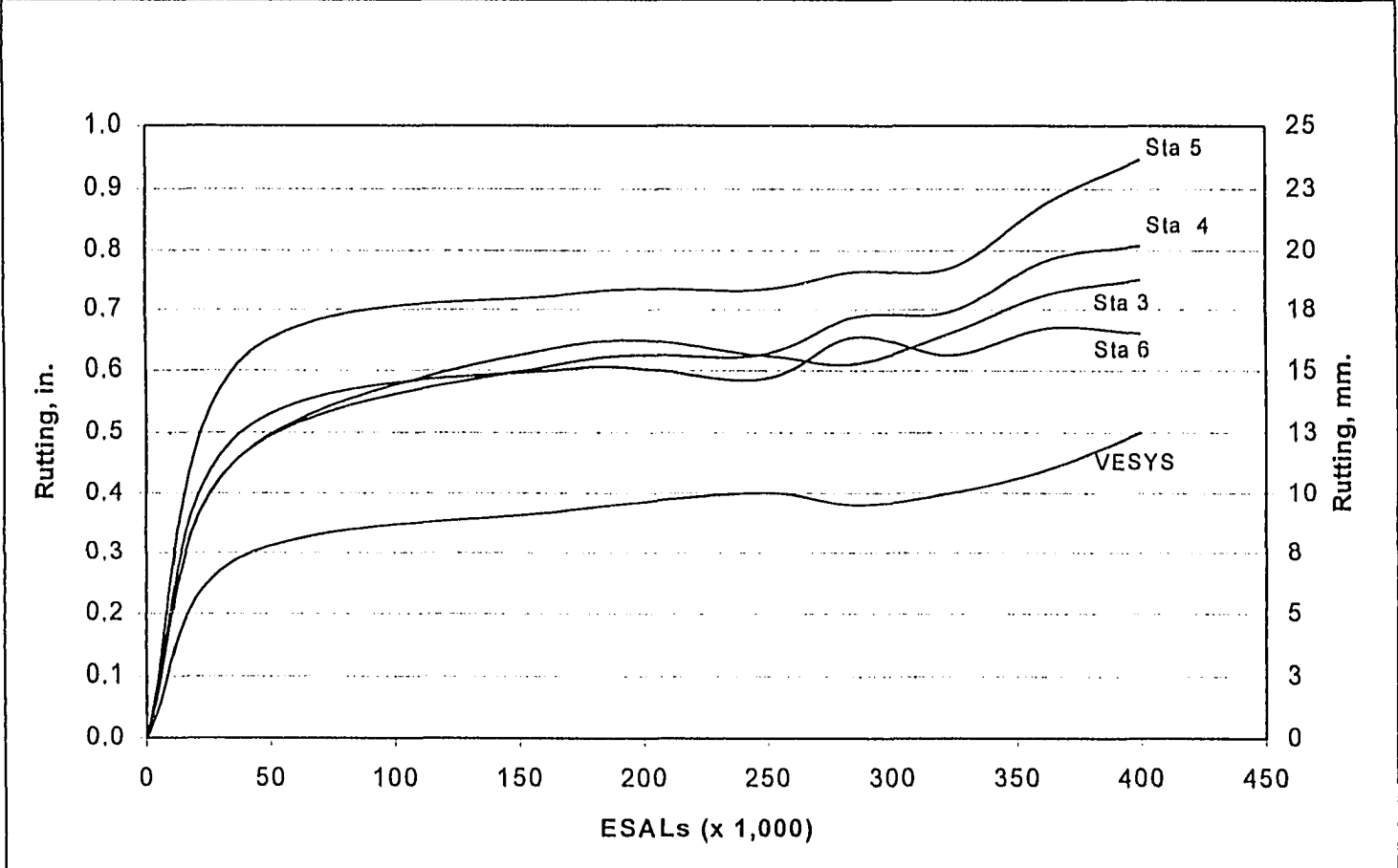


Figure 4. 3 Comparison of rutting development between VESYS 3A-M and observed data for lane 004

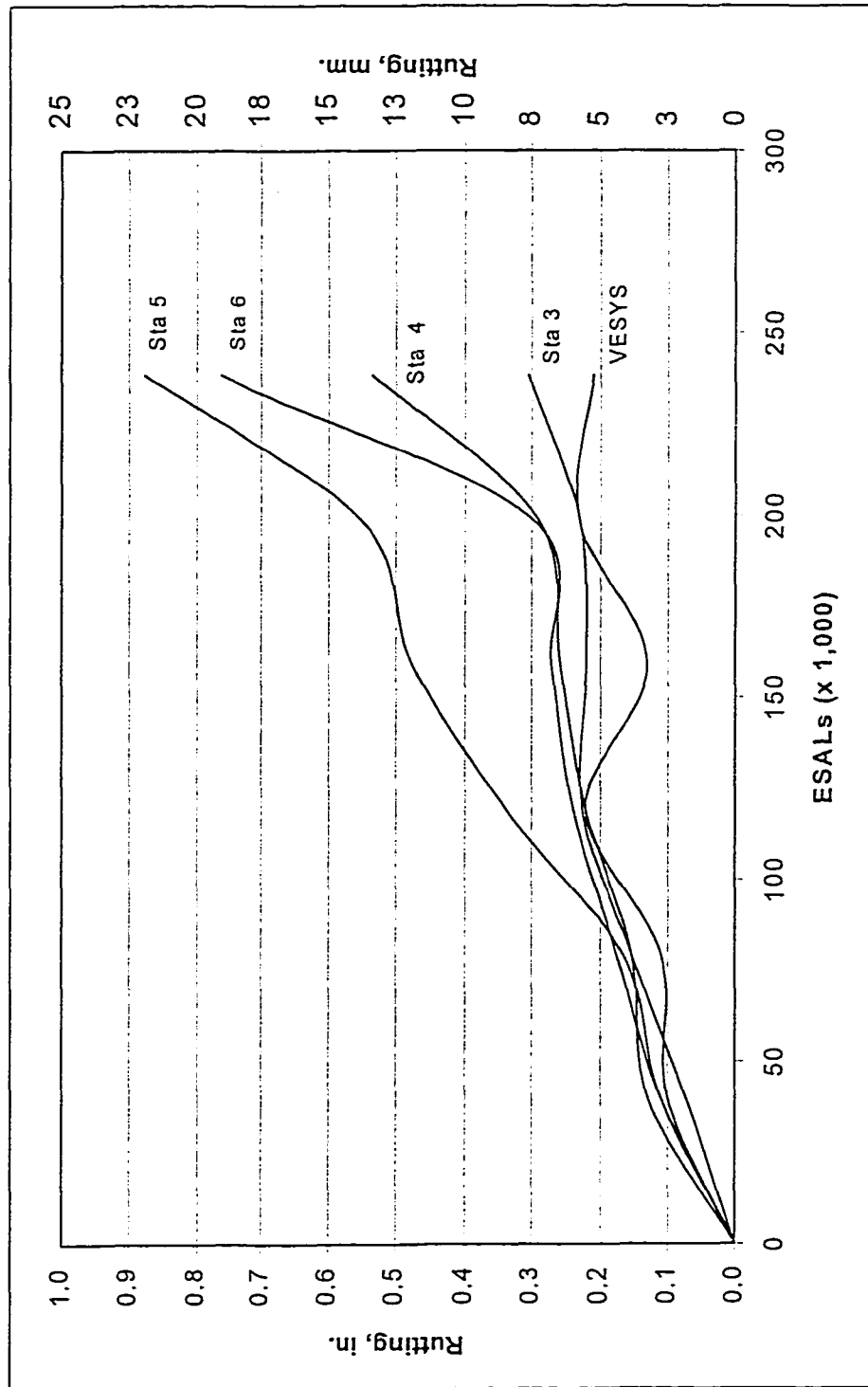


Figure 4. 4 Comparison of rutting development between VESYS 3A-M and observed data for lane 005

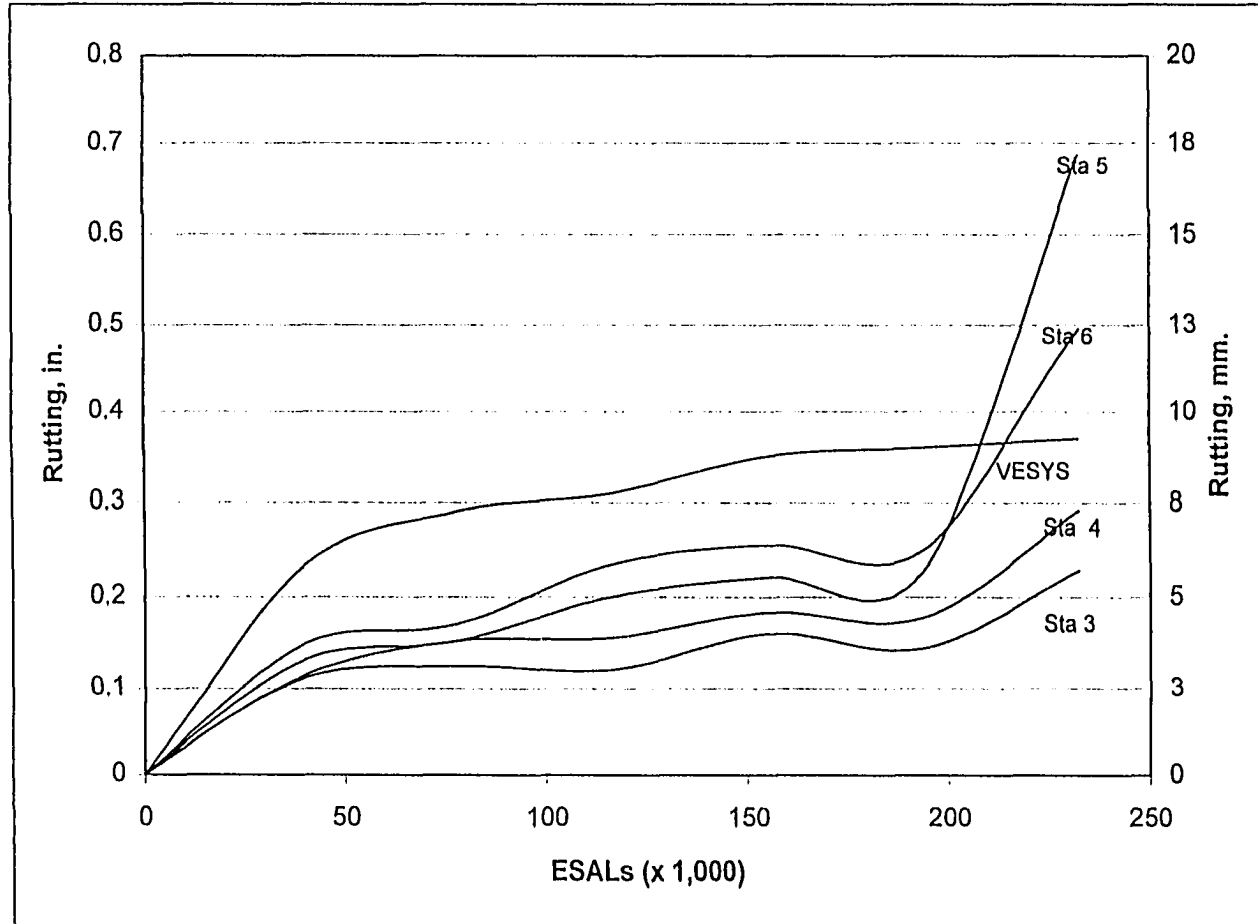


Figure 4. 5 Comparison of rutting development between VESYS 3A-M and observed data for lane 006

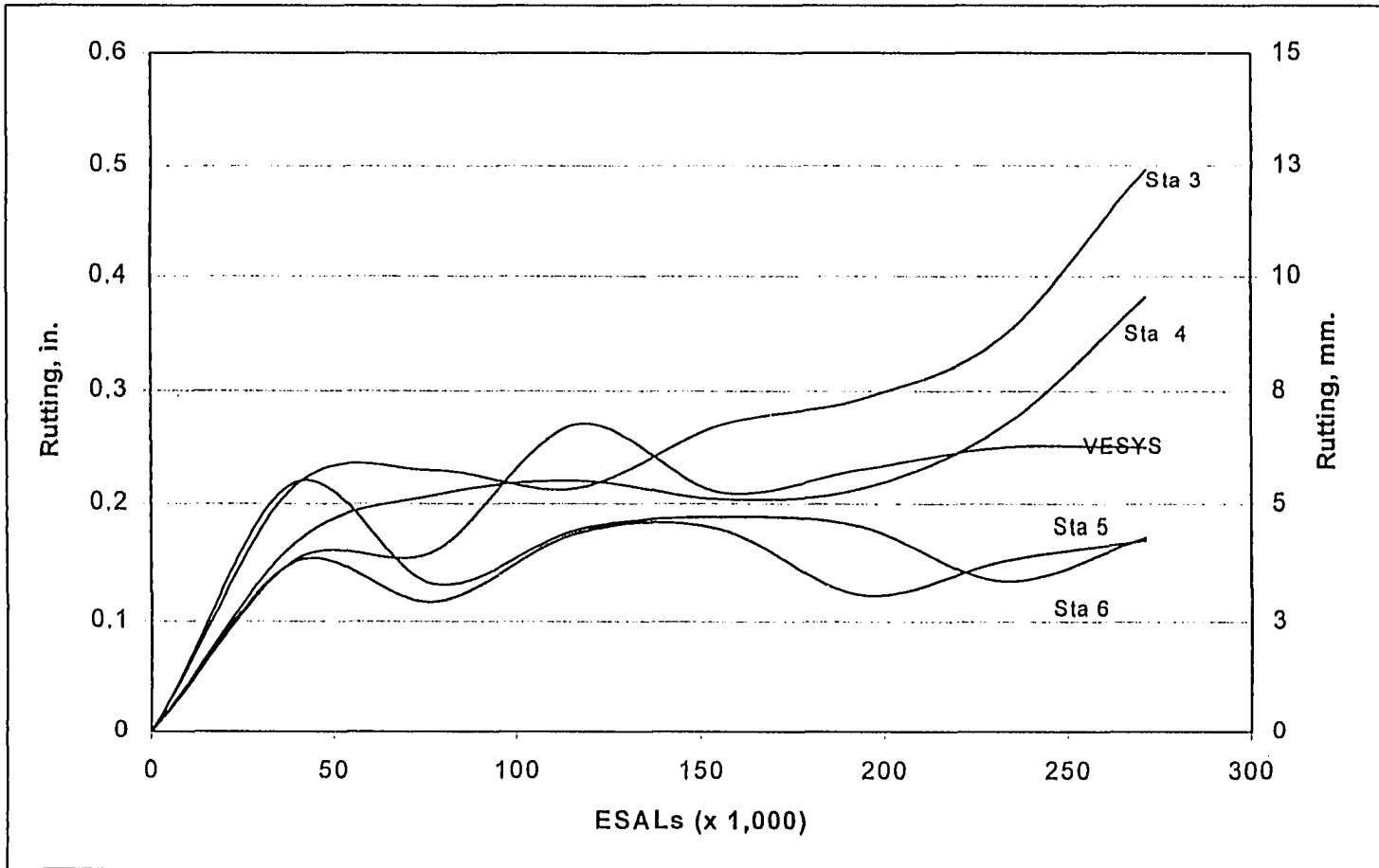


Figure 4. 6 Comparison of rutting development between VESYS 3A-M and observed data for lane 007

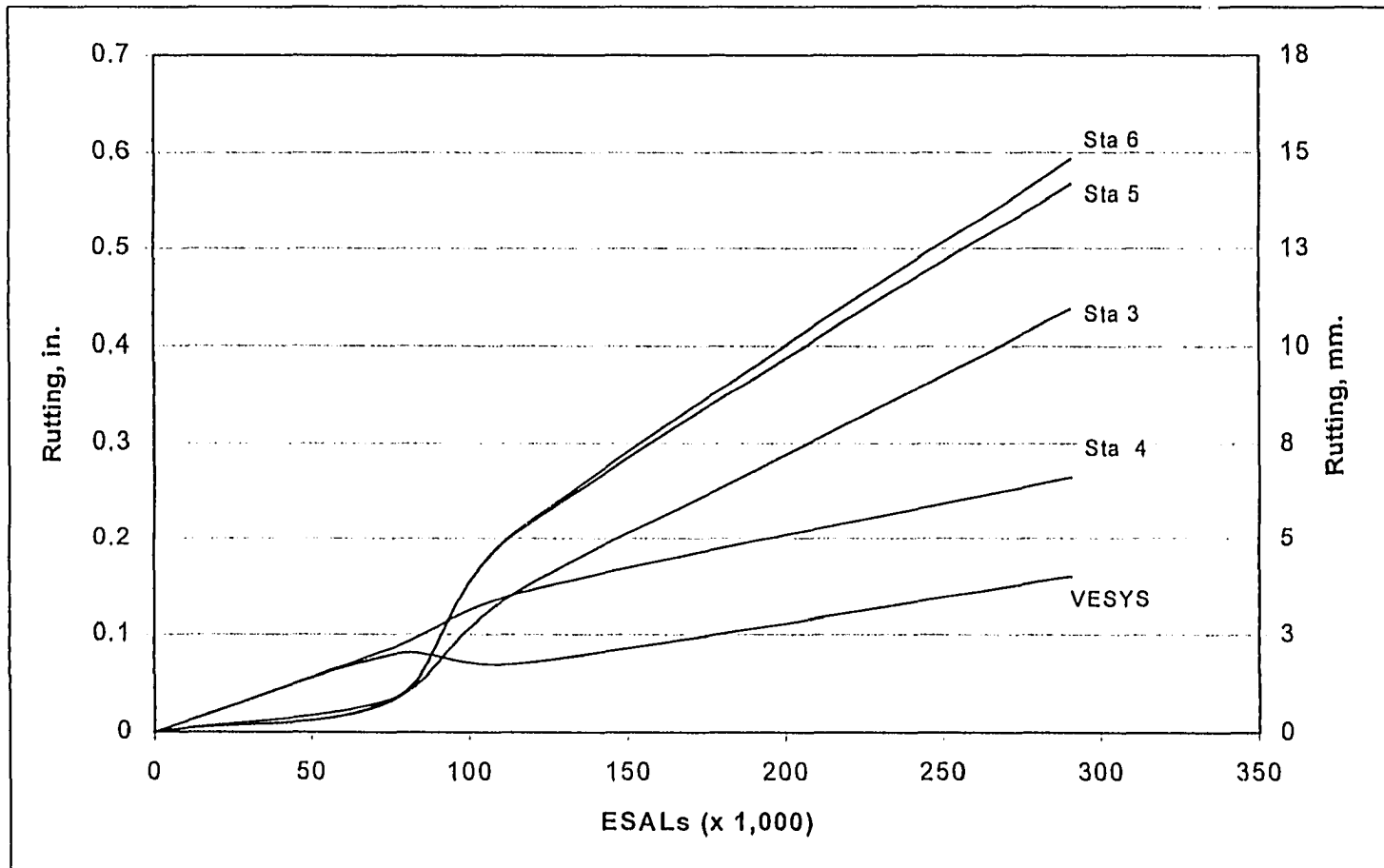


Figure 4. 7 Comparison of rutting development between VESYS 3A-M and observed data for lane 008

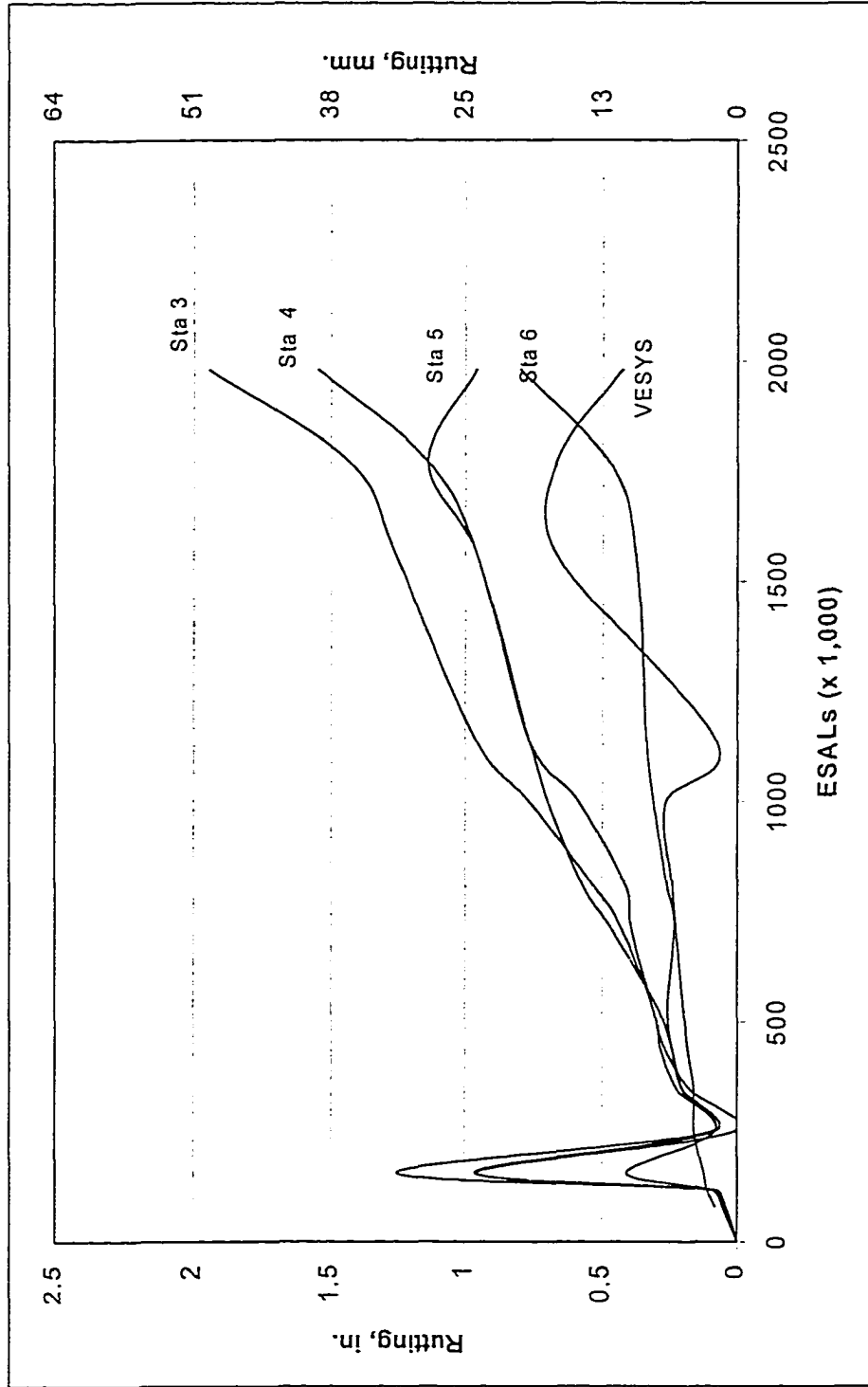


Figure 4. 8 Comparison of rutting development between VESYS 3A-M and observed data for lane 009

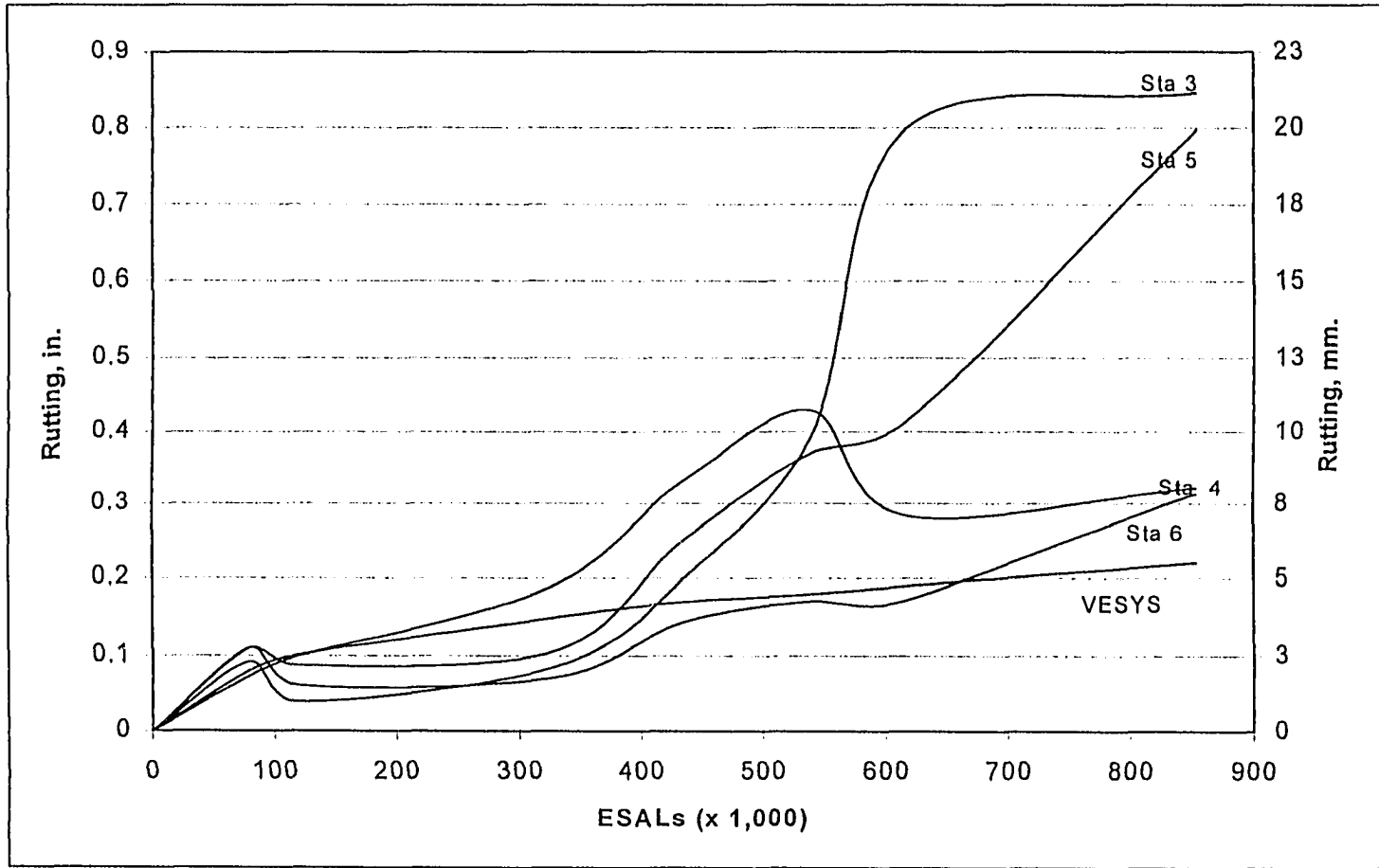


Figure 4. 9 Comparison of rutting development between VESYS 3A-M and observed data for lane 010

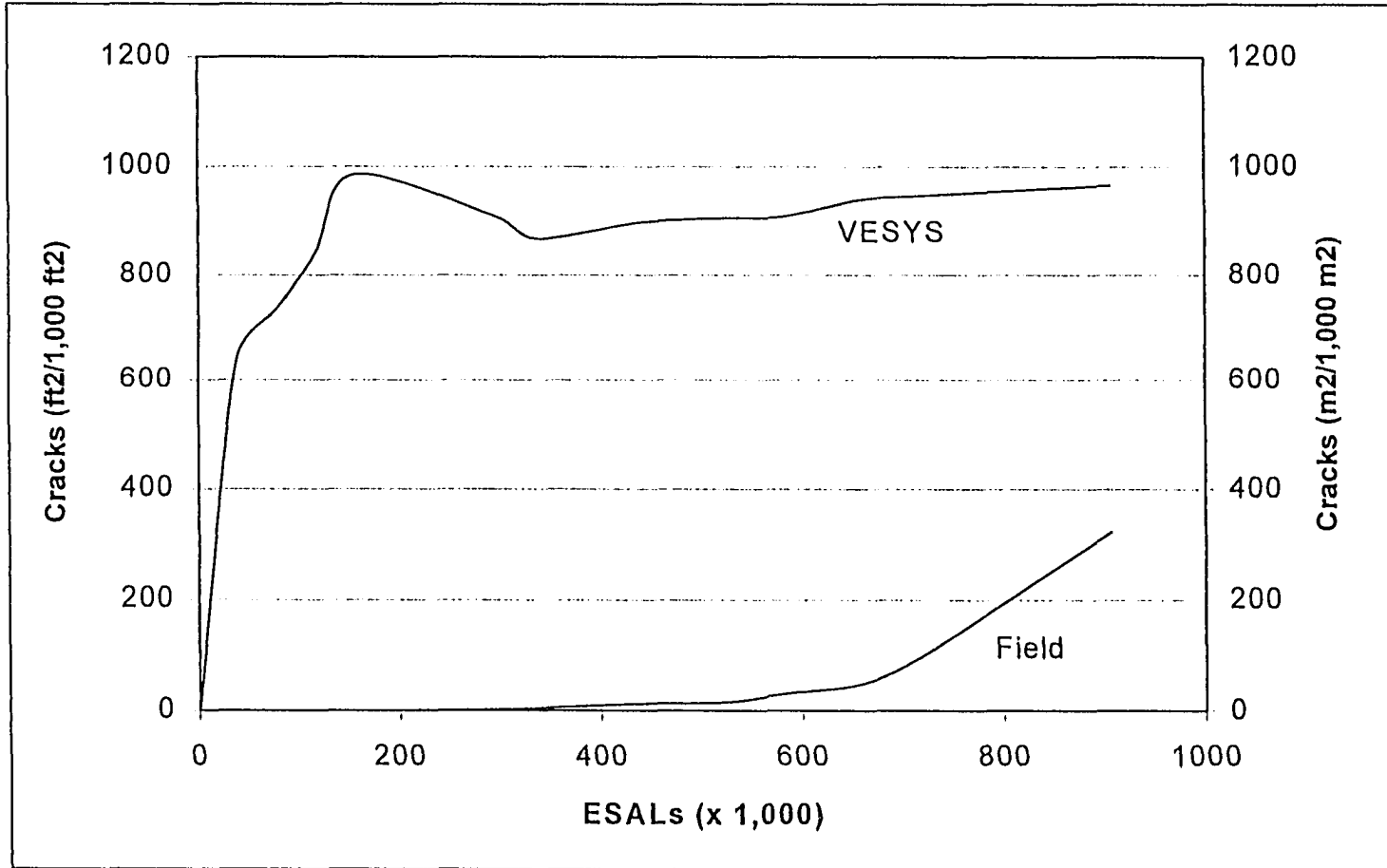


Figure 4. 10 Comparison of crack development between VESYS 3A-M prediction and observed data for lane 002

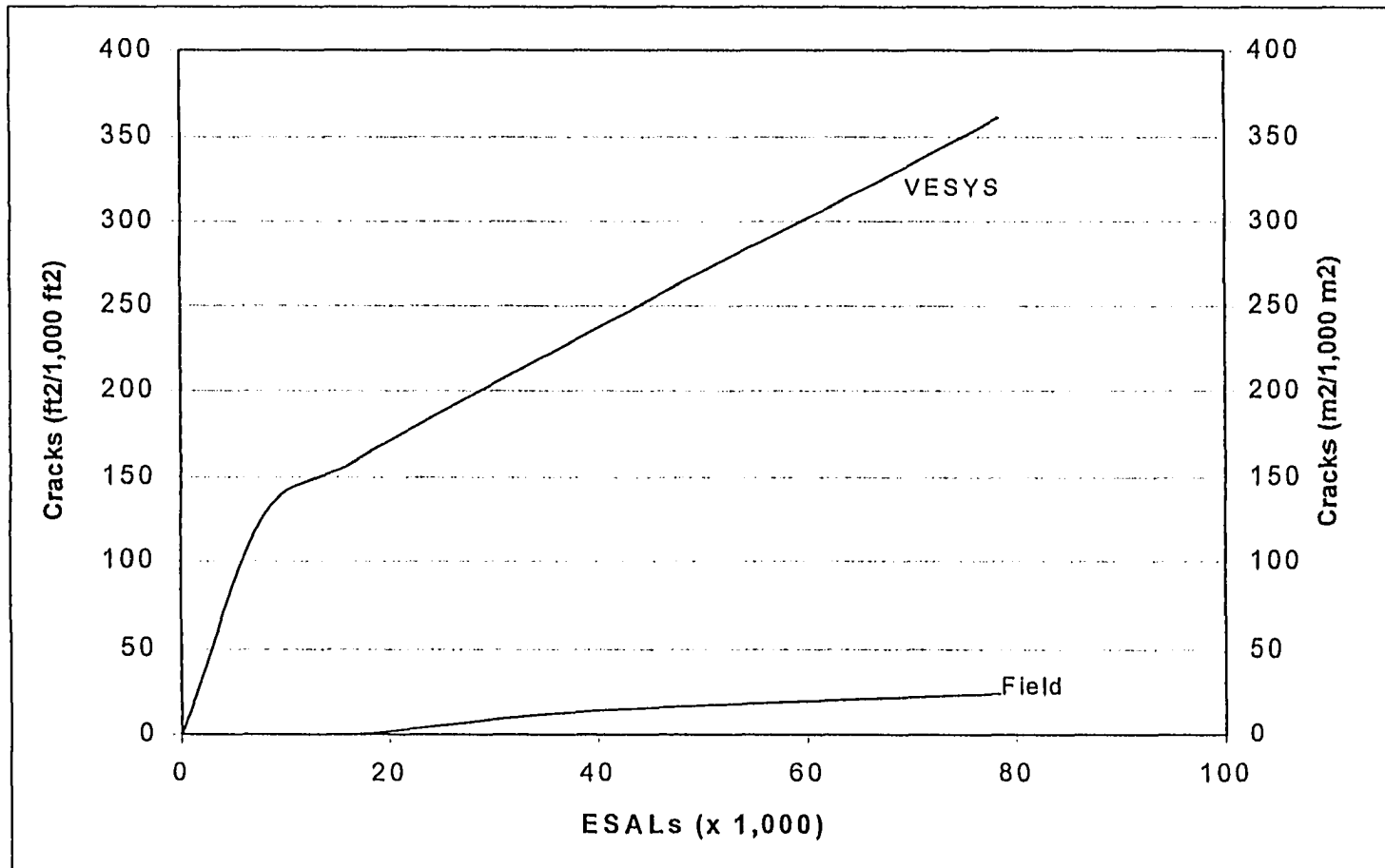


Figure 4. 11 Comparison of crack development between VESYS 3A-M prediction and observed data for lane 003

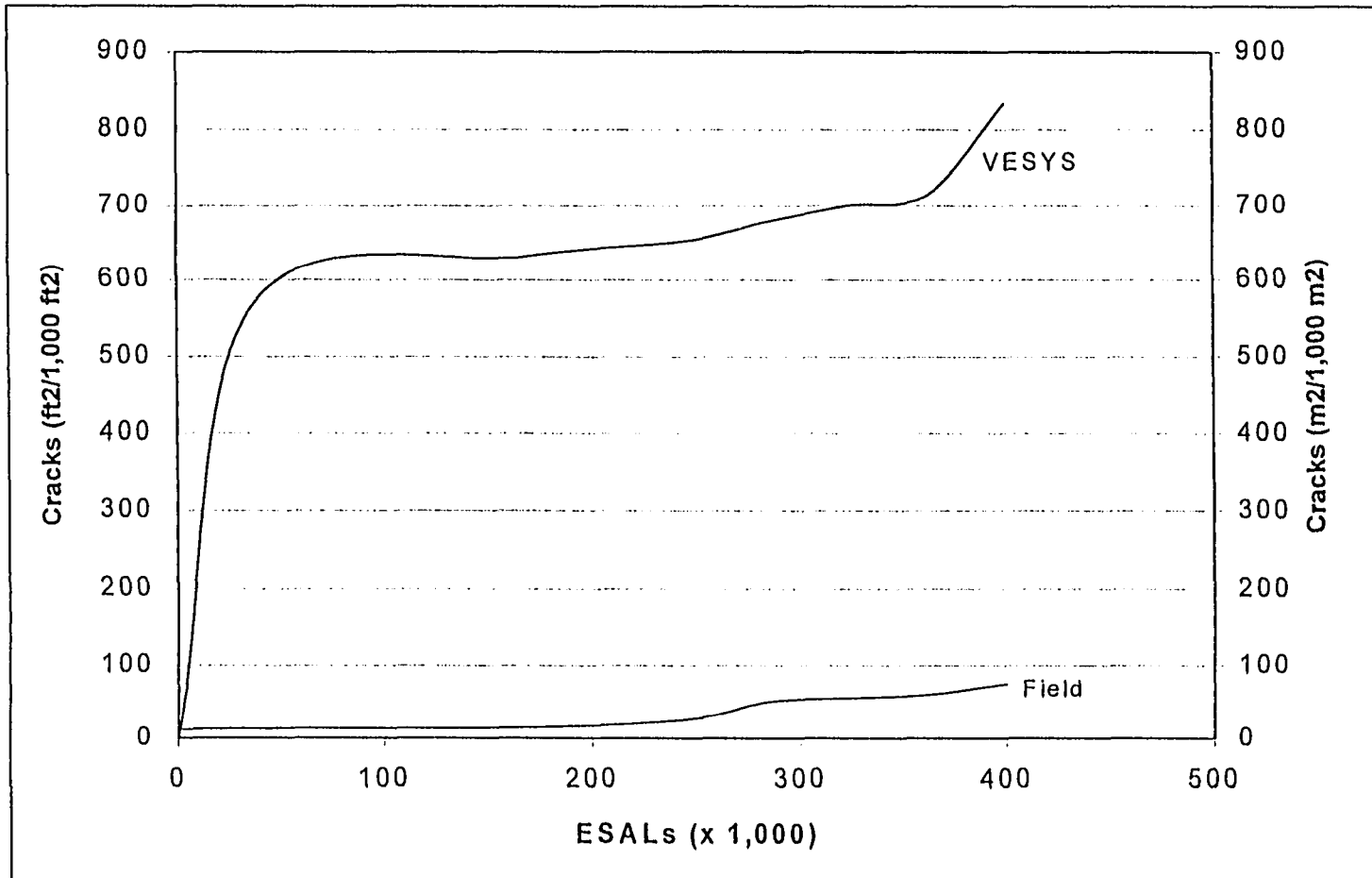


Figure 4. 12 Comparison of crack development between VESYS 3A-M prediction and observed data for lane 004

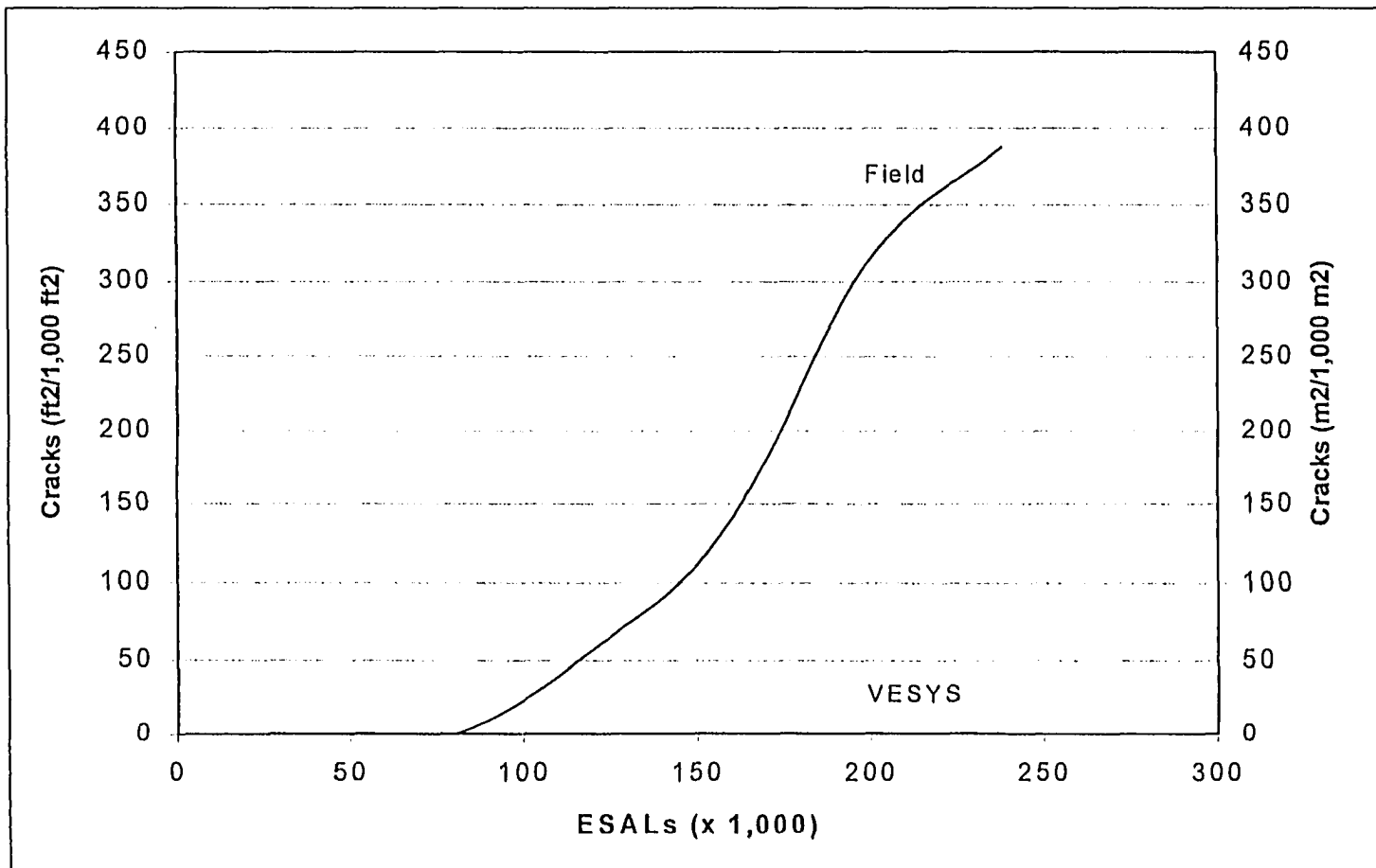


Figure 4. 13 Comparison of crack development between VESYS 3A-M prediction and observed data for lane 005

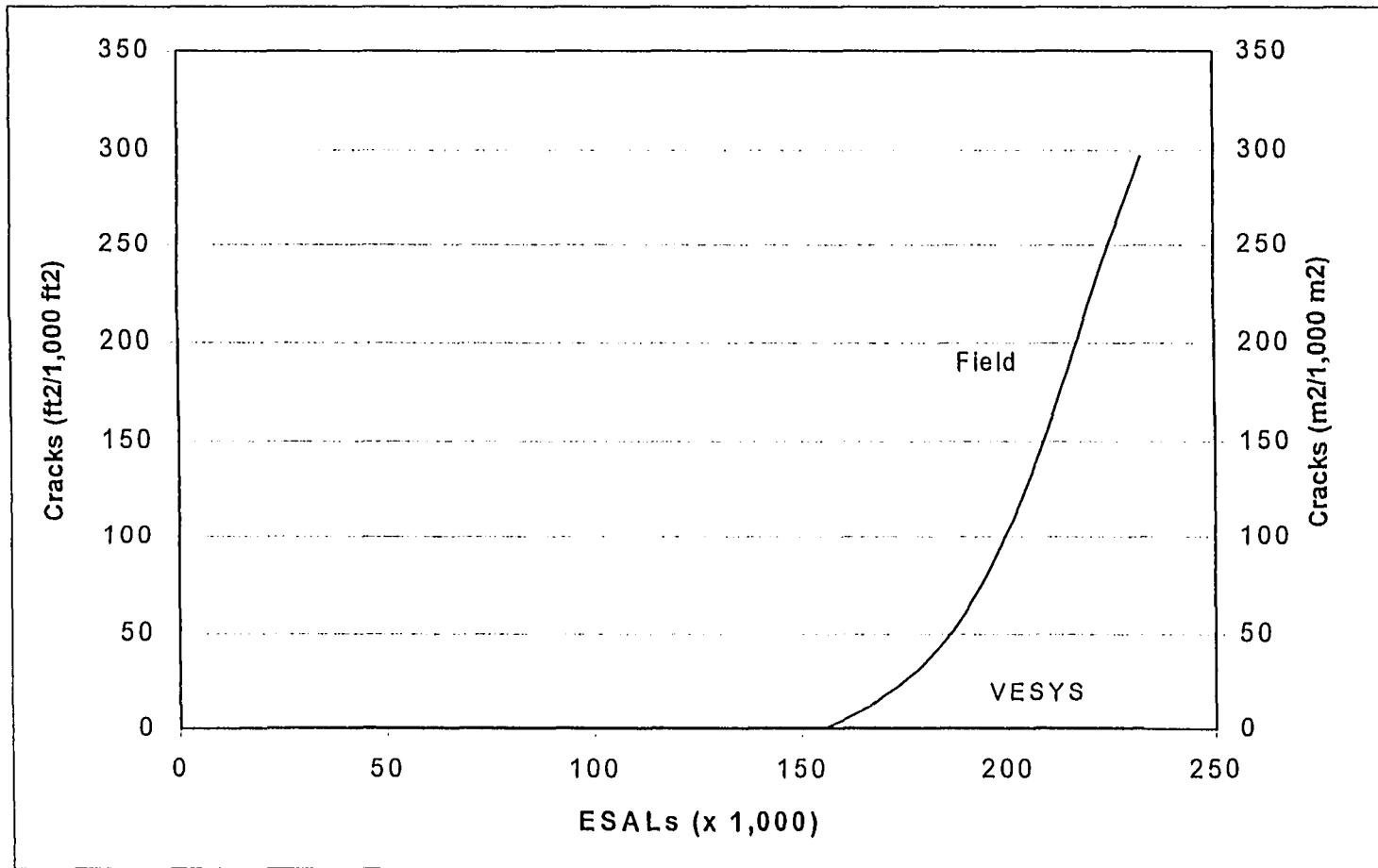


Figure 4. 14 Comparison of crack development between VESYS 3A-M prediction and observed data for lane 006

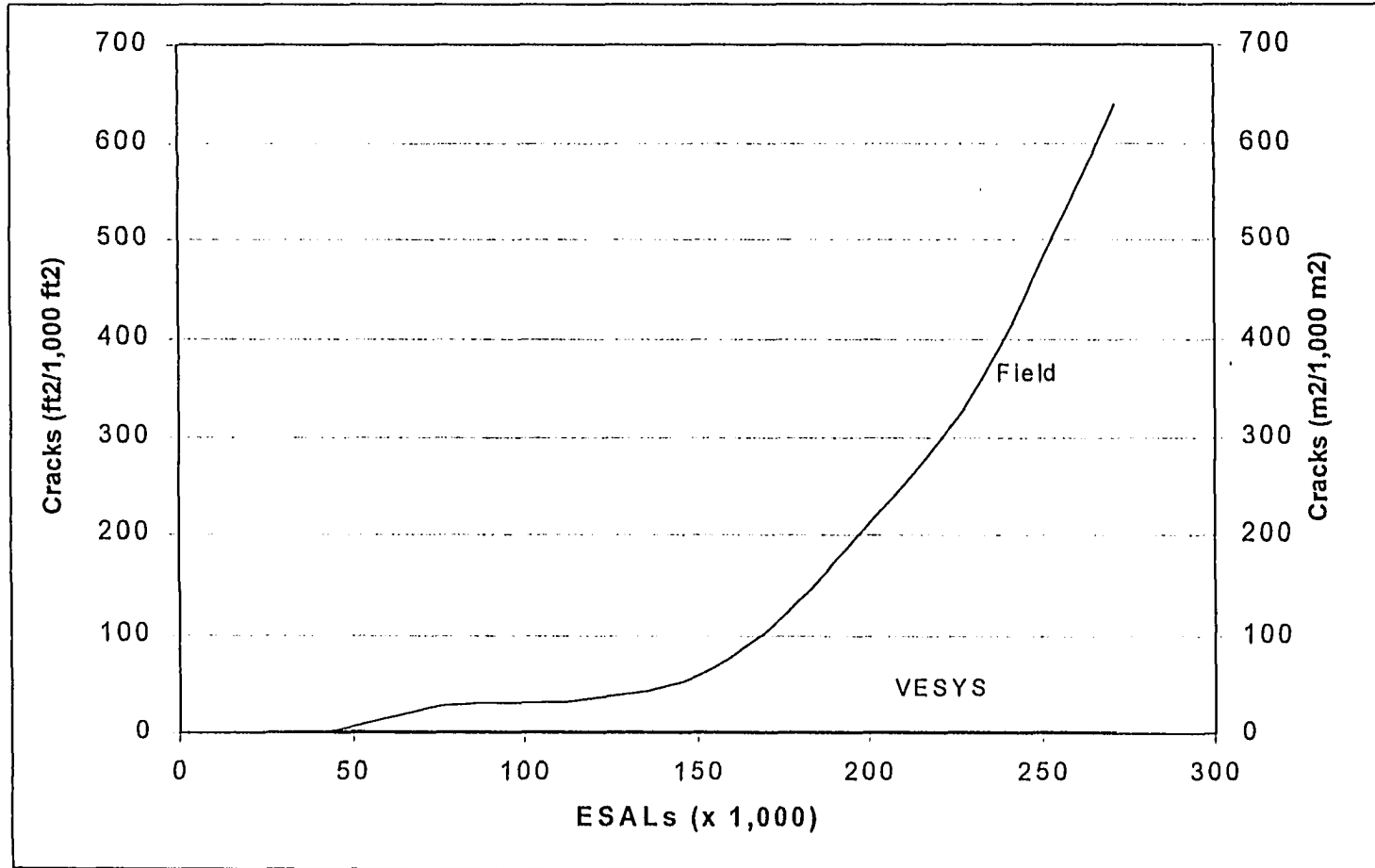


Figure 4. 15 Comparison of crack development between VESYS 3A-M prediction and observed data for lane 007

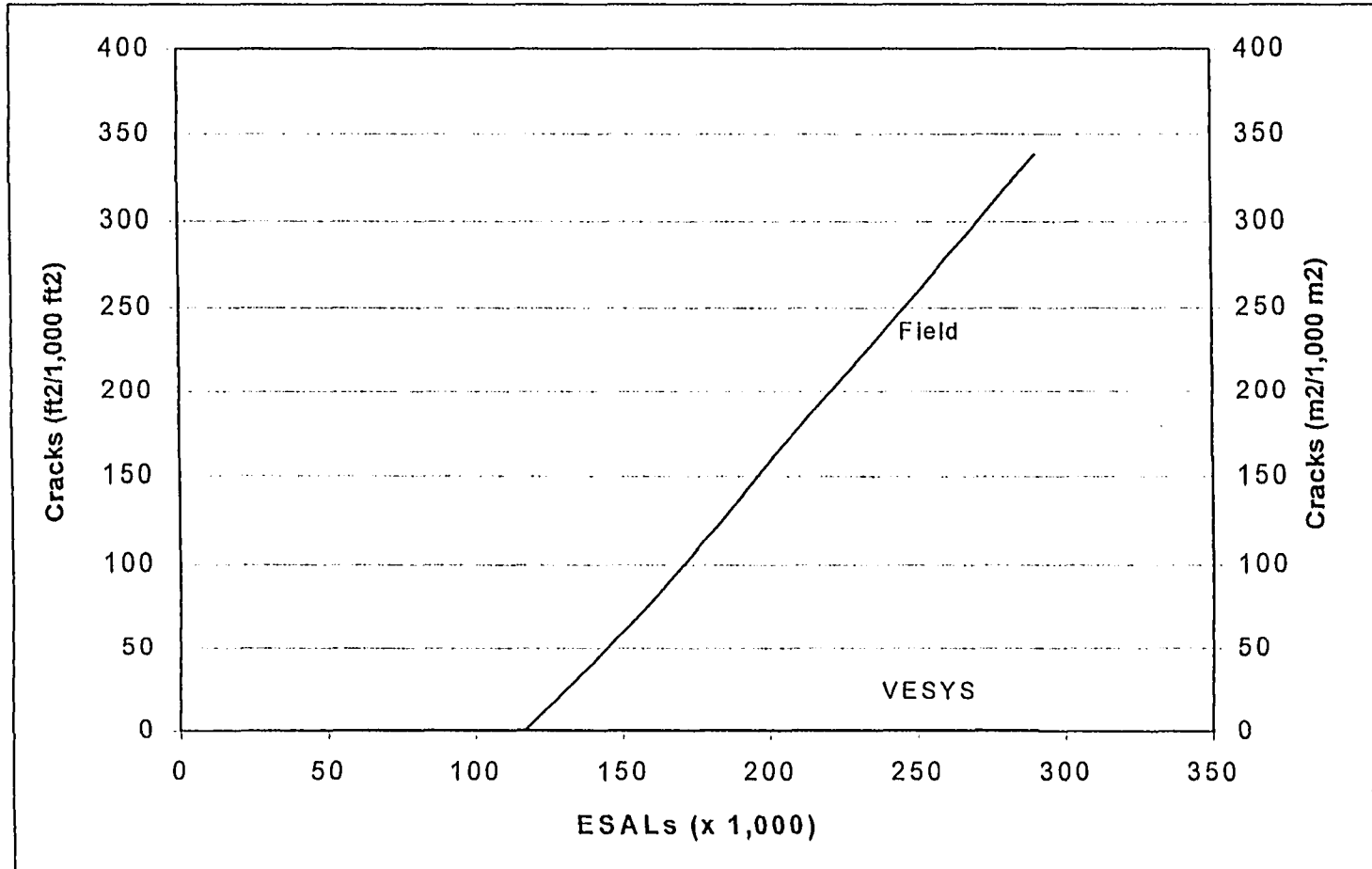


Figure 4. 16 Comparison of crack development between VESYS 3A-M prediction and observed data for lane 008

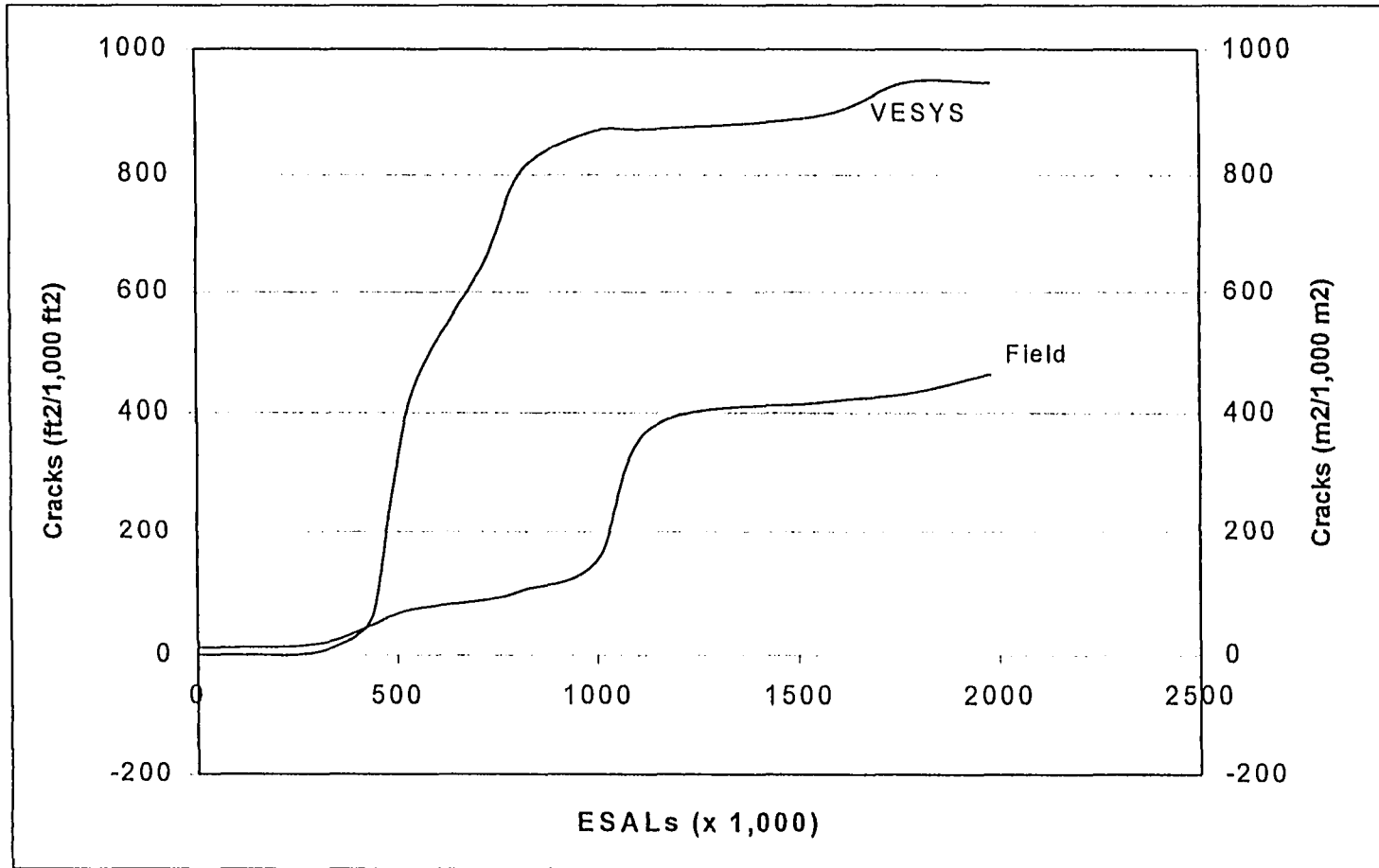


Figure 4. 17 Comparison of crack development between VESYS 3A-M prediction and observed data for lane 009

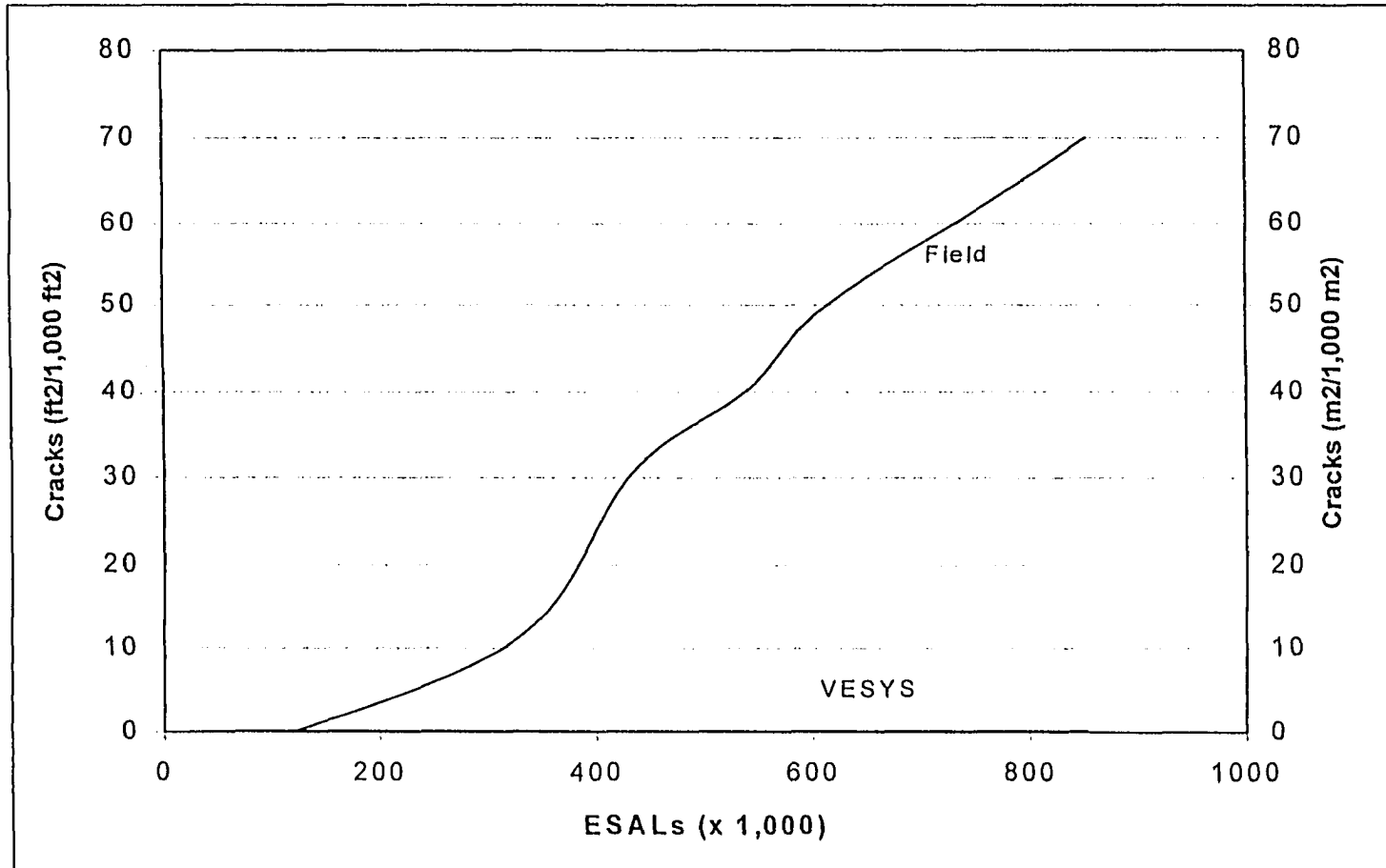


Figure 4. 18 Comparison of crack development between VESYS 3A-M prediction and observed data for lane 010

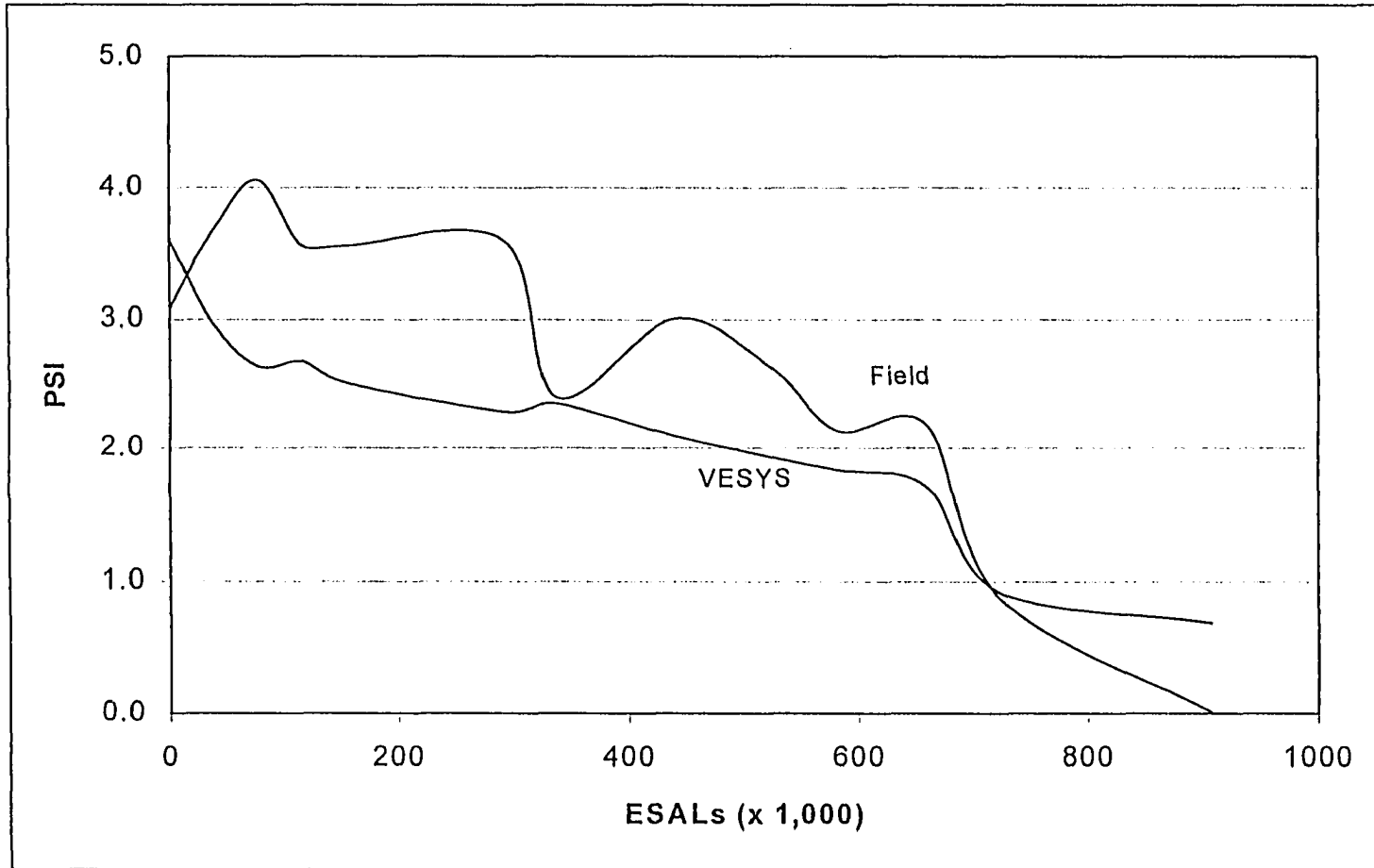


Figure 4. 19 Comparison of PSI development between VESYS 3A-M prediction and observed data for lane 002

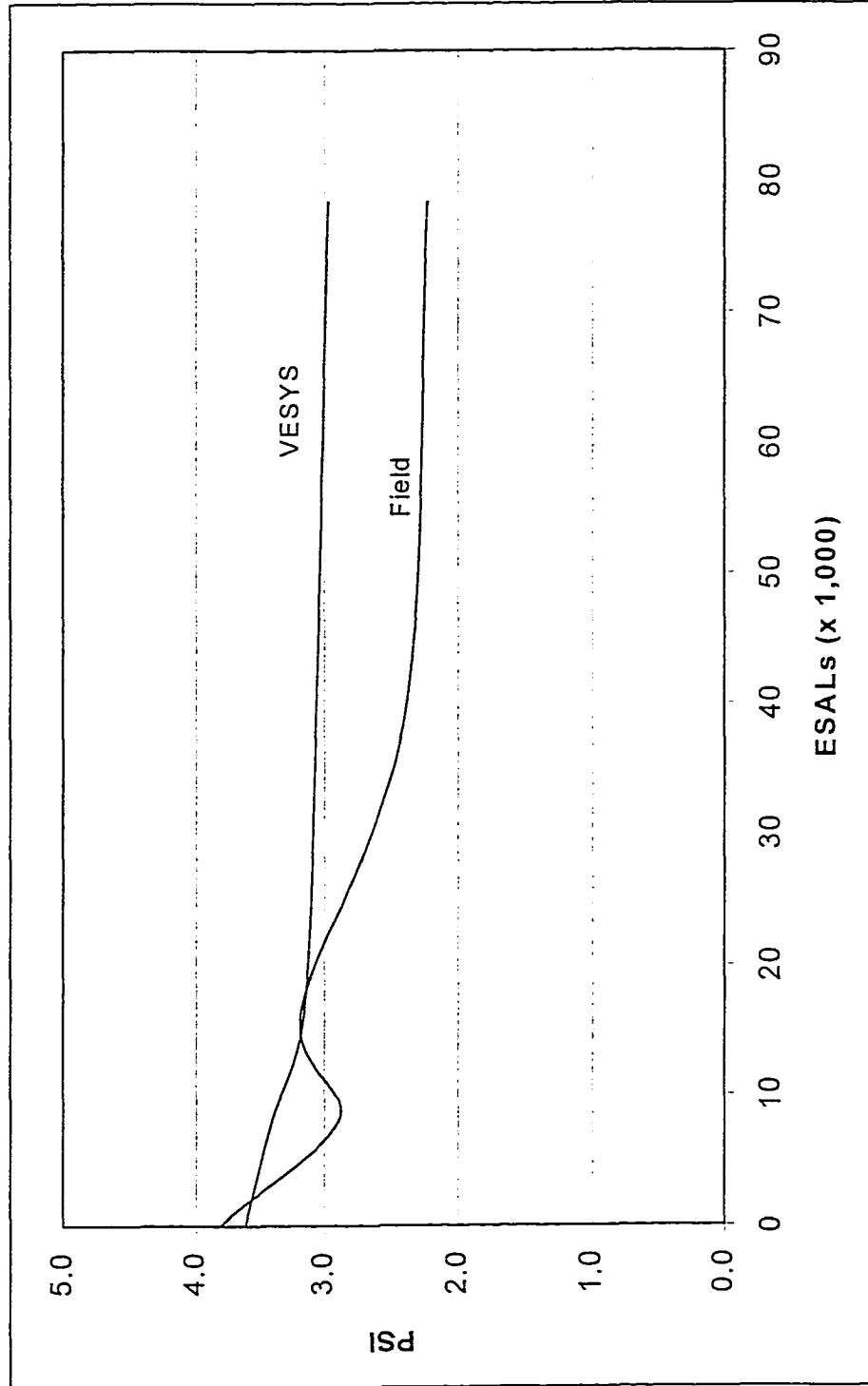


Figure 4. 20 Comparison of PSI development between VESYS 3A-M prediction and observed data for lane 003

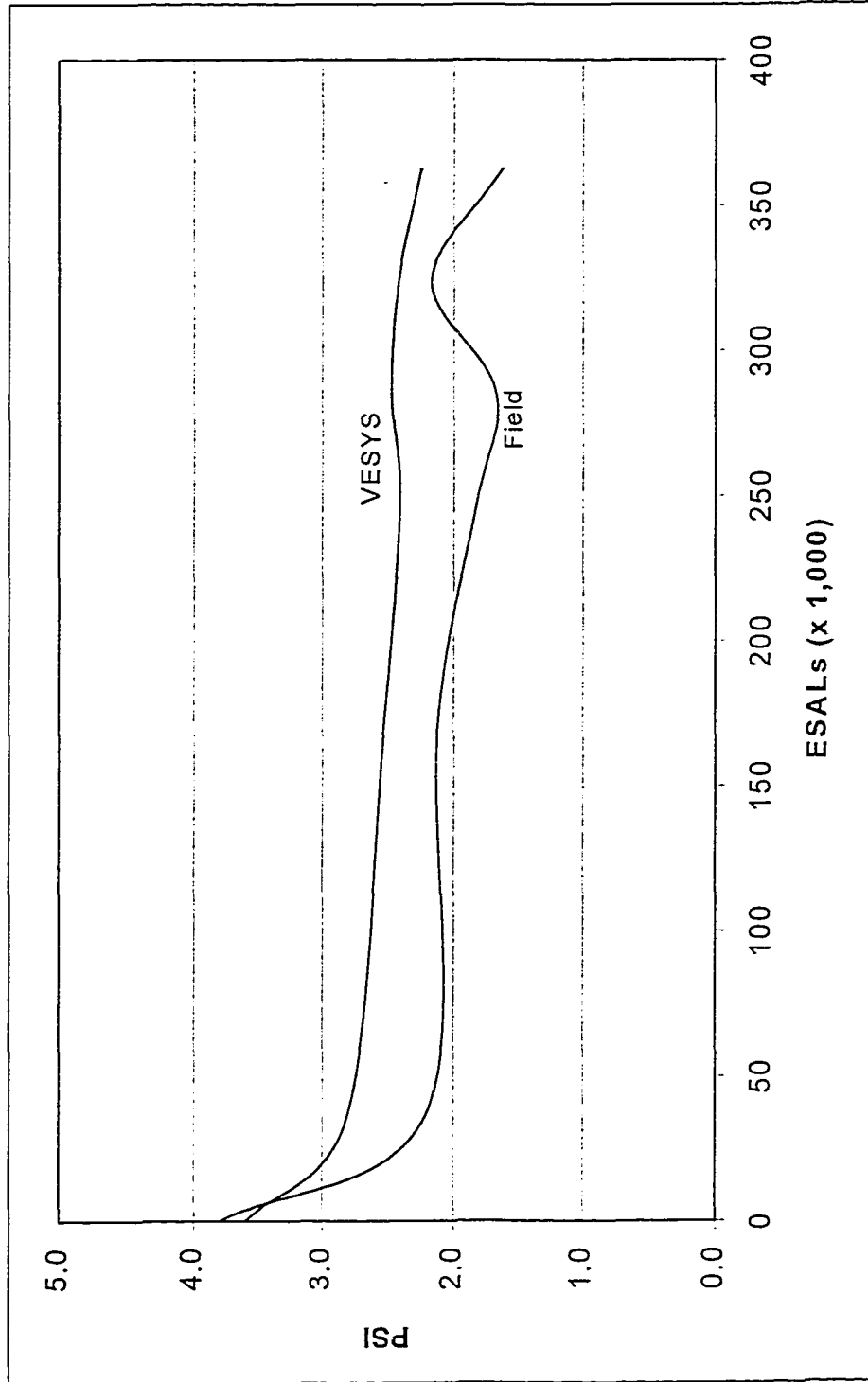


Figure 4. 21 Comparison of PSI development between VESYS 3A-M prediction and observed data for lane 004

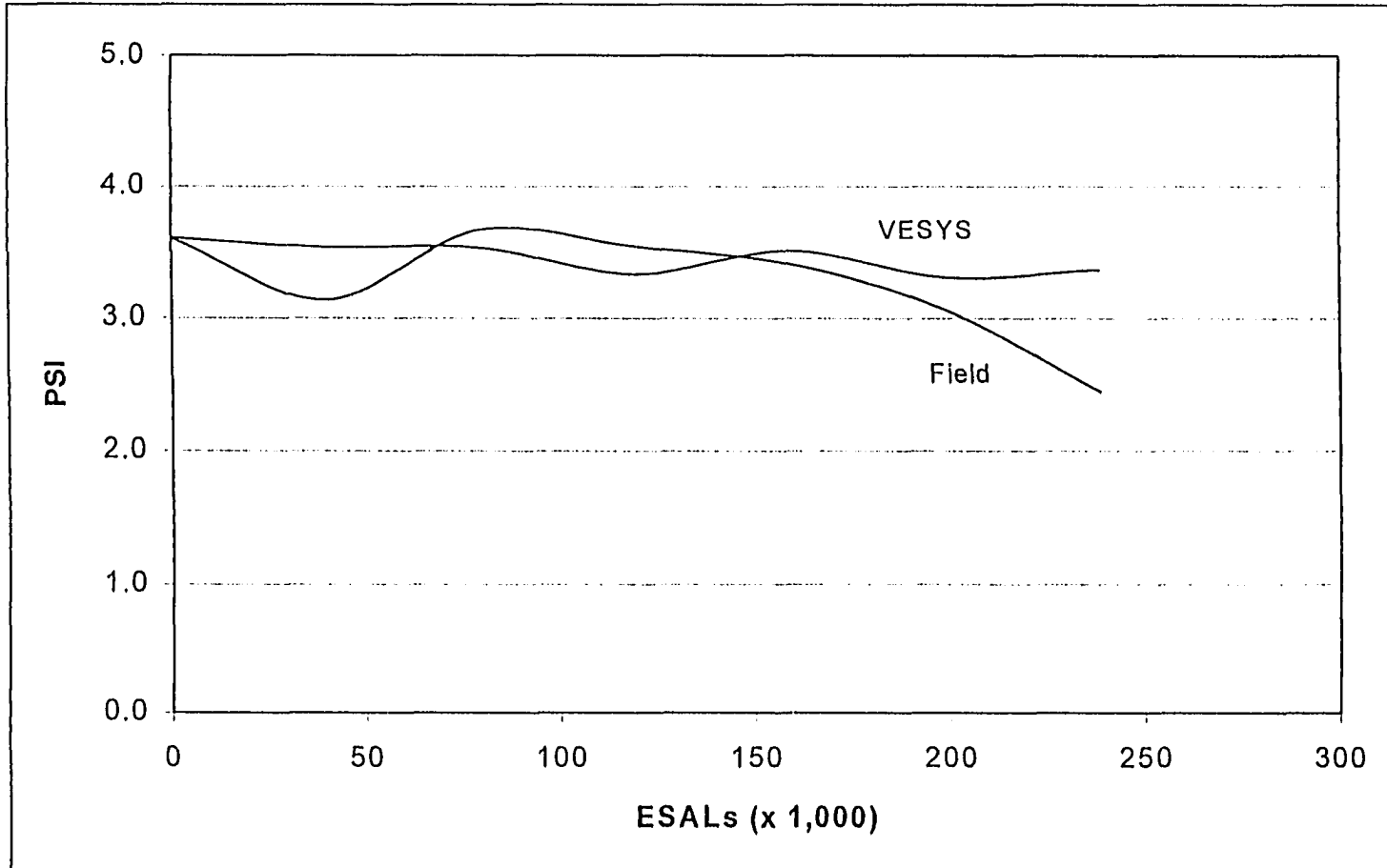


Figure 4. 22 Comparison of PSI development between VESYS 3A-M prediction and observed data for lane 005

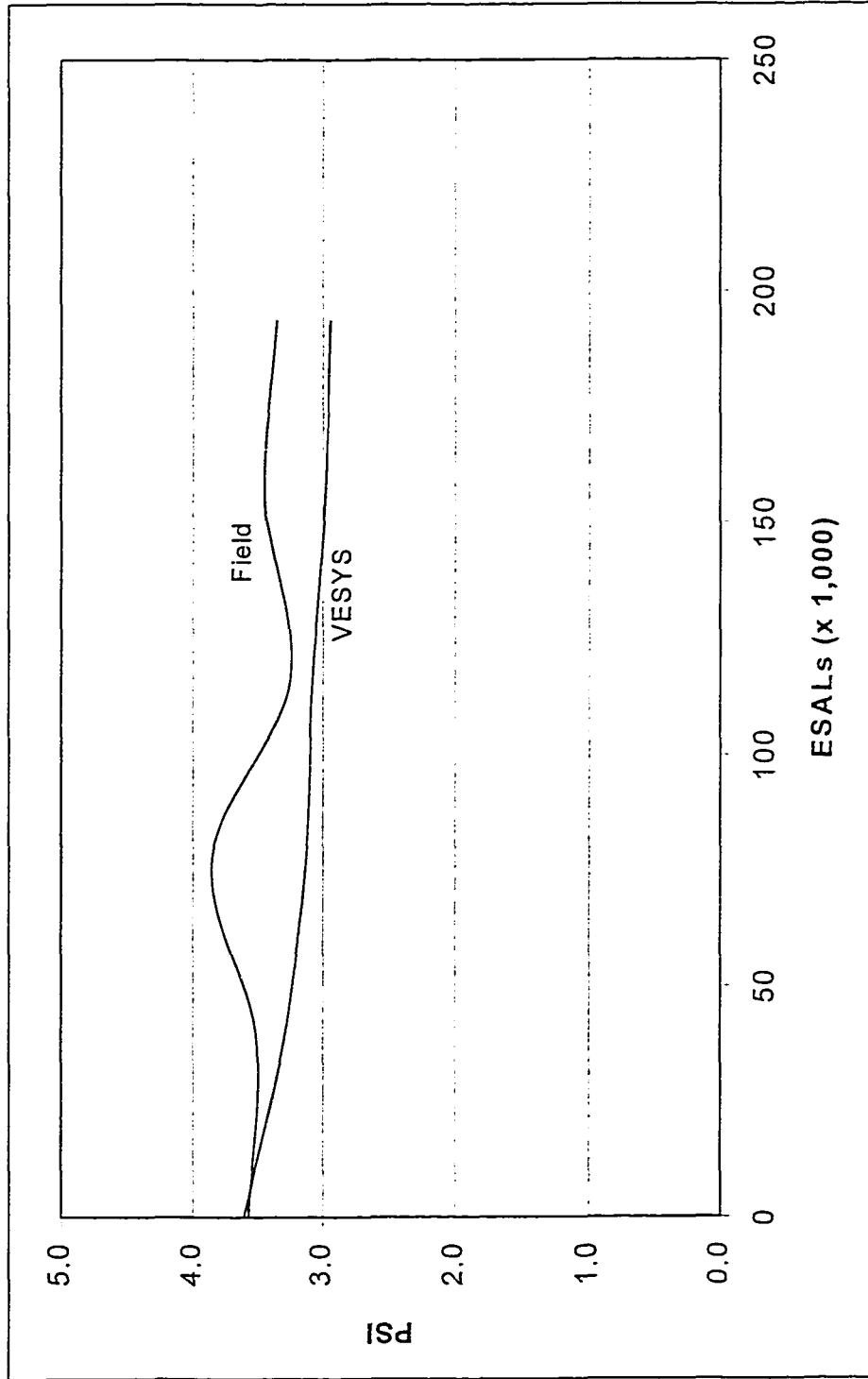


Figure 4. 23 Comparison of PSI development between VESYS 3A-M prediction and observed data for lane 006

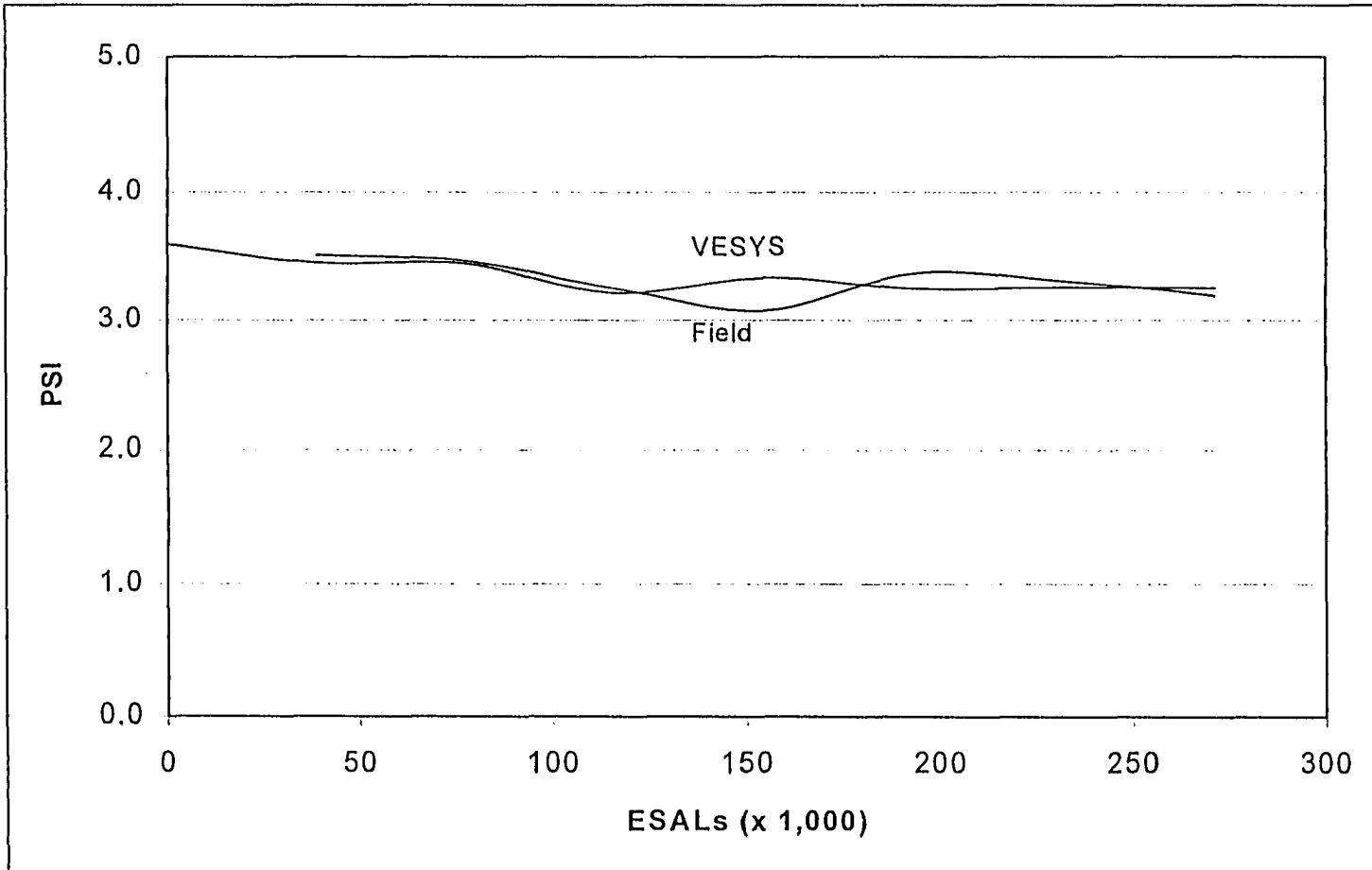


Figure 4. 24 Comparison of PSI development between VESYS 3A-M prediction and observed data for lane 007

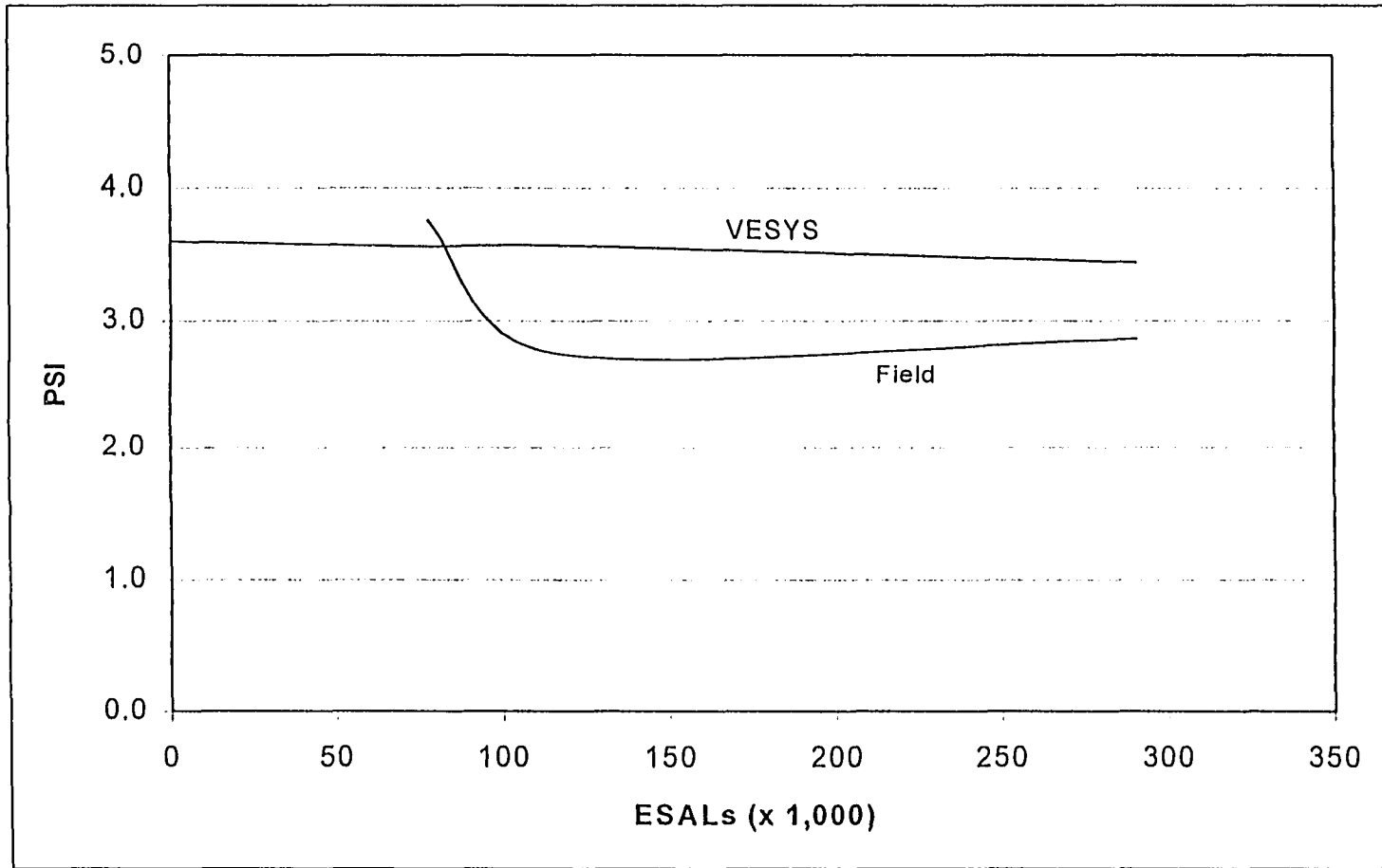


Figure 4. 25 Comparison of PSI development between VESYS 3A-M prediction and observed data for lane 008

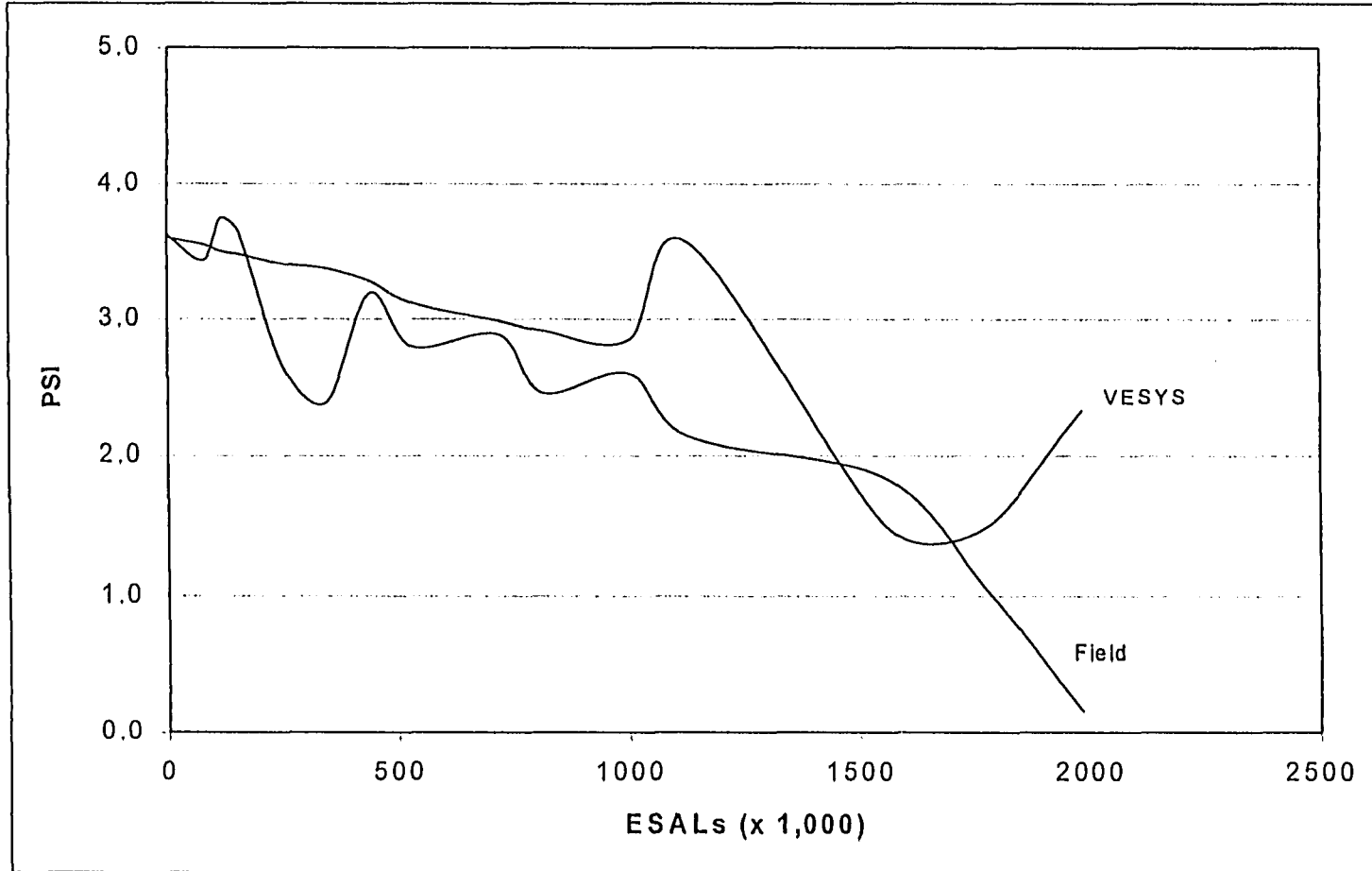


Figure 4. 26 Comparison of PSI development between VESYS 3A-M prediction and observed data for lane 009

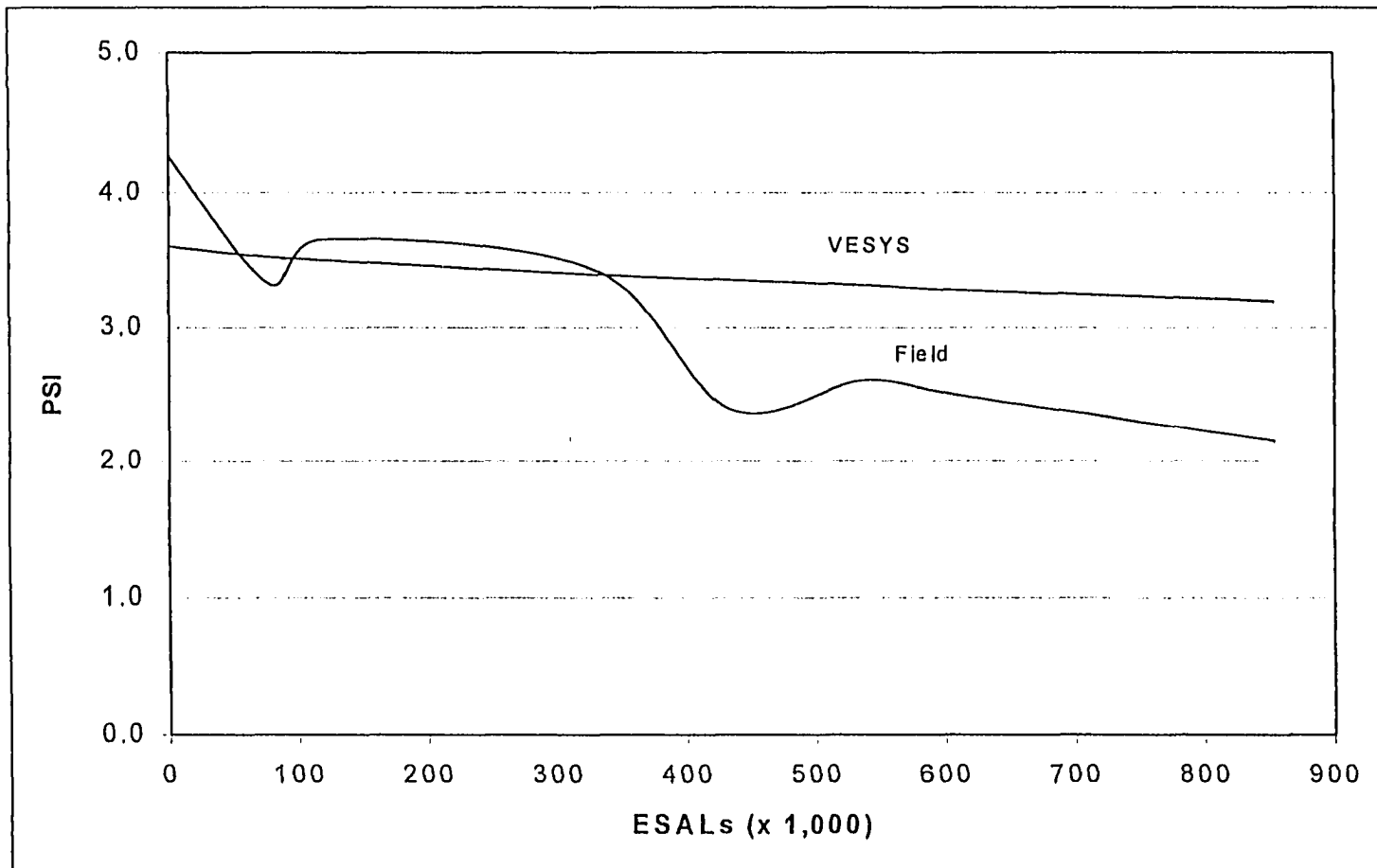


Figure 4. 27 Comparison of PSI development between VESYS 3A-M prediction and observed data for lane 010

CHAPTER 5

RELATIVE PERFORMANCE COMPARISON USING OBSERVED DATA

Rut Depth Data

One of the criteria that can be used to evaluate the performance of a flexible pavement is its ability to carry loads before reaching a critical rut depth. The slower the rut depth development, the better the pavement structure performs. Figure 5.1 was obtained by averaging the rut depth on stations 4, 5, 6 and 7 since these stations are in the middle of each test lane so that the touchdown effect can be ignored and a uniform load application can be expected. As shown in Figure 5.1, the ALF loading was terminated at different rut depths on the test lanes. In lane 002, for example, the ALF loading continued after 271,000 passes where the rut depth reached approximately 25-mm (1-in.), while the loading on lanes 006 and 008 was terminated with rut depths of less than 15-mm. (0.60-in.).

Therefore, to compare the relative performance for each lane, a rut depth of 19-mm.(0.75-in.) was chosen as a basis for the comparison. Since not all the lanes were loaded until the rut depth reached 19-mm. (0.75 in.), a simple regression was performed to determine the relationship between rut depth and the

number of ESALs for each test lane. Table 5.1 presents each model and the coefficient of determination (R^2).

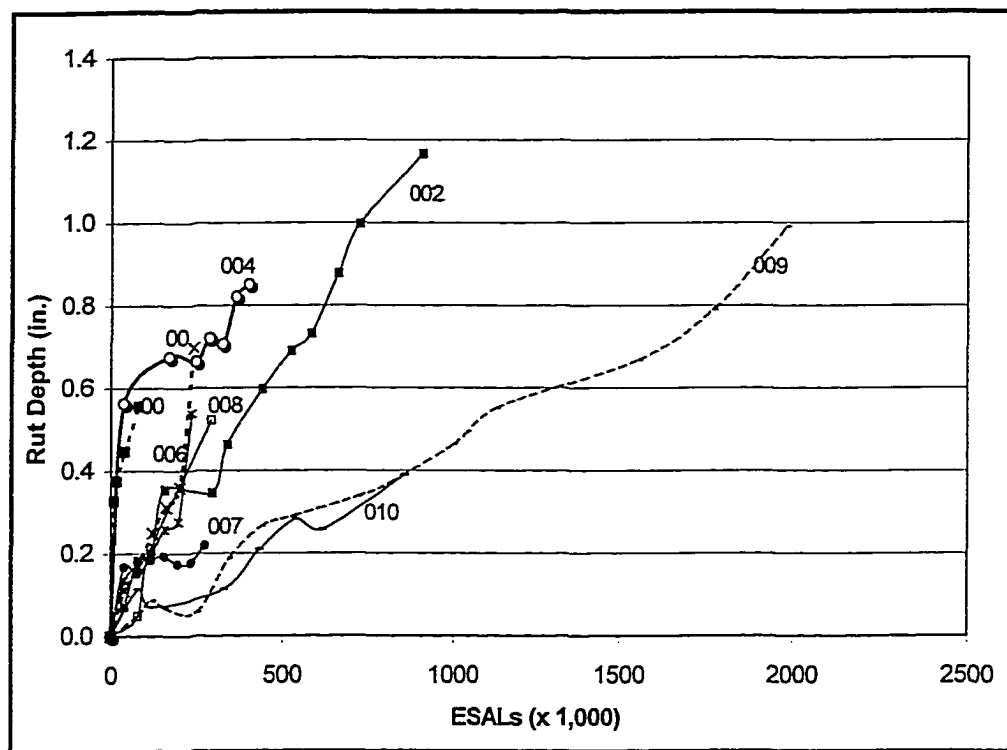


Figure 5. 1 Average rutting development for lanes 002 through 010

Using the above models, the approximate number of ESAL applications required to produce a rut depth of 19-mm.(0.75-in.) was determined and the relative performance comparison was shown in Figure 5.2. It can be seen from Figure 5.2 that lane 010, constructed using 305-mm. (12-in.) of 4 percent plant mix soil cement base without subbase material, provided the best performance in terms of rutting resistance, followed by lanes 009 and 002; whereas lanes 004, 005, 006, 007 and 008 have comparable performance. Lane 002, which is the crushed stone control section, performed better than lanes 003, 004, 005, 006, 007 and 008.

A post-mortem evaluation showed that the deformation occurred not only in the surface layer but also in the base layers [62]. Therefore, the hypothesis that the base layer contributed to the rut depth development can be justified.

Table 5. 1 Regression model for rut depth versus ESALs

| Lanes | Model | R ² |
|-------|---|----------------|
| 02 | Rut = 0.0012 ESAL + 0.05 | 0.98 |
| 03 | Rut = 0.0031 ESAL + 0.3149 | 0.99 |
| 04 | Rut = 1E-6 ESAL ² + 1E-4 ESAL + 0.5689 | 0.90 |
| 05 | Rut = 1E-5 ESAL ² - 0.0014 ESAL + 0.1694 | 0.93 |
| 06 | Rut = 1E-5 ESAL ² - 0.0017 ESAL + 0.2025 | 0.91 |
| 07 | Rut = 6E-10 ESAL ⁴ - 4E-7 ESAL ³ + 7E-5 ESAL ² - 0.0054 ESAL + 0.285 | 0.95 |
| 08 | Rut = 0.0021 ESAL - 0.0743 | 0.97 |
| 09 | Rut = 0.0005 ESAL + 0.0126 | 0.98 |
| 10 | Rut = 0.0004 ESAL + 0.0388 | 0.91 |

Roughness Data

Figure 5.3 summarizes the IRI for lanes 002 through 010 where each plot is the average of the three lines of the profile data described earlier. Data from the first 152-cm. (60-in.) of the profile, where the touchdown of the load occurs, were excluded to eliminate the effect of premature distress occurring there.

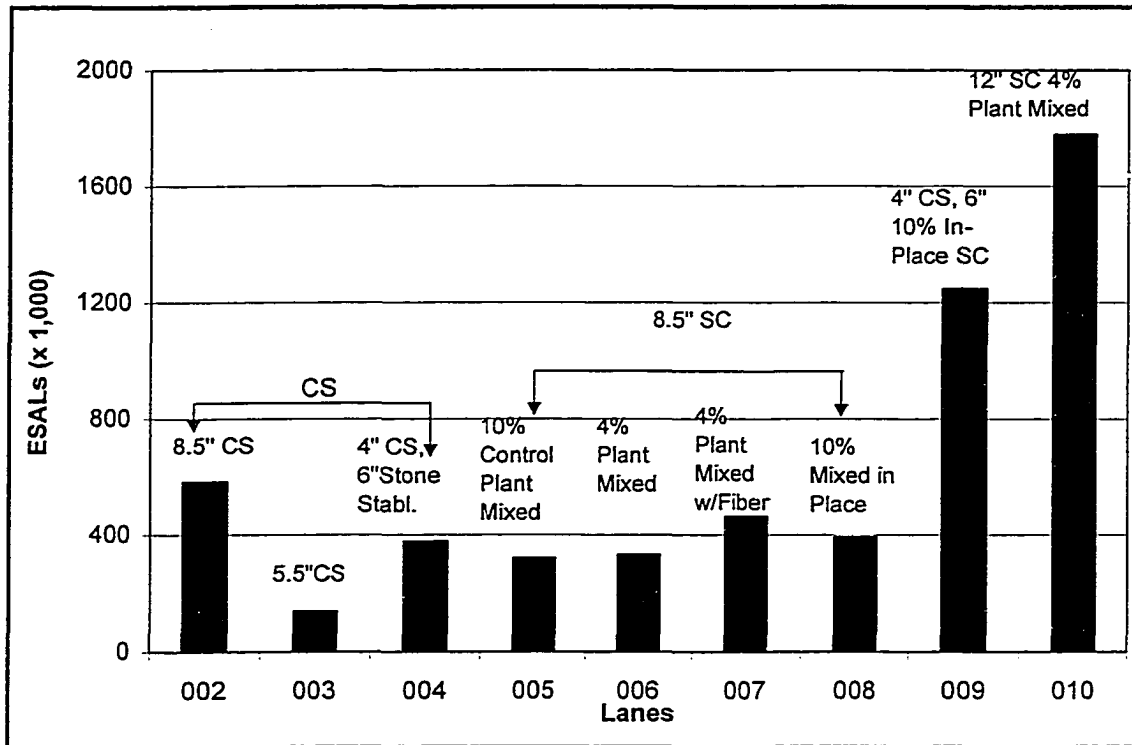


Figure 5. 2 Performance comparison at a rut depth of 19-mm. (0.75 in.)

To express the roughness in terms of serviceability index (SI), the following equation suggested by Patterson [18] was used :

$$SI = 5.0e^{-0.181/RI} \quad (5.1)$$

Where: IRI is in m/km

The results are shown in Table 5.2. As can be seen from the Table, at the end of the loading the SI value for all test sections is below 2.0, meaning that the sections have reached an unacceptable condition.

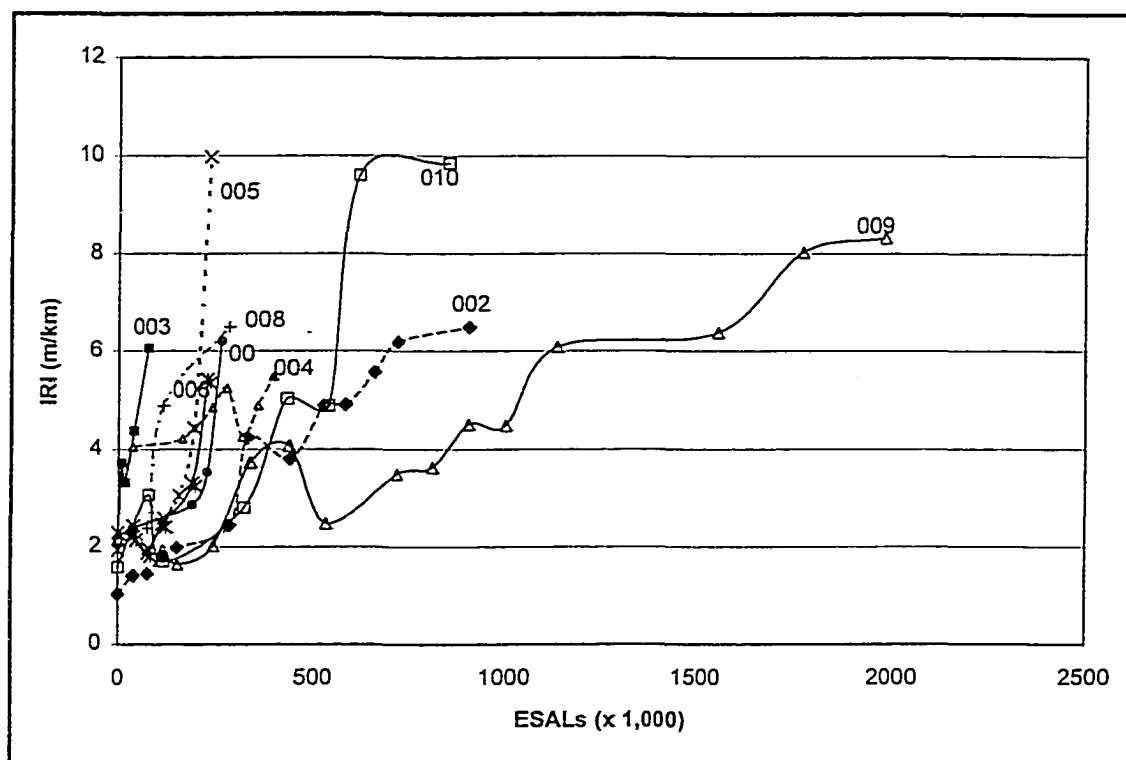


Figure 5. 3 Summary of roughness development for lanes 002 through 010

Table 5. 2 Approximate relation between IRI and SI for each lane

| Lanes | Beginning of Test | | | End of Test | | |
|-------|-------------------|-------|-----|-------------|------|-----|
| | ESALs | IRI | SI | ESALs | IRI | SI |
| 002 | 0 | 1.03 | 4.2 | 853,000 | 6.49 | 1.6 |
| 003 | 0 | 2.12 | 3.4 | 74,000 | 6.06 | 1.7 |
| 004 | 35,000 | 4.05* | 2.4 | 382,000 | 5.48 | 1.9 |
| 005 | 0 | 1.94 | 3.5 | 222,000 | 9.97 | 0.8 |
| 006 | 0 | 2.29 | 3.3 | 222,000 | 5.41 | 1.9 |
| 007 | 37,000 | 2.38* | 3.3 | 259,000 | 6.2 | 1.6 |
| 008 | 74,000 | 2.38* | 3.3 | 311,000 | 6.5 | 1.6 |
| 009 | 111,000 | 1.93* | 3.5 | 1,863,000 | 8.32 | 1.1 |
| 010 | 0 | 1.59 | 3.8 | 815,000 | 9.84 | 0.9 |

*No data available at ESALs = 0

In Figure 5.3, the roughness development of each lane shows large variability, making performance comparisons difficult. Therefore, to make the relative performance comparison among the lanes, an analysis similar to that used to compare the rutting development was conducted. First, a regression analysis was performed on data from each lane to develop a relationship between ESALs and IRI. Then, setting $IRI = 3.8$ as the terminal ride quality level, the number of ESALs required to reach an IRI of 3.8 was predicted from the regression equations.

Figure 5.4 presents the performance comparison of the lanes using both the rutting and roughness criteria. It shows a comparable result and pattern of performance from both criteria. Both show that lanes 002, 009 and 010 perform best despite the fact that these three are ordered differently for the two criteria. Based on the rutting criteria, lane 010 is the best, while based on roughness criteria, lane 009 is the best. For other lanes both rutting and roughness criteria show that these lanes have a relatively similar performance.

Cracking Development

Field surface cracking was recorded by sketching the cracks on a surface distress map. Each lane was divided into 4 panels, each containing 48 sub panels. The use of the distress map will help not only in determining the intensity of the cracking but also in identifying the location of distress. The length of each crack was measured using a distance-measuring device called Plan Wheel. In this measurement, only cracks having width more than 0.1 mm. (0.04 in.) were

recorded. The field surface crack measurements were conducted at intervals of approximately 25,000 ALF passes.

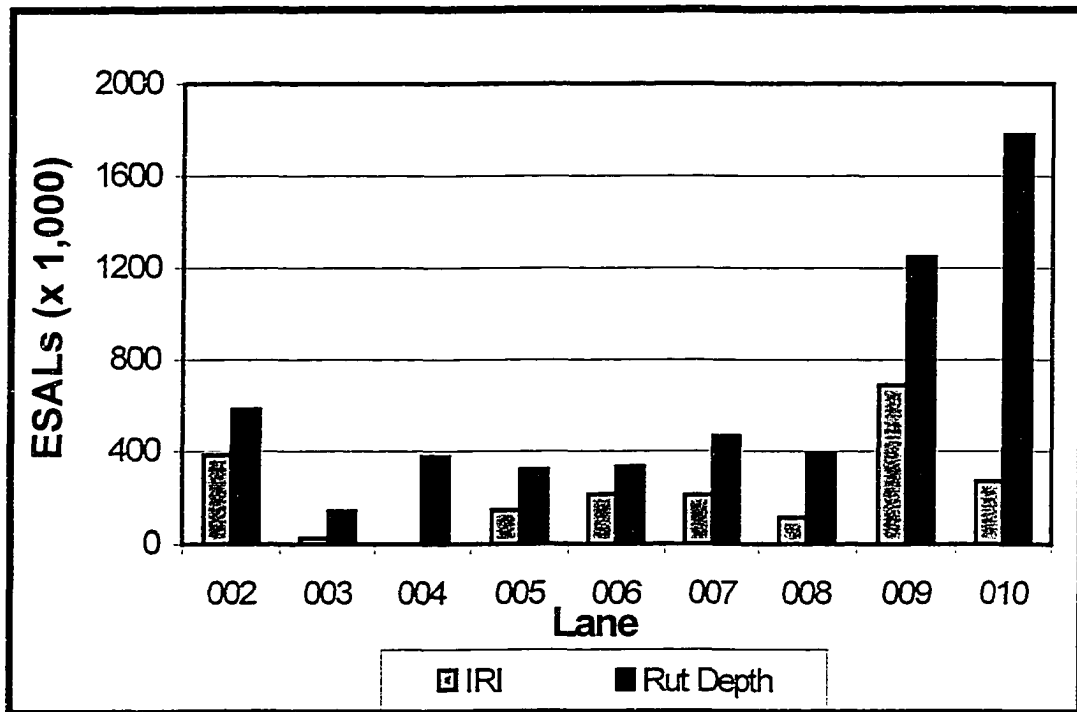


Figure 5. 4 Performance comparison based on rutting and roughness

The field data, which were in lineal m/m² was then converted to m²/1,000 m² to conform to the VESYS definition. VESYS defines the intensity of fatigue cracks as follows:

$$ICA = \frac{N}{BL} \times 1,000 \quad (5.2)$$

Where:

N= number of square meter (square feet) in one or both wheel path, containing class I cracking,

B = band width of wheel paths, usually taken as 0.61 m. (2 ft.) per wheel path,

L = length of pavement section, m (ft).

Almost all the cracks on the test sections occurred only in areas subjected to ALF loading. The fatigue cracks initially occurred as individual longitudinal cracks; then, transverse cracks appeared and progressed as the longitudinal cracks grew longer and wider. These transverse and longitudinal cracks gradually interconnected into an alligator cracking pattern as traffic increased.

Figure 5.4 shows the crack development for lanes 002 through 010. As can be shown from the Figure, the overall evaluation showed that lanes 009 and 002 provided the best performance in resisting cracking followed by lanes 004 and 010. As for lane 010, even though it seems to have a good crack resistance, the result is not conclusive because the loading was terminated at approximately 759,000 ESAL when the IRI reached 10. Lane 04 also showed good cracking resistance. This performance pattern is very similar to those obtained from both the roughness and rutting evaluations.

The crack development in Figure 5.4 also showed that the crushed stone base material, lanes 002, 004 and 009, resisted cracking much better than the soil cement bases, represented by lanes 004, 005, 006, 007, 008 and 010. It also indicated that in-place soil cement, represented by lane 008, has a slightly better performance in resisting cracking than that of plant-mixed soil cement which occur in lanes 005, 006 and 007, which have the worst performance. As

shown in Figure 5.4, after about 200,000 ESALs lanes 005, 006 and 007 developed very steep crack development curves.

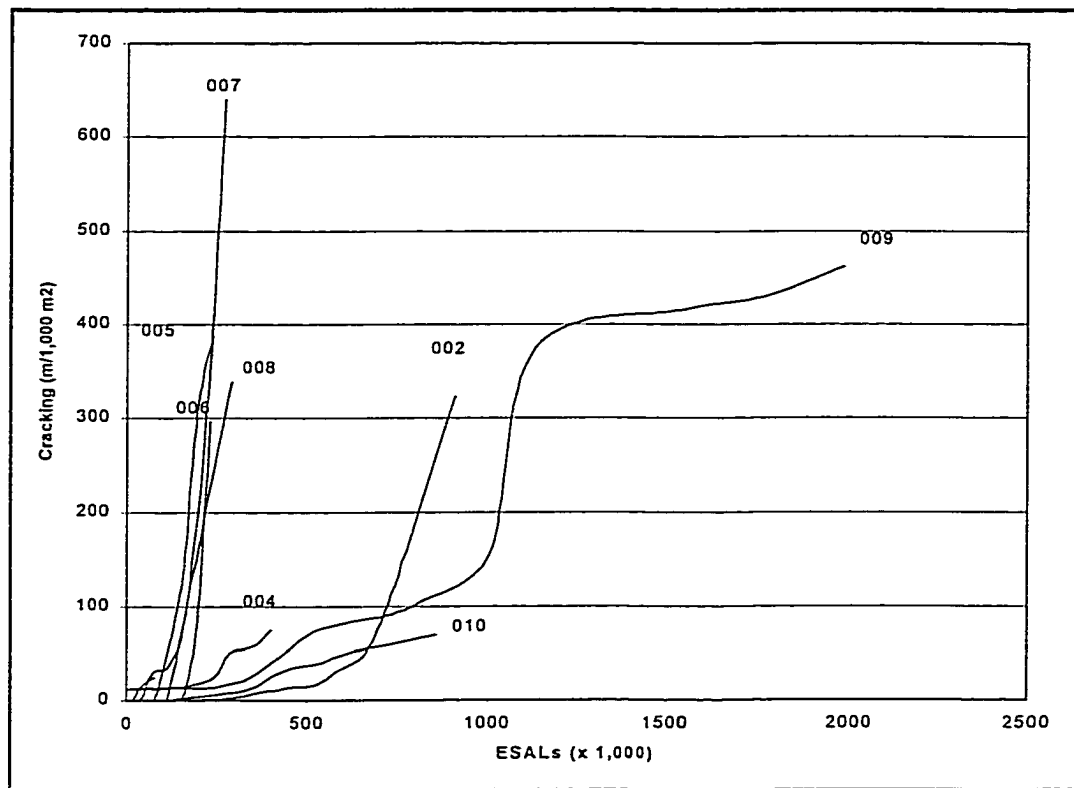


Figure 5. 5 Crack development for lanes 002 through 010

The data in Figure 5.4 show no clear difference in cracking development as a result of the percentage of cement in the soil cement of lanes 005, 006 and 007. The data also show that the best performance was achieved when using stone as the base over a soil cement subbase in lane 009. In other words, using soil cement as the subbase, rather than as base material, gives superior cracking resistance. When used as bases, the soil cement materials form shrinkage cracks which later reflect to the surface. However, the stone base intercepted those cracks and delayed their reflection to the surface. Post-mortem evaluations showed that there was evidence of cracking in the soil cement bases [62].

Reflection cracking plus softening of the soil cement immediately below the HMA may help explain why lanes 005 through 008 failed according to the roughness criteria. The rapid roughness development on these lanes may be due to the premature cracking, water penetration and softening of the soil cement that later contributed to the acceleration of the roughness development.

CHAPTER 6

IMPLEMENTATION OF ALF RESULTS

Methodology

The methodology used to evaluate the performance of the ALF materials when constructed at different soil conditions and traffic level is described as follows:

1. Overview the pavement design practices in Louisiana
2. Obtain information on roadbed soil conditions in Louisiana
3. Group parishes having relatively similar soil conditions
4. Select the levels of traffic representing the Louisiana road systems
5. Design the pavement structure for each set of ALF materials based on the soil conditions and traffic levels
6. Analyze the pavement sections using VESYS 3A-M and predict their life in terms of rutting and present serviceability index (PSI), and
7. Compare the predicted life among the sections.

Each of the items above is discussed in the following sections.

Pavement Design Practices in Louisiana

The Louisiana DOTD adopted the AASHTO pavement design guidelines [41] for their routine design with modifications for some of the input parameters to take into account the Louisiana conditions. Tables 6.1 through 6.3 present the suggested input parameters for use in design.

Surface Materials. There are five surface material types commonly used in Louisiana: Type 3, Type 7, Type 8, Type 8F, and Type 9. The use of each type of the materials depends on the design traffic volume as shown in Table 6.1. For example, Type 8, the material used at the ALF test sections, is recommended for roads with current average daily traffic (ADT) ranging from 2,500 to 6,999. For other traffic levels, the suggested surface material types are presented in Table 6.1. The suggested thickness for each layer of the surface material can be seen in Tables 6.2.

Table 6. 1 Pavement type with respect to traffic volume

| Current Traffic Volume, ADT | Wearing Course | Binder Course | Shoulder Wearing |
|-----------------------------|----------------|---------------|------------------|
| Less than 2,500 | Type 3 | Type 3 | Type 9 |
| 2,500 – 6,999 | Type 8 | Type 8 | Type 9 |
| 7,000 and up | Type 8F | Type 8 | Type 9 |
| General Aviation Airport | Type 7 | Type 7 | - |

Structural Coefficients. Table 6. 3 presents the layer coefficients ("a" values) commonly used in Louisiana. The layer coefficient for Type 8 was 0.44 assuming that the average moduli for this asphalt type was about 3,100 MPa (450,000 psi).

Another specific material type, the soil cement, was assigned a layer coefficient of 0.14.

Table 6. 2 Surface lift thickness specification

| Course | Minimum | Maximum | Preferred |
|-----------------|----------------|--------------|----------------|
| Wearing Course | 38 mm (1.5 in) | 51 mm (2 in) | 38 mm (1.5 in) |
| Binder Course | 51 mm (2 in) | 76 mm (3 in) | 51 mm (2 in) |
| Base Course | 51 mm (2 in) | - | - |
| Leveling Course | 25 mm (1 in) | Varies | - |

Serviceability Index. Table 6.4 shows the suggested serviceability index for Louisiana. As can be seen from the Table, the initial serviceability index for Interstate and Primary roads were 4.3. This value was based on the average value encountered in new road constructions in Louisiana, which ranges between 4.2 to 4.6 [67]. In addition, serviceability of 4.3 is the minimum acceptable value being targeted for major highways as the La DOTD implements the rolling profilograph for construction control and acceptance.

Reliability Level. According to the AASHTO guidelines [41], reliability is defined as “the probability that a pavement section designed using design-performance process will perform satisfactorily over the traffic and environment conditions for the design period.” The suggested values for reliability level varies with the functional class. For the Interstate system, for example, AASHTO suggests values between 85 to 99.99, while Louisiana suggested 99. Table 6.5 presents the suggested reliability levels for both AASHTO and Louisiana.

Table 6. 3 Layer coefficients for some materials commonly used in Louisiana

| Layer | Material Type | Layer Coefficients | |
|------------------------|--------------------------------------|-----------------------|-------------------------|
| | | U.S. Units (SN/in) | Metric Units (SN/mm) |
| Surface | Type 8 WC, BC | 0.44 | 0.01732 |
| Course | Type 8F | 0.44 | 0.01732 |
| | Type 3 WC | 0.42 | 0.01654 |
| | Type 3 BC | 0.42 | 0.01654 |
| Untreated Materials | Sand Clay Gravel | 0.07 | 0.00276 |
| | Sand/Shell, Shell | 0.14 | 0.00551 |
| Base Course | Crushed Stone or Crushed Slag | 0.14 | 0.00551 |
| | Recycled Portland Cement Concrete | 0.14 | 0.00551 |
| Cement | Soil Cement | 0.14 | 0.00551 |
| Treated or | Sand Clay Gravel | 0.14 | 0.00551 |
| Cement | Sand/Shell, Shell (5%) | 0.20 | 0.00787 |
| Stabilized | Recycled Portland Cement Concrete | 0.20 | 0.00787 |
| Base Course | | | |
| Asphalt Base Course | Hot Mix Base Course | 0.33 | 0.01299 |
| Subbase Course | Soil Cement | 0.14 | 0.00551 |
| | Crushed Stone | 0.14 | 0.00551 |
| | Sand/Shell, Shell | 0.14 | 0.00551 |
| | Sand Clay Gravel | 0.11 | 0.00433 |
| | Sand | 0.11 | 0.00433 |
| | Old Gravel, Shell Roadbed (8") | 0.11 | 0.00433 |

Table 6. 4 Serviceability index suggested for each functional class

| Functional Class | Δ PSI | P_i | P_t |
|------------------|--------------|-------|-------|
| Interstate | 1.5 | 4.3 | 2.8 |
| Primary | 1.8 | 4.3 | 2.5 |
| Collectors | 2.0 | 4.0 | 2.0 |
| Local | 2.0 | 3.5 | 1.5 |

Table 6. 5 Reliability level for each location and functional class

| Location | Functional Class | AASHTO Suggested Reliability Level | Louisiana Reliability Level |
|----------|------------------|------------------------------------|-----------------------------|
| Urban | Interstate | 85 – 99.99 | 99 |
| | Principal | 80-99 | 97 |
| | Collectors | 80 – 95 | 90 |
| | Local | 50 – 80 | 70 |
| Rural | Interstate | 80 – 99.99 | 97 |
| | Principal | 75 – 95 | 95 |
| | Collectors | 75 – 95 | 85 |
| | Local | 50 – 80 | 70 |

Overall Standard Deviation. The application of the reliability concept requires the selection of a standard deviation representative of local conditions. In lieu of availability of local data, AASHTO suggests a value of 0.45 and 0.35 for flexible and rigid pavements, respectively. Louisiana DOTD suggests that 0.47 be used for flexible pavements.

Roadbed Condition

Generally, the soil condition in Louisiana can be categorized as fair to poor due to the nature of the land. Temple and Shah [68] divided the principal soils in Louisiana into eight categories as follows:

- Silty clay
- Lime treated soil
- Silty sand
- Silty-clayey sand
- Clay loam
- Fine sand
- Well graded sand
- Heavy clay.

This classification was mostly based on data from soil survey reports [69] for Louisiana parishes. Even though the soil survey report used different names for each local area, when these classifications were related to the AASHTO method the soils generally fell into the categories listed above.

Resilient Moduli

The use of the resilient modulus value to define the soil characteristics in Louisiana is relatively new. It was after the extensive tests on resilient moduli as part of the Louisiana ALF base project in 1987 [68] and tests by Mohammad, et al., [70] that laboratory determination of resilient moduli became part of standard laboratory work. For this reason, only a few resilient modulus data points are available to describe soil characteristics across Louisiana. Before 1986 soil support values (R-values) were used to characterize the soil in pavement design. Roland [71] has performed extensive work on estimating soil support values from soil classifications and other engineering properties. Another correlation was

developed to relate the R-values to resilient moduli. Figure 6.1 shows the relationship between soil classification and resilient modulus, while Figure 6.2 shows the relationship between R-values and resilient modulus. In general, the resilient modulus for soils across Louisiana range from 48.3 MPa (7,000 psi) to 82.7 MPa (12,000 psi).

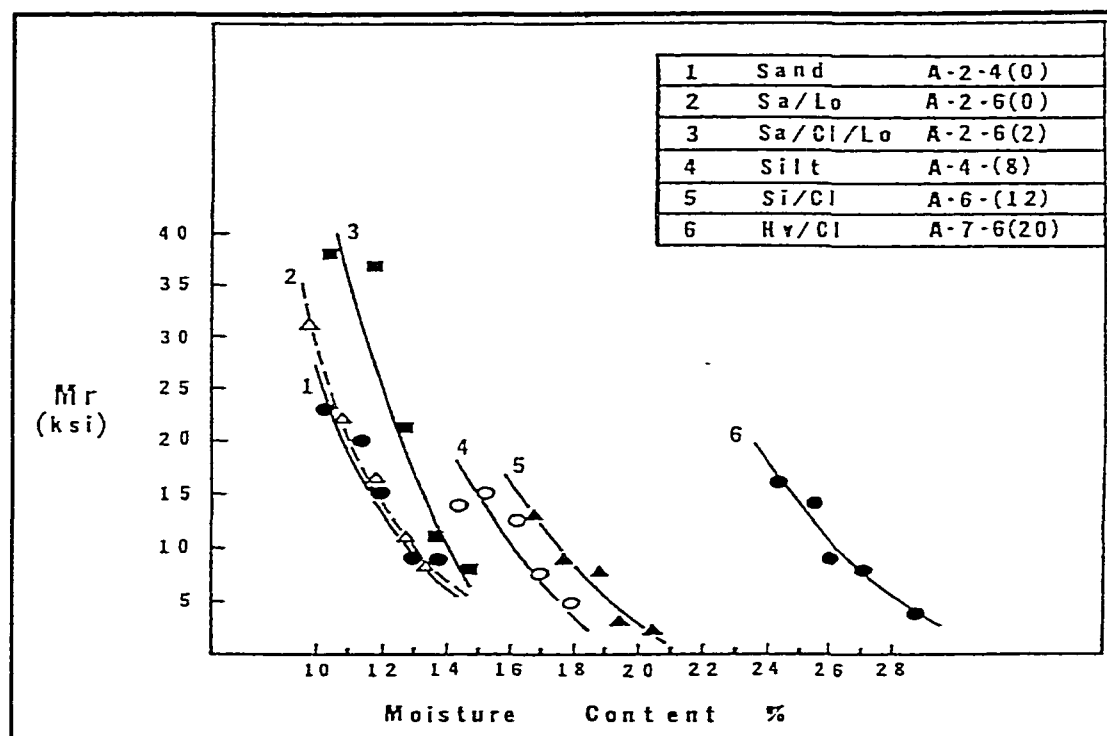


Figure 6. 1 Resilient modulus for typical Louisiana soil types [67]

It also a policy of the La DOTD not to permit a subgrade soil modulus to fall below 41.4 MPa (6,000 psi). When a soil has a modulus below 41.4 MPa (6,000 psi), the soil will be improved to raise the subgrade modulus to a minimum value of 41.4 MPa (6,000 psi).

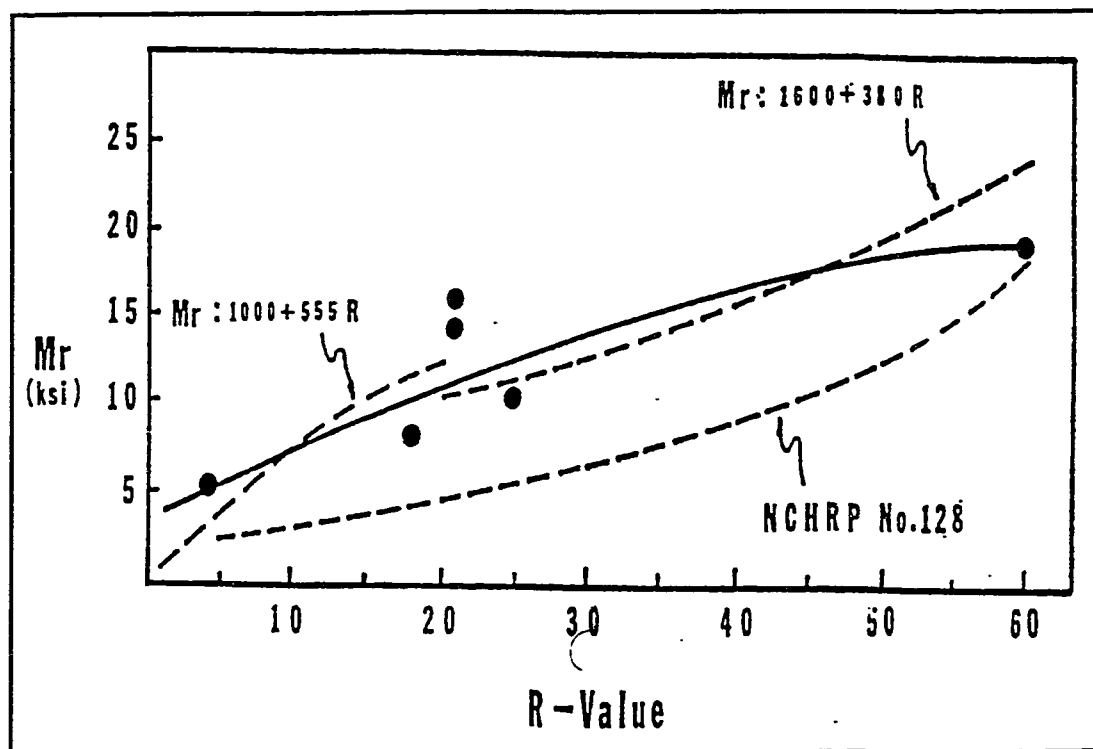


Figure 6.2 Soil resilient modulus – R-values correlation [67]

Grouping Parishes with Similar Soil Condition

The Louisiana soil conditions can be divided into three levels of moduli values: low, medium, and high as presented in Table 6.6. Low moduli are assigned to parishes with moduli ranging between 52.4 MPa (7,600 psi) to 57.9 MPa (8,400 psi); medium values for those with moduli ranging between 60.7 MPa (8,800 psi) to 65.5 MPa (9,500 psi); and high values for those with moduli ranging between 68.3 MPa (9,900 psi) to 77.9 MPa (11,300 psi) or more.

Table 6. 6 Range of moduli used in the analysis

| Level | Moduli Range, MPa (psi) | Parishes |
|-------|---------------------------------|--|
| I | 52.4 – 58.0 (7,600 – 8,400) | Allen, Ascension, Assumption, Concordia, East Baton Rouge, Iberville, Jefferson, Jefferson Davis, Orleans, St. Bernard, St. Charles, St. James, St. John, St. Martin, Vermillion. |
| II | 60.7 – 65.5 (8,800 – 9,500) | Acadia, Avoyelles, Beauregard, Bossier, Calcasieu, Cameron, Desoto, East Carrol, Evangeline, Catahoula, Iberia, Jackson, Lafourche, Lasalle, Livingston, Madison, Morehouse, Pointe Coupee, Richland, Sabine, St. Helena, St. Landry, St. Mary, St. Tammany, Tensas, Terrebonne, Vernon, Washington, Webster, West Baton Rouge, West Carrol. |
| III | 68.2 – 77.9 (9,900 – 11,300) | Bienville, Caddo, Caldwell, Clairborne, East Feliciana, Franklin, Grant, Lafayette, Lincoln, Natchitoches, Ouachita, Plaquemines, Rapides, Red River, Tangipahoa, Union, West Feliciana, Winn. |

Traffic Analysis

To determine the level of traffic common on Louisiana highways, a search of the Louisiana traffic monitoring report was conducted. In addition, the criteria used by the pavement design and geotechnical section of the LaDOTD was also considered. As shown in Table 6.1, the LaDOTD sets a criteria that Type 8 material be used for roads with ADT more than 2,500. From the 1996 traffic monitoring report, it was found that the ADT for Louisiana roadway system varies from as low as 500 to as high as 150,000. High-volume traffics were encountered

at urban Interstate systems, while moderate traffic volumes were mostly encountered in urban state highway system. Reviewing the pattern of traffic volume in Louisiana, Table 6.7 is presented to classify the traffic levels to be used in this study.

Table 6. 7 Traffic level used in the study

| Level | ADT Range | Design ADT |
|-------|-----------------|------------|
| I | 2,500 – 5,9999 | 4,000 |
| II | 6,000 – 9,999 | 8,000 |
| III | 10,000 – 19,999 | 15,000 |
| IV | 20,000 – 29,999 | 25,000 |
| V | 30,000 – 49,999 | 40,000 |
| VI | >50,000 | 75,000 |

Conversion of ADT to ESALs

In order for the traffic data to be useful in pavement design, volume data must be converted to the number of 18,000 equivalent single axle loads (ESALs). Equation 6.1 can be used to compute the number of ESALs for 1 year from ADT data [71]:

$$ESAL = ADT \times TKS \times DD \times LD \times TF \times 365 \times \left(1 + \frac{GR}{100}\right)^n \quad (6. 1)$$

Where:

ESAL = Number of 80 kN ESAL applications in the design lane for year 1

ADT = Initial two-way average daily traffic, vehicle per day

TKS = Percent of ADT that is heavy trucks (FHWA class 5 or greater)

DD = Directional distribution of truck traffic

LD = Lane distribution of trucks in design lane

TF = Average truck factor for all trucks, ESALs per truck

GR = growth rate in percent per year

N = number of years in the analysis period

Note that the truck factor (TF) in the above equation is the average of all vehicle class in lieu of more detail data. Otherwise, more detail truck factor for each class should be used, as discussed in the next section.

Growth Rate. Future traffic can be reasonably estimated from the current traffic level by giving an appropriate traffic growth rate. The following factors should be considered when selecting a traffic growth rate [72]:

- Historical trends exhibited by ADT and ADTT traffic volumes
- Future highway system changes and land usage in the vicinity
- General expected future trends in truck volumes in the vicinity, based upon economic, political, and other factors.

Unless a detailed study is needed for a specific location, the LaDOTD office of planning usually uses 3 percent as the estimated traffic growth.

Directional Distribution. The directional distribution is the percent of truck traveling in one direction. In most cases, it is reasonable to assume that 50 percent of the truck traffic is traveling in each direction [72].

Lane Distribution. The lane distribution factor is the percentage of truck traffic in the design lane, usually the outer lane. The lane distribution may vary among roads depending of the number of lanes and the traffic volume. In many of occasions, outer lanes usually carry more truck traffic than the inner lanes. In

lieu of project-specific data, Table 6.8 can be used to estimate the lane distribution factor.

Table 6. 8 Lane distribution factor guidelines from AASHTO [41]

| Number of Lanes in Both Directions | 80 kN ESAL Traffic in Design Lane (%) |
|------------------------------------|---------------------------------------|
| 1 | 100 |
| 2 | 80 – 100 |
| 3 | 60 – 80 |
| >4 | 50 – 75 |

Calculation of the Total Number of ESALs

An MS Excel spreadsheet macro was developed to calculate the number of ESALs for the whole performance period, as shown in Table 6.9. To determine the percentage of ADT for each functional class, one can use Table 6. 10, based on the 1986 average classification counts for Louisiana roads. The definition of functional class is presented in Table 6.11. The average truck factor for Louisiana traffic, expressed in ESALs/truck, is presented in Table 6.12 for terminal serviceability of 2.5 and Table 6.13 for terminal serviceability of 2.0. These statewide averages are used for pavement design and were developed from all the W-4 weight tables developed in the state vehicle weighing program. The value in Table 6.12 was obtained from the 1996 data. These data are usually updated annually.

Table 6. 9 A sample of spreadsheet used to calculate 18-kips ESALs

| Functional Class: | | 02 (Rural Principal Areas) | | | | |
|-------------------------------|-------|----------------------------|-----------------|--|---------------------------------|-----------------------|
| Performance Period: | | 20 | | | | |
| ADT/ADTT: | | 4,000 | | | | |
| Directional Distribution (%): | | 50 | | | | |
| Lane Distribution (%): | | 90 | | | | |
| Class | % ADT | ADT per Class | % Annual Growth | Avg. Initial Truck Factor (ESAL/Truck) | % Annual Growth in Truck Factor | Accumulated 18K ESALs |
| 1 | 0.52 | 21 | 3 | 0.0005 | 0 | 46 |
| 2 | 68.36 | 2,734 | 3 | 0.0005 | 0 | 6,034 |
| 3 | 16.42 | 657 | 3 | 0.0188 | 0 | 54,497 |
| 4 | 0.46 | 18 | 3 | 0.1932 | 0 | 15,689 |
| 5 | 2.13 | 85 | 3 | 0.1932 | 0 | 72,648 |
| 6 | 1.22 | 49 | 3 | 0.4092 | 0 | 88,132 |
| 7 | 0.03 | 1 | 3 | 0.4092 | 0 | 2,167 |
| 8 | 1.23 | 49 | 3 | 0.8814 | 0 | 191,389 |
| 9 | 8.8 | 352 | 3 | 1.1 | 0 | 1,708,891 |
| 10 | 0.49 | 20 | 3 | 1.45 | 0 | 125,431 |
| 11 | 0.18 | 7 | 3 | 1.84 | 0 | 58,470 |
| 12 | 0.02 | 1 | 3 | 1.84 | 0 | 6,497 |
| 13 | 0.12 | 5 | 3 | 1.84 | 0 | 38,980 |
| Total | 100 | 3,999 | | | Total | 2,368,870 |

Table 6. 10 Classification counts (%) of vehicles

| FC* | TV** | CYCLE % | CARS % | 2A-4T % | BUSSES % | 2A-SU % | 3A-SU % | 4A-SU % | 4A-ST % | 5A-ST % | 6A-ST % | 5A-MT % | 6A-MT % | 7A-MT % | NONE % | NOT CLASSED % | AXLE FACTOR |
|-----|-----------|---------|--------|---------|----------|---------|---------|---------|---------|---------|---------|---------|---------|---------|--------|---------------|-------------|
| 01 | 1,820,026 | 0.77 | 62.38 | 11.88 | 0.34 | 2.12 | 0.90 | 0.04 | 3.59 | 12.27 | 0.41 | 0.62 | 0.11 | 0.19 | 0.00 | 4.36 | 0.797 |
| 02 | 301,393 | 0.52 | 68.36 | 16.42 | 0.46 | 2.13 | 1.22 | 0.03 | 1.23 | 6.36 | 0.49 | 0.18 | 0.02 | 0.12 | 0.00 | 2.46 | 0.882 |
| 06 | 333,947 | 0.49 | 64.85 | 19.10 | 0.45 | 2.71 | 1.50 | 0.22 | 1.38 | 5.80 | 0.56 | 0.21 | 0.19 | 0.30 | 0.00 | 2.28 | 0.885 |
| 07 | 424,785 | 0.43 | 70.31 | 19.66 | 0.34 | 2.59 | 1.14 | 0.05 | 0.79 | 2.53 | 0.18 | 0.00 | 0.00 | 0.07 | 0.00 | 3.37 | 0.942 |
| 08 | 90,255 | 0.99 | 69.62 | 21.50 | 0.55 | 2.22 | 0.87 | 0.10 | 0.61 | 0.88 | 0.09 | 0.00 | 0.00 | 0.05 | 0.00 | 4.63 | 0.967 |
| 11 | 654,774 | 0.70 | 67.61 | 13.38 | 0.23 | 1.84 | 1.19 | 0.12 | 1.93 | 7.30 | 0.46 | 0.31 | 0.06 | 0.39 | 0.00 | 4.48 | 0.857 |
| 12 | 10,703 | 0.13 | 86.82 | 5.04 | 0.00 | 1.82 | 1.26 | 0.04 | 0.74 | 3.06 | 0.04 | 0.03 | 0.00 | 0.00 | 0.00 | 1.03 | 0.942 |
| 14 | 1,704,121 | 0.28 | 74.12 | 16.64 | 0.17 | 1.91 | 0.92 | 0.04 | 0.67 | 2.19 | 0.21 | 0.03 | 0.01 | 0.13 | 0.00 | 2.67 | 0.949 |
| 16 | 141,205 | 0.35 | 74.41 | 15.92 | 0.23 | 1.69 | 2.44 | 0.09 | 0.49 | 1.87 | 0.21 | 0.00 | 0.00 | 0.06 | 0.00 | 4.14 | 0.949 |
| 17 | 114,653 | 0.93 | 80.05 | 13.04 | 0.24 | 1.55 | 0.46 | 0.03 | 0.37 | 0.30 | 0.05 | 0.00 | 0.00 | 0.14 | 0.00 | 5.36 | 0.971 |

*FC = Functional class. See Table 11

**TV = Total volume

Table 6. 11 FHWA functional class description

| Code | Description | Code | Description |
|------|---------------------------------|------|--|
| | Rural | | Urban |
| 01 | Principal Arterial – Interstate | 11 | Principal Arterial – Interstate |
| 02 | Principal Arterial – Other | 12 | Principal Arterial – Other Freeways and Expressways |
| 06 | Minor Arterial | 14 | Principal Arterial – Other |
| 07 | Major Collector | 16 | Minor Arterial |
| 08 | Minor Collector | 17 | Collector |
| 09 | Local | 19 | Local |

Table 6. 12 1996 Louisiana equivalency factors for each classification vehicle for $PSI_i = 2.5$

| FHWA Vehicle Classification | Description | Equivalency Factors |
|-----------------------------|--|---------------------|
| 1 | Motorcycles | 0.0005 |
| 2 | Passenger Cars | 0.0005 |
| 3 | Other Two-Axle, Four-Tire Single Unit Vehicles | 0.0188 |
| 4 | Buses | 0.1932 |
| 5 | Two-Axle, Six-Tire Single Unit Trucks | 0.1932 |
| 6 | Three-Axle Single Unit Truck | 0.4095 |
| 7 | Four or More Axle Single Unit Trucks | 0.4095 |
| 8 | Four or Less Axle Single Trailer Trucks | 0.8814 |
| 9 | Five Axle Single Trailer Trucks | 1.1000 |
| 10 | Six or More Axle Single Trailer Trucks | 1.4500 |
| 11 | Five or Less Axle Multi Trailer Trucks | 1.8400 |
| 12 | Six Axle Multi Trailer Trucks | 1.8400 |
| 13 | Seven or More Axle Multi Trailer Trucks | 1.8400 |

Table 6. 13 1996 Louisiana equivalency factors for each classification vehicle for $PSI_e = 2.0$

| FHWA Vehicle Classification | Description | Equivalency Factors |
|-----------------------------|--|---------------------|
| 1 | Motorcycles | 0.0004 |
| 2 | Passenger Cars | 0.0004 |
| 3 | Other Two-Axle, Four-Tire Single Unit Vehicles | 0.0143 |
| 4 | Buses | 0.1694 |
| 5 | Two-Axle, Six-Tire Single Unit Trucks | 0.1694 |
| 6 | Three-Axle Single Unit Truck | 0.3836 |
| 7 | Four or More Axle Single Unit Trucks | 0.3836 |
| 8 | Four or Less Axle Single Trailer Trucks | 0.8523 |
| 9 | Five Axle Single Trailer Trucks | 1.0450 |
| 10 | Six or More Axle Single Trailer Trucks | 1.4500 |
| 11 | Five or Less Axle Multi Trailer Trucks | 1.8400 |
| 12 | Six Axle Multi Trailer Trucks | 1.8400 |
| 13 | Seven or More Axle Multi Trailer Trucks | 1.8400 |

Analysis Method

Using the subgrade modulus (Table 6.6) and traffic levels (Table 6.7) discussed in the previous sections, the cells in Table 6.14 represents the combinations of subgrade modulus and traffic level included in this study. Tables 6.15 and 6.16 summarize the actual values of the traffic levels and subgrade moduli used in the analysis. For each traffic level and subgrade shown in cells 1 through 18 in Table 6.14, nine pavement sections representing lanes 002 through 010 of the ALF study were included for a total of 162 sections. Each section was

designed using the AASHTO method to determine the layer thicknesses for each section. These results are presented in Tables A5.1 through A5.9 in Appendix 5.

Once the thickness for each pavement was determined, VESYS 3A-M was run using material information and thicknesses for each pavement to predict the rut depth and PSI at the end of the performance period.

Table 6. 14 Design combinations of subgrade and traffic level included in this study

| | | Traffic Level | | | | | |
|----------|-----|---------------|----|-----|----|----|----|
| | | I | II | III | IV | V | VI |
| Subgrade | I | 1 | 2 | 3 | 4 | 5 | 6 |
| | II | 7 | 8 | 9 | 10 | 11 | 12 |
| | III | 13 | 14 | 15 | 16 | 17 | 18 |

Table 6. 15 Summary of traffic level used in the analysis

| Level | Average ADT | ESALs |
|-------|-------------|------------|
| I | 4,000 | 2,370,000 |
| II | 8,000 | 4,740,000 |
| III | 15,000 | 8,883,000 |
| IV | 25,000 | 14,805,000 |
| V | 40,000 | 23,690,000 |
| VI | 75,000 | 44,446,000 |

Table 6. 16 Summary of subgrade level used in the study

| Level | Modulus, psi |
|-------|--------------|
| I | 8,000 |
| II | 9,150 |
| III | 10,600 |

Performance Criteria

There are two criteria used in this study to evaluate the pavement performance: rutting and serviceability index. A pavement is considered to perform satisfactorily when it meets these two requirements while carrying the design traffic. The Louisiana DOTD sets the criteria for the maximum rutting allowed to occur in a roadway at 19 mm (0.75 in). At this rut level, the road is usually in a deteriorated condition and the wheelpath ruts begin to hold water causing a safety problem. In addition, setting rut level deeper than 19 mm (0.75 in) might cause danger to drivers particularly during rainy seasons where hydroplaning might occur. From the VESYS analysis it was also found that at this rut level, the serviceability index is usually below 2.0. The second performance criterion is the serviceability index (PSI). In this study the lowest acceptable serviceability is 2.5, based on the La DOTD requirements for primary road functional class (Table 6.4). At a P_i of 2.5, the road should receive rehabilitation to restore the riding quality.

Results and Discussions

Rutting Evaluation

Figures 6.3 through 6.8 show the VESYS predictions of rutting at the end of the 20-year performance period for pavements designed in parishes with subgrade moduli of 55.2 MPa (8,000 psi). As can be observed from Figures 6.3 through 6.8, in the regions with subgrade moduli of 55.2 MPa (8,000 psi) and traffic up to about 40,000 ADT, VESYS predicted that all pavement sections could perform satisfactorily under given conditions except for those designed using materials similar to those in lane 004. One can also observe that at the traffic level up to 15,000 ADT, pavements designed using soil cement bases experienced little rutting compared with pavements with crushed stone materials. However, at the higher traffic level, the pattern changes. Pavements with soil cement bases rutted to the same level or higher than pavements with crushed stone bases. For example, at 25,000 ADT pavements designed using crushed stone materials (lanes 002 and 003) and soil cement materials (lane 005, 007 and 008) were predicted to rut to about 51 mm (0.5 in). At 40,000 ADT pavements with materials similar to lanes 005, 007 and 008 rutted to about 16.5 mm (0.65 in), while pavements with crushed stone bases were predicted to rut to about 15 mm (0.60 in). At 75,000 ADT, pavements with similar materials to lanes 005, 007 and 008 were even predicted to rut to about 25 mm (1 in).

In general, pavements with materials similar to those in lanes 006 and 010 outperformed all other material combinations at any traffic level included in this

study. Pavements with sandwiched sections (lane 009), however, outperformed all conventional configurations at the higher levels of traffic.

Figures 6.9 through 6.14 show the rutting prediction at the end of the 20-year performance when designed in parishes with subgrade moduli of 63.1 MPa (9,150 psi). As can be seen from the figures, the patterns are almost identical to those in parishes with subgrade moduli of 55.2 MPa (8,000 psi). For example, up to 40,000 ADT all pavement sections performed satisfactorily. At traffic levels up to 15,000 ADT, pavements with soil cement bases outperformed those with crushed stone bases. At the higher traffic level, say at 40,000 ADT, pavements with crushed stone bases (lanes 002 and 003) outperformed pavements designed using materials similar to lanes 005, 007 and 008. Pavements with crushed stone bases performed satisfactorily even with 75,000 ADT. Again, pavements with bases similar to lanes 006 and 010 outperformed all other pavements at any traffic levels.

Figures 6.15 through 6.20 show the rutting prediction at the end of the 20-year performance when designed in parishes with subgrade modulus of 73.1 MPa (10,600 psi). Up to traffic level of 25,000 ADT all pavements performed satisfactorily since none of them was predicted to rut more than 19 mm (0.75 in). At 40,000 ADT, pavements with crushed stone bases could fail since the rutting in these pavements is slightly less than 19 mm (0.75 in). At the higher traffic level, say 75,000 ADT, pavements designed using materials similar to lanes 006, 009 and 010 would perform well. Surprisingly, pavements designed using materials similar to lanes 002 and 003 also performed well.

As Figures 6.3 through 6.20 show, pavements designed using materials similar to those used in Lane 004 of ALF test section have the worst performance at all locations in Louisiana and at all traffic levels included in the study. Therefore, combinations of crushed stone and stone-stabilized select soil for base and subbase materials should be avoided until reasons for their poor performance can be evaluated.

Figures 6.3 through 6.21 also show that pavements designed using soil cement bases show superior performance to those designed using crushed stone materials. These predictions are, in fact, in line with the performance observed for existing soil cement pavements in Louisiana. However, one should note that the VESYS model used in this study cannot model the cracks occurring in the soil cement that reflect through the HMA material and form surface cracks. These cracks have become a major issue because once they become prevalent, water infiltrates through the surface materials. Once water penetrates and stays in the base, the strength of the base material is reduced. Eventually, the pavement performance will be shortened as has been demonstrated very noticeably in the ALF test sections.

The results showing that pavements designed using materials of Lanes 006 and 010 (soil cement bases) have better performance than those designed using crushed stone materials seem to contradict the results from the ALF test sections. As presented in Chapter 3, lane 002 which was constructed using crushed stone material had better performance than those of lanes 005 through 008. One should keep in mind that this simulation study assumed that the material

properties for the bases and subbases are uniform throughout the performance period and there was no water in the subbase. When the ALF experiment was conducted, these conditions were not met. A post-mortem evaluation revealed the presence of water in both the base and subbase. The post-mortem evaluation also revealed that the soil cement bases experienced rutting, which is not expected for this type of materials. The effect of water in the subbase is more serious in the soil cement bases than those in crushed stone bases because water can stay longer in soil cement bases than in crushed stone bases causing the base to soften. In addition, studies of moisture-induced damage in flexible pavements confirm that the strength and moduli of asphaltic concrete mixtures are adversely affected by the presence of moisture [73]. Other studies also confirmed that wheel loads on flooded sections are many times more damaging than those on a dry pavements [74].

Serviceability Evaluation

All the sections in this simulation study were designed to meet class 2 functional requirements. The La DOTD practice involves designing class 2 roads with an initial serviceability index (SI) of 4.3 and a terminal serviceability index of 2.5. Figure 6.21 through 6.38 show the predicted PSI for pavements designed using materials similar to those used in Lanes 002 through 10. The Figures show that at the average subgrade modulus of 55.1 MPa (8,000 psi) and traffic of up to 15,000 ADT, VESYS predicted that, except for pavements with lane 004 materials, all pavements designed either using crushed stone bases or soil cement bases

should carry the design traffic at serviceability levels above the minimum for any area in Louisiana. As shown in the figures, at the end of the performance period all pavements have a PSI of 2.5 or higher.

At the traffic level of 25,000 ADT, only pavements with soil cement bases have a PSI above 2.5. Pavements with crushed stone bases fell below 2.5, the allowable minimum value for the class 2 functional class. At a higher traffic level, say, at the ADT of 40,000, only pavements designed using materials similar to lanes 006 and 010 could have a PSI above 2.5 at the end of the performance period. However, at the traffic level of 75,000 ADT no ALF pavement sections have a PSI above 2.5.

In parishes that have an average subgrade modulus of 63.1 MPa (9,150 psi), see Figures 6.27 through 6.32, and up to traffic level of 15,000 ADT, VESYS predicted that almost all pavements designed using ALF materials should perform satisfactorily. At the end of the performance period, the serviceability index is at or above 2.5 except for those designed using materials similar to those used in Lane 004, which has a PSI at 2.48. At the higher traffic level, say, at 25,000 ADT, only pavements designed using cement treated materials performed satisfactorily. At 40,000 ADT only pavements designed using materials similar to lanes 006 and 010 were predicted to perform as expected. However, at traffic level higher than 75,000 ADT, none of the pavements would perform satisfactorily since at the end of the performance period, all pavements had predicted PSI below 2.5.

In parishes that have an average subgrade modulus of 73.1 MPa (10,600 psi), see Figures 6.33 through 6.38, and up to traffic level of 25,000 ADT, VESYS

predicted that almost all pavements designed using ALF materials should perform satisfactorily. At the end of the performance period, the serviceability index is at or above 2.5 except for those designed using materials similar to those used in Lanes 002 and 003, which has a PSI at 2.49. At the higher traffic level, say, at 40,000 ADT, only pavements designed using cement treated materials performed satisfactorily. Pavements designed using materials similar to lane 009 has a PSI of 2.48 at the end of performance period. However, at traffic level higher than 75,000 ADT, none of the pavements would perform satisfactorily since at the end of the performance period, all pavements had predicted PSI below 2.5.

Why is It Different from the ALF Results?

As shown in Chapter 5, based on the ALF test results, lanes 002, 009 and 010 outperformed other test sections and were recommended for use in new pavement constructions. In this simulation study, however, materials similar to those used in lanes 006, 009 and 010 outperformed other material types and combinations. These differences can be explained as follows:

1. Typical section. The thickness of the ALF test sections were based on the typical sections in Louisiana, i.e., 38 mm (1.5 in) for wearing course, 51 mm (2 in) for binder course, 216 mm (8.5 in) for base either soil cement or crushed stone materials, and 89 mm (3.5 in) for subbase totaling 394 mm (15.5 in) for the whole structure. In other words, it seems that the thicknesses were not designed to carry the same traffic levels but were

selected to keep the pavement geometry at the test site about the same. In designing an individual pavement using different materials with different resilient modulus and "a" values, those cross sections made with materials having higher resilient moduli would have thinner layers. The resilient moduli for crushed stone material ranges from 137.9 MPa (20,000 psi) to 482.6 MPa (70,000 psi) while that for soil cement material ranges from 689.5 MPa (100,000 psi) to 3792.1 MPa (550,000 psi). Realizing the difference between soil cement and crushed stone materials, one would expect that the thickness of the pavement made from these two materials would be different when designed for the same number of equivalent single axle loads (ESALs). Likewise, one would expect that the number of ESALs carried to failure would vary for the same layer thickness of these two materials in a pavement, as in the case of the ALF test sections.

2. Environmental Effect. As mentioned in the previous section, this simulation study assumes the uniformity of the material properties. For example, the study assumed that the resilient modulus for soil cement is constant at 1034.2 MPa (150,000 psi) for the whole performance period. Data from the ALF test sections showed that lanes with soil cement bases experienced surface cracks. These cracks were caused by the reflection of cracks initiated in the soil cement bases due to shrinkage. Rainfall data also showed that the rate of the total rainfall in the ALF site was high during the experiment. The surface cracks allowed the water to infiltrate the pavement structure. In addition, the water table in the ALF site is high particularly

when the water level of the Mississippi River was at its peak. The presence of water in the base and subbase may reduce the strength and the resilient modulus of the pavement structure substantially. This hypothesis was supported by the post mortem evaluation in which there was evidence that rutting also occurred in the pavements with soil cement bases and subbases, which was not expected to occur for this type of material. As for lane 009, the inverted section, the water pore pressure effect should not be as severe as in other lanes with soil cement bases due to the existence of crushed stone layer between HMA and soil cement material. This layer could function both as crack resistant interlayer and for drainage. Therefore, the performance of this lane was much better than other lanes with only soil cement bases.

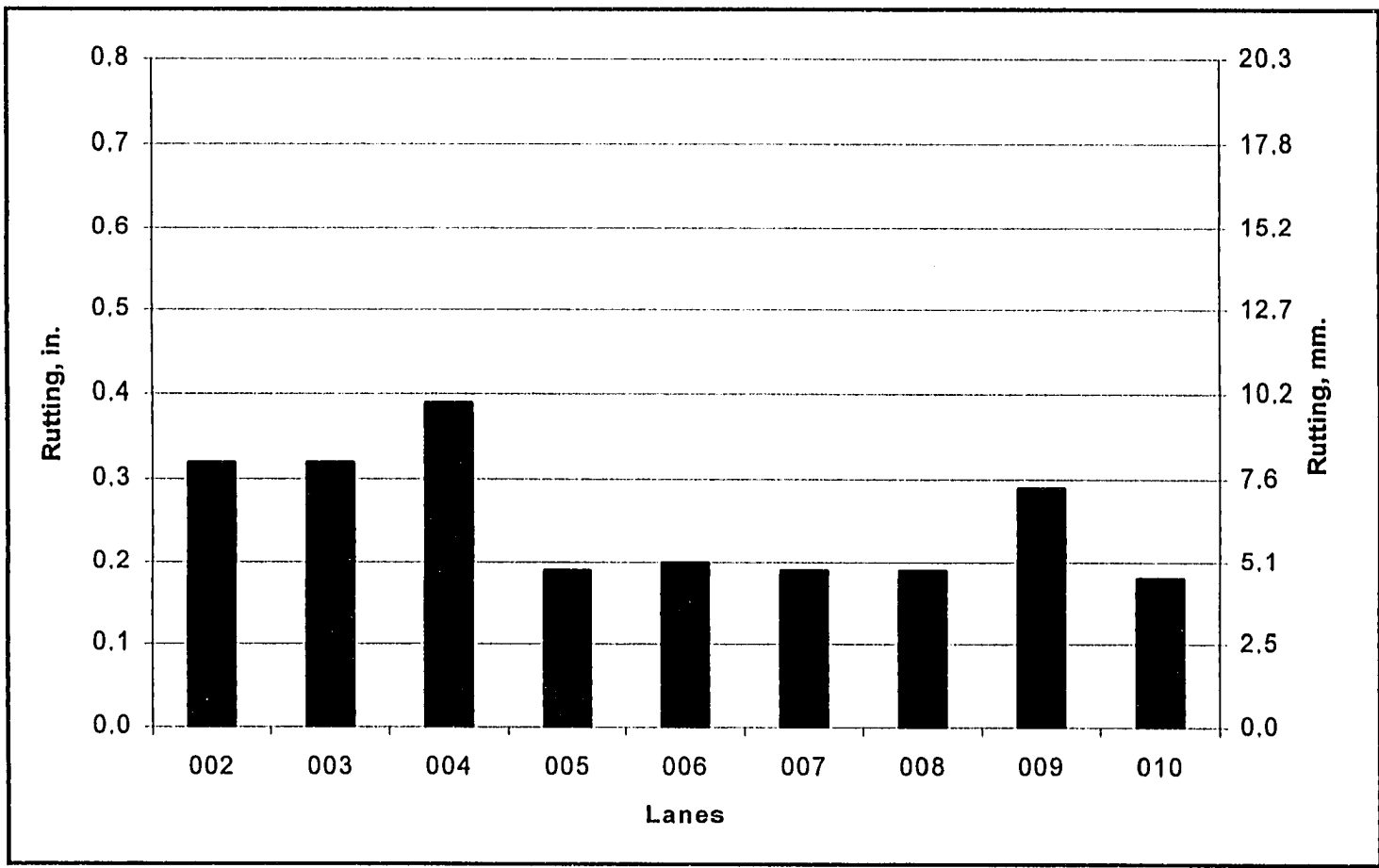


Figure 6. 3 Predicted rutting comparison at the end of a 20-year performance period for pavements designed for an average ADT of 4,000 and subgrade modulus of 8,000 psi

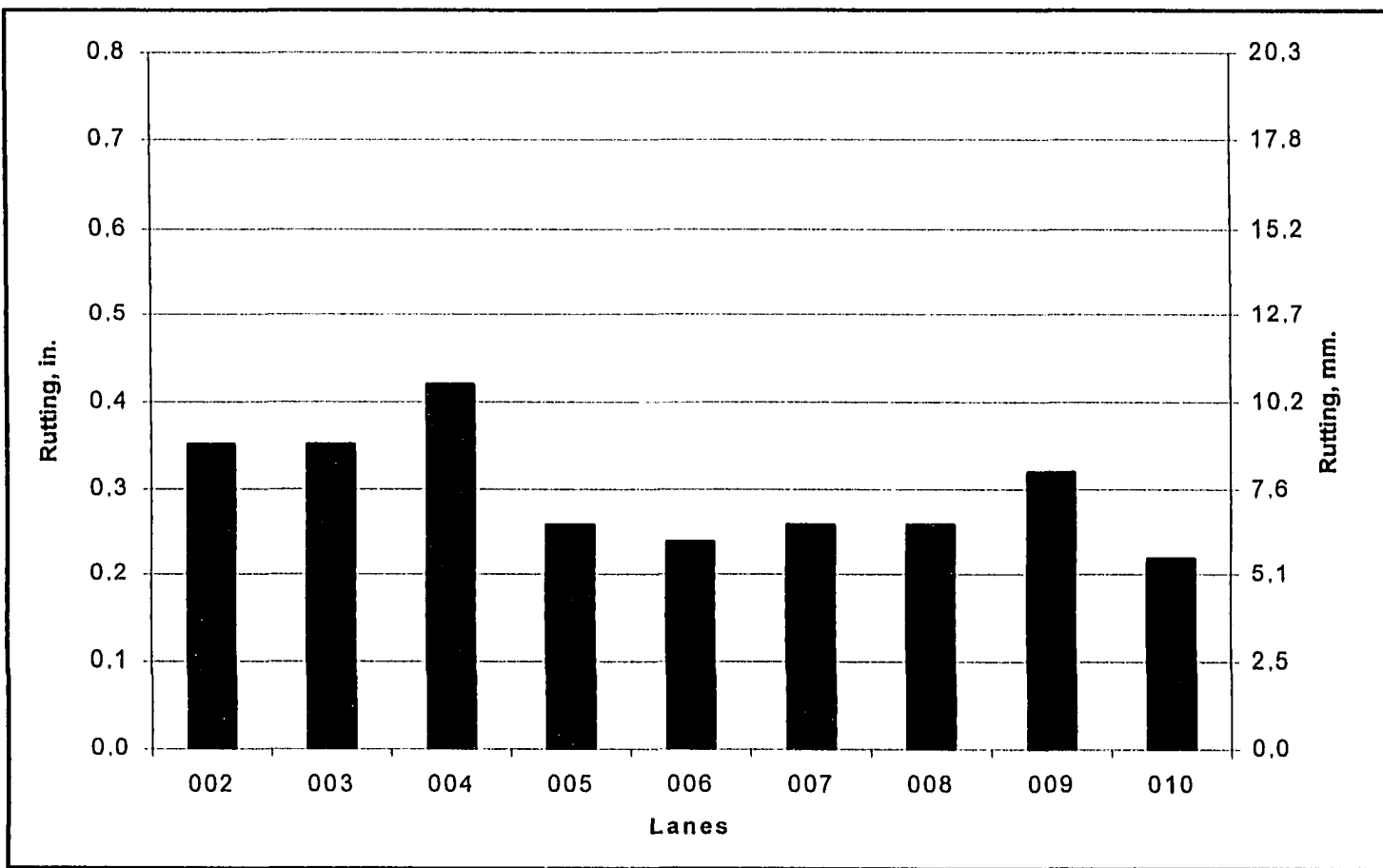


Figure 6. 4 Predicted rutting comparison at the end of a 20-year performance period for pavements designed for an average ADT of 8,000 and subgrade modulus of 8,000 psi

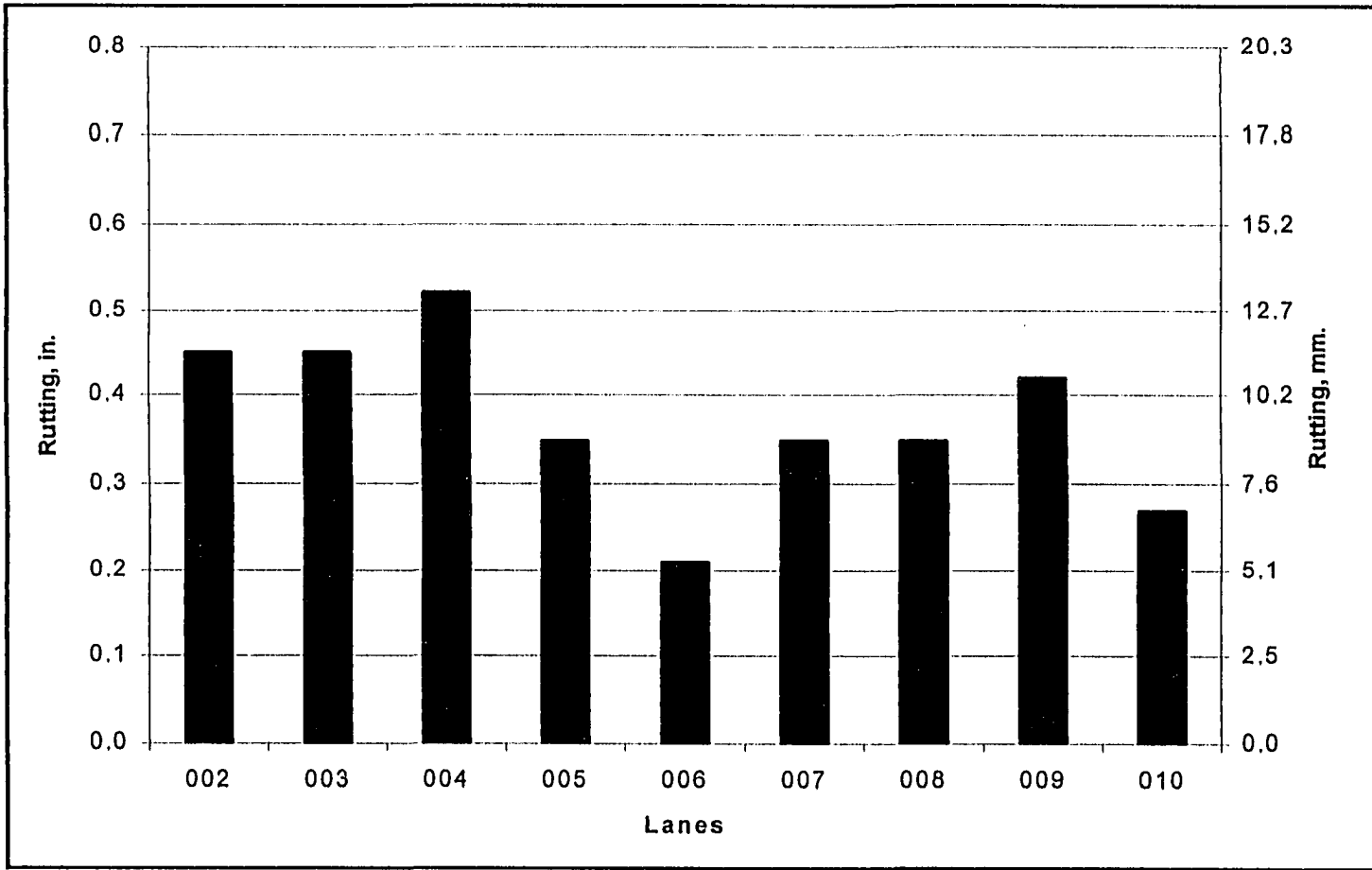


Figure 6. 5 Predicted rutting comparison at the end of a 20-year performance period for pavements designed for an average ADT of 15,000 and subgrade modulus of 8,000 psi

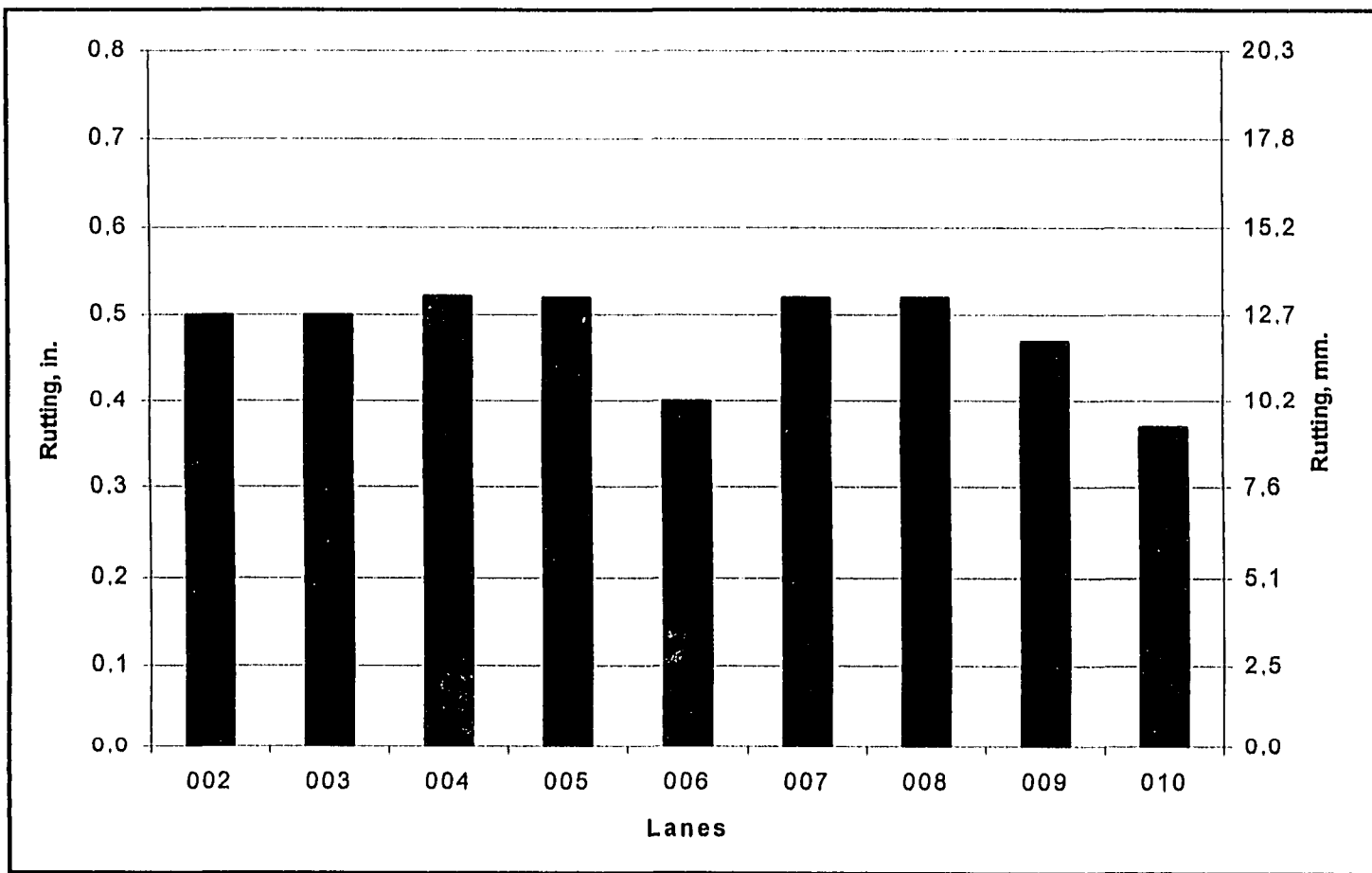


Figure 6. 6 Predicted rutting comparison at the end of a 20-year performance period for pavements designed for an average ADT of 25,000 and subgrade modulus of 8,000 psi

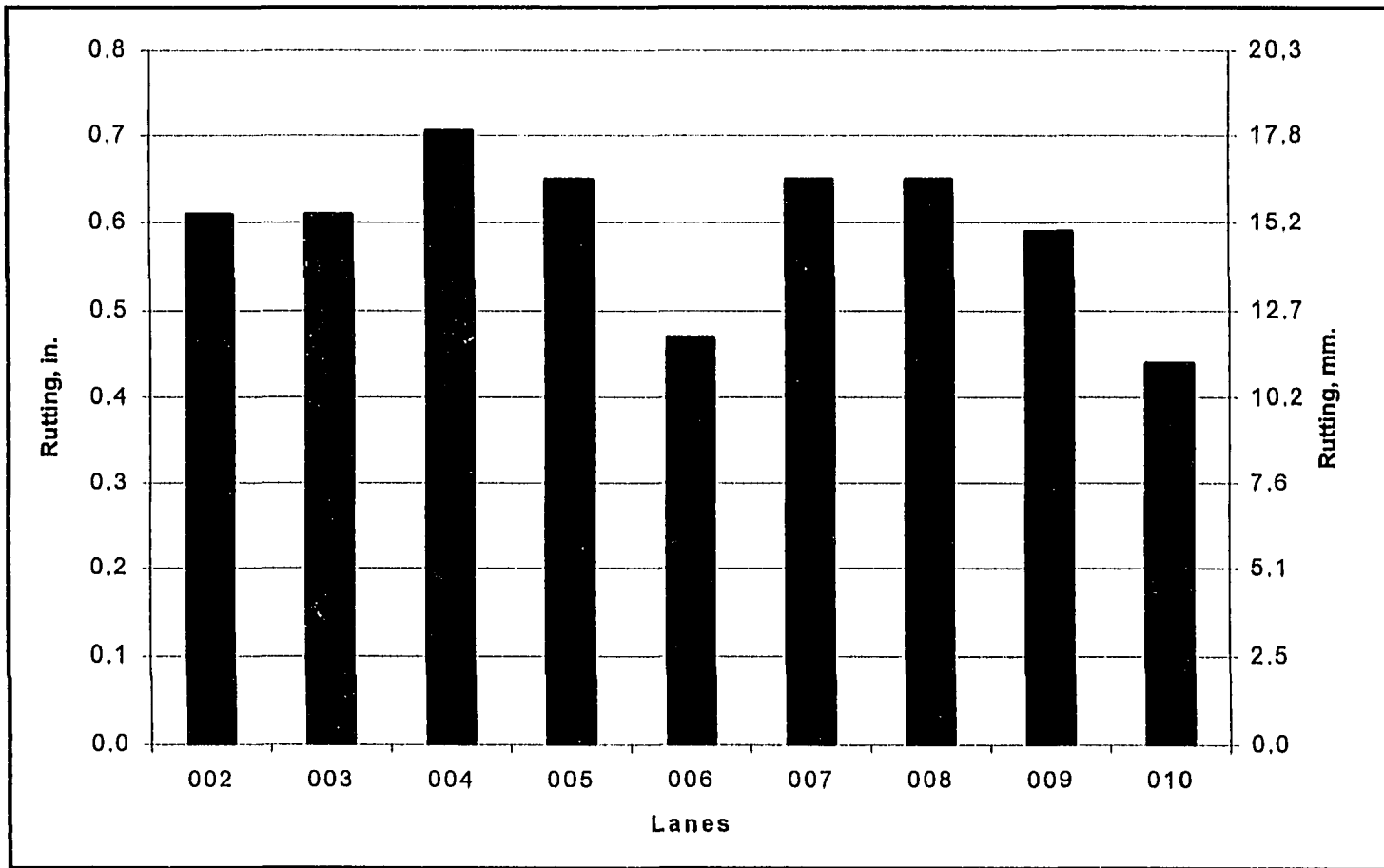


Figure 6. 7 Predicted rutting comparison at the end of a 20-year performance period for pavements designed for an average ADT of 40,000 and subgrade modulus of 8,000 psi

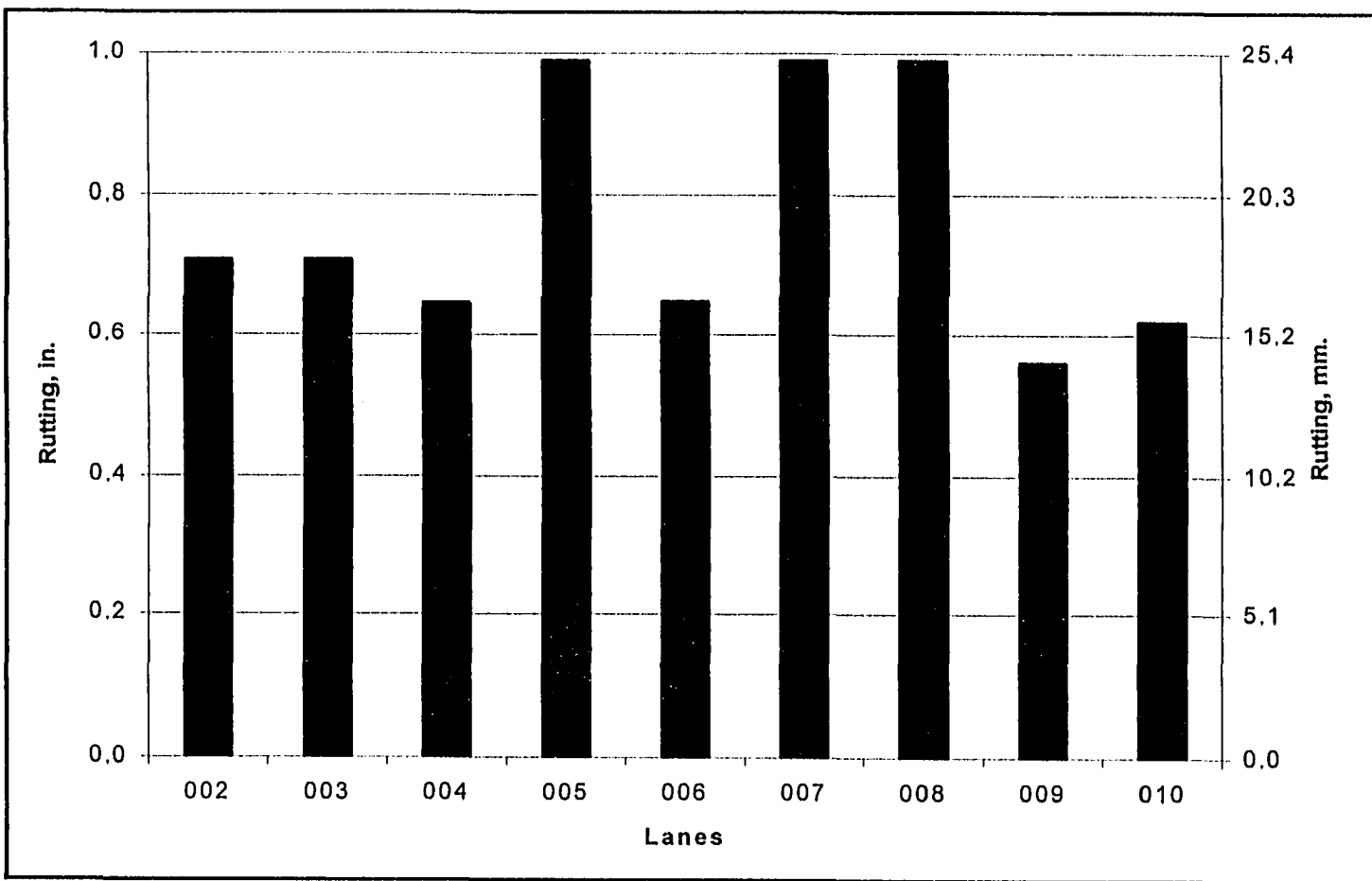


Figure 6. 8 Predicted rutting comparison at the end of a 20-year performance period for pavements designed for an average ADT of 75,000 and subgrade modulus of 8,000 psi

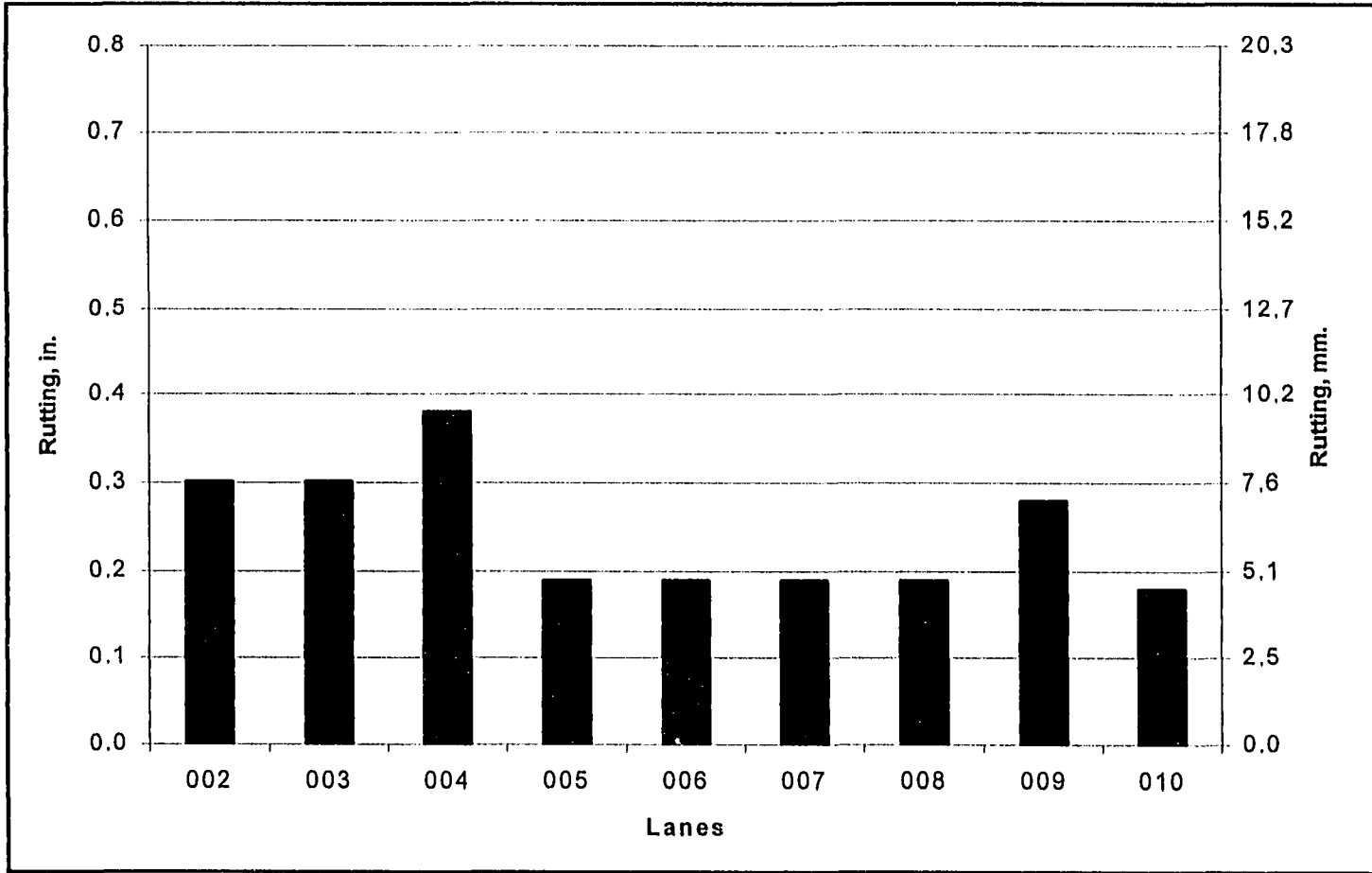


Figure 6. 9 Predicted rutting comparison at the end of a 20-year performance period for pavements designed for an average ADT of 4,000 and subgrade modulus of 9,150 psi

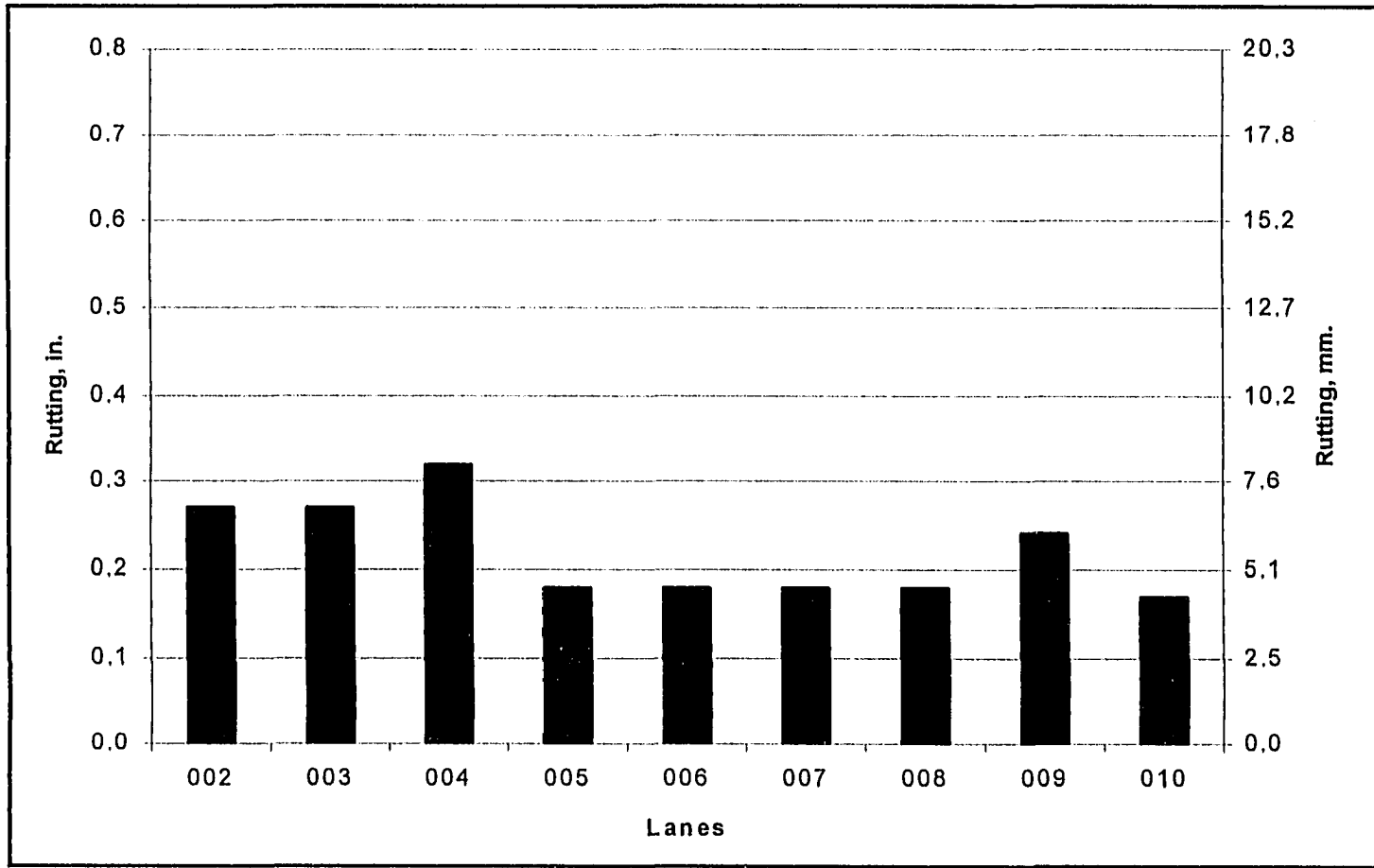


Figure 6. 10 Predicted rutting comparison at the end of a 20-year performance period for pavements designed for an average ADT of 8,000 and subgrade modulus of 9,150 psi

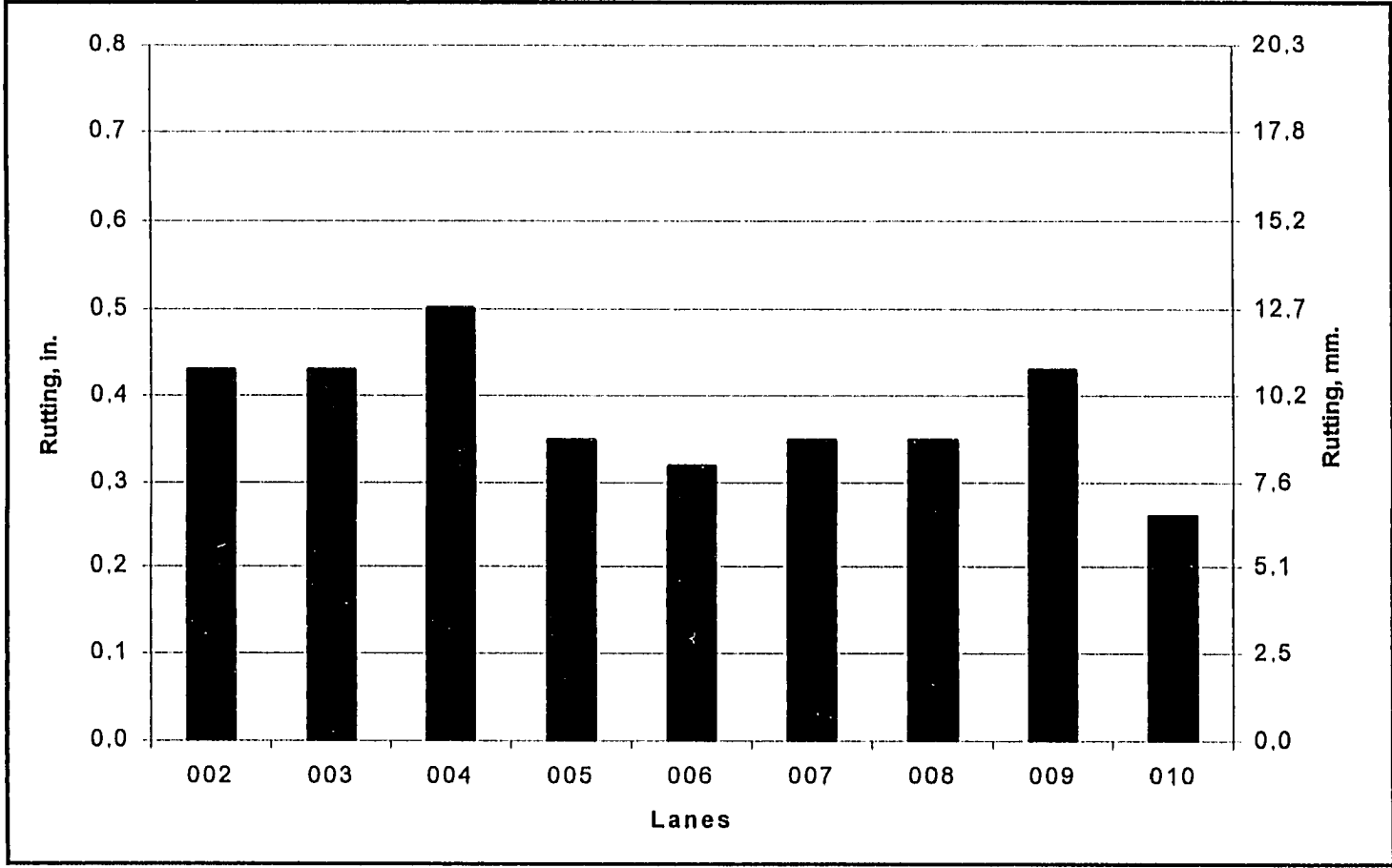


Figure 6. 11 Predicted rutting comparison at the end of a 20-year performance period for pavements designed for an average ADT of 15,000 and subgrade modulus of 9,150 psi

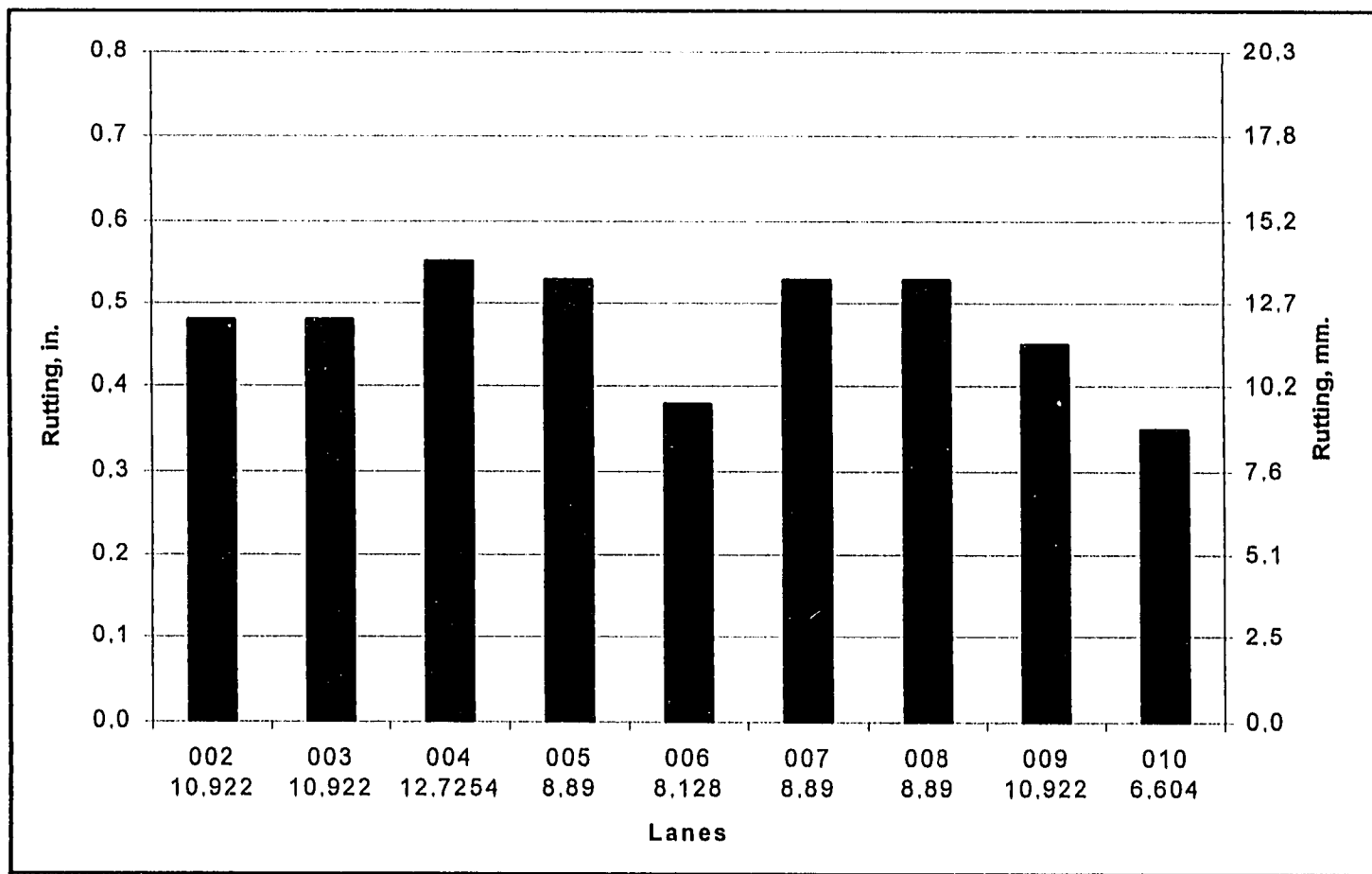


Figure 6. 12 Predicted rutting comparison at the end of a 20-year performance period for pavements designed for an average ADT of 25,000 and subgrade modulus of 9,150 psi

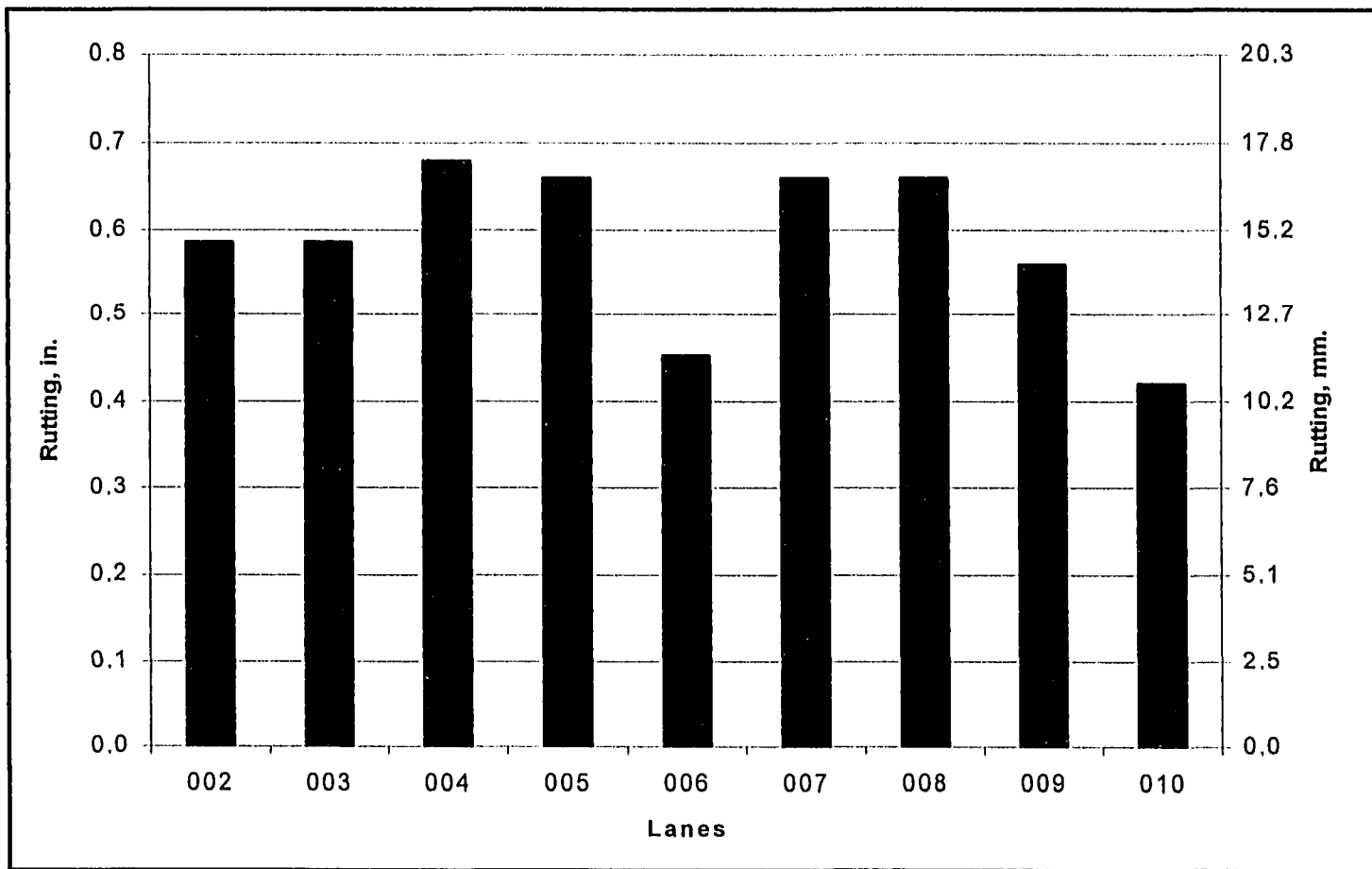


Figure 6. 13 Predicted rutting comparison at the end of a 20-year performance period for pavements designed for an average ADT of 40,000 and subgrade modulus of 9,150 psi

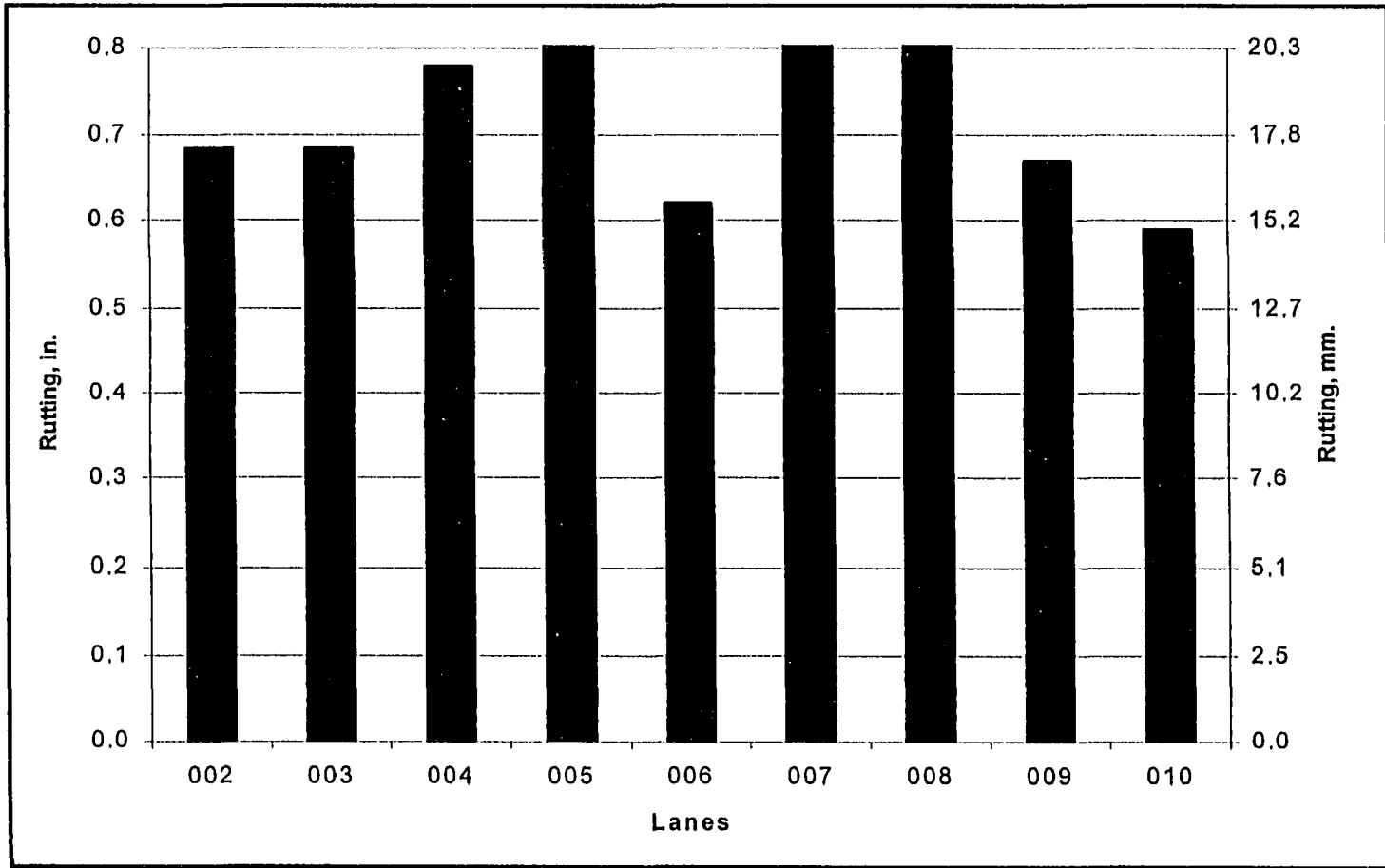


Figure 6. 14 Predicted rutting comparison at the end of a 20-year performance period for pavements designed for an average ADT of 75,000 and subgrade modulus of 9,150 psi

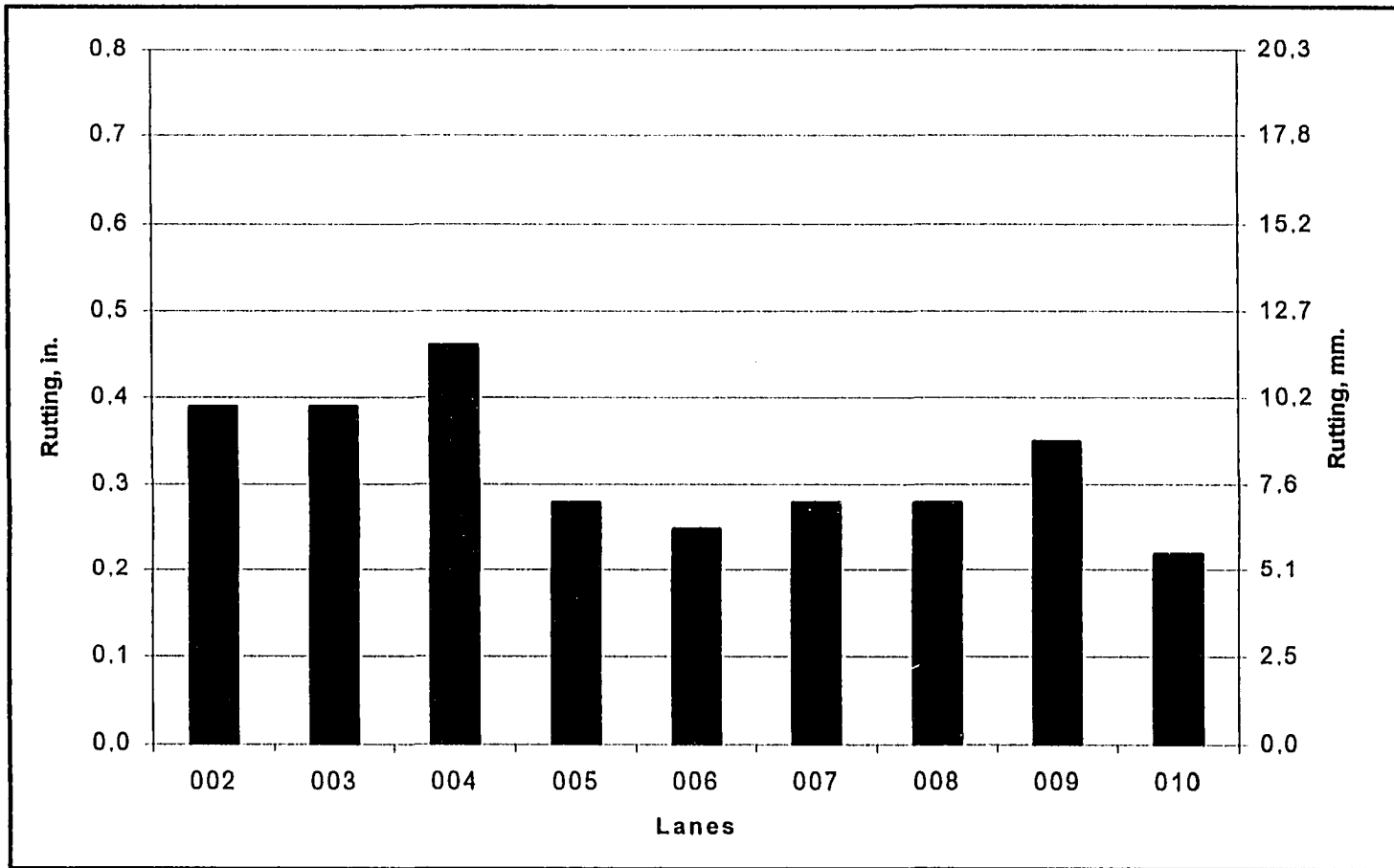


Figure 6. 15 Predicted rutting comparison at the end of a 20-year performance period for pavements designed for an average ADT of 4,000 and subgrade modulus of 10,600 psi

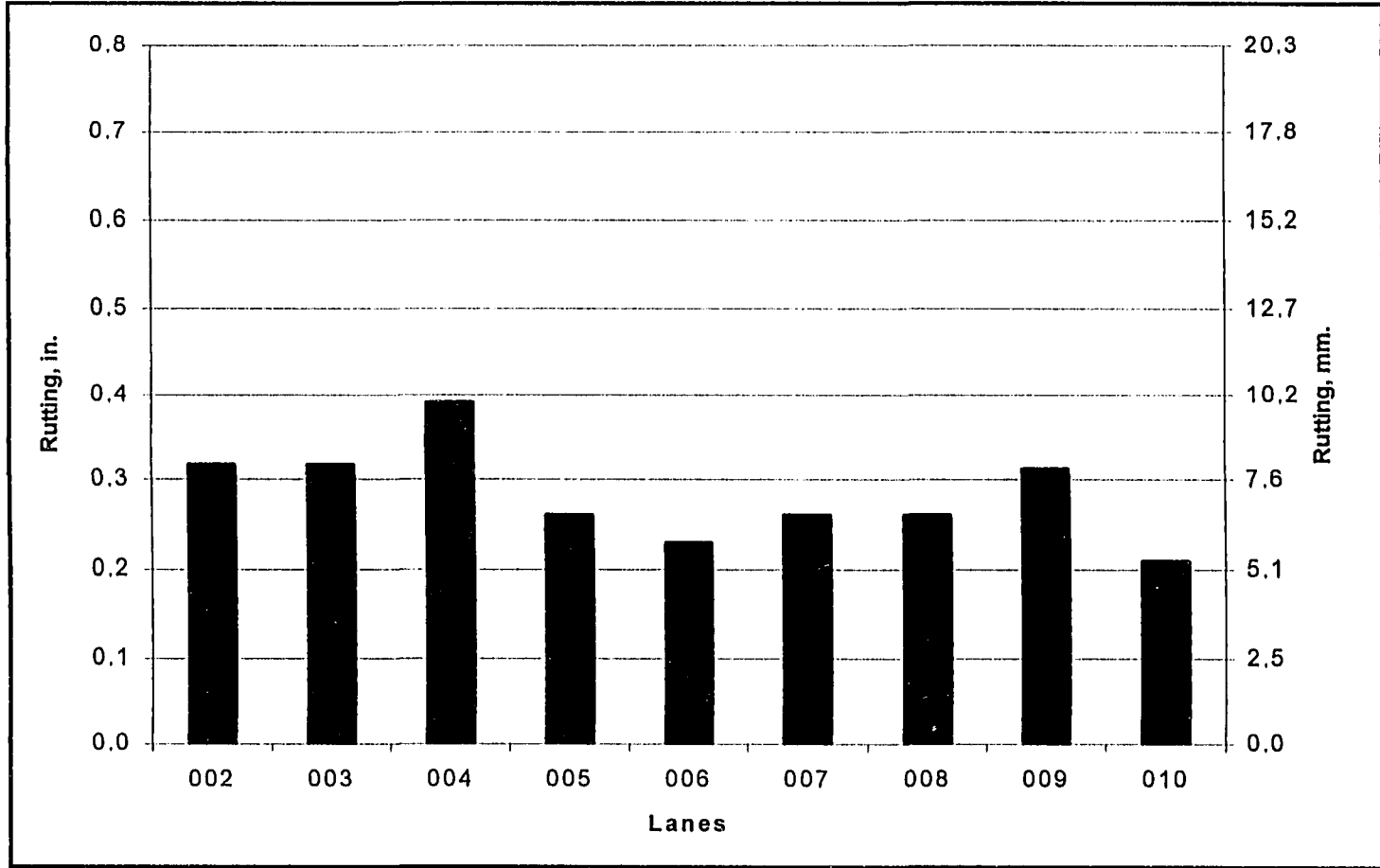


Figure 6. 16 Predicted rutting comparison at the end of a 20-year performance period for pavements designed for an average ADT of 8,000 and subgrade modulus of 10,600 psi

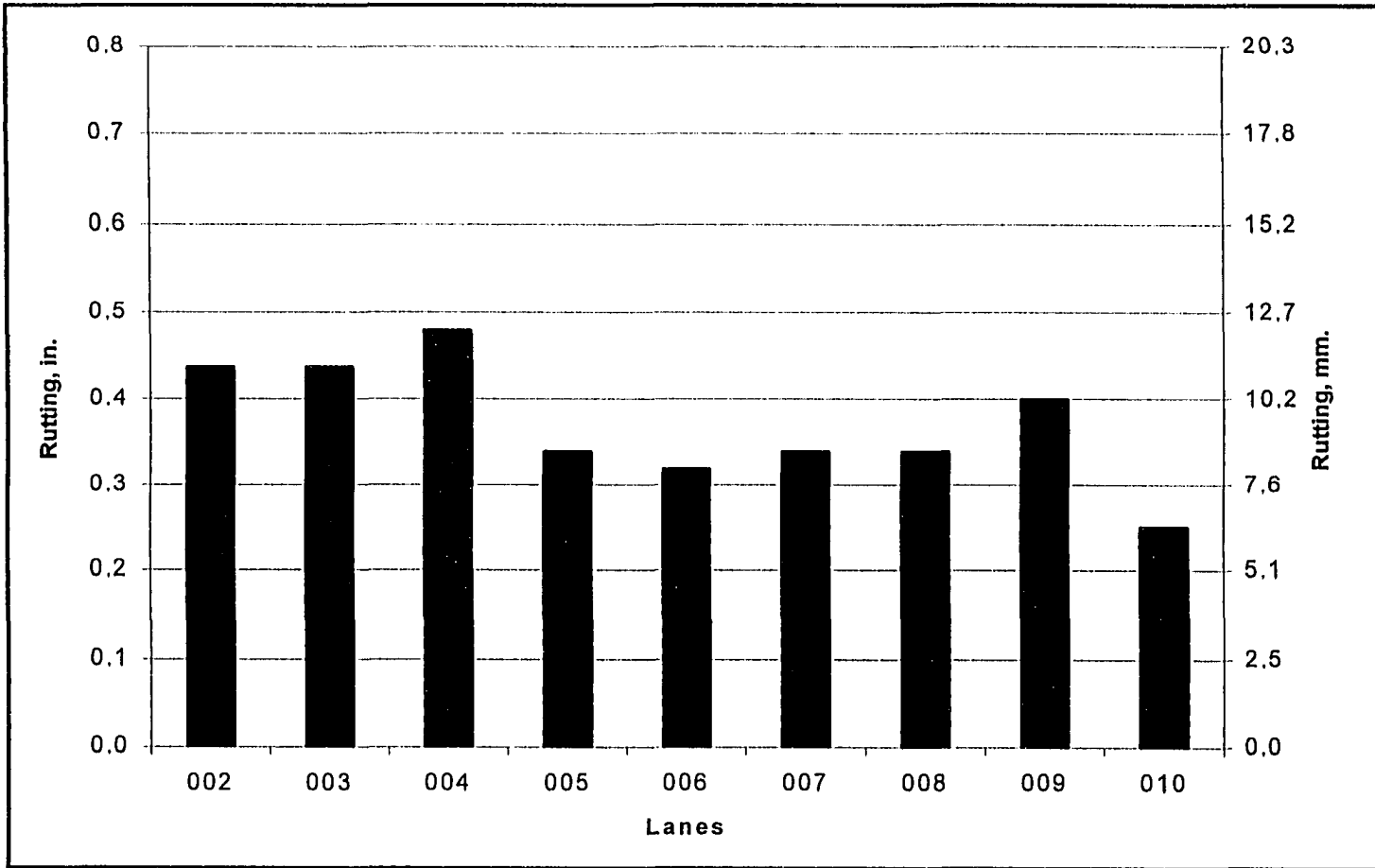


Figure 6. 17 Predicted rutting comparison at the end of a 20-year performance period for pavements designed for an average ADT of 15,000 and subgrade modulus of 10,600 psi

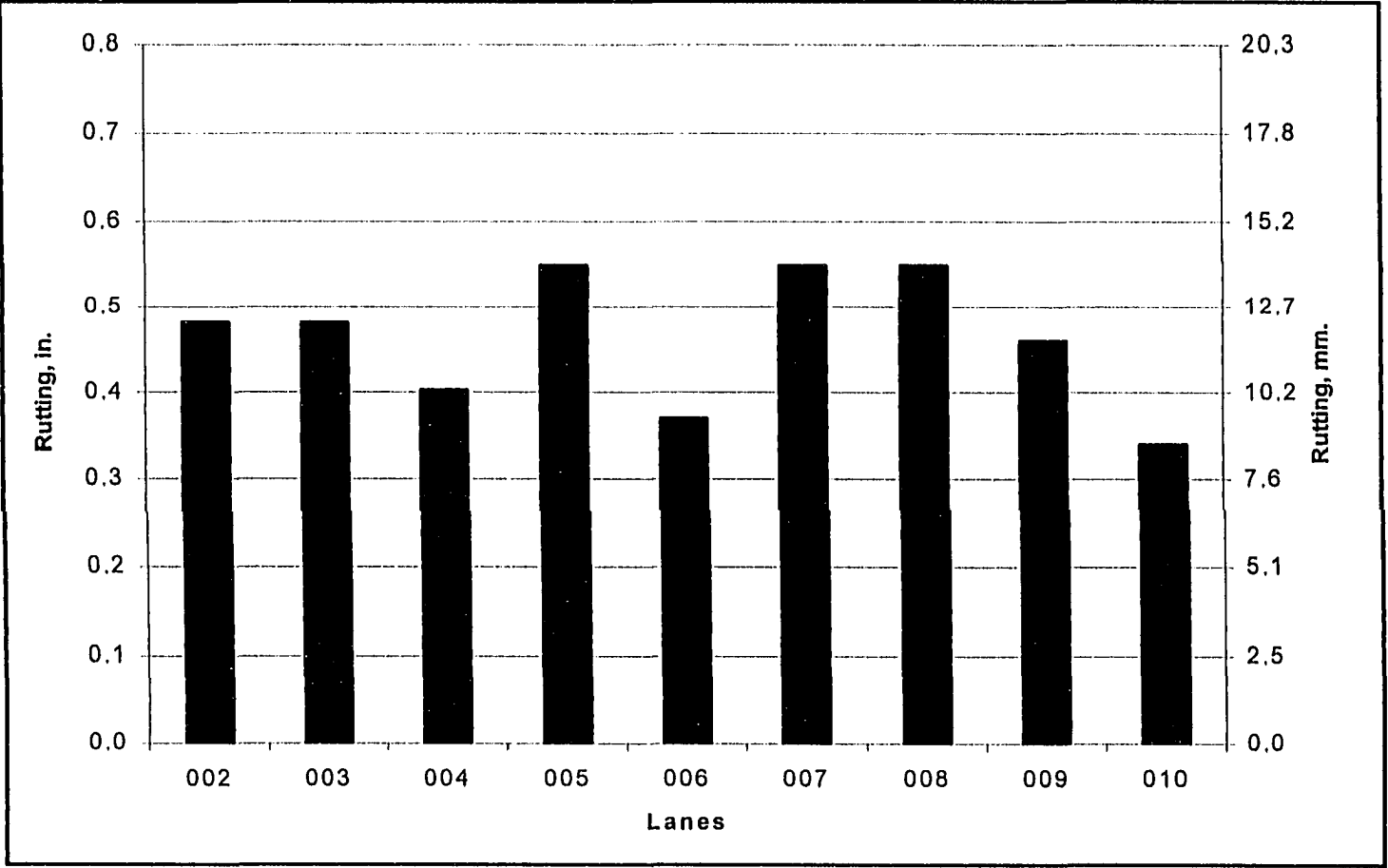


Figure 6. 18 Predicted rutting comparison at the end of a 20-year performance period for pavements designed for an average ADT of 25,000 and subgrade modulus of 10,600 psi

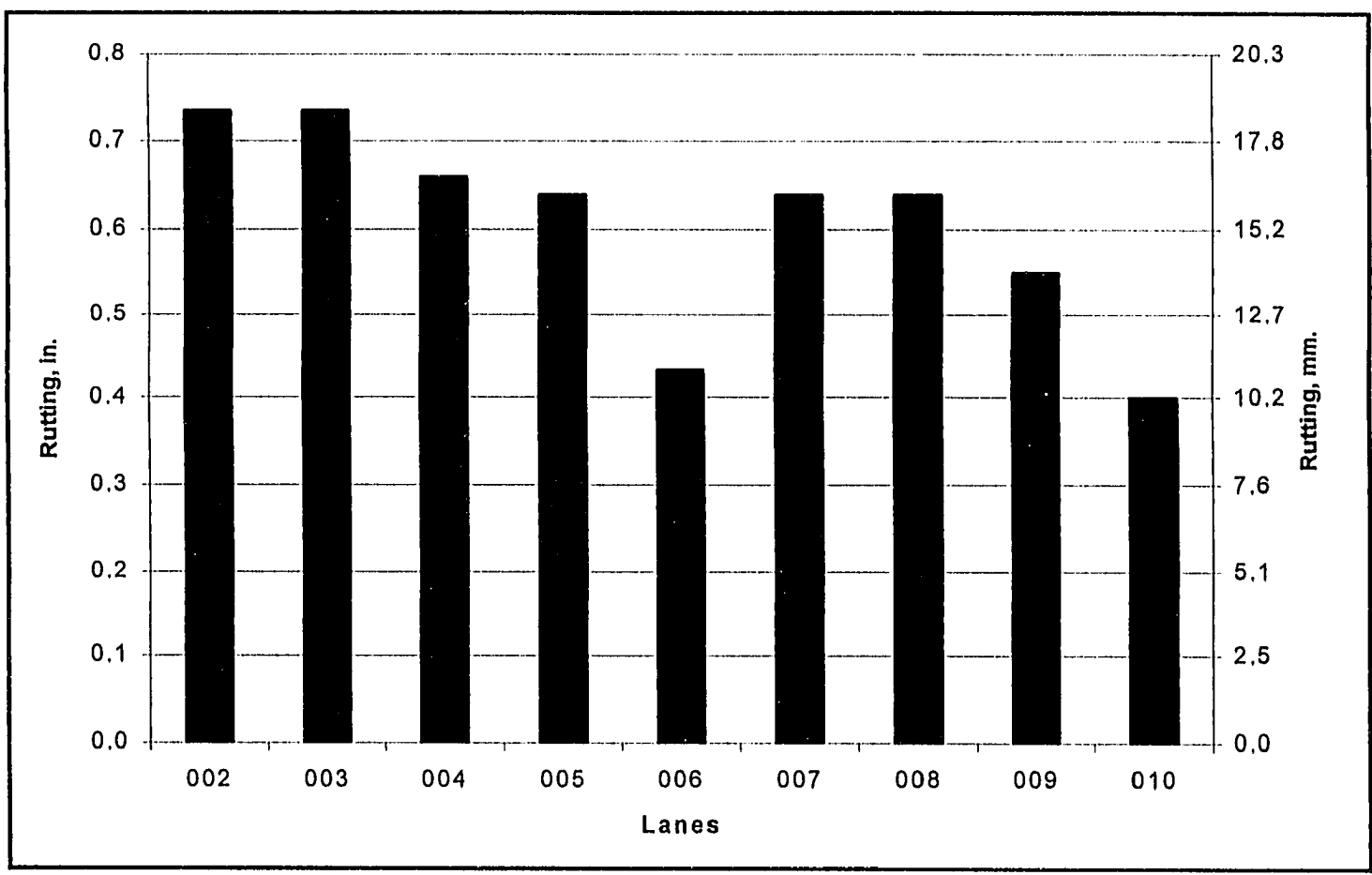


Figure 6. 19 Predicted rutting comparison at the end of a 20-year performance period for pavements designed for an average ADT of 40,000 and subgrade modulus of 10,600 psi

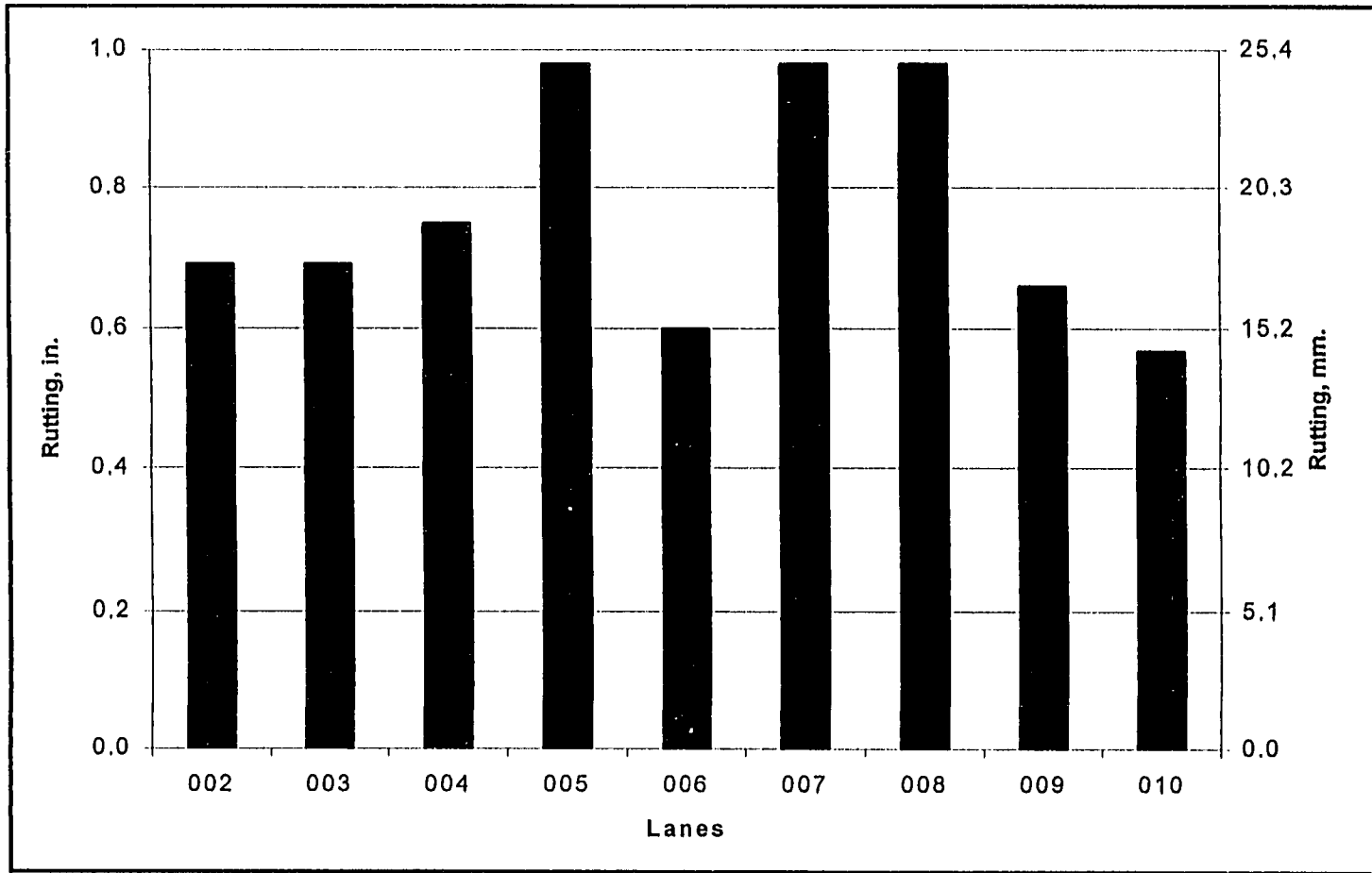


Figure 6. 20 Predicted rutting comparison at the end of a 20-year performance period for pavements designed for an average ADT of 75,000 and subgrade modulus of 10,600 psi

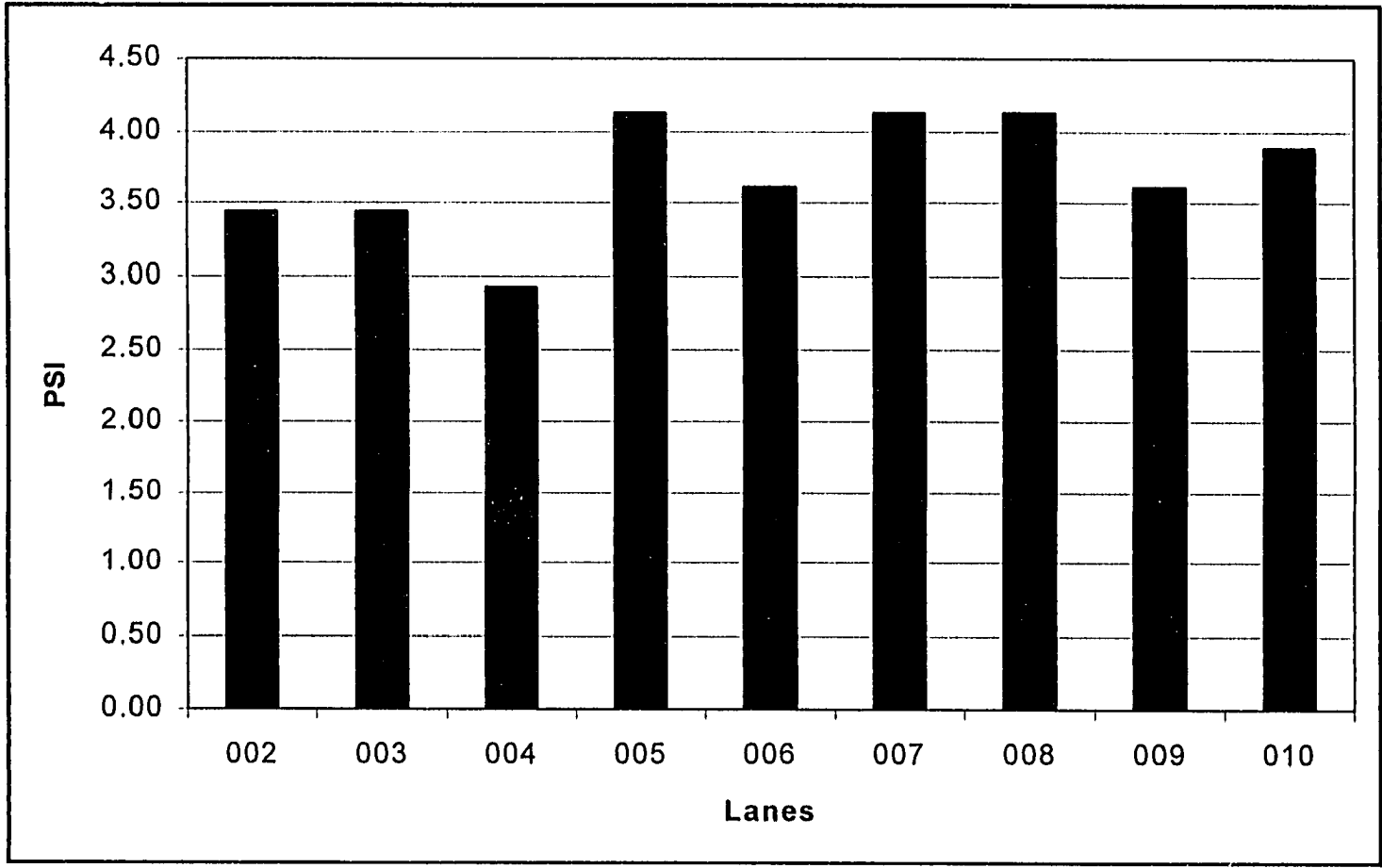


Figure 6. 21 Predicted PSI comparison at the end of a 20-year performance period for pavements designed for an average ADT of 4,000 and subgrade modulus of 8,000 psi

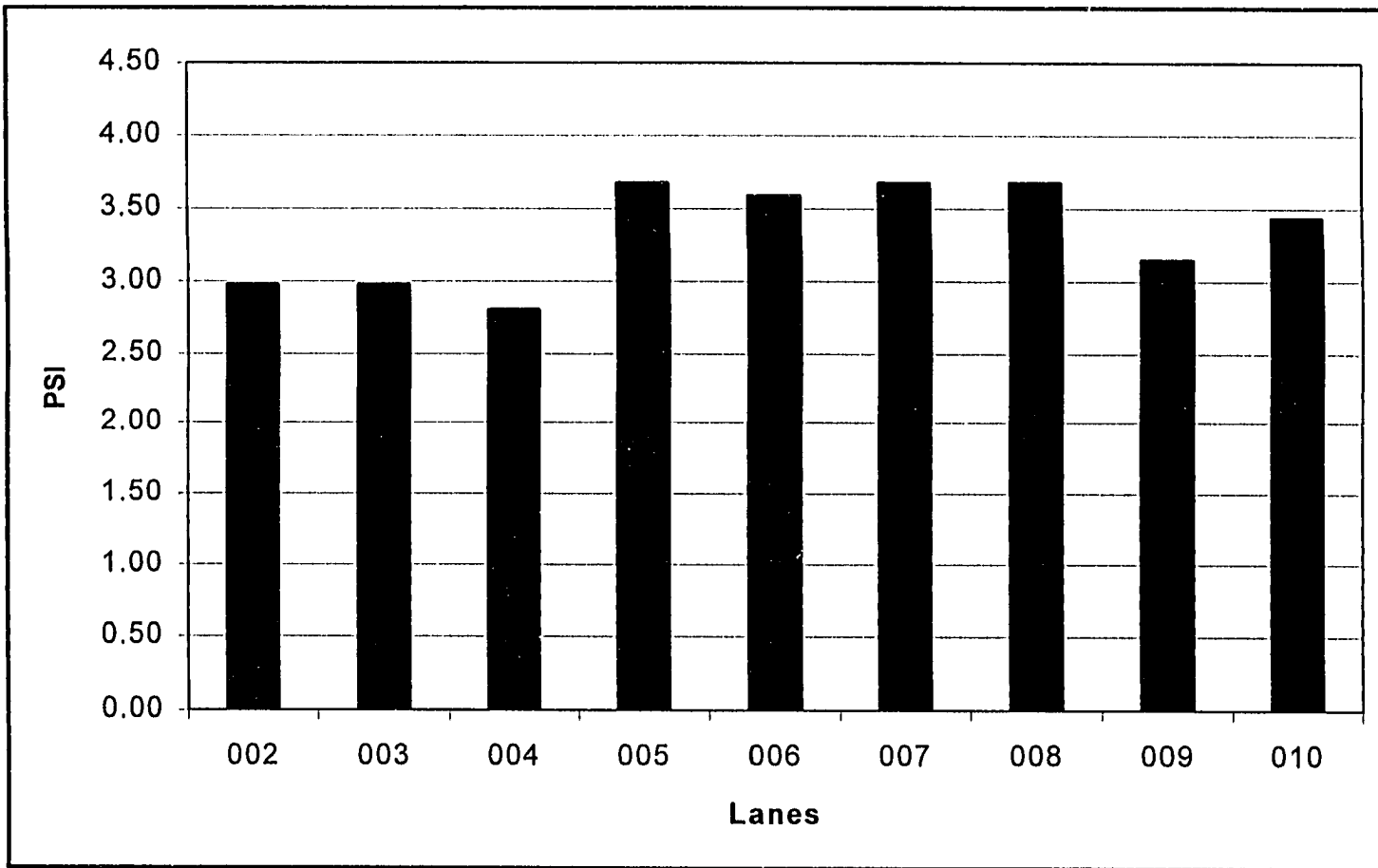


Figure 6. 22 Predicted PSI comparison at the end of a 20-year performance period for pavements designed for an average ADT of 8,000 and subgrade modulus of 8,000 psi

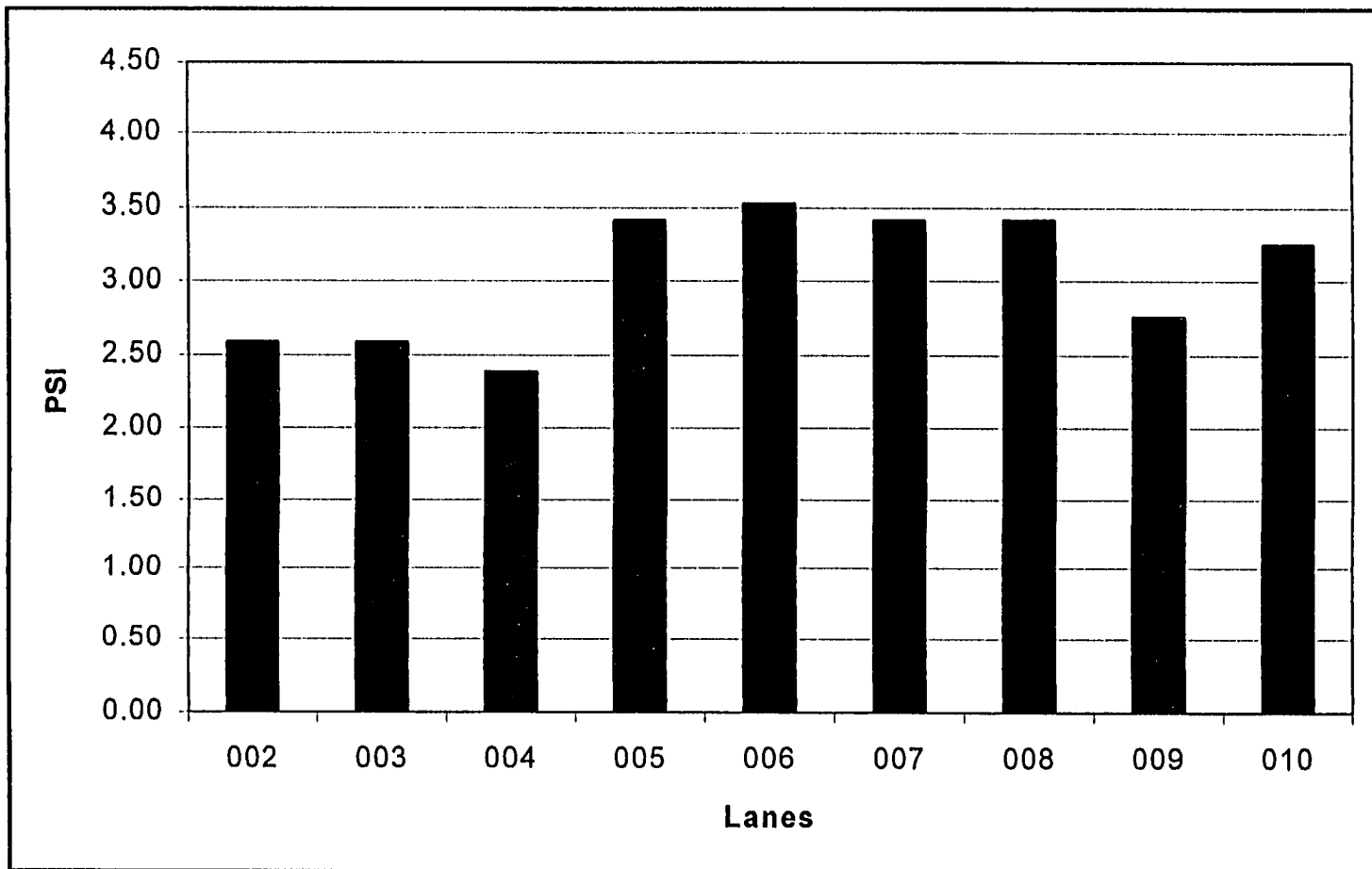


Figure 6. 23 Predicted PSI comparison at the end of a 20-year performance period for pavements designed for an average ADT of 15,000 and subgrade modulus of 8,000 psi

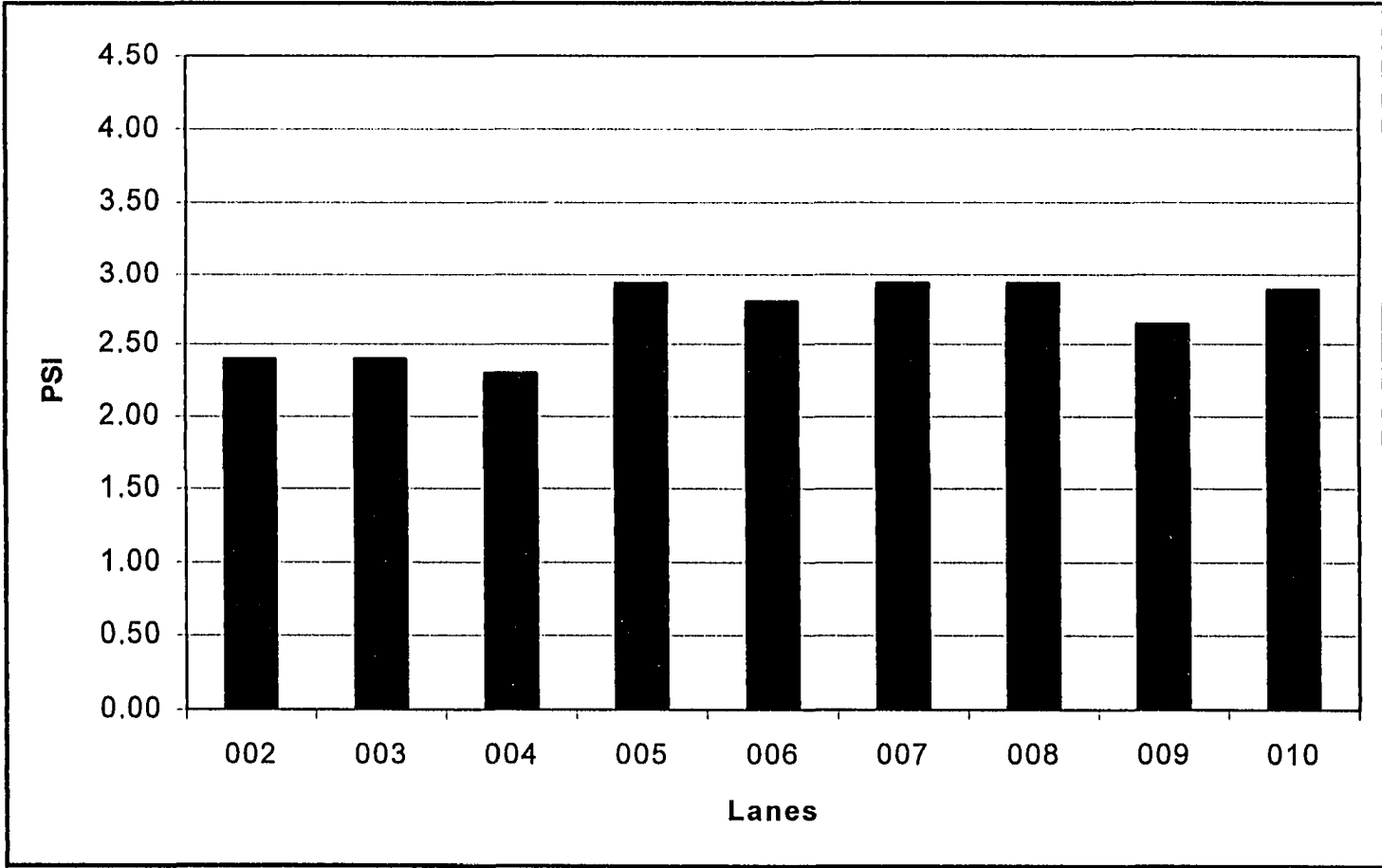


Figure 6. 24 Predicted PSI comparison at the end of a 20-year performance period for pavements designed for an average ADT of 25,000 and subgrade modulus of 8,000 psi

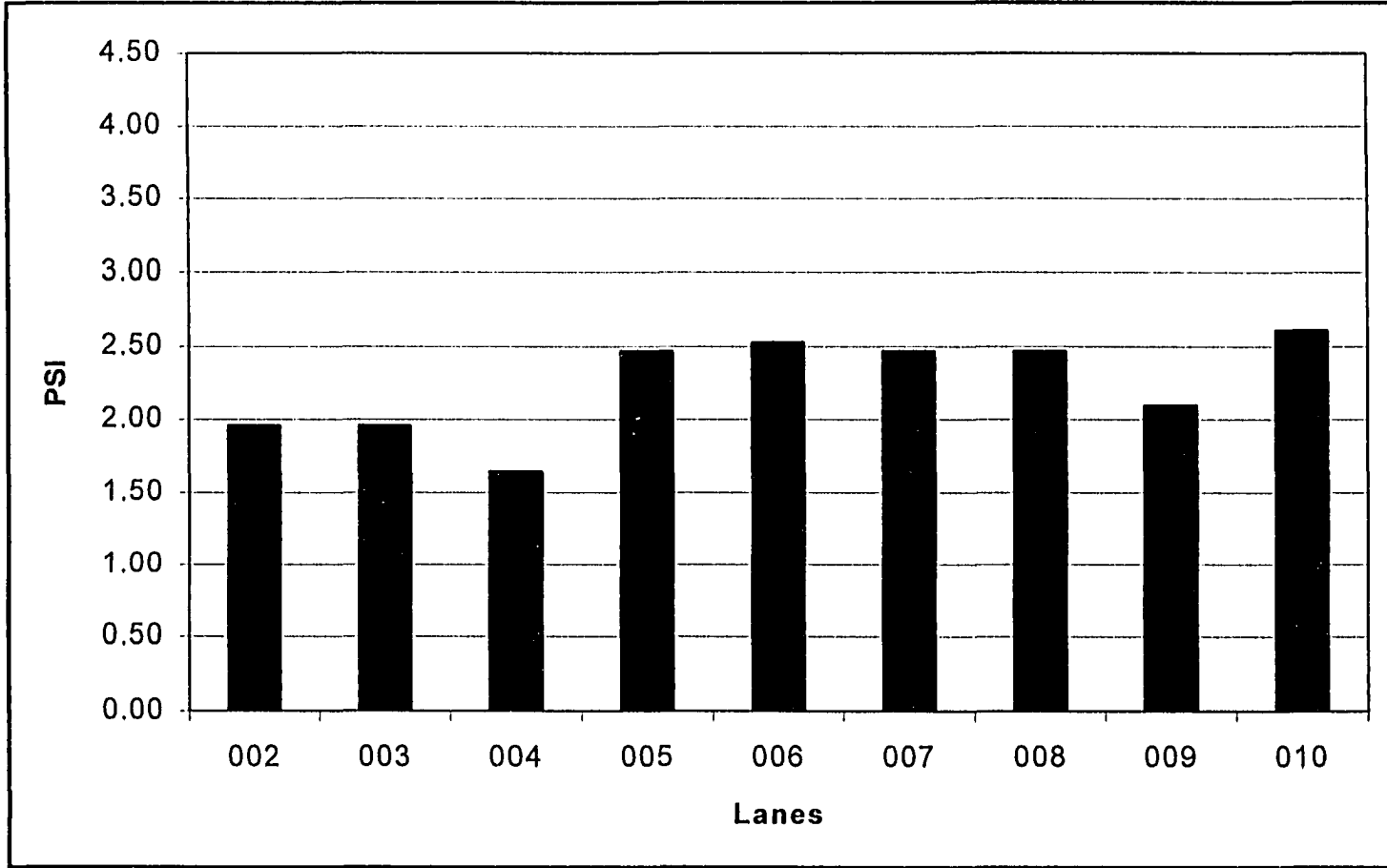


Figure 6. 25 Predicted PSI comparison at the end of a 20-year performance period for pavements designed for an average ADT of 40,000 and subgrade modulus of 8,000 psi

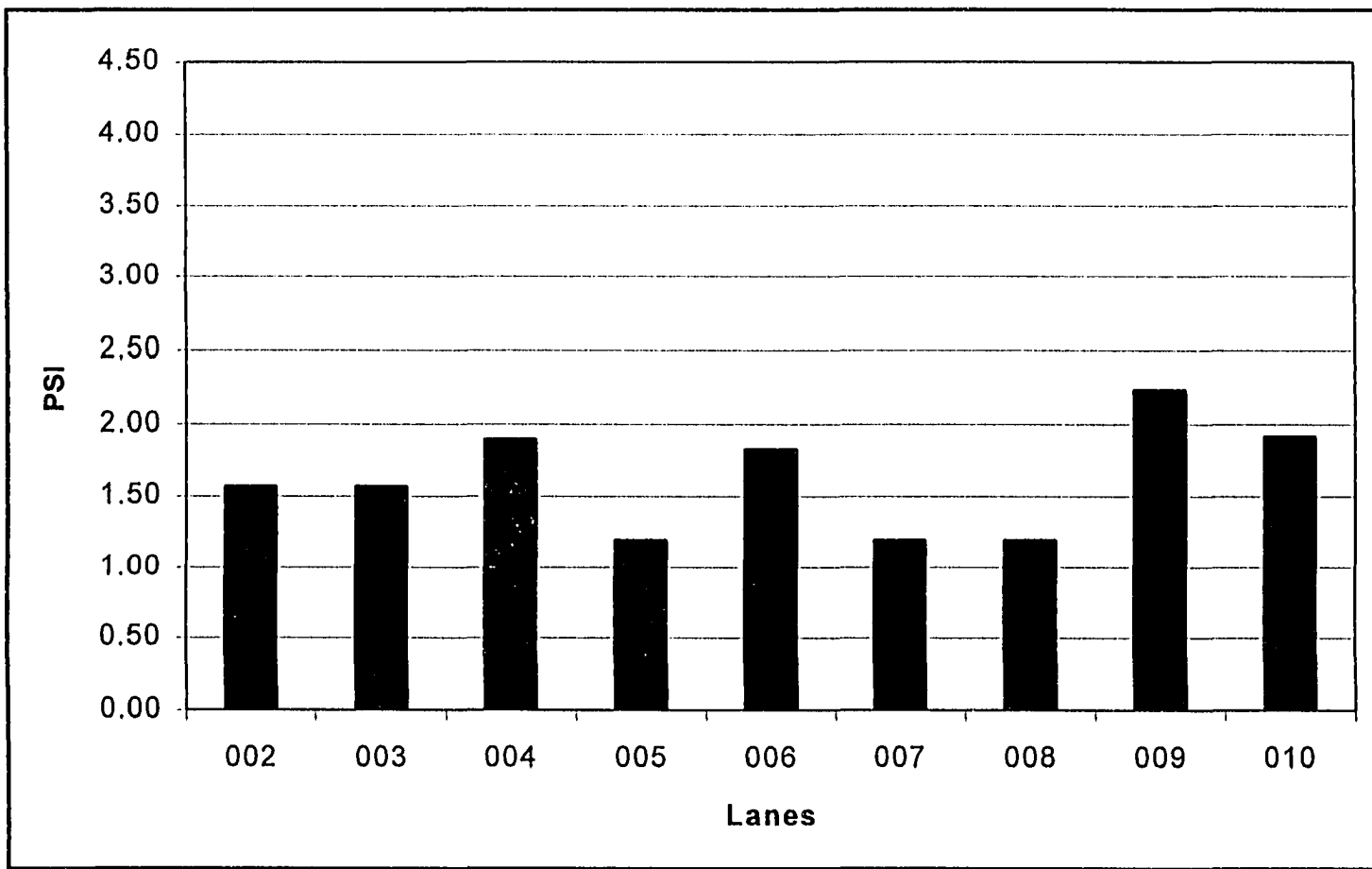


Figure 6. 26 Predicted PSI comparison at the end of a 20-year performance period for pavements designed for an average ADT of 75,000 and subgrade modulus of 8,000 psi

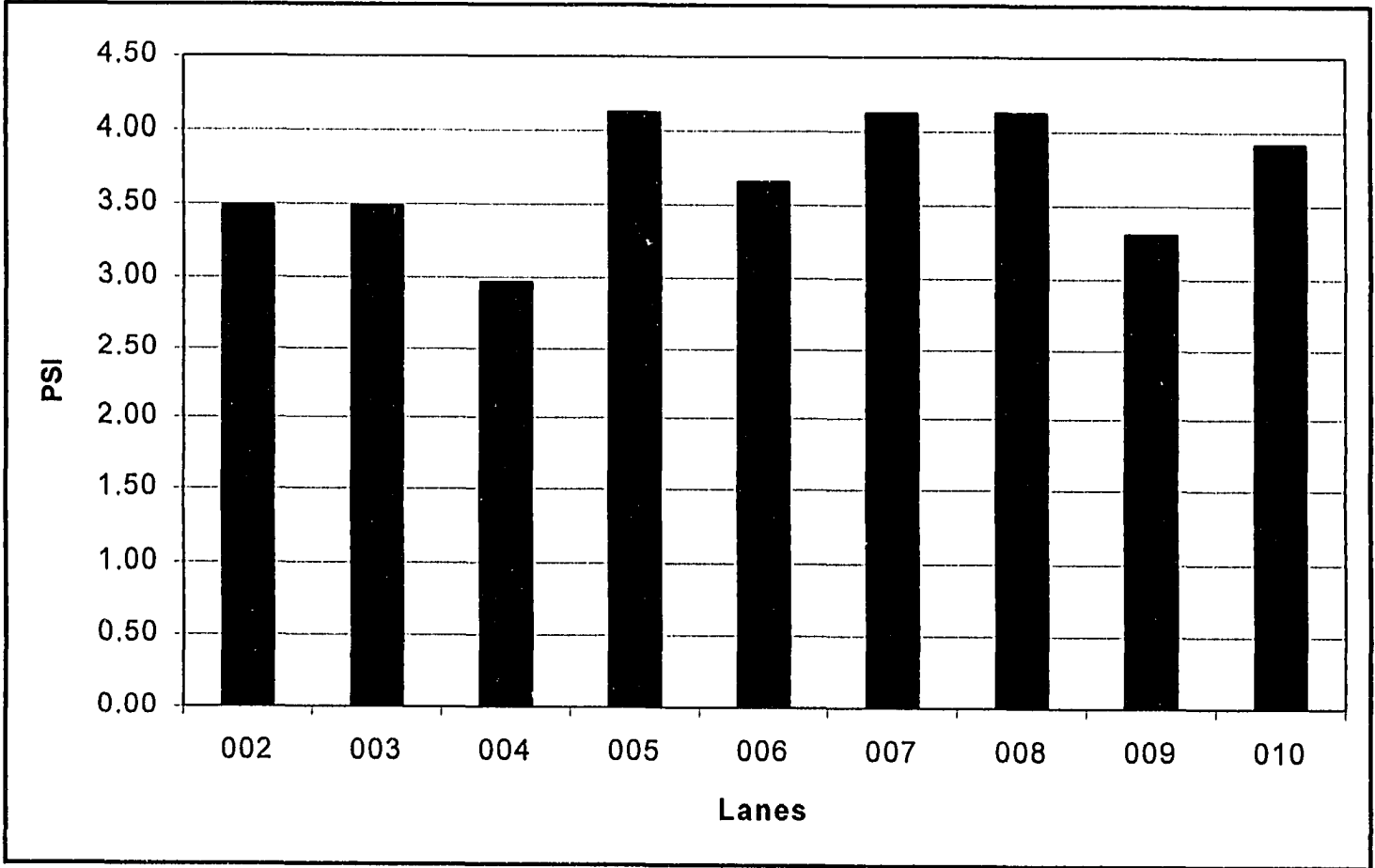


Figure 6. 27 Predicted PSI comparison at the end of a 20-year performance period for pavements designed for an average ADT of 4,000 and subgrade modulus of 9,150 psi

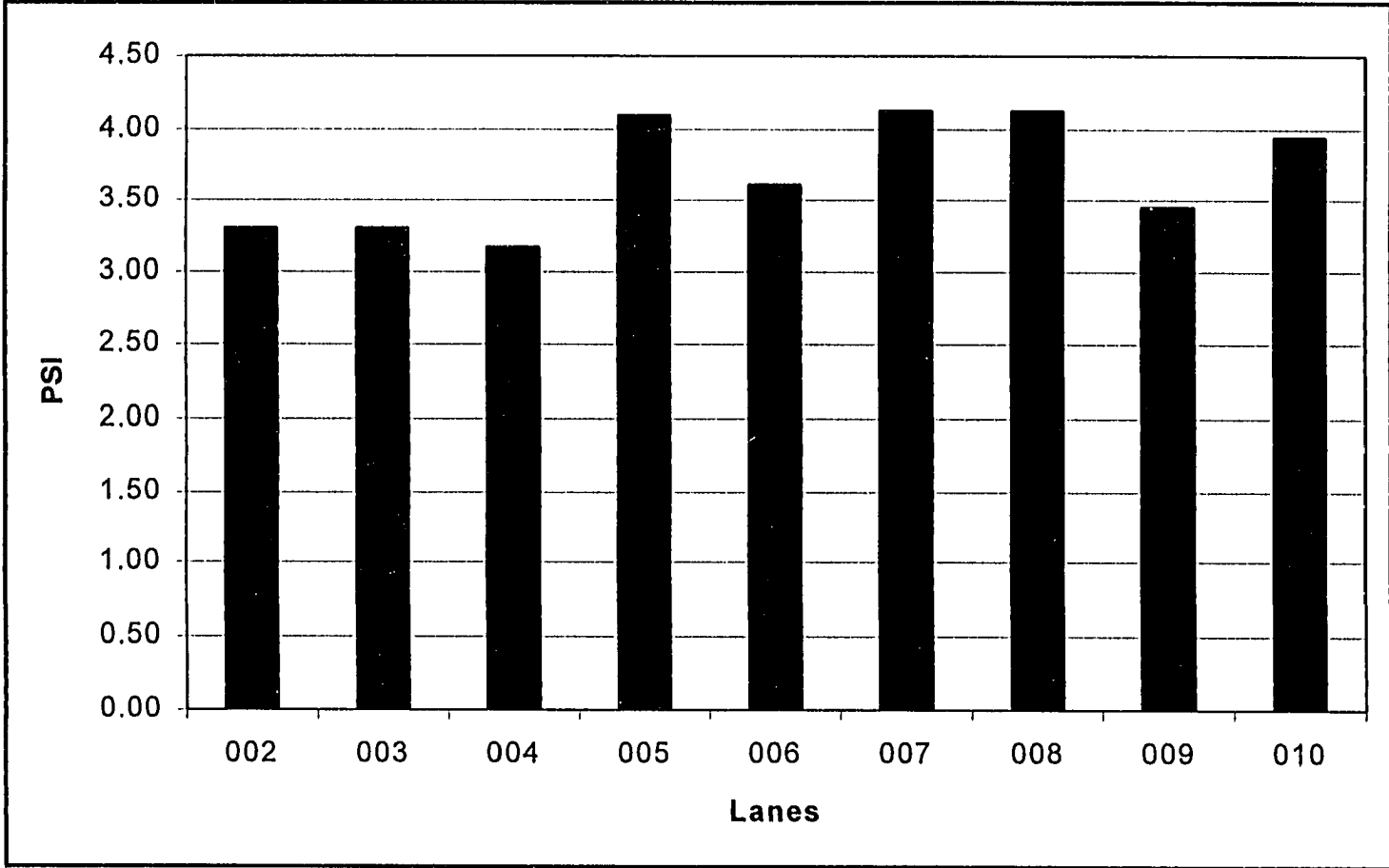


Figure 6. 28 Predicted PSI comparison at the end of a 20-year performance period for pavements designed for an average ADT of 8,000 and subgrade modulus of 9,150 psi

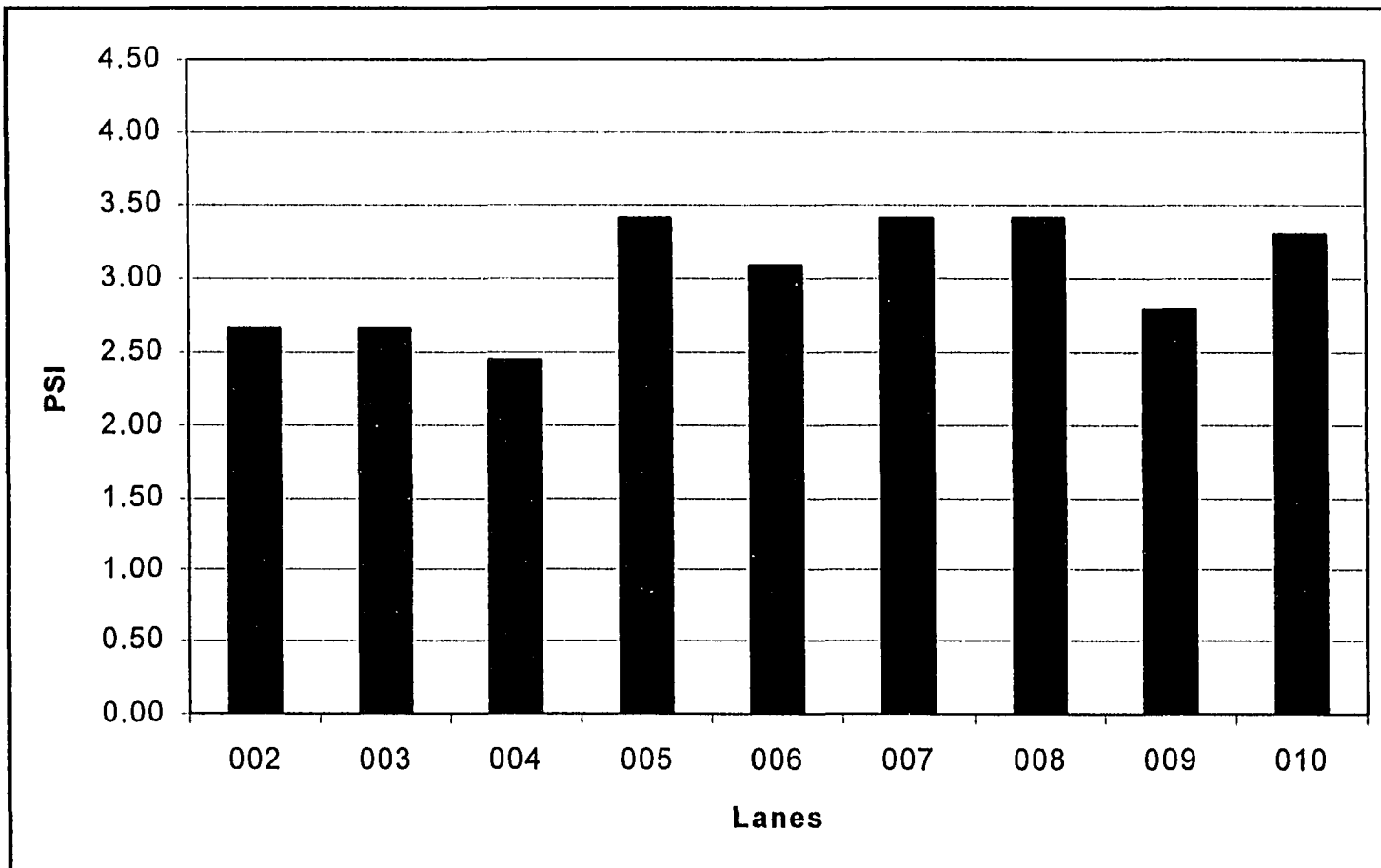


Figure 6. 29 Predicted PSI comparison at the end of a 20-year performance period for pavements designed for an average ADT of 15,000 and subgrade modulus of 9,150 psi

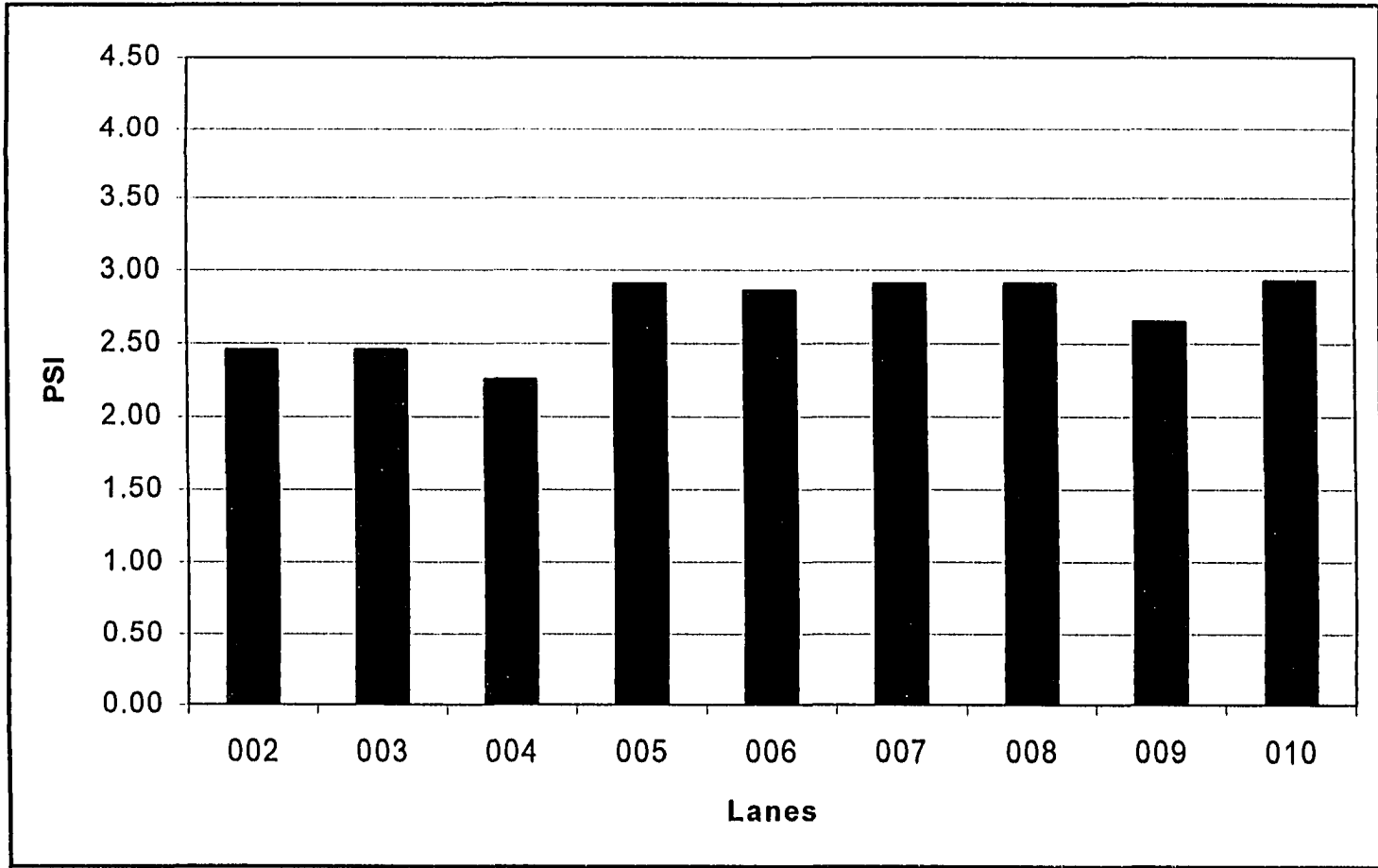


Figure 6. 30 Predicted PSI comparison at the end of a 20-year performance period for pavements designed for an average ADT of 25,000 and subgrade modulus of 9,150 psi

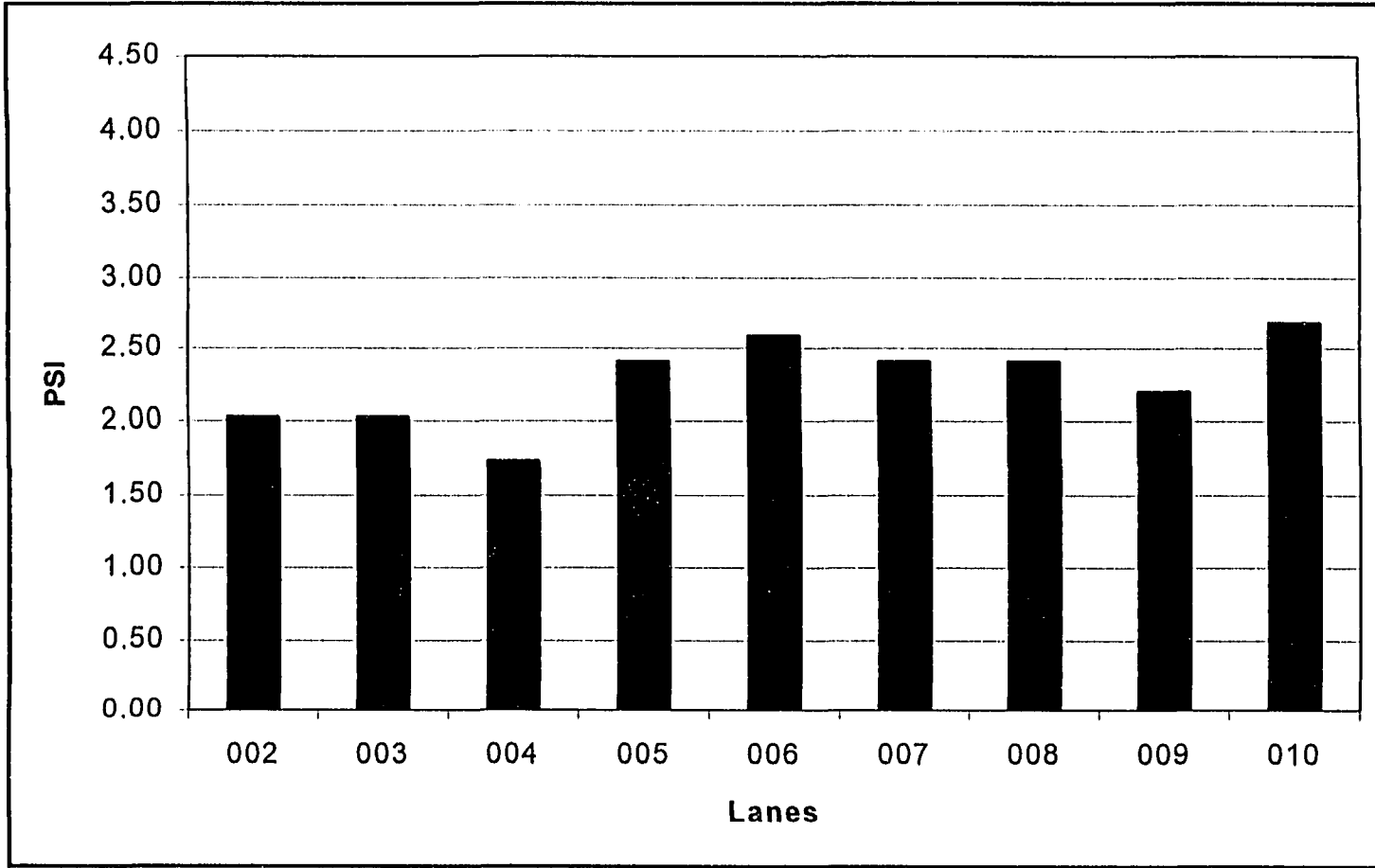


Figure 6. 31 Predicted PSI comparison at the end of a 20-year performance period for pavements designed for an average ADT of 40,000 and subgrade modulus of 9,150 psi

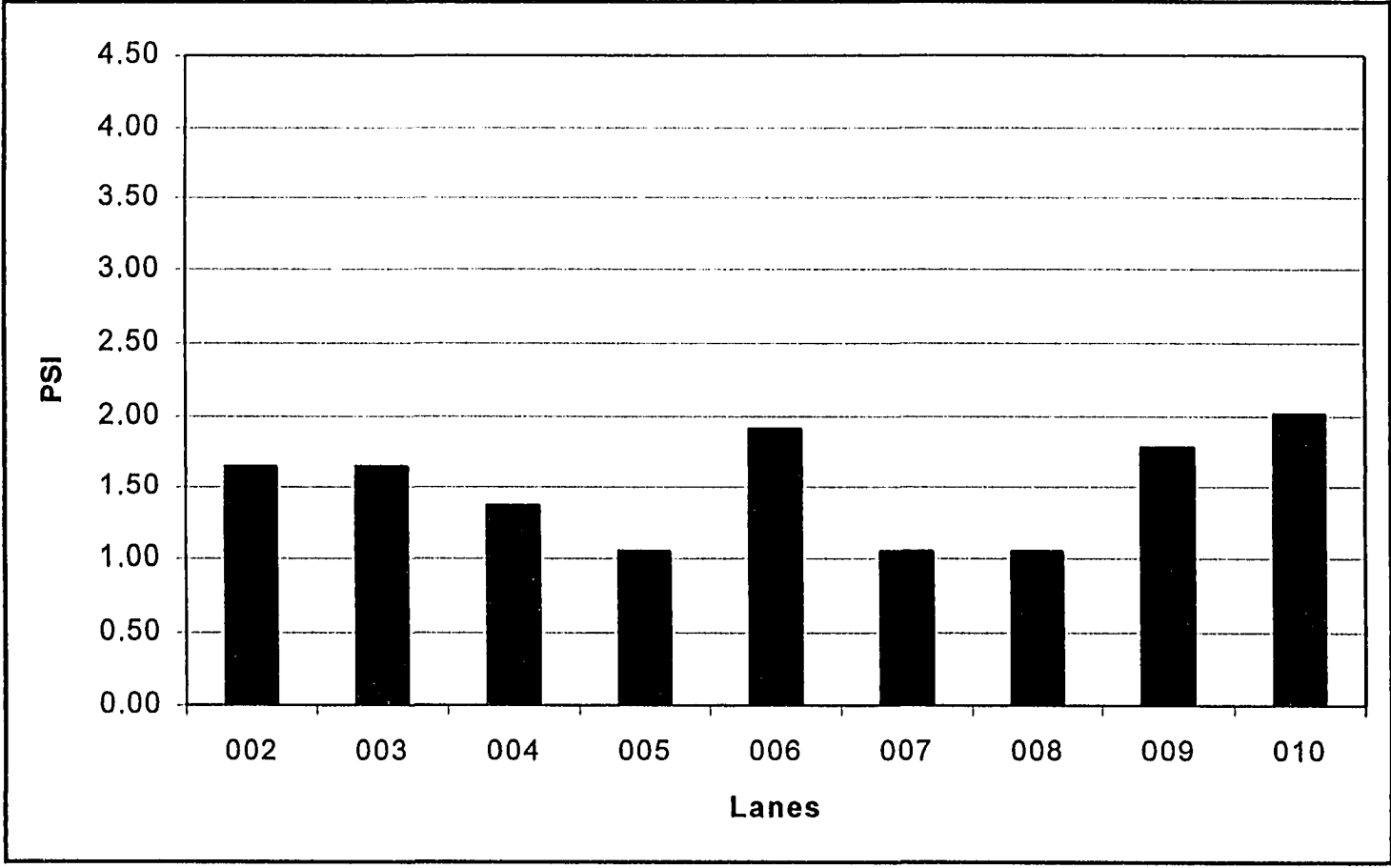


Figure 6. 32 Predicted PSI comparison at the end of a 20-year performance period for pavements designed for an average ADT of 75,000 and subgrade modulus of 9,150 psi

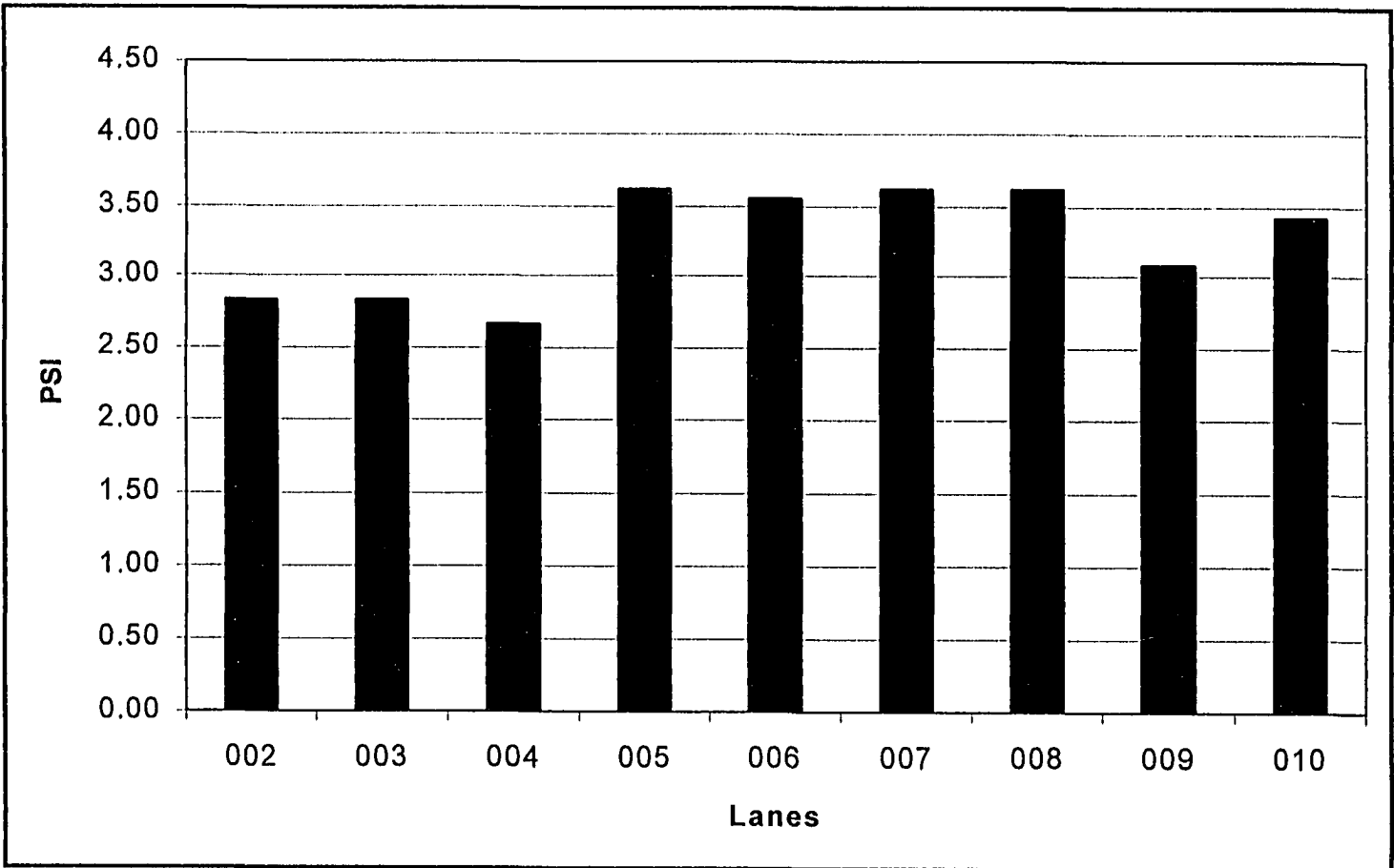


Figure 6. 33 Predicted PSI comparison at the end of a 20-year performance period for pavements designed for an average ADT of 4,000 and subgrade modulus of 10,600 psi

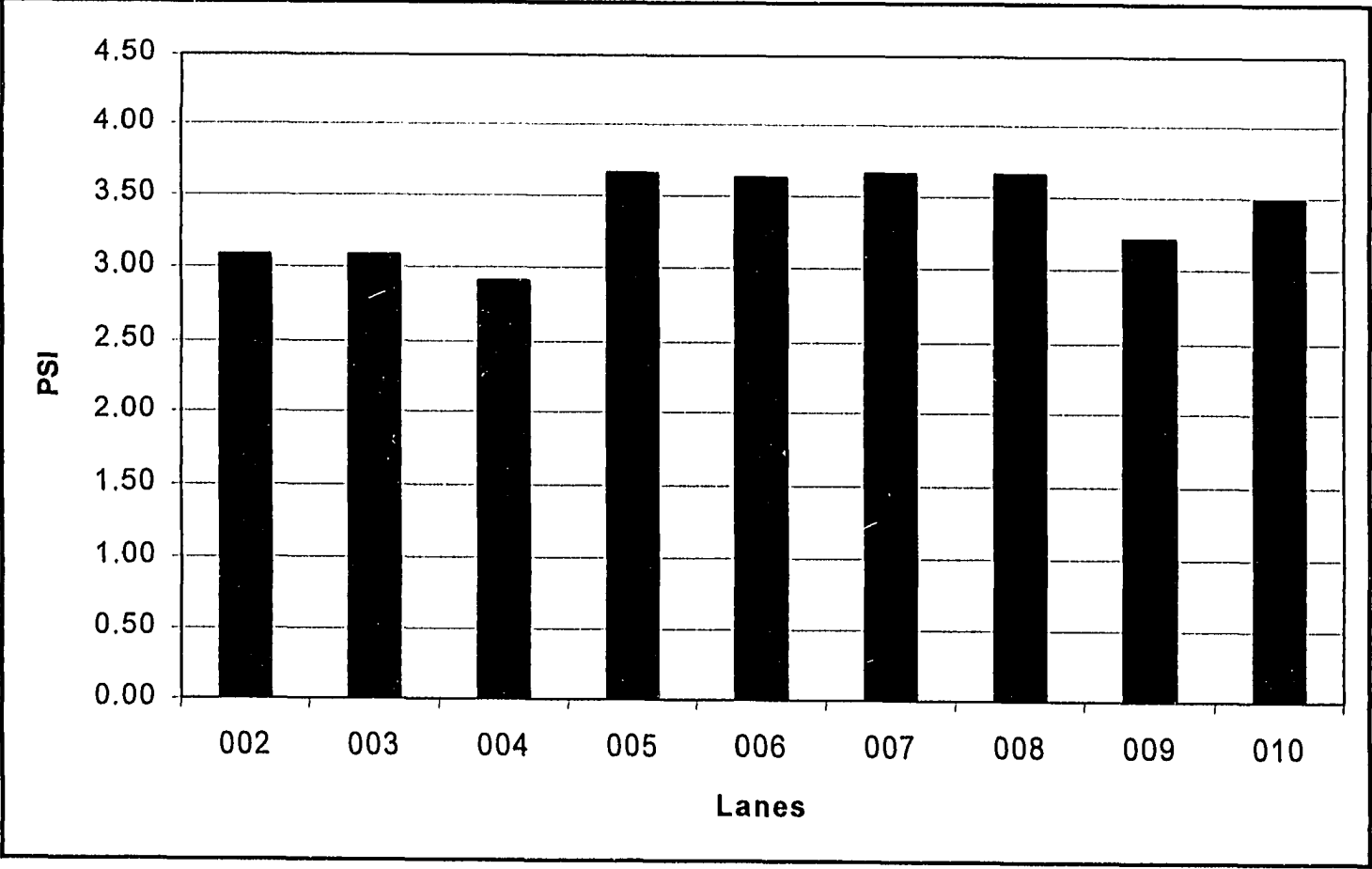


Figure 6. 34 Predicted PSI comparison at the end of a 20-year performance period for pavements designed for an average ADT of 8,000 and subgrade modulus of 10,600 psi

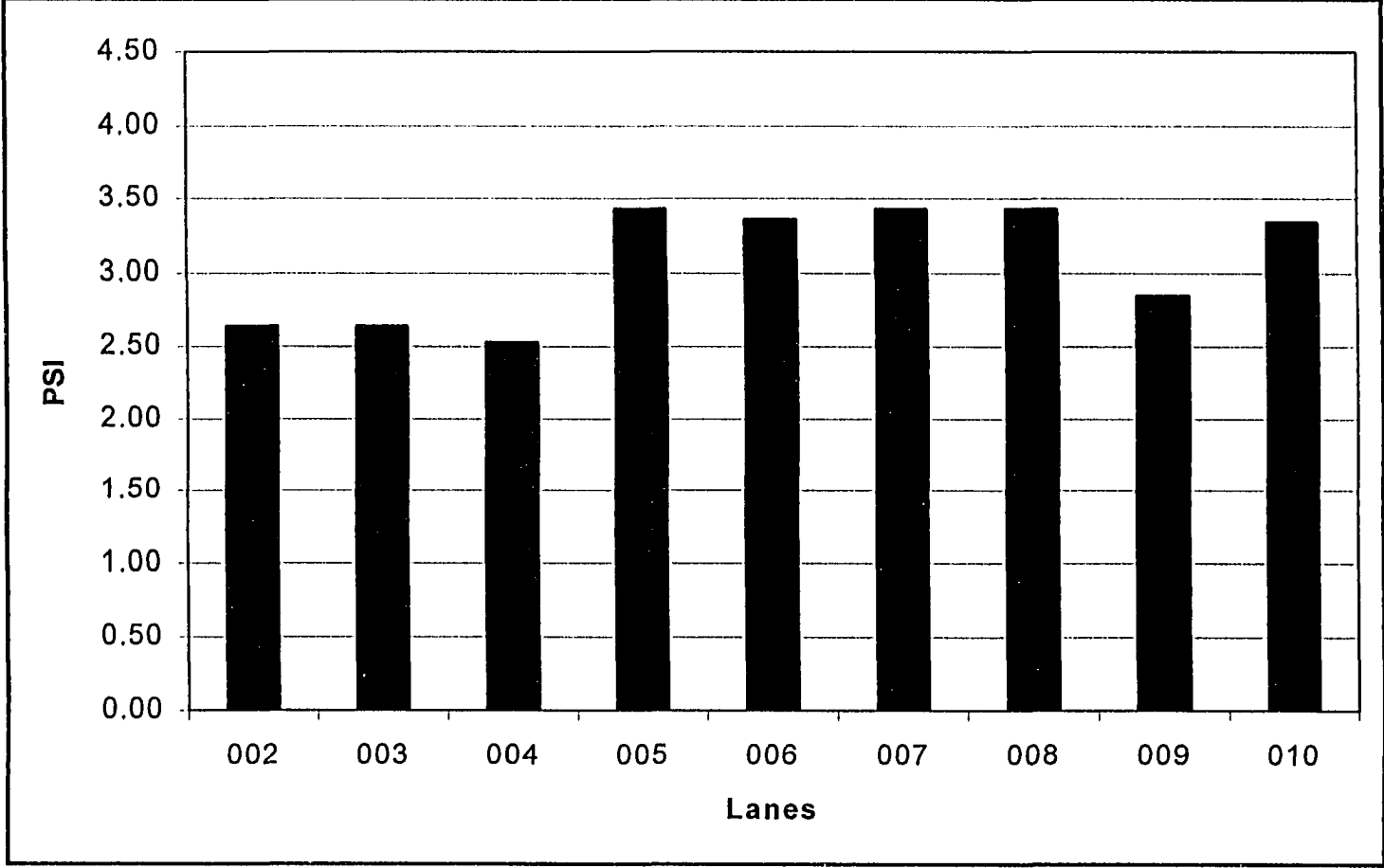


Figure 6. 35 Predicted PSI comparison at the end of a 20-year performance period for pavements designed for an average ADT of 15,000 and subgrade modulus of 10,600 psi

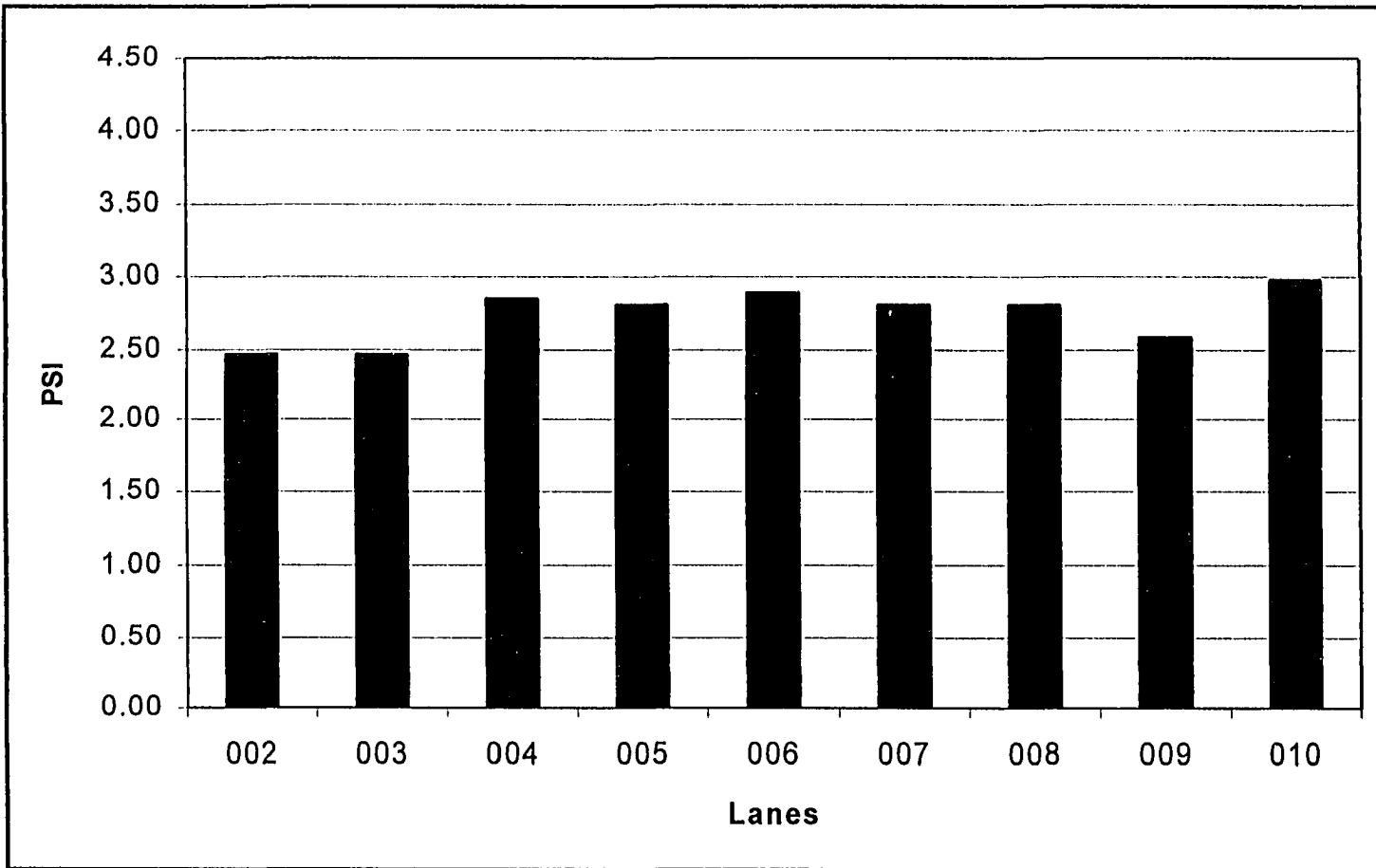


Figure 6. 36 Predicted PSI comparison at the end of a 20-year performance period for pavements designed for an average ADT of 25,000 and subgrade modulus of 10,600 psi

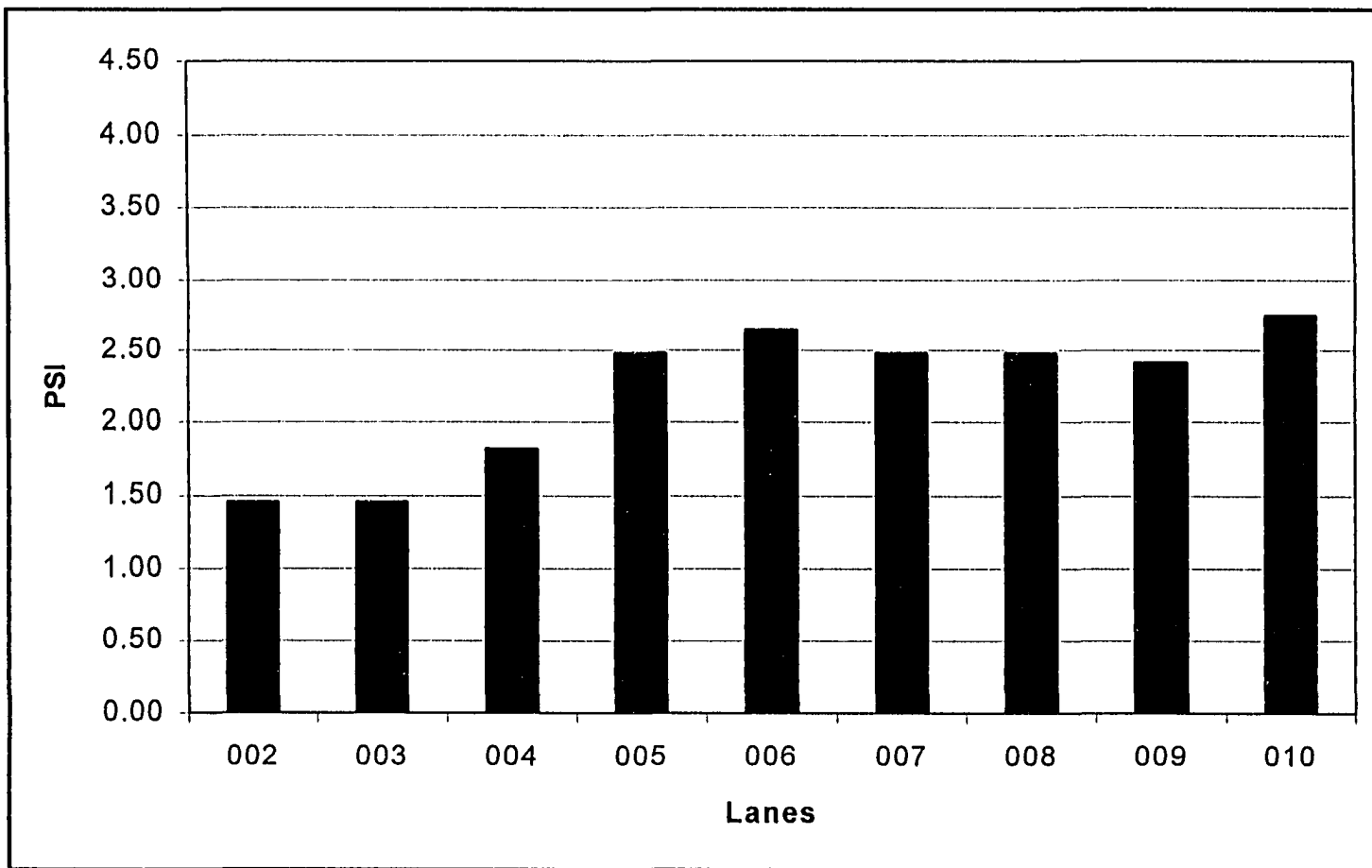


Figure 6. 37 Predicted PSI comparison at the end of a 20-year performance period for pavements designed for an average ADT of 40,000 and subgrade modulus of 10,600 psi

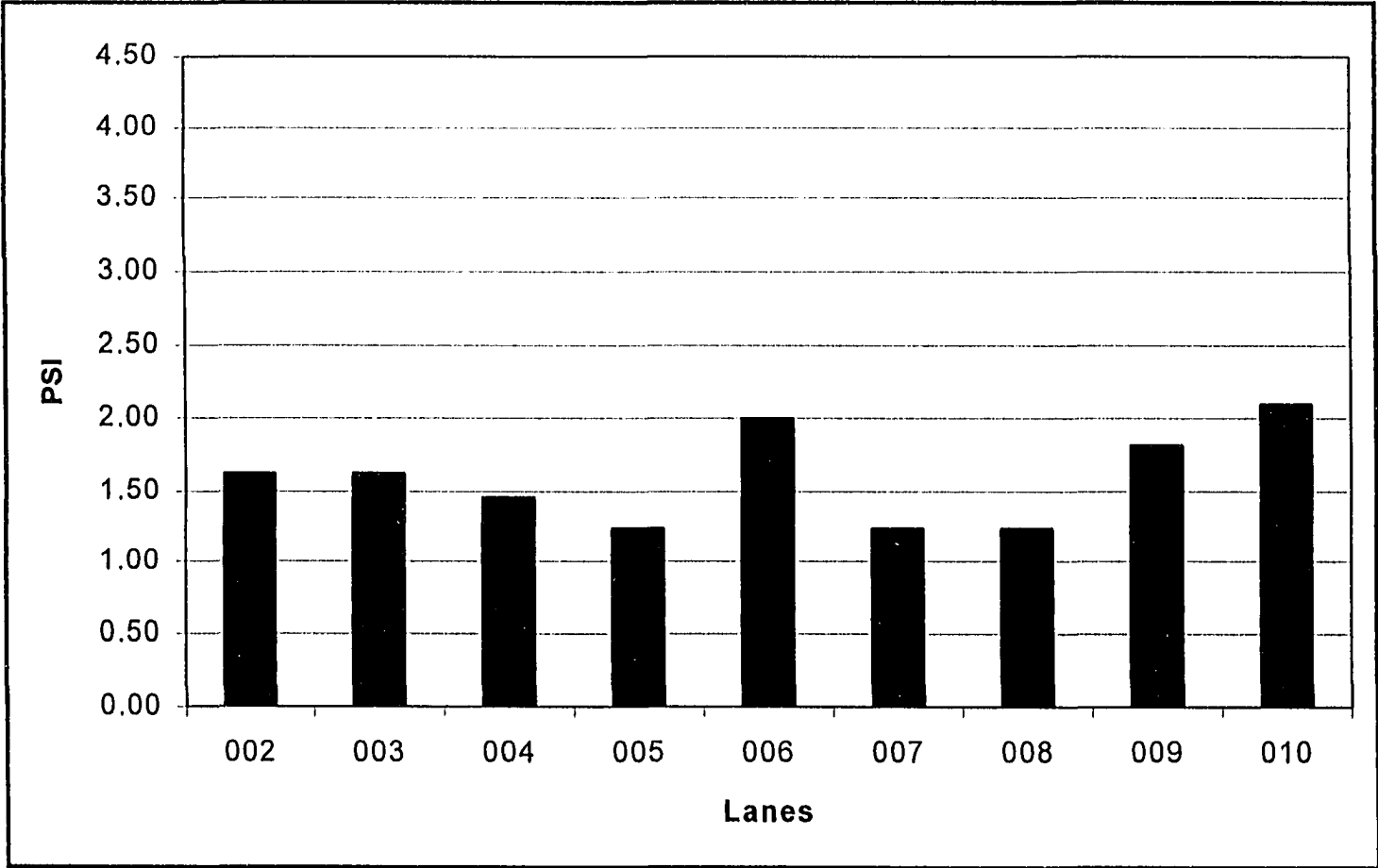


Figure 6. 38 Predicted PSI comparison at the end of a 20-year performance period for pavements designed for an average ADT of 75,000 and subgrade modulus of 10,600 psi

CHAPTER 7

CONCLUSIONS AND RECOMMENDATIONS

Based on the analysis of data from the ALF site as discussed in Chapter 5, the following conclusions are drawn:

The 216-mm. (8.5-in.) crushed stone base (lane 002), 102-mm. (4-in.) crushed stone base over 152-mm. (6-in.) of 10 percent mixed in place soil cement (lane 009) and 12 in. of 4 percent plant mixed soil cement base (lane 010) performed better than any of other base combinations for all the performance criteria considered.

1. For this series of tests, the 216-mm. (8.5-in.) crushed stone base performed better than any of the 216-mm. (8.5-in.) soil cement bases in terms of rut, roughness and crack development. This is a surprising finding and is counter to the general experience and pavement design practices in Louisiana.
2. The soil cement bases with 4 percent cement performed as well as those with 10 percent cement, compare the performance of lanes 006 and 007 with 005.
3. The mixed in-place soil cement performed as well as the plant mixed soil cement, compare lanes 008 and 009 with 005.

4. The 4 percent, 305-mm. (12-in.) soil cement base performed much better in both rutting and cracking than any of the other 216-mm.(8.5-in.) soil cement bases with either 4 or 10 percent cement.
5. The combination of 102-mm. (4-in.) crushed stone base over 152-mm. (6-in.) of 10 percent soil cement (lane 009) outperformed all of the 216-mm.(8.5-in.) soil cement bases as well as the 216-mm.(8.5-in.) crushed stone bases. Additionally this material configuration should have the least problem with reflection cracking from the soil cement through the HMA surface.
6. Crushed stone bases should definitely be considered for use in Louisiana even in those areas where the subgrade is relatively soft with predicted moduli of around 35 MPa (5 ksi).
7. Combinations of crushed stone over soil cement appear to be an excellent material combination to carry traffic loads while resisting rutting and should retard the occurrence of reflection cracking.
8. Soil cement bases using 4 percent and mixed in-place should be constructed and their performance observed and compared to the more standard 10 percent plant mixed soil cement base.

Based on the discussions on the performance of ALF materials when constructed in different environment and traffic levels as presented in Chapter 6 , the following conclusions are drawn:

1. Pavement structures using crushed stone materials for the base similar to those used in the ALF test sections should be limited initially to roadways

with ADT not more than 25,000 or the number of ESALs not more than 23.7 million ESALs for a 20 year design period.

2. Soil cement bases can structurally be used in any areas with ADT not more than 40,000 or the number of ESALs less than 44.4 million for the 20 year design period. However, one should be cautious when using this material in the areas where a high rainfall or the potential for a high water table exists since water may weaken the structure and cause a substantial reduction in pavement life.
3. None of the material combination used in the ALF test section performed satisfactorily in the areas when the ADT was more than 75,000. In such situations, a full depth hot mix asphalt or a rigid pavement should be considered.
4. Inverted sections such as that used in lane 009 of ALF test section provided the best overall performance characteristics of all the materials. The results from the Louisiana ALF experiment showed that the inverted section provided better performance due to its ability to substantially reduce the reflection cracking initiated in the soil cement material underneath.
5. The different results between the ALF experiment and the simulation study are believed to be principally due to the approach used in designing the thickness of the section, which is set to have similar total thickness for the different materials and the inability of the model to change the material characteristic due to environmental changes.

Recommendations

1. Recommendations for material usage in the field. The various pavement material combination tested in the ALF test sections have been analyzed using a simulation study to evaluate the predicted performance in different subgrade conditions and traffic situations. Based on the analysis, the following recommendations presented in Table 7.1 are made regarding the use of each cross section type.

Table 7. 1 Recommended use of ALF test materials based on traffic and subgrade modulus

| Subgrade Resilient Moduli, MPa (psi) | Traffic, ADT | Recommended Base Materials |
|--------------------------------------|-----------------------------------|------------------------------------|
| 52.4 – 58.0 (7,600 – 8,400) | $\leq 15,000$ | Lanes 002 and 003 |
| | $15,000 < \text{ADT} \leq 40,000$ | Lanes 005, 006, 007, 008, 009, 010 |
| | $> 40,000$ | Full depth or rigid pavements |
| 60.7 – 65.5 (8,800 – 9,500) | $\leq 25,000$ | Lanes 002 and 003 |
| | $25,000 < \text{ADT} \leq 40,000$ | Lanes 005, 006, 007, 008, 009, 010 |
| | $> 40,000$ | Full depth or rigid pavements |
| 68.2 – 77.9 (9,900 – 11,300) | $\leq 25,000$ | Lanes 002 and 003 |
| | $25,000 < \text{ADT} \leq 40,000$ | Lanes 005, 006, 007, 008, 009, 010 |
| | $> 40,000$ | Full depth or rigid pavements |

2. Implementation. Since results from both the ALF experiment and the simulation study showed that the inverted section has outstanding performance, the La DOTD should start incorporating this pavement structure into appropriate new construction or reconstruction projects on an experimental basis. Any construction projects should be routinely examined and to assess performance under traffic on experimental conditions.

3. Further ALF research. A further and more detail study is needed for soil cement material in order to determine its material properties and its behavior in different level of stress and, more importantly, to determine the effect of water presence in the soil cement to its performance. In addition, further research is needed to seek any method to reduce the reflection cracking from the soil cement to the hot mix asphalt surface.
4. Duplication. In any experimental program, duplication of a few test sections is critical in helping to define the variations in test results. It could be very desirable to replicate at least one of the granular base sections and one of the cement stabilized base sections to begin to assess variability.

APPENDIX 1. RESILIENT MODULUS DATA

Table A1. 1 Predicted layer moduli for lane 002

| Passes x 1,000 | ESALs, x 1,000 | Date | Surf. Temp | Pav. Temp | AC Uncorrected, ksi | AC Corrected, ksi | Base, ksi | Subbase, ksi | Subgrade, ksi |
|-------------------|-------------------|----------|---------------|--------------|---------------------------|-------------------------|-----------|-----------------|------------------|
| 0 | 0 | 12/27/95 | 70.1 | 63.7 | 318.0 | 254.0 | 20.9 | 5.9 | 6.6 |
| 25 | 39 | 2/21/96 | 73.6 | 66.9 | 298.0 | 241.0 | 20.4 | 4.7 | 6.8 |
| 50 | 77 | 2/27/96 | 78.6 | 71.5 | 300.0 | 300.0 | 20.0 | 4.3 | 3.9 |
| 75 | 116 | 3/12/96 | 71.8 | 65.3 | 437.0 | 349.0 | 20.0 | 5.1 | 4.0 |
| 125 | 193 | 3/12/96 | 90.2 | 82 | 107.0 | 192.0 | 20.0 | 5.3 | 3.2 |
| 143 | 221 | 4/20/96 | 111.2 | 101.1 | 103.0 | 453.0 | 20.0 | 5.9 | 3.2 |
| 217 | 336 | 4/24/96 | 110.4 | 100.4 | 100.0 | 440.0 | 20.0 | 5.3 | 2.7 |
| 243 | 523 | 5/8/96 | 106 | 96.4 | 75.0 | 263.0 | 20.0 | 5.0 | 2.5 |
| 300 | 933 | 9/13/96 | 100 | 90.9 | 111.0 | 278.0 | 20.0 | 5.0 | 2.7 |
| 322 | 1092 | 9/19/96 | 82.6 | 75.1 | 217.0 | 281.0 | 20.0 | 5.1 | 3.0 |
| Average | | | | | 206.6 | 305.1 | 20.1 | 5.2 | 3.9 |

Table A1. 2 Predicted layer moduli for lane 003

| Passes x 1,000 | ESALs, x 1,000 | Date | Surf. Temp | Pav. Temp | AC Uncorrected, ksi | AC Corrected, ksi | Base, ksi | Subbase, ksi | Subgrade, ksi |
|-------------------|-------------------|---------|---------------|--------------|---------------------------|-------------------------|-----------|-----------------|------------------|
| 0 | 0 | 1/16/96 | 78.2 | 71.1 | 533 | 533 | 20.1 | 10 | 5 |

Table A1. 3 Predicted layer moduli for lane 004

| Passes x 1,000 | ESALs, x 1,000 | Date | Surf. Temp, °F | Pav. Temp, °F | AC Uncorrected, ksi | AC Corrected, ksi | Base, ksi | Subbase, ksi | Subgrade, ksi |
|-------------------|-------------------|---------|----------------------|---------------------|---------------------------|-------------------------|-----------|-----------------|------------------|
| 0 | 0 | 1/17/96 | 69.6 | 63.3 | 629 | 490 | 22.6 | 14.8 | 4.9 |
| 210 | 325 | 8/16/96 | 97.6 | 88.7 | 150 | 323 | 20 | 5 | 1.9 |
| 258 | 400 | 8/23/96 | 87.3 | 79.4 | 150 | 225 | 20 | 5 | 2 |
| 325 | 504 | 9/5/96 | 99.9 | 90.8 | 211 | 591 | 28.9 | 7.9 | 2.5 |
| Average | | | | | 285 | 407.25 | 22.875 | 8.175 | 2.825 |

Table A1. 4 Predicted layer moduli for lane 005

| Passes x 1,000 | ESALs, x 1,000 | Date | Surf. Temp., °F | Pav. Temp., °F | AC Uncorrected, ksi | AC Corrected, ksi. | Base, ksi | Subbase, ksi | Subgrade, ksi |
|-------------------|-------------------|----------|-----------------------|----------------------|---------------------------|-----------------------|--------------|-----------------|------------------|
| 0 | 0 | 6/19/97 | 110 | 100 | 139 | 611 | 153 | 17.7 | 3.3 |
| 25 | 40 | 10/17/97 | 110 | 100 | 77 | 339 | 150 | 5.2 | 4.9 |
| 50 | 79 | 10/31/97 | 100 | 90.9 | 102 | 275 | 150 | 5.1 | 4.6 |
| 100 | 159 | 12/2/97 | 74 | 67.3 | 303 | 258 | 150 | 5.2 | 4.8 |
| 125 | 199 | 12/16/97 | 90 | 81.8 | 228 | 399 | 150 | 5.2 | 4.9 |
| 175 | 278 | 2/17/98 | 60 | 54.5 | 351 | 200 | 151 | 5.2 | 3.9 |
| Average | | | | | 200 | 347 | 151 | 7.3 | 4.4 |

Table A1. 5 Predicted layer moduli for lane 006

| Passes x 1,000 | ESALs, x 1,000 | Date | Surf. Temp., °F | Pav. Temp., °F | AC Uncorrected, ksi | AC Corrected, ksi. | Base, ksi | Subbase, ksi | Subgrade, ksi |
|-------------------|-------------------|----------|--------------------|-------------------|---------------------------|--------------------------|--------------|-----------------|------------------|
| 0 | 0 | 6/19/97 | 125 | 113.6 | 75 | 450 | 150 | 5 | 2.6 |
| 25 | 39 | 10/7/97 | 94 | 85.5 | 150 | 300 | 103 | 5 | 3.2 |
| 50 | 77 | 10/20/97 | 100 | 90.9 | 76 | 205 | 100 | 5 | 6.1 |
| 75 | 116 | 11/3/97 | 70 | 63.6 | 300 | 240 | 100 | 5.1 | 4.5 |
| 100 | 155 | 12/1/97 | 80 | 72.7 | 250 | 263 | 100 | 5.1 | 4.6 |
| 125 | 194 | 12/16/97 | 80 | 72.7 | 250 | 263 | 151 | 5.5 | 3.7 |
| 175 | 271 | 2/17/98 | 60 | 54.5 | 350 | 192 | 150 | 5 | 2 |
| Average | | | | | 207 | 273 | 122 | 5.1 | 3.8 |

Table A1. 6 Predicted layer moduli for lane 007

| Passes x 1,000 | ESALs, x 1,000 | Date | Surf. Temp., °F | Pav. Temp., °F | AC Uncorrected, ksi | AC Corrected, ksi. | Base, ksi | Subbase, ksi | Subgrade, ksi |
|-------------------|-------------------|----------|--------------------|-------------------|---------------------------|--------------------------|-----------|-----------------|------------------|
| 25 | 39 | 10/7/97 | 110 | 100 | 75 | 375 | 151 | 5 | 3.9 |
| 50 | 77 | 10/20/97 | 100 | 90.9 | 75 | 300 | 150 | 5.3 | 5 |
| 75 | 116 | 10/31/97 | 100 | 90.9 | 75 | 203 | 154 | 5.1 | 4.2 |
| 125 | 155 | 12/1/97 | 80 | 72.7 | 250 | 675 | 151 | 5.9 | 3.9 |
| Average | | | | | 119 | 388 | 152 | 5.3 | 4.3 |

Table A1. 7 Predicted layer moduli for lane 008

| Passes x 1,000 | ESALs, x 1,000 | Date | Surf. Temp., °F | Pav. Temp., °F | AC Uncorrected, ksi | AC Corrected, ksi. | Base, ksi | Subbase, ksi | Subgrade, ksi |
|-------------------|-------------------|----------|--------------------|-------------------|---------------------------|--------------------------|--------------|-----------------|------------------|
| 0 | 0 | 2/12/96 | 68.9 | 62.6 | 433 | 321 | 156 | 15.3 | 4.7 |
| 25 | 38.75 | 11/30/96 | 88.7 | 80.6 | 164 | 246 | 151 | 13.5 | 4.1 |
| 50 | 77.5 | 12/6/96 | 66.1 | 60.1 | 350 | 227 | 150 | 7.9 | 3.6 |
| 75 | 155 | 2/13/97 | 81.8 | 74.4 | 262 | 328 | 155 | 8.3 | 3.8 |
| Average | | | | | 302 | 281 | 153 | 11.3 | 4.1 |

Table A1. 8 Predicted layer moduli for lane 009

| Passes x 1,000 | ESALs, x 1,000 | Date | Surf. Temp., °F | Pav. Temp., °F | AC Uncorrected, ksi | AC Corrected, ksi. | Base, ksi | Subbase, ksi | Subgrade, ksi |
|-------------------|-------------------|---------|--------------------|-------------------|---------------------------|--------------------------|-----------|-----------------|------------------|
| 0 | 0 | 2/12/96 | 72.3 | 65.7 | 522 | 443 | 20.1 | 161.4 | 10.2 |
| 25 | 39 | 2/21/96 | 73.6 | 66.9 | 710 | 603 | 20.9 | 151.8 | 9.7 |
| 50 | 78 | 12/6/96 | 84.7 | 77 | 710 | 922 | 20.7 | 152.3 | 9.4 |
| 100 | 157 | 2/13/97 | 67.2 | 61.1 | 800 | 559 | 37.7 | 150 | 5.5 |
| 225 | 626 | 4/23/97 | 73 | 66.4 | 699 | 559 | 21.8 | 157.2 | 8.1 |
| 275 | 813 | 5/8/97 | 80 | 72.7 | 481 | 536 | 21.3 | 150 | 7 |
| 300 | 907 | 5/16/97 | 81 | 73.6 | 422 | 540 | 21 | 150 | 6.5 |
| 325 | 1000 | 5/20/97 | 101 | 91.8 | 186 | 539 | 20.3 | 150 | 5.7 |
| 360 | 1132 | 5/29/97 | 108 | 98.2 | 142 | 539 | 20.4 | 150 | 5.5 |
| 385 | 1344 | 6/3/97 | 99 | 90 | 201 | 503 | 20.6 | 150 | 6 |
| 410 | 1557 | 6/6/97 | 109 | 99.1 | 127 | 432 | 20.2 | 150 | 4.9 |
| 435 | 1769 | 6/12/97 | 111 | 100.9 | 136 | 510 | 20.2 | 150 | 5 |
| Average | | | | | 428 | 557 | 22 | 152 | 7.0 |

Table A1. 9 Predicted layer moduli for lane 010

| Passes x 1,000 | ESALs, x 1,000 | Date | Surf. Temp., °F | Pav. Temp., °F | AC Uncorrected, ksi | AC Corrected, ksi. | Base, ksi | Subbase, ksi | Subgrade, ksi |
|-------------------|-------------------|---------|-----------------------|-------------------|---------------------------|-----------------------|-----------|-----------------|------------------|
| 0 | 0 | 2/13/96 | 57.6 | 52.4 | 412 | 222 | 178.6 | 0 | 5.5 |
| 25 | 39 | 2/21/96 | 73.6 | 66.9 | 327 | 281 | 150.6 | 0 | 5.2 |
| 50 | 79 | 12/3/96 | 68.6 | 62.4 | 300 | 240 | 150 | 0 | 4.6 |
| 75 | 118 | 1/7/97 | 66.1 | 60.1 | 300 | 205 | 150.1 | 0 | 4.6 |
| 100 | 158 | 2/7/97 | 63 | 57.3 | 380 | 228 | 151.2 | 0 | 5.1 |
| 150 | 368 | 4/23/97 | 112 | 101.8 | 87 | 435 | 169 | 0 | 4.7 |
| 193 | 548 | 4/23/97 | 112 | 101.8 | 75 | 375 | 153.9 | 0 | 4.6 |
| Average | | | | | 269 | 284 | 158 | 0 | 4.9 |

APPENDIX 2. RUTTING DATA

Table A2. 1 Rut depth for lane 002

| Load | Date Data Taken | Passes | ESALs | Rutting | | | | | | | | | |
|-------|-----------------|--------|---------|---------|-------|-------|-------|-------|-------|-------|-------|------|------|
| | | | | Sta 1 | Sta 2 | Sta 3 | Sta 4 | Sta 5 | Sta 6 | Sta 7 | Sta 8 | | |
| 10000 | 2/6/96 | 0 | 0 | 0.00 | 0.00 | 0.00 | 0.00 | 0.00 | 0.00 | 0.00 | 0.00 | 0.00 | 0.00 |
| 10000 | 2/19/96 | 25000 | 38,750 | 0.04 | 0.05 | 0.04 | 0.04 | 0.04 | 0.05 | 0.11 | 0.08 | 0.06 | 0.06 |
| 10000 | 2/26/96 | 50000 | 77,500 | 0.20 | 0.15 | 0.18 | 0.18 | 0.18 | 0.18 | 0.18 | 0.18 | 0.18 | 0.16 |
| 10000 | 3/11/96 | 75000 | 116,250 | 0.21 | 0.15 | 0.23 | 0.19 | 0.19 | 0.19 | 0.19 | 0.23 | 0.15 | 0.15 |
| 10000 | 4/19/96 | 100000 | 155,000 | 0.43 | 0.33 | 0.43 | 0.33 | 0.33 | 0.38 | 0.33 | 0.38 | 0.24 | 0.24 |
| 10000 | 4/19/96 | 188830 | 292,687 | 0.39 | 0.42 | 0.40 | 0.40 | 0.40 | 0.40 | 0.36 | 0.24 | 0.28 | 0.28 |
| 10000 | 4/25/96 | 217553 | 337,207 | 0.52 | 0.40 | 0.41 | 0.42 | 0.42 | 0.42 | 0.43 | 0.58 | 0.23 | 0.23 |
| 14000 | 5/6/96 | 231945 | 440,830 | 0.84 | 0.77 | 0.73 | 0.76 | 0.76 | 0.65 | 0.55 | 0.42 | 0.27 | 0.27 |
| 14000 | 5/9/96 | 243644 | 525,062 | 1.11 | 1.08 | 0.96 | 1.04 | 1.04 | 0.76 | 0.53 | 0.42 | 0.31 | 0.31 |
| 14000 | 5/10/96 | 251525 | 581,806 | 1.15 | 1.18 | 1.19 | 1.10 | 1.10 | 0.76 | 0.57 | 0.49 | 0.31 | 0.31 |
| 14000 | 5/24/96 | 262219 | 658,802 | 1.30 | 1.41 | 1.27 | 1.34 | 1.34 | 0.95 | 0.69 | 0.53 | 0.34 | 0.34 |
| 14000 | 6/18/96 | 271000 | 722,026 | 1.26 | 1.41 | 1.26 | 1.35 | 1.35 | 1.27 | 0.80 | 0.57 | 0.46 | 0.46 |
| 14000 | 9/12/96 | 296775 | 907,606 | 1.37 | 1.60 | 1.45 | 1.53 | 1.53 | 1.34 | 1.04 | 0.76 | 0.50 | 0.50 |

Table A2. 2 Rut depth for lane 003

| Load | Date Data Taken | Passes | ESALs | Rutting | | | | | | | | | | |
|-------|-----------------|--------|--------|---------|-------|-------|-------|-------|-------|-------|-------|------|--|--|
| | | | | Sta 1 | Sta 2 | Sta 3 | Sta 4 | Sta 5 | Sta 6 | Sta 7 | Sta 8 | | | |
| 10000 | 6/11/96 | 0 | 0 | | | | | | | | | | | |
| 10000 | 6/17/96 | 5,234 | 8,217 | 0.37 | 0.40 | 0.33 | 0.33 | 0.29 | 0.29 | 0.29 | 0.39 | 0.33 | | |
| 10000 | 6/18/96 | 10,448 | 16,403 | 0.44 | 0.40 | 0.40 | 0.44 | 0.33 | 0.29 | 0.29 | 0.44 | 0.29 | | |
| 10000 | 6/21/96 | 25,000 | 39,250 | 0.61 | 0.52 | 0.60 | 0.52 | 0.44 | 0.44 | 0.36 | 0.48 | 0.40 | | |
| 10000 | 6/28/96 | 49,990 | 78,484 | 0.75 | 0.76 | 0.76 | 0.68 | 0.56 | 0.56 | 0.44 | 0.56 | 0.48 | | |

Table A2. 3 Rut depth for lane 004

| Load | Date Data Taken | Passes | ESALs | Rutting | | | | | | | |
|-------|-----------------|---------|---------|---------|-------|-------|-------|-------|-------|-------|-------|
| | | | | Sta 1 | Sta 2 | Sta 3 | Sta 4 | Sta 5 | Sta 6 | Sta 7 | Sta 8 |
| 10000 | 7/15/96 | 23857 | 36,978 | 0.42 | 0.53 | 0.46 | 0.46 | 0.61 | 0.50 | 0.69 | 0.88 |
| 10000 | 8/2/96 | 109,000 | 168,950 | 0.72 | 0.77 | 0.64 | 0.61 | 0.73 | 0.60 | 0.76 | 0.99 |
| 10000 | 8/9/96 | 158,977 | 246,414 | 0.88 | 0.81 | 0.62 | 0.62 | 0.73 | 0.59 | 0.71 | 0.98 |
| 10000 | 8/12/96 | 183,982 | 285,172 | 0.92 | 0.84 | 0.61 | 0.69 | 0.76 | 0.65 | 0.78 | 1.03 |
| 10000 | 8/16/96 | 209,000 | 323,950 | 0.88 | 0.92 | 0.66 | 0.70 | 0.77 | 0.62 | 0.73 | 0.99 |
| 10000 | 8/20/96 | 233,984 | 362,675 | 0.99 | 1.18 | 0.73 | 0.78 | 0.88 | 0.67 | 0.95 | 1.08 |
| 10000 | 8/23/96 | 258,000 | 399,900 | 1.06 | 1.28 | 0.75 | 0.81 | 0.95 | 0.66 | 0.99 | 1.03 |

Table A2. 4 Rut depth for lane 005

| Load | Date Data Taken | Passes | ESALs | Rutting | | | | | | | | | |
|-------|-----------------|--------|---------|---------|-------|-------|-------|-------|-------|-------|-------|------|------|
| | | | | Sta 1 | Sta 2 | Sta 3 | Sta 4 | Sta 5 | Sta 6 | Sta 7 | Sta 8 | | |
| 10000 | 10/7/97 | 0 | 0 | 0.00 | 0.00 | 0.00 | 0.00 | 0.00 | 0.00 | 0.00 | 0.00 | 0.00 | 0.00 |
| 10000 | 10/10/97 | 25000 | 39,750 | 0.07 | 0.07 | 0.07 | 0.13 | 0.11 | 0.11 | 0.11 | 0.09 | 0.11 | 0.11 |
| 10000 | 10/31/97 | 50000 | 79,500 | 0.15 | 0.10 | 0.15 | 0.15 | 0.17 | 0.17 | 0.18 | 0.18 | 0.15 | 0.15 |
| 10000 | 11/3/97 | 75000 | 119,250 | 0.18 | 0.20 | 0.23 | 0.22 | 0.34 | 0.34 | 0.24 | 0.20 | 0.22 | 0.22 |
| 10000 | 12/11/97 | 100033 | 159,052 | 0.19 | 0.18 | 0.22 | 0.26 | 0.48 | 0.48 | 0.27 | 0.24 | 0.18 | 0.18 |
| 10000 | 12/18/97 | 125035 | 198,806 | 0.22 | 0.19 | 0.23 | 0.29 | 0.55 | 0.55 | 0.30 | 0.30 | 0.23 | 0.23 |
| 10000 | 1/8/97 | 150064 | 238,602 | 0.38 | 0.24 | 0.31 | 0.53 | 0.88 | 0.88 | 0.76 | 0.61 | 0.69 | 0.69 |

Table A2.5 Rut depth for lane 003

| Load | Date Data Taken | Passes | ESALs | Rutting | | | | | | | | | |
|-------|-----------------|--------|---------|---------|-------|-------|-------|-------|-------|-------|-------|------|------|
| | | | | Sta 1 | Sta 2 | Sta 3 | Sta 4 | Sta 5 | Sta 6 | Sta 7 | Sta 8 | | |
| 10000 | 9/29/97 | 0 | 0 | 0.00 | 0.00 | 0.00 | 0.00 | 0.00 | 0.00 | 0.00 | 0.00 | 0.00 | 0.00 |
| 10000 | 10/10/97 | 25000 | 38,750 | 0.15 | 0.12 | 0.11 | 0.11 | 0.13 | 0.13 | 0.15 | 0.15 | 0.15 | 0.16 |
| 10000 | 10/20/97 | 50000 | 77,500 | 0.20 | 0.15 | 0.13 | 0.15 | 0.15 | 0.15 | 0.17 | 0.21 | 0.21 | 0.18 |
| 10000 | 11/3/97 | 75000 | 116,250 | 0.18 | 0.16 | 0.12 | 0.16 | 0.20 | 0.20 | 0.24 | 0.21 | 0.21 | 0.20 |
| 10000 | 12/5/97 | 100000 | 155,000 | 0.21 | 0.25 | 0.16 | 0.18 | 0.22 | 0.22 | 0.26 | 0.37 | 0.37 | 0.32 |
| 10000 | 12/16/97 | 125041 | 193,814 | 0.18 | 0.15 | 0.15 | 0.18 | 0.23 | 0.23 | 0.25 | 0.45 | 0.45 | 0.42 |
| 10000 | 1/8/97 | 150036 | 232,556 | 0.20 | 0.23 | 0.23 | 0.29 | 0.69 | 0.69 | 0.50 | 0.67 | 0.67 | 0.70 |

Table A2. 6 Rut depth for lane 007

| Load | Date Data Taken | Passes | ESALs | Rutting | | | | | | | | |
|-------|-----------------|--------|---------|---------|-------|-------|-------|-------|-------|-------|-------|------|
| | | | | Sta 1 | Sta 2 | Sta 3 | Sta 4 | Sta 5 | Sta 6 | Sta 7 | Sta 8 | |
| 10000 | 10/7/97 | 0 | 0 | 0.00 | 0.00 | 0.00 | 0.00 | 0.00 | 0.00 | 0.00 | 0.00 | 0.00 |
| 10000 | 10/10/97 | 25000 | 38,750 | 0.20 | 0.29 | 0.21 | 0.17 | 0.15 | 0.22 | 0.14 | 0.11 | |
| 10000 | 10/31/97 | 50000 | 77,500 | 0.23 | 0.42 | 0.23 | 0.21 | 0.12 | 0.13 | 0.15 | 0.16 | |
| 10000 | 11/6/97 | 75000 | 116,250 | 0.26 | 0.41 | 0.21 | 0.22 | 0.18 | 0.18 | 0.16 | 0.18 | |
| 10000 | 11/25/97 | 100000 | 155,000 | 0.36 | 0.49 | 0.27 | 0.20 | 0.18 | 0.19 | 0.20 | 0.29 | |
| 10000 | 12/16/97 | 125024 | 193,787 | 0.27 | 0.57 | 0.29 | 0.21 | 0.12 | 0.18 | 0.18 | 0.19 | |
| 10000 | 1/8/97 | 150061 | 232,595 | 0.40 | 0.73 | 0.35 | 0.27 | 0.15 | 0.14 | 0.15 | 0.23 | |
| 10000 | 2/6/98 | 175156 | 271,492 | 0.59 | 1.09 | 0.50 | 0.38 | 0.17 | 0.17 | 0.15 | 0.32 | |

Table A2. 7 Rut depth for lane 008

| Load | Date Data Taken | Passes | ESALs | Rutting | | | | | | | | |
|-------|-----------------|--------|---------|---------|-------|-------|-------|-------|-------|-------|-------|------|
| | | | | Sta 1 | Sta 2 | Sta 3 | Sta 4 | Sta 5 | Sta 6 | Sta 7 | Sta 8 | |
| 10000 | | 0 | 0 | 0.00 | 0.00 | 0.00 | 0.00 | 0.00 | 0.00 | 0.00 | 0.00 | 0.00 |
| 10000 | 12/23/96 | 50000 | 77,500 | 0.04 | 0.04 | 0.04 | 0.09 | 0.04 | 0.04 | 0.04 | 0.04 | 0.06 |
| 10000 | 1/31/97 | 75000 | 116,250 | 0.27 | 0.30 | 0.15 | 0.14 | 0.21 | 0.21 | 0.29 | 0.19 | |
| 10000 | 2/21/97 | 125000 | 290,750 | 0.40 | 0.51 | 0.44 | 0.27 | 0.57 | 0.59 | 0.66 | 0.31 | |

Table A2. 8 Rut depth for lane 009

| Load | Date Data Taken | Passes | ESALs | Rutting | | | | | | | | | |
|-------|-----------------|--------|-----------|---------|-------|-------|-------|-------|-------|-------|-------|------|------|
| | | | | Sta 1 | Sta 2 | Sta 3 | Sta 4 | Sta 5 | Sta 6 | Sta 7 | Sta 8 | | |
| 10000 | 11/22/96 | 0 | 0 | 0.00 | 0.00 | 0.00 | 0.00 | 0.00 | 0.00 | 0.00 | 0.00 | 0.00 | 0.00 |
| 10000 | 11/23/96 | 50000 | 78,500 | 0.12 | 0.04 | 0.06 | 0.05 | 0.04 | 0.04 | 0.06 | 0.06 | 0.06 | 0.04 |
| 10000 | 1/14/97 | 75000 | 117,750 | 0.08 | 0.08 | 0.09 | 0.08 | 0.09 | 0.09 | 0.10 | 0.08 | 0.08 | 0.07 |
| 10000 | 2/13/97 | 100045 | 157,071 | 1.11 | 1.18 | 1.26 | 0.97 | 0.95 | 0.95 | 0.41 | 0.38 | 0.38 | 0.02 |
| 12300 | 2/21/97 | 125000 | 250,652 | 0.09 | 0.08 | 0.10 | 0.09 | 0.02 | 0.02 | 0.09 | 0.05 | 0.05 | 0.09 |
| 12300 | 3/11/97 | 150000 | 344,402 | 0.19 | 0.20 | 0.23 | 0.20 | 0.17 | 0.17 | 0.21 | 0.18 | 0.18 | 0.14 |
| 12300 | 3/21/97 | 175055 | 438,358 | 0.44 | 0.33 | 0.29 | 0.25 | 0.27 | 0.27 | 0.25 | 0.30 | 0.30 | 0.12 |
| 12300 | 4/18/97 | 200057 | 532,116 | 0.20 | 0.00 | 0.32 | 0.30 | 0.32 | 0.32 | 0.26 | 0.28 | 0.28 | 0.20 |
| 12300 | 4/29/97 | 250048 | 719,582 | 0.25 | 0.43 | 0.44 | 0.48 | 0.40 | 0.40 | 0.24 | 0.24 | 0.24 | 0.16 |
| 12300 | 5/11/97 | 275056 | 813,362 | 0.52 | 0.49 | 0.54 | 0.57 | 0.42 | 0.42 | 0.27 | 0.23 | 0.23 | 0.22 |
| 12300 | 5/21/97 | 325063 | 1,000,888 | 0.63 | 0.77 | 0.77 | 0.70 | 0.59 | 0.59 | 0.32 | 0.26 | 0.26 | 0.22 |
| 12300 | 5/30/97 | 360069 | 1,132,161 | 0.76 | 0.91 | 0.95 | 0.76 | 0.76 | 0.76 | 0.34 | 0.34 | 0.34 | 0.37 |
| 14600 | 6/6/97 | 410077 | 1,557,229 | 1.12 | 1.22 | 1.26 | 0.95 | 0.95 | 0.95 | 0.38 | 0.38 | 0.38 | 0.38 |
| 14600 | 6/11/97 | 435077 | 1,769,729 | 1.17 | 1.87 | 1.43 | 1.13 | 1.14 | 1.14 | 0.48 | 0.41 | 0.41 | 0.44 |
| 14600 | 7/10/97 | 460077 | 1,982,229 | 1.65 | 2.30 | 1.95 | 1.55 | 0.96 | 0.96 | 0.80 | 0.66 | 0.66 | 0.64 |

Table A2. 9 Rut depth for lane 010

| Load | Date Data Taken | Passes | ESALs | Rutting | | | | | | | | | |
|-------|-----------------|---------|---------|---------|-------|-------|-------|-------|-------|-------|-------|------|------|
| | | | | Sta 1 | Sta 2 | Sta 3 | Sta 4 | Sta 5 | Sta 6 | Sta 7 | Sta 8 | | |
| 10000 | 11/15/96 | 0 | 0 | 0.00 | 0.00 | 0.00 | 0.00 | 0.00 | 0.00 | 0.00 | 0.00 | 0.00 | 0.00 |
| 10000 | 12/23/96 | 50,000 | 79,000 | 0.19 | 0.18 | 0.09 | 0.07 | 0.11 | 0.11 | 0.11 | 0.16 | 0.16 | 0.09 |
| 10000 | 1/10/97 | 75,000 | 118,500 | 0.07 | 0.07 | 0.04 | 0.10 | 0.09 | 0.09 | 0.06 | 0.04 | 0.04 | 0.08 |
| 12300 | 2/21/97 | 125,000 | 328,500 | 0.18 | 0.10 | 0.09 | 0.19 | 0.11 | 0.07 | 0.07 | 0.09 | 0.09 | 0.10 |
| 12300 | 3/11/97 | 150,000 | 433,500 | 0.50 | 0.33 | 0.20 | 0.33 | 0.25 | 0.14 | 0.14 | 0.12 | 0.12 | 0.14 |
| 12300 | 3/21/97 | 175,000 | 538,500 | 0.60 | 0.29 | 0.39 | 0.43 | 0.37 | 0.17 | 0.17 | 0.16 | 0.16 | 0.16 |
| 12300 | 4/18/97 | 193,285 | 615,297 | 0.83 | 0.83 | 0.80 | 0.28 | 0.41 | 0.17 | 0.17 | 0.16 | 0.16 | 0.14 |
| 12300 | 4/29/97 | 250,048 | 853,702 | 0.92 | 0.90 | 0.85 | 0.32 | 0.80 | 0.31 | 0.31 | 0.13 | 0.13 | 0.20 |

APPENDIX 3. ROUGHNESS DATA

Table A3. 1 IRI and RN values for lane 002

| Load | Data Taken | Passes | ESALs | Average IRI, m/km | | | Average RN | | |
|--------|------------|---------|---------|-------------------|----------------|-----------------|-----------------|----------------|-----------------|
| | | | | Sample Interval | | | Sample Interval | | |
| | | | | 25 mm (1 in.) | 152 mm (6 in.) | 304 mm (12 in.) | 25 mm (1 in.) | 152 mm (6 in.) | 304 mm (12 in.) |
| | 2/6/96 | 0 | 0 | 1.03 | 0.94 | 1.32 | 3.3 | 3.64 | 3.62 |
| 10,000 | 2/19/96 | 25,000 | 38,750 | 1.41 | 1.39 | 1.08 | 3.21 | 3.46 | 3.76 |
| 10,000 | 2/26/96 | 50,000 | 77,500 | 1.45 | 1.39 | 1.18 | 3.41 | 3.57 | 3.69 |
| 10,000 | 3/11/96 | 75,000 | 116,250 | 1.8 | 1.59 | 1.52 | 3.05 | 3.36 | 3.43 |
| 10,000 | 4/19/96 | 100,000 | 155,000 | 1.98 | 1.81 | 1.7 | 3 | 3.33 | 3.4 |
| 10,000 | 4/19/96 | 188,830 | 292,687 | 2.44 | 1.92 | 1.87 | 2.75 | 3.16 | 3.24 |
| 10,000 | 4/25/96 | 217,553 | 337,207 | 4.23 | 3.86 | 3.95 | 2.17 | 2.39 | 2.44 |
| 14,000 | 5/6/96 | 231,945 | 440,830 | 3.8 | 3.67 | 3.64 | 2.19 | 2.4 | 2.42 |
| 14,000 | 5/9/96 | 243,644 | 525,062 | 4.88 | 5.03 | 4.78 | 1.86 | 1.9 | 2 |
| 14,000 | 5/10/96 | 251,525 | 581,806 | 4.91 | 4.51 | 4.39 | 1.8 | 2 | 2.03 |
| 14,000 | 5/24/96 | 262,191 | 658,601 | 5.56 | 5.29 | 5.19 | 1.69 | 1.82 | 1.94 |
| 14,000 | 6/18/96 | 271,000 | 722,026 | 6.18 | 6.19 | 6.28 | 1.51 | 1.63 | 1.6 |
| 14,000 | 9/12/96 | 296,775 | 907,606 | 6.49 | 5.98 | 6.05 | 1.41 | 1.63 | 1.61 |

Table A3. 2 IRI and RN values for lane 003

| Load | Date Data Taken | Passes | ESALs | Average IRI, m/km | | | Average RN | | |
|--------|-----------------------|--------|--------|-------------------|-------------------|--------------------|------------------|-------------------|--------------------|
| | | | | Sample Interval | | | Sample Interval | | |
| | | | | 25 mm (1 in.) | 152 mm (6 in.) | 304 mm (12 in.) | 25 mm (1 in.) | 152 mm (6 in.) | 304 mm (12 in.) |
| 10,000 | 6/11/96 | 0 | 0 | 2.12 | 2.13 | 2.05 | 3.07 | 3.15 | 3.14 |
| 10,000 | 6/17/96 | 5,234 | 8,217 | 3.72 | 3.2 | 3.22 | 2.37 | 2.69 | 2.67 |
| 10,000 | 6/18/96 | 10,448 | 16,403 | 3.32 | 2.75 | 2.63 | 2.6 | 2.86 | 2.87 |
| 10,000 | 6/21/96 | 25,000 | 39,250 | 4.37 | 4.18 | 4.08 | 1.99 | 2.22 | 2.31 |
| 10,000 | 6/28/96 | 49,990 | 78,484 | 6.06 | 5.28 | 5.16 | 1.57 | 1.95 | 1.95 |

Table A3. 3 IRI and RN values for lane 004

| Load | Date Data Taken | Passes | ESALs | Average IRI, m/km | | | Average RN | | |
|--------|-----------------------|---------|---------|-------------------|-------------------|--------------------|------------------|-------------------|--------------------|
| | | | | Sample Interval | | | Sample Interval | | |
| | | | | 25 mm (1 in.) | 152 mm (6 in.) | 304 mm (12 in.) | 25 mm (1 in.) | 152 mm (6 in.) | 304 mm (12 in.) |
| 10,000 | 7/15/96 | 23,857 | 36,978 | 4.05 | 3.52 | 3.55 | 2.16 | 2.47 | 2.38 |
| 10,000 | 8/2/96 | 109,000 | 168,950 | 4.22 | 3.97 | 4.2 | 2.08 | 2.2 | 2.09 |
| 10,000 | 8/9/96 | 158,977 | 246,414 | 4.85 | 4.47 | 4.36 | 1.81 | 1.94 | 2.04 |
| 10,000 | 8/12/96 | 183,982 | 285,172 | 5.25 | 4.7 | 4.63 | 1.75 | 1.9 | 2.05 |
| 10,000 | 8/16/96 | 209,000 | 323,950 | 4.25 | 4.08 | 4.4 | 2.15 | 2.28 | 2.26 |
| 10,000 | 8/20/96 | 233,984 | 362,675 | 4.89 | 4.42 | 4.21 | 1.77 | 2.1 | 2.12 |
| 10,000 | 8/23/96 | 258,000 | 399,900 | 5.48 | 4.88 | 4.62 | 1.73 | 1.84 | 2.05 |

Table A3. 4 IRI and RN values for lane 005

| Load | Date Data Taken | Passes | ESALs | Average IRI, m/km | | | Average RN | | |
|--------|-----------------|---------|---------|-------------------|-------------------|--------------------|------------------|-------------------|--------------------|
| | | | | Sample Interval | | | Sample Interval | | |
| | | | | 25 mm (1 in.) | 152 mm (6 in.) | 304 mm (12 in.) | 25 mm (1 in.) | 152 mm (6 in.) | 304 mm (12 in.) |
| 10,000 | 10/7/97 | 0 | 0 | 1.94 | 1.54 | 1.38 | 3.18 | 3.51 | 3.62 |
| 10,000 | 10/10/97 | 25,000 | 39,750 | 2.43 | 2.38 | 2.23 | 2.69 | 2.75 | 3.14 |
| 10,000 | 10/31/97 | 50,000 | 79,500 | 1.97 | 1.72 | 1.74 | 3.17 | 3.39 | 3.39 |
| 10,000 | 11/3/97 | 75,000 | 119,250 | 2.59 | 2.3 | 2.01 | 2.83 | 3.01 | 3.11 |
| 10,000 | 12/11/97 | 100,003 | 159,005 | 3.05 | 2.84 | 2.86 | 2.62 | 2.75 | 2.77 |
| 10,000 | 12/18/97 | 125,035 | 198,806 | 4.43 | 4.14 | 3.97 | 2.09 | 2.29 | 2.31 |
| 10,000 | 1/8/97 | 150,064 | 238,602 | 9.97 | 9.76 | 9.4 | 1.1 | 1.14 | 1.19 |

Table A3. 5 IRI and RN values for lane 006

| Load | Date Data Taken | Passes | ESALs | Average IRI, m/km | | | Average RN | | |
|--------|-----------------|---------|---------|-------------------|----------------|-----------------|-----------------|----------------|-----------------|
| | | | | Sample Interval | | | Sample Interval | | |
| | | | | 25 mm (1 in.) | 152 mm (6 in.) | 304 mm (12 in.) | 25 mm (1 in.) | 152 mm (6 in.) | 304 mm (12 in.) |
| 10,000 | 9/29/97 | 0 | 0 | 2.29 | 2.16 | 2.14 | 2.9 | 3.13 | 3.12 |
| 10,000 | 10/10/97 | 25,000 | 38,750 | 2.21 | 1.83 | 1.63 | 3 | 3.37 | 3.49 |
| 10,000 | 10/20/97 | 50,000 | 77,500 | 1.87 | 1.46 | 1.56 | 3.25 | 3.5 | 3.45 |
| 10,000 | 11/3/97 | 75,000 | 116,250 | 2.47 | 2.09 | 2.13 | 2.8 | 3.27 | 3.28 |
| 10,000 | 12/16/97 | 125,041 | 193,814 | 3.31 | 2.77 | 2.37 | 2.36 | 2.72 | 3.01 |
| 10,000 | 1/8/97 | 150,036 | 232,556 | 5.41 | 4.69 | 4.72 | 1.73 | 1.99 | 1.95 |

Table A3. 6 IRI and RN values for lane 007

| Load | Date Data Taken | Passes | ESALs | Average IRI, m/km | | | Average RN | | |
|--------|-----------------|---------|---------|-------------------|----------------|-----------------|-----------------|----------------|-----------------|
| | | | | Sample Interval | | | Sample Interval | | |
| | | | | 25 mm (1 in.) | 152 mm (6 in.) | 304 mm (12 in.) | 25 mm (1 in.) | 152 mm (6 in.) | 304 mm (12 in.) |
| 10,000 | 10/10/97 | 25,000 | 38,750 | 2.38 | 2.36 | 2.36 | 2.93 | 3 | 3.05 |
| 10,000 | 12/16/97 | 125,024 | 193,787 | 2.86 | 2.86 | 3.03 | 2.69 | 2.9 | 2.87 |
| 10,000 | 1/8/97 | 150,061 | 232,595 | 3.53 | 3.26 | 3.21 | 2.19 | 2.4 | 2.56 |
| 10,000 | 2/6/98 | 175,156 | 271,492 | 6.2 | 5.57 | 5.15 | 1.6 | 1.89 | 2.01 |

Table A3. 7 IRI and RN values for lane 008

| Load | Date Data Taken | Passes | ESALs | Average IRI, m/km | | | Average RN | | |
|--------|-----------------|---------|---------|-------------------|----------------|-----------------|-----------------|----------------|-----------------|
| | | | | Sample Interval | | | Sample Interval | | |
| | | | | 25 mm (1 in.) | 152 mm (6 in.) | 304 mm (12 in.) | 25 mm (1 in.) | 152 mm (6 in.) | 304 mm (12 in.) |
| 10,000 | 12/23/96 | 50,000 | 77,500 | 2.38 | 2.19 | 2.49 | 2.93 | 3.02 | 2.87 |
| 10,000 | 1/31/97 | 75,000 | 116,250 | 4.89 | 4.21 | 3.95 | 1.9 | 2.21 | 2.25 |
| 12,300 | 2/21/97 | 125,000 | 290,750 | 6.5 | 6.11 | 6.14 | 1.25 | 1.36 | 1.34 |

Table A3. 8 IRI and RN values for lane 009

| Load | Date Data Taken | Passes | ESALs | Average IRI, m/km | | | Average RN | | |
|--------|-----------------------|---------|-----------|-------------------|-------------------|--------------------|------------------|-------------------|--------------------|
| | | | | Sample Interval | | | Sample Interval | | |
| | | | | 25 mm (1 in.) | 152 mm (6 in.) | 304 mm (12 in.) | 25 mm (1 in.) | 152 mm (6 in.) | 304 mm (12 in.) |
| 10,000 | 1/14/97 | 75,000 | 117,750 | 1.93 | 2.24 | 2.12 | 3.04 | 2.69 | 3.05 |
| 10,000 | 2/13/97 | 100,045 | 157,071 | 1.65 | 1.66 | 1.95 | 3.32 | 3.45 | 3.34 |
| 12,300 | 2/21/97 | 125,000 | 250,652 | 2.03 | 1.7 | 1.59 | 3.07 | 3.36 | 3.46 |
| 12,300 | 3/11/97 | 150,000 | 344,402 | 3.73 | 3.06 | 3.08 | 2.3 | 2.75 | 2.72 |
| 12,300 | 3/21/97 | 175,055 | 438,358 | 4.07 | 2.97 | 3.02 | 2.14 | 2.68 | 2.73 |
| 12,300 | 4/18/97 | 200,057 | 532,116 | 2.48 | 2.46 | 3 | 2.82 | 2.88 | 2.65 |
| 12,300 | 4/29/97 | 250,048 | 719,582 | 3.49 | 3.29 | 3.29 | 2.37 | 2.54 | 2.73 |
| 12,300 | 5/11/97 | 275,056 | 813,362 | 3.63 | 3.38 | 3.12 | 2.29 | 2.58 | 2.66 |
| 12,300 | 5/15/97 | 300,000 | 906,902 | 4.51 | 4.24 | 3.95 | 2.03 | 2.14 | 2.42 |
| 12,300 | 5/21/97 | 325,063 | 1,000,888 | 4.48 | 3.85 | 3.9 | 2.08 | 2.35 | 2.34 |
| 12,300 | 5/30/97 | 360,069 | 1,132,161 | 6.08 | 5.69 | 5.42 | 1.47 | 1.64 | 1.7 |
| 14,600 | 6/6/97 | 410,077 | 1,557,229 | 6.38 | 6.07 | 5.81 | 1.45 | 1.59 | 1.67 |
| 14,600 | 6/11/97 | 435,077 | 1,769,729 | 8.03 | 7.71 | 7.62 | 1.1 | 1.16 | 1.2 |
| 14,600 | 7/10/97 | 460,077 | 1,982,229 | 8.32 | 8.03 | 8.2 | 1.02 | 1.12 | 1.14 |

Table A3. 9 IRI and RN values for lane 010

| Load | Date Data Taken | Passes | ESALs | Average IRI, m/km | | | Average RN | | |
|--------|-----------------|---------|---------|-------------------|----------------|-----------------|-----------------|----------------|-----------------|
| | | | | Sample Interval | | | Sample Interval | | |
| | | | | 25 mm (1 in.) | 152 mm (6 in.) | 304 mm (12 in.) | 25 mm (1 in.) | 152 mm (6 in.) | 304 mm (12 in.) |
| 10,000 | 11/15/96 | 0 | 0 | 1.59 | 1.4 | 1.53 | 3.4 | 3.62 | 3.59 |
| 10,000 | 12/23/96 | 50,000 | 79,000 | 3.06 | 2.94 | 2.76 | 2.69 | 2.85 | 2.9 |
| 10,000 | 1/10/97 | 75,000 | 118,500 | 1.71 | 1.55 | 1.55 | 3.2 | 3.51 | 3.52 |
| 12,300 | 2/21/97 | 125,000 | 328,500 | 2.8 | 2.34 | 2.22 | 2.69 | 3 | 2.96 |
| 12,300 | 3/11/97 | 150,000 | 433,500 | 5.03 | 4.13 | 4.29 | 1.82 | 2.26 | 2.14 |
| 12,300 | 3/21/97 | 175,000 | 538,500 | 4.89 | 3.99 | 4.23 | 1.98 | 2.34 | 2.21 |
| 12,300 | 4/18/97 | 193,285 | 615,297 | 9.6 | 9.41 | 10.18 | 0.53 | 0.59 | 0.54 |
| 12,300 | 4/29/97 | 250,048 | 853,702 | 9.84 | 9.14 | 8.6 | 0.61 | 0.78 | 0.85 |

APPENDIX 4. PSI DATA

Table A4. 1 PSI for lane 002

| ESALs X 1,000 | Slope Variance (x 1E-6) | Cracks (ft ² /1000 ft ²) | Rutting (in.) | PSI |
|------------------|-------------------------------|--|------------------|------|
| 0 | 9.38 | 0 | 0.08 | 3.08 |
| 39 | 4.106 | 0 | 0.06 | 3.67 |
| 77 | 2.05 | 0 | 0.18 | 4.06 |
| 116 | 4.52 | 0 | 0.20 | 3.56 |
| 155 | 3.736 | 0 | 0.37 | 3.55 |
| 293 | 3.31 | 2.592 | 0.39 | 3.59 |
| 337 | 4.21 | 4.913 | 0.42 | 3.39 |
| 441 | 4.163 | 13.037 | 0.67 | 3.01 |
| 525 | 4.575 | 15.977 | 0.83 | 2.62 |
| 582 | 6.807 | 30.6379 | 0.91 | 2.13 |
| 659 | 3.354 | 48.587 | 1.06 | 2.19 |
| 722 | 12.463 | 102.745 | 1.17 | 0.88 |
| 908 | 16.382 | 323.4 | 1.34 | 0.01 |

Table A4. 2 PSI for lane 003

| ESALs X 1,000 | Slope Variance (x 1E-6) | Cracks (ft ² /1000 ft ²) | Rutting (in.) | PSI |
|------------------|-------------------------------|--|------------------|------|
| 0 | 3.3 | 0 | 0.12 | 3.80 |
| 8 | 10.278 | 0 | 0.31 | 2.89 |
| 16 | 6.48 | 0 | 0.37 | 3.18 |
| 39 | 14.762 | 13.926 | 0.48 | 2.39 |
| 78 | 13.982 | 24.371 | 0.61 | 2.23 |

Table A4. 3 PSI for lane 004

| ESALs x 1,000 | Slope Variance (x 1E-6) | Cracks (ft ² /1000 ft ²) | Rutting (in.) | PSI |
|------------------|-------------------------------|--|------------------|------|
| 0 | | 11.605 | 0.00 | 5.00 |
| 37 | 17.927 | 13 | 0.51 | 2.20 |
| 169 | 14.97 | 14.7 | 0.64 | 2.12 |
| 246 | 21.448 | 25.912 | 0.64 | 1.83 |
| 285 | 23.515 | 49.90264 | 0.68 | 1.67 |
| 324 | 12.16 | 55 | 0.69 | 2.17 |
| 363 | 20.099 | 60 | 0.76 | 1.62 |
| 400 | 21.193 | 74.6605 | 0.79 | 1.51 |

Table A4. 4 PSI for lane 005

| ESALs x 1,000 | Slope Variance (x 1E-6) | Cracks (ft ² /1000 ft ²) | Rutting (in.) | PSI |
|------------------|-------------------------------|--|------------------|------|
| 0 | 4.603 | 0 | 0.05 | 3.60 |
| 39 | 8.68 | 0 | 0.11 | 3.13 |
| 79 | 3.984 | 0 | 0.16 | 3.66 |
| 119 | 3.972 | 56.092 | 0.26 | 3.53 |
| 159 | 4.311 | 136.942 | 0.31 | 3.40 |
| 198 | 6.151 | 311.408 | 0.34 | 3.06 |
| 239 | 8.472 | 387.6159 | 0.62 | 2.44 |

Table A4. 5 PSI for lane 006

| ESALs x 1,000 | Slope Variance (x 1E-6) | Cracks (ft ² /1000 ft ²) | Rutting (in.) | PSI |
|------------------|-------------------------------|--|------------------|------|
| 0 | 4.828 | 0 | 0.04 | 3.57 |
| 38 | 5.126 | 0 | 0.13 | 3.50 |
| 77 | 3.003 | 0 | 0.15 | 3.85 |
| 116 | 7.068 | 0 | 0.18 | 3.25 |
| 155 | 5.307 | 0 | 0.21 | 3.44 |
| 194 | 5.307 | 75.434 | 0.20 | 3.36 |
| 232 | 7.673 | 297.0945 | 0.43 | 2.82 |

Table A4. 6 PSI for lane 007

| ESALs x 1,000 | Slope Variance (x 1E-6) | Cracks (ft ² /1000 ft ²) | Rutting (in.) | PSI |
|------------------|-------------------------------|--|------------------|------|
| 0 | | 0 | 0.00 | |
| 39 | 4.817 | 0 | 0.19 | 3.52 |
| 77 | 4.823 | 29.787 | 0.17 | 3.47 |
| 116 | 6.481 | 34.815 | 0.20 | 3.25 |
| 155 | 7.906 | 68.084 | 0.21 | 3.07 |
| 194 | 4.823 | 185.684 | 0.20 | 3.38 |
| 233 | 4.823 | 357.4422 | 0.23 | 3.31 |
| 271 | 4.823 | 640.224 | 0.31 | 3.19 |

Table A4. 7 PSI for lane 008

| ESALs x 1,000 | Slope Variance (x 1E-6) | Cracks (ft ² /1000 ft ²) | Rutting (in.) | PSI |
|------------------|-------------------------------|--|------------------|------|
| 0 | | 0 | 0.00 | |
| 77 | 3.608 | 0 | 0.05 | 3.76 |
| 116 | 13.973 | 0 | 0.18 | 2.74 |
| 291 | 6.623 | 338.487 | 0.47 | 2.86 |

Table A4. 8 PSI for lane 009

| ESALs x 1,000 | Slope Variance (x 1E-6) | Cracks (ft ² /1000 ft ²) | Rutting (in.) | PSI |
|------------------|-------------------------------|--|------------------|------|
| 0 | 4.235 | 11.992 | 0.04 | 3.62 |
| 79 | 5.528 | 12 | 0.05 | 3.44 |
| 118 | 3.442 | 12.5 | 0.09 | 3.75 |
| 157 | 4.059 | 13 | 0.09 | 3.64 |
| 251 | 15.63 | 14.313 | 0.07 | 2.65 |
| 344 | 20.303 | 24.7579 | 0.20 | 2.39 |
| 438 | 6.501 | 50 | 0.26 | 3.19 |
| 532 | 10.438 | 74.6605 | 0.30 | 2.80 |
| 719 | 8.145 | 90.521 | 0.39 | 2.89 |
| 813 | 12.986 | 105 | 0.45 | 2.46 |
| 1000 | 7.951 | 153.963 | 0.59 | 2.60 |
| 1132 | 10.353 | 374.85 | 0.71 | 2.13 |
| 1557 | 8.946 | 415.8553 | 0.89 | 1.83 |
| 1769 | 14.04 | 430 | 1.04 | 1.07 |
| 1982 | 14.616 | 461.8895 | 1.31 | 0.16 |

Table A4. 9 PSI for lane 010

| ESALs x 1,000 | Slope Variance (x 1E-6) | Cracks (ft ² /1000 ft ²) | Ruttin g (in.) | PSI |
|------------------|-------------------------------|---|----------------------|------|
| 0 | 1.532 | 0 | 0.04 | 4.26 |
| 79 | 6.779 | 0 | 0.10 | 3.32 |
| 118 | 4.22 | 0 | 0.07 | 3.65 |
| 328 | 5.495 | 11.218 | 0.11 | 3.43 |
| 433 | 19.669 | 30.5603 | 0.23 | 2.39 |
| 538 | 13.243 | 40 | 0.34 | 2.60 |
| 615 | 13.795 | 50 | 0.42 | 2.49 |
| 854 | 15.983 | 70 | 0.57 | 2.15 |

APPENDIX 5. THICKNESS DESIGN DATA

Table A5. 1 Thickness design using lane 002 materials

| Cell No. | Surface, in. | Base, in. | Subbase, in. |
|----------|--------------|-----------|--------------|
| 1 | 5.0 | 12.0 | 7.0 |
| 2 | 5.0 | 16.0 | 6.0 |
| 3 | 6.0 | 15.0 | 8.0 |
| 4 | 6.0 | 18.0 | 8.0 |
| 5 | 7.0 | 17.0 | 9.0 |
| 6 | 7.0 | 21.0 | 8.0 |
| 7 | 5.0 | 12.0 | 4.0 |
| 8 | 5.0 | 16.0 | 4.0 |
| 9 | 6.0 | 15.0 | 5.0 |
| 10 | 6.0 | 18.0 | 4.0 |
| 11 | 7.0 | 17.0 | 5.0 |
| 12 | 7.0 | 21.0 | 4.0 |
| 13 | 5.0 | 10.0 | 4.0 |
| 14 | 5.0 | 16.0 | 0.0 |
| 15 | 6.0 | 13.0 | 4.0 |
| 16 | 6. | 16.0 | 4.0 |
| 17 | 7.0 | 15.0 | 4.0 |
| 18 | 7.0 | 18.0 | 4.0 |

Table A5. 2 Thickness design using lane 003 materials

| Cell No. | Surface, in. | Base, in. | Subbase, in. |
|----------|--------------|-----------|--------------|
| 1 | 5.0 | 12.0 | 7.0 |
| 2 | 5.0 | 16.0 | 6.0 |
| 3 | 6.0 | 15.0 | 8.0 |
| 4 | 6.0 | 18.0 | 8.0 |
| 5 | 7.0 | 17.0 | 9.0 |
| 6 | 7.0 | 21.0 | 8.0 |
| 7 | 5.0 | 12.0 | 4.0 |
| 8 | 5.0 | 16.0 | 4.0 |
| 9 | 6.0 | 15.0 | 5.0 |
| 10 | 6.0 | 18.0 | 4.0 |
| 11 | 7.0 | 17.0 | 5.0 |
| 12 | 7.0 | 21.0 | 4.0 |
| 13 | 5.0 | 10.0 | 4.0 |
| 14 | 5.0 | 16.0 | 0.0 |
| 15 | 6.0 | 13.0 | 4.0 |
| 16 | 6. | 16.0 | 4.0 |
| 17 | 7.0 | 15.0 | 4.0 |
| 18 | 7.0 | 18.0 | 4.0 |

Table A5. 3 Thickness design using lane 004 materials

| Cell No. | Surface, in. | Base, in. | Subbase 1, in. | Subbase 2, in. |
|----------|-----------------|-----------|-------------------|-------------------|
| 1 | 5.0 | 7.0 | 7.0 | 7.0 |
| 2 | 5.0 | 10.0 | 8.0 | 7.0 |
| 3 | 6.0 | 10.0 | 7.0 | 8.0 |
| 4 | 6.0 | 12.0 | 8.0 | 8.0 |
| 5 | 7.0 | 11.0 | 8.0 | 9.0 |
| 6 | 7.0 | 14.0 | 9.0 | 10.0 |
| 7 | 5.0 | 7.0 | 5.0 | 7.0 |
| 8 | 5.0 | 10.0 | 5.0 | 7.0 |
| 9 | 6.0 | 10.0 | 7.0 | 4.0 |
| 10 | 6.0 | 12.0 | 8.0 | 5.0 |
| 11 | 7.0 | 11.0 | 8.0 | 5.0 |
| 12 | 7.0 | 14.0 | 9.0 | 6.0 |
| 13 | 5.0 | 7.0 | 4.0 | 6.0 |
| 14 | 5.0 | 10.0 | 4.0 | 6.0 |
| 15 | 6.0 | 10.0 | 5.0 | 4.0 |
| 16 | 6.0 | 12.0 | 6.0 | 4.0 |
| 17 | 7.0 | 11.0 | 6.0 | 4.0 |
| 18 | 7.0 | 14.0 | 7.0 | 4.0 |

Table A5. 4 Thickness design using lane 005 materials

| Cell No. | Surface, in. | Base, in. | Subbase, in. |
|----------|--------------|-----------|--------------|
| 1 | 4.0 | 16.0 | 6.0 |
| 2 | 4.0 | 19.0 | 7.0 |
| 3 | 4.0 | 22.0 | 8.0 |
| 4 | 5.0 | 22.0 | 7.0 |
| 5 | 5.0 | 24.0 | 9.0 |
| 6 | 6.0 | 24.0 | 9.0 |
| 7 | 4.0 | 15.0 | 4.0 |
| 8 | 4.0 | 19.0 | 4.0 |
| 9 | 4.0 | 22.0 | 5.0 |
| 10 | 5.0 | 21.0 | 4.0 |
| 11 | 5.0 | 24.0 | 5.0 |
| 12 | 6.0 | 24.0 | 5.0 |
| 13 | 4.0 | 13.0 | 4.0 |
| 14 | 4.0 | 16.0 | 4.0 |
| 15 | 4.0 | 20.0 | 4.0 |
| 16 | 5.0 | 22.0 | 0.0 |
| 17 | 5.0 | 22.0 | 4.0 |
| 18 | 6.0 | 22.0 | 4.0 |

Table A5. 5 Thickness design using lane 006 materials

| Cell No. | Surface, in. | Base, in. | Subbase, in. |
|----------|--------------|-----------|--------------|
| 1 | 4.0 | 18.0 | 7.0 |
| 2 | 4.0 | 22.0 | 7.0 |
| 3 | 5.0 | 22.0 | 7.0 |
| 4 | 5.0 | 25.0 | 8.0 |
| 5 | 5.0 | 28.0 | 9.0 |
| 6 | 6.0 | 28.0 | 9.0 |
| 7 | 4.0 | 18.0 | 4.0 |
| 8 | 4.0 | 22.0 | 4.0 |
| 9 | 5.0 | 22.0 | 4.0 |
| 10 | 5.0 | 25.0 | 4.0 |
| 11 | 5.0 | 28.0 | 5.0 |
| 12 | 6.0 | 28.0 | 5.0 |
| 13 | 4.0 | 15.0 | 4.0 |
| 14 | 4.0 | 19.0 | 4.0 |
| 15 | 5.0 | 19.0 | 4.0 |
| 16 | 5.0 | 22.0 | 4.0 |
| 17 | 5.0 | 25.0 | 4.0 |
| 18 | 6.0 | 26.0 | 4.0 |

Table A5. 6 Thickness design using lane 007 materials

| Cell No. | Surface, in. | Base, in. | Subbase, in. |
|----------|--------------|-----------|--------------|
| 1 | 4.0 | 16.0 | 6.0 |
| 2 | 4.0 | 19.0 | 7.0 |
| 3 | 4.0 | 22.0 | 8.0 |
| 4 | 5.0 | 22.0 | 7.0 |
| 5 | 5.0 | 24.0 | 9.0 |
| 6 | 6.0 | 24.0 | 9.0 |
| 7 | 4.0 | 15.0 | 4.0 |
| 8 | 4.0 | 19.0 | 4.0 |
| 9 | 4.0 | 22.0 | 5.0 |
| 10 | 5.0 | 21.0 | 4.0 |
| 11 | 5.0 | 24.0 | 5.0 |
| 12 | 6.0 | 24.0 | 5.0 |
| 13 | 4.0 | 13.0 | 4.0 |
| 14 | 4.0 | 16.0 | 4.0 |
| 15 | 4.0 | 20.0 | 4.0 |
| 16 | 5.0 | 22.0 | 0.0 |
| 17 | 5.0 | 22.0 | 4.0 |
| 18 | 6.0 | 22.0 | 4.0 |

Table A5. 7 Thickness design using lane 008 materials

| Cell No. | Surface, in. | Base, in. | Subbase, in. |
|----------|--------------|-----------|--------------|
| 1 | 4.0 | 16.0 | 6.0 |
| 2 | 4.0 | 19.0 | 7.0 |
| 3 | 4.0 | 22.0 | 8.0 |
| 4 | 5.0 | 22.0 | 7.0 |
| 5 | 5.0 | 24.0 | 9.0 |
| 6 | 6.0 | 24.0 | 9.0 |
| 7 | 4.0 | 15.0 | 4.0 |
| 8 | 4.0 | 19.0 | 4.0 |
| 9 | 4.0 | 22.0 | 5.0 |
| 10 | 5.0 | 21.0 | 4.0 |
| 11 | 5.0 | 24.0 | 5.0 |
| 12 | 6.0 | 24.0 | 5.0 |
| 13 | 4.0 | 13.0 | 4.0 |
| 14 | 4.0 | 16.0 | 4.0 |
| 15 | 4.0 | 20.0 | 4.0 |
| 16 | 5.0 | 22.0 | 0.0 |
| 17 | 5.0 | 22.0 | 4.0 |
| 18 | 6.0 | 22.0 | 4.0 |

Table A5. 8 Thickness design using lane 009 materials

| Cell No. | Surface, in. | Base, in. | Subbase 1, in. | Subbase 2, in. |
|----------|-----------------|-----------|-------------------|-------------------|
| 1 | 5.0 | 6.0 | 5.0 | 9.0 |
| 2 | 5.0 | 6.0 | 9.0 | 7.0 |
| 3 | 6.0 | 6.0 | 8.0 | 10.0 |
| 4 | 6.0 | 6.0 | 11.0 | 10.0 |
| 5 | 7.0 | 6.0 | 10.0 | 11.0 |
| 6 | 7.0 | 6.0 | 14.0 | 10.0 |
| 7 | 5.0 | 6.0 | 5.0 | 6.0 |
| 8 | 5.0 | 6.0 | 9.0 | 5.0 |
| 9 | 6.0 | 6.0 | 8.0 | 6.0 |
| 10 | 6.0 | 6.0 | 11.0 | 6.0 |
| 11 | 7.0 | 6.0 | 10.0 | 7.0 |
| 12 | 7.0 | 6.0 | 14.0 | 6.0 |
| 13 | 5.0 | 6.0 | 4.0 | 4.0 |
| 14 | 5.0 | 6.0 | 7.0 | 6.0 |
| 15 | 6.0 | 6.0 | 7.0 | 5.0 |
| 16 | 6.0 | 6.0 | 10.0 | 4.0 |
| 17 | 7.0 | 6.0 | 9.0 | 4.0 |
| 18 | 7.0 | 6.0 | 12.0 | 6.0 |

Table A5. 9 Thickness design using lane 010 materials

| Cell No. | Surface, in. | Base, in. | Subbase, in. |
|----------|--------------|-----------|--------------|
| 1 | 4.0 | 6.0 | 13.0 |
| 2 | 4.0 | 6.0 | 17.0 |
| 3 | 4.0 | 6.0 | 20.0 |
| 4 | 5.0 | 6.0 | 20.0 |
| 5 | 5.0 | 6.0 | 23.0 |
| 6 | 6.0 | 6.0 | 23.0 |
| 7 | 4.0 | 6.0 | 12.0 |
| 8 | 4.0 | 6.0 | 15.0 |
| 9 | 4.0 | 6.0 | 19.0 |
| 10 | 5.0 | 6.0 | 18.0 |
| 11 | 5.0 | 6.0 | 21.0 |
| 12 | 6.0 | 6.0 | 21.0 |
| 13 | 4.0 | 6.0 | 10.0 |
| 14 | 4.0 | 6.0 | 13.0 |
| 15 | 4.0 | 6.0 | 17.0 |
| 16 | 5.0 | 6.0 | 16.0 |
| 17 | 5.0 | 6.0 | 19.0 |
| 18 | 6.0 | 6.0 | 19.0 |

REFERENCES

1. Freeme, C.R. Maree, J.H., and Viljoen, A.W. Mechanistic Design of Asphalt Pavements and Verifications Using the Heavy Vehicle Simulator. Proceedings of the Fifth International Conferences on the Structural Design of Asphalt Pavements. University of Michigan, Ann Arbor, 1982. Pp. 156-173.
2. Al-Omary, B., and Darter, M.I. Effect of Pavement Deterioration Types on IRI and Rehabilitation. Transportation Research Record 1505, TRB, National Research Council, Washington, DC, 1995.
3. Research Plans, Strategic Highway Research Program. Final Report, TRB, National Research Council, Washington, D.C., May 1986.
4. Metcalf, J.B. Application of Full-Scale Accelerated Pavement Testing. NCHRP Synthesis 235, Transportation Research Board, National Research Council, Washington, D.C., 1996.
5. Rao, J.S., Shah, N.S., Mueller, G.L., Shahin, M.Y., George, K.P., and Carpenter, S.M. Using Pavement Performance Data to Develop Mechanistic-empirical Concepts for Deteriorated and Rehabilitated Pavements. Research Report No. FHWA-RD-93-162. FHWA. US Department of Transportation, Washington, D.C. 1994.
6. Rauhut, J.B., Lytton, R.L., and Darter, M.I. Pavement Damage Functions for Cost Allocations. Research Report No. FHWA/RD-82/126. FHWA. US Department of Transportation, Washington, DC, July, 1982.
7. Statton, J.E., and Kadar, P. *The Performance of Pavement Rehabilitations Under Accelerated Loading - The Callington ALF Trial*. Proceedings 15th. ARRB Conference Part 2. Australia. 1992. pp.328-345.
8. Bonaquist, R. Summary of Pavement Performance Tests Using the Accelerated Loading Facility, 1986-1990. *Transportation Research Record 1354*. Transportation Research Board. Washington, D.C. 1992. pp 74-85.
9. Johnson-Clark, J.R., Sharp, K.G., Walter, P.D. *The Performance of Pavements with Geotextile Reinforced Seals: The Brewarrina, N.S.W. ALF Trial*. Research Report 241. Australian Road Research Board Ltd. Vermont, Victoria. Australia. February 1993.

10. Bonaquist, R., Surdahl, R., and Mogawer, W. Effect of Tire Pressure on Flexible Pavement Response and Performance. *Transportation Research Record 1227*. Transportation Research Board. Washington, D.C. 1989. pp 97-106.
11. Sebaaly, P., Tabatabaee, N., Bonaquist, R., and Anderson, D. Evaluating Structural Damage of Flexible Pavements Using Cracking and Falling Weight Deflectometer Data. *Transportation Research Record 1227*. Transportation Research Board. Washington, D.C., 1989. pp 115-127.
12. Kadar, P. *The Performance of Overlay Treatment and Modified Binders Under Accelerated Full Scale Loading- The Callington ALF Trial*. 27 November 1990. Australian Road Research Board Ltd. Vermont, Victoria. Australia.
13. Sharp, K.G. The Efficiency and Effectiveness of the Australian Accelerated Loading Facility (ALF) Program. *Road and Transport Research*. Vol.1, No. 2, June 1992, pp. 104-107.
14. Kenis, W.J. *VESYS 3A-M User's Manual*. FHWA. Office of Research, Development, and Technology. Washington, D.C. Undated.
15. Hudson, W.R. Road Roughness: Its Elements and Measurement. *Transportation Research Record 836*, TRB, National Research Council, Washington, DC, 1981.
16. Carey, W.N., and Irick, P.E., "The Pavement Serviceability Performance Concept," *HRB Bulletin 250*, Washington, D.C., 1960.
17. Hodges, J.W., Rolt, J., and Jones, T.E. *The Kenya Road Transport Cost Study: Research on Road Deterioration*. Laboratory Report 673, TRRL, Crowthorne, England, 1975.
18. Patterson, W.O. International Roughness Index: Relationship to Other Measures of Roughness and Riding Quality. *Transportation Research Record 1084*, TRB, National Research Council, Washington, DC, 1986.
19. Sayers, M.W., T.D. Gillespie, and C.A.V. Queiroz, "The International Road Roughness Experiment: A Basis for Establishing a Standard Scale for Road Roughness Measurements," *Transportation Research Record 1084*, TRB, National Research Council, Washington, DC, 1986. pp. 76 -85.
20. Sayers, M.W., "Two Quarter-Car Models for Defining Road Roughness: IRI and HRI," *Transportation Research Record 1215*, TRB, National Research Council, Washington, DC, 1990. pp. 165 - 171.

21. Sayers, M.W., "Profiles of Roughness," Transportation Research Record 1260, TRB, National Research Council, Washington, DC, 1990.
22. Sayers, M.W. On the Calculation of International Roughness Index from Longitudinal Road Profile. Transportation Research Record 1501, TRB, National Research Council, Washington, DC, 1995.
23. Way, G.B., and Eisenberg, J. Pavement Management System for Arizona Phase II: Verification of Performance Prediction Models and Development of Database. Arizona Department of Transportation, 1988.
24. Zaniewski, J.P., Perera, R.W., and Mamlouk, M.S. Feedback of Pavement Management Performance Data for Pavement Design. Transportation Research Record 1272, TRB, Washington, D.C.
25. Potter, D.W. The Development of Road Roughness with Time- an Investigation. Internal Report AAIR 346-1, Australian Road Research Board, Melbourne, 1972.
26. Uzan, J. , and Lytton, R.L. Structural Design of Flexible Pavements: a Simple Predictive System. Transportation Research Record 888, TRB, Washington, D.C., 1982.
27. Lytton, R.L., Michalak, C.H., and Scullion, the Texas Flexible Pavement System, Volume 1, Proceedings, Fifth International Conference Structural Design of Asphalt Pavements, the University of Michigan, Ann Arbor, 1982.
28. Paterson, W.D.O. Road Deterioration and Maintenance Effects, Model for Planning and Management. The Highway Design and Maintenance Standards Services, World Bank. The John Hopkins University Press. 1988.
29. Watanada, T. Herral, C.G., and Patterson, W.D.O. Highway Design and Maintenance Standards Model-HDM3. World Bank, the John Hopkins University Press. 1988.
30. Garcia-Diaz, A. and Riggins, M. Serviceability and Distress Methodology for Predicting Pavement Performance. Transportation Research Record 977, TRB, National Research Council, Washington, DC, 1984.
31. George, K.P., Rajagopal, A.S., and Lim, L.K. Models For Predicting Pavement Deterioration. Transportation Research Record 1215, TRB, National Research Council, Washington, DC, 1989.
32. Cumbaa, S.L. Correlation of Profile-Based and Response-Type Roughness Devices for Louisiana's Highway Performance Monitoring System.

- Transportation Research Record 1260, TRB, National Research Council, Washington, DC, 1990.
33. Smith, K.D., T.E. Hoerner, and M.I. Darter. Effect of Initial Pavement Smoothness on Future Smoothness and Pavement Life. *Transportation Research Record 1570*, TRB, National Research Council, Washington, DC, 1997.
 34. Touma, B.E., Croveti, J.A., Shahin, M.Y. Effect of Various Load Distributions on Backcalculated Moduli Values in Flexible Pavements. *Transportation Research Record 1293*. Transportation Research Board. Washington, D.C. 1991. pp 31-41.
 35. Chou, Y.J., Lytton, R.L. Accuracy and Consistency of Backcalculated Pavement Layer Moduli. *Transportation Research Record 1293*. Transportation Research Board. Washington, D.C. 1991. pp 72-85.
 36. Parker, F. Estimation of Paving Materials Design Moduli from Falling Weight Deflectometer Measurements. *Transportation Research Record 1293*. Transportation Research Board. Washington, D.C. 1991. pp 42-51.
 37. Nazarian, S., Tandon, V., Briggs, R.C. Development of an Absolute Calibration System for Nondestructive Testing Devices. *Transportation Research Record 1293*. Transportation Research Board. Washington, D.C. 1991. pp 24-30.
 38. Uddin, W., Meyer, A.H., Hudson, W.R. Rigid Bottom Considerations for Nondestructive Evaluation of Pavement. *Transportation Research Record 1070*. Transportation Research Board. Washington, D.C. 1991. pp 21-29.
 39. Houssein, M., and L.Scofield. Correlation Between Backcalculated and Laboratory-Determined Asphalt Concrete Moduli. *Transportation Research Record 1377*. Transportation Research Board. Washington, D.C. 1992. pp 67-76.
 40. Roberts, F.L., Wedgeworth, J.B., Pumphrey, N.D. *Analysis and Evaluation of Methods for Backcalculation of M_R Values*. Research Report No. FHWA/LA-9-263. Final Report. Federal Highway Administration. January 1993.
 41. AASHTO. AASHTO Guide for Design of Pavement Structures. American Association of State Highway and Transportation Officials. Washington, D.C. 1986.
 42. Baltzer, S., and J.M. Jansen. Temperature Correction of Asphalt Moduli for FWD Measurements. Proc., 4th International Conference on Bearing Capacity of Roads and Airfields, Vol. 1, Minneapolis, Minn., 1994.

43. Johnson, A.M., and R.L. Baus. Alternative Method for Temperature Correction of Backcalculated Equivalent Pavement Moduli. *Transportation Research Record 1355*. Transportation Research Board. Washington, D.C. 1992.
44. Ullidtz, P. *Pavement Analysis*. Elsevier, New York, 1987.
45. Ali, H.A., and Parker, N.A. Using Time Series to Incorporate Seasonal Variations in Pavement Design. *Transportation Research Record 1539*, TRB, National Research Council, Washington, DC, 1996.
46. Ali, H.A., and Lopez, A. Statistical Analyses of Temperature and Moisture Effects on Pavement Structural Properties Based on Seasonal Monitoring Data. *Transportation Research Record 1540*, TRB, National Research Council, Washington, DC, 1997
47. Solaimanian, M., and Kennedy, T.W. Predicting Maximum Pavement Surface Temperature Using Maximum Air Temperature and Hourly Solar Radiation. *Transportation Research Record 1417*, TRB, National Research Council, Washington, DC, 1993. Pp.1-11.
48. Sousa, J.B., and Solaimanian, M. Abridged Procedure to Determine Permanent Deformation of Asphalt Concrete Pavements. *Transportation Research Record 1448*, TRB, National Research Council, Washington, DC, 1994. pp 25-32
49. Ullidtz, P., and B.K. Larsen. Mathematical Model for Predicting Pavement Performance, *Transportation Research Record 949*. Transportation Research Board. Washington, D.C. 1983.
50. Tayabji, S.D., P.J. Nussbaum, and A.T. Ciolko. Evaluation of Heavily Loaded Cement-Stabilized Bases. In *Transportation Research Record 839*, TRB, National Research Council, Washington, D.C., 1982, pp. 6 – 11.
51. Huntington, G., K. Ksaibati, and W. Oyler. Sulfate Expansion of Cement-Treated Bases. In *Transportation Research Record 1486*, TRB, National Research Council, Washington, D.C., 1995, pp. 59 – 67.
52. Thompson, M.R. High-Strength Stabilized Base Thickness Design Procedure. In *Transportation Research Record 1440*, TRB, National Research Council, Washington, D.C., 1994, pp. 1 – 7.
53. Ksaibati, K., and T.L. Conklin. Field Performance Evaluation of Cement-Treated Bases With and Without Fly Ash. In *Transportation Research Record 1440*, TRB, National Research Council, Washington, D.C., 1994, pp. 16 – 21.
54. Kota, P.B., T. Scullion, and D.N. Little. Investigation of Performance of Heavily Stabilized Bases in Houston, Texas, District. In *Transportation Research Record*

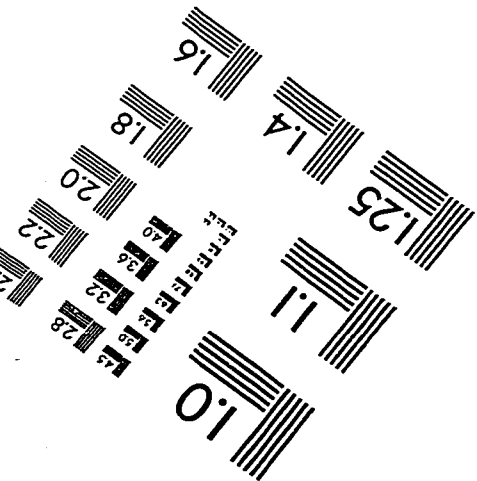
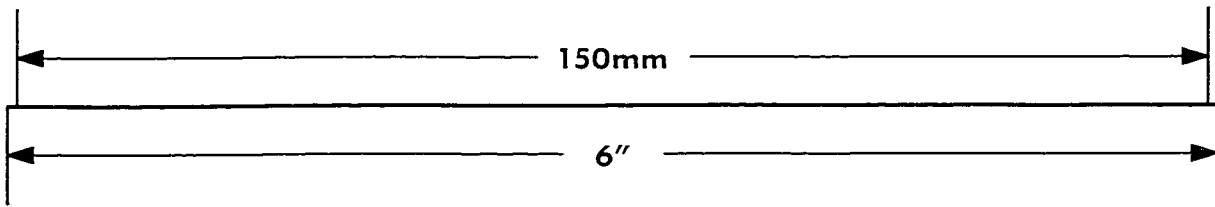
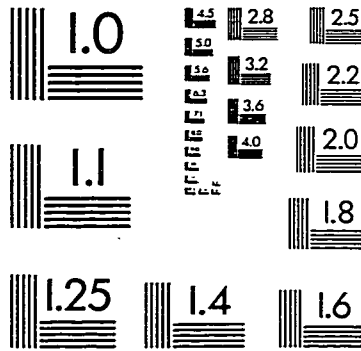
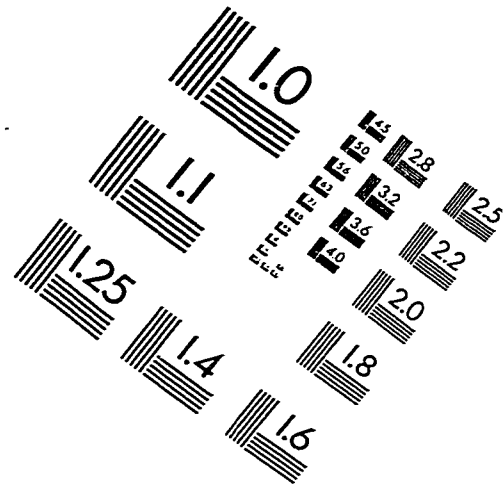
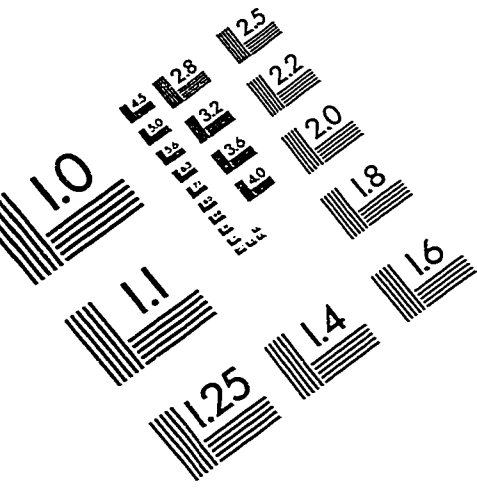
- 1486, TRB, National Research Council, Washington, D.C., 1995, pp. 68 – 76.
55. Corley-Lay, J.B. Comparison of Road Mix and Plant Mix Cement Treated Aggregate Base Course. In *Transportation Research Record 1589*, TRB, National Research Council, Washington, D.C., 1997, pp. 76 – 82.
 56. Tutumluer, E., and R.D. Barksdale. Inverted Flexible Pavement Response and Performance. In *Transportation Research Record 1482*, TRB, National Research Council, Washington, D.C., 1995, pp. 102 – 110.
 57. Johnson, W.V. Comparative Studies of Combinations of Treated and Untreated Bases and Subbases for Flexible Pavements. *Bulletin 289*, HRB, National Research Council, Washington, D.C., 1960, pp. 44-61.
 58. McGhee, K.H. *Pavement Design Performance Studies*. Final Report on Phase C Research Report BHRC 70-R44, Virginia Highway Research Council, 1971.
 59. Van Vuuren, D.J. Pavement Performance in the S12 Road Experiment, an AASHO Satellite Test Road in South Africa. Third International Conference on the Structural Design of Asphalt Pavements, Volume 1, *Proceeding*, London, 1972.
 60. Barksdale, R.D., S.F. Brown, and F. Chan. *NCHRP Report 315: Potential Benefits of Geosynthetics in Flexible Pavements*. TRB, National Research Council, Washington, D.C., 1989.
 61. Metcalf, J.B., S. Romanoschie, and L. Yongqi. Construction and Comparison of Louisiana's Conventional and Alternative Bases under Accelerated Loading. Interim Report 1, Phase 1. Louisiana Transportation Research Center. Louisiana Department of Transportation and Development. Baton Rouge. 1998.
 62. Metcalf, J.B., S. Romanoschie, and L. Yongqi. The Louisiana Accelerated Loading Facility. Report 2, Experiment 1, Phase 3. Louisiana Transportation
 63. Yoder, E.J., R.T. Milhous. Comparison of Different Methods of Measuring Pavement Condition. Interim Report. NCHRP 7. HRB. National Science Academy of Science. Washington, D.C., 1964.
 64. Hadley, W.O. *A Mechanistic Evaluation and Analysis of the Performance of Louisiana Experimental Test Sections*. Research Report No. FHWA/LA-83/78-5. Louisiana Department of Transportation and Development. December 1983.
 65. Anderson, D.I., Peterson, D.E., McBride, J.C., Shepherd, L.D. *Field Verification and Implementation of the VESYS IIM Structural Subsystem in Utah*. Research Report No. FHWA-RD-78-510. Final Report. Federal Highway Administration. February 1978.

66. Rauhut, J.B., Jordahl, P.R. *Effects of Flexible Highways of Increased Legal Vehicle Weights Using VESYS IIM*. Research Report No. FHWA-RD-77-116. Federal Highway Administration. January 1978.
67. Temple, W.H., and Walter Carpenter, Jr. *Implementation of the New AASHTO Pavement Design Procedure in Louisiana*. Final Report No. FHWA/LA-90/218. Louisiana Transportation Research Center. Louisiana Department of Transportation and Development. Baton Rouge. 1990.
68. Temple, W.H., and S.C. Shah. *Louisiana Experimental Base Project*. Report No. FHWA/LA-87/192. Louisiana Transportation Research Center. Louisiana Department of Transportation and Development. Baton Rouge. 1987.
69. USDA. *Soil Survey of Parishes in Louisiana*. United States Department of Agriculture. Soil Conservation Service and Forest Service. 1970.
70. Mohammad, L.N., Puppala, A.J., and Alavilli, P. "Effect of Instrumentation on Resilient Modulus of Sands," *Dynamic Geotechnical Testing: Second Volume*, ASTM STP 1213, American Society for Testing Materials, Philadelphia, 1995.
71. Roland, H.L. *Texas Triaxial R-Value Correlation*. Louisiana Department of Highways, Research Section, March 1963.
72. NHI. *Techniques for Pavement Rehabilitation. A Training Course Reference Manual*. 6th Edition. National Highway Institute, Federal Highway Administration. Washington, D.C. 1997.

VITAE

Mr. Ludfi Djakfar is a native of Indonesia. He earned his bachelor degree in Civil Engineering from Brawijaya University, Malang, Indonesia in 1988. After his graduation, he worked as a teaching and research assistant at the same University for about five years. He later got a scholarship to pursue a higher degree in Louisiana Tech University. Mr. Djakfar earned his Master of Science degree in Civil Engineering in 1996. When he pursued his master degree he worked on the research project, the Performance Comparison of Base Materials Under Accelerated Loading, funded by the Louisiana Transportation Research Center. His involvement in this research effort continued until he earned his doctorate degree. In addition to this research, he was also involved in another research work titled "Preliminary Assessment of Pavement Damage Due to Heavier Loads on Louisiana Highways", funded also by the Louisiana Transportation Research Center. He published several papers and research reports during his years at Louisiana Tech University.

IMAGE EVALUATION TEST TARGET (QA-3)



APPLIED IMAGE, Inc
 1653 East Main Street
 Rochester, NY 14609 USA
 Phone: 716/482-0300
 Fax: 716/288-5989

© 1993, Applied Image, Inc., All Rights Reserved

